REPORT DOCUMENTATION PAGE

Form Approved
OMB No. 0704-0188

1. REPORT DATE *(DD-MM-YYYY)*	2. REPORT TYPE	3. DATES COVERED *(From - To)*
21/Aug/2001	DISSERTATION	

4. TITLE AND SUBTITLE
OXIDIZED AND REDUCED BIOGENIC NITROGEN COMPUND EMISSIONS INTO THE RURAL TROSPOSHERE: CHARACTERIZATION AND MODELING

5a. CONTRACT NUMBER

5b. GRANT NUMBER

5c. PROGRAM ELEMENT NUMBER

6. AUTHOR(S)
CAPT ROELLE PAUL A

5d. PROJECT NUMBER

5e. TASK NUMBER

5f. WORK UNIT NUMBER

7. PERFORMING ORGANIZATION NAME(S) AND ADDRESS(ES)
NORTH CAROLINA STATE UNIVERSITY

8. PERFORMING ORGANIZATION REPORT NUMBER
CI01-206

9. SPONSORING/MONITORING AGENCY NAME(S) AND ADDRESS(ES)
THE DEPARTMENT OF THE AIR FORCE
AFIT/CIA, BLDG 125
2950 P STREET
WPAFB OH 45433

10. SPONSOR/MONITOR'S ACRONYM(S)

11. SPONSOR/MONITOR'S REPORT NUMBER(S)

12. DISTRIBUTION/AVAILABILITY STATEMENT
Unlimited distribution
In Accordance With AFI 35-205/AFIT Sup 1

13. SUPPLEMENTARY NOTES

14. ABSTRACT

20010904 047

15. SUBJECT TERMS

16. SECURITY CLASSIFICATION OF:			17. LIMITATION OF ABSTRACT	18. NUMBER OF PAGES	19a. NAME OF RESPONSIBLE PERSON
a. REPORT	b. ABSTRACT	c. THIS PAGE		218	19b. TELEPHONE NUMBER *(Include area code)*

Oxidized and Reduced Biogenic Nitrogen Compound Emissions into the Rural Troposphere: Characterization and Modeling

By

PAUL ANDREW ROELLE

A dissertation submitted to the Graduate Faculty of
North Carolina State University
in partial fulfillment of the
requirements for the Degree of
Doctor of Philosophy

DEPARTMENT OF MARINE, EARTH, AND ATMOSPHERIC SCIENCES

Raleigh

2001

APPROVED BY:

S. Pal Arya

Rohit Mathur

Jeffrey Peirce

Allen Riordan

Viney P. Aneja
Chair of Advisory Committee

The views expressed in this article are those of the author and do not reflect the official policy or position of the United States Air Force, Department of Defense, or the U.S. Government

BIOGRAPHY

Paul Andrew Roelle was born at Clark Air Force Base in the Philippines. The son of an Air Force Master Sergeant, Paul moved with his family from the Philippines to Ohio, and then to Northern Virginia. Paul graduated from Lake Braddock Secondary School in Burke, Virginia in 1987.

In 1987, Paul was awarded an Air Force ROTC scholarship and entered the AFROTC program at the Pennsylvania State University. While at Penn State, Paul was involved with the University Student Government (USG) as a Fraternity Senator and was a member of the Phi Delta Theta Fraternity. During his junior year, Paul attended the U.S. Army Airborne school at Ft. Benning, Georgia, where he earned his parachute wings in August of 1990.

Paul earned a Bachelor's of Science degree in Meteorology and a minor in Technical Writing in May, 1991 and accepted a commission in the United States Air Force as a second lieutenant. While waiting to enter the active duty Air Force, Paul met his future wife and spent three months traveling throughout Europe and Northern Africa.

At his first assignment in Ft. Polk, Louisiana, Paul served as the Staff Weather Officer to both the 5th Infantry Division and 2nd Armored Cavalry Regiment. Upon completion of his assignment at Ft. Polk, 1st Lieutenant Roelle was awarded with the Army Commendation Medal and was selected to attend the Air Force's Institute of Technology Civilian Institute program to pursue a Masters of Science in Atmospheric Science. In the fall of 1994, Paul began graduate study in air quality at the North Carolina State University under the direction of Dr. Viney P. Aneja. While at NC State,

Paul and . were married on October 14th, 1995 and Paul was promoted to Captain two days later.

During the summer of 1996, after completing the MS in Atmospheric Science with a minor in statistics, Paul and his wife were reassigned to Hanscom Air Force Base, Massachusetts. At Hanscom AFB, Paul served a short time as an Acquisition Meteorologist, but was then picked to serve as an Executive Officer. During his final year at Hanscom, Paul was selected to be the program manager for the Department of Defense's Automated Message Handling System (AMHS). Paul was named the Company Grade Officer of the Quarter and Company Grade Officer of the Year 2 years in a row. Paul also volunteered and was selected to be the Officer in Charge of the Patriot Honor Guard, a position which made him responsible for the funeral/retirement/parade duties throughout the Northeast US and Canada. Captain Roelle was awarded the Air Force Commendation Medal upon completion of his assignment at Hanscom AFB. While at Hanscom, Paul and Cynthia volunteered as first aid responders in Centennial Olympic Park during the 1996 Summer Olympics in Atlanta, Georgia. They were both on duty the night of the bombing and the US Air Force awarded Paul the Commendation Medal for heroism for his assistance with treating the injured and evacuating the Park.

During his final year at Hanscom, Paul competed for and was awarded one of four Air Force PhD assignments to study Atmospheric Science. In the fall of 1998, Captain Roelle began his PhD program under the direction of Dr. Viney P. Aneja. While pursuing his PhD, Paul remained an active volunteer and was awarded the Military

Outstanding Volunteer Service Medal and was Honorable Mention for the NC State University Deborah S. Moore memorial volunteer service award.

To date, Paul has published 16 journal articles and has presented his research at 20 scientific meetings throughout North America, Europe and Asia. Upon completion of the PhD program in August, 2001, Paul and his wife will spend a few weeks traveling throughout Italy and then begin their new assignment at the Air Force Combat Climatology Center in Asheville, North Carolina.

ACKNOWLEDGMENTS

I would like to recognize the following people and organizations for their support and guidance throughout my course work, research efforts, and thesis preparation. First, I would like to thank Cynthia Roelle for all her support and for helping with this manuscript and with presentations during my PhD program. My sincere thanks to the chair of my graduate committee, Dr. Viney Aneja, who always had time for me, and earnestly nurtured my development both personally and professionally. Dr. Jeffrey Peirce and his graduate students were also an invaluable resource, assisting me in technical discussions, soil analysis and field campaigns. I am very thankful to Dr. Rohit Mathur and Mr. Jeff Vukovich of the North Carolina Supercomputing Center who were invaluable in all aspects of the modeling efforts. Thanks also to Dr. S. Pal Arya and Dr. Al Riordan for their technical reviews and guidance throughout my PhD program.

Thanks to all the members of the NC State Air Quality Group, both past members who paved the way for this research and present members who helped me in innumerous ways. Thanks also to the US Environmental Protection Agency, especially Dr. Bruce Gay and Mr. Bob Seila for all their assistance and support. Additional thanks to Mr. George Murray and Mr. Mark Yirka of the North Carolina Department of Environment and Natural Resources for their help with calibrating, servicing and technical expertise with the analytical equipment. I am also grateful to the United States Air Force, because this would not have been possible without their sponsorship.

This research has been partially funded through the National Science Foundation via Duke University (Contract No. 99-SC-NSF-1019 – Nitrogen Oxide Flux From Sludge

Amended Soil). Partial funding for this research was also received from the North Carolina Department of Environment, Health and Natural Resources (Contract No. EA01001 – Technical Air Quality Services Contract).

Mention of trade names or commercial products does not constitute endorsement or recommendation for use.

TABLE OF CONTENTS

LIST OF TABLES

LIST OF FIGURES

Chapter III.

Chapter IV.

ABSTRACT

ROELLE, PAUL ANDREW. Oxidized and Reduced Biogenic Nitrogen Compound Emissions into the Rural Troposphere: Characterization and Modeling. (Under the direction of Viney Pal Aneja.)

Nitrogen compound emissions are known to have profound effects on air quality. Consequences associated with increased emissions of oxidized and reduced nitrogen species are known to be increased tropospheric ozone production, fine particulate aerosol production, nitrate contamination of drinking water, eutrophication and acidification of soil and water bodies. It is well recognized that soil emissions can contribute a substantial percent of the total inventory for both the oxidized and reduced species, but great uncertainty still exists in this inventory. Using a dynamic flow-through chamber technique in conjunction with a state-of-the-art mobile laboratory, this research attempts to characterize and model these oxidized and reduced biogenic nitrogen compound emissions into the rural troposphere.

North Carolina has relatively recently witnessed the increased use of both municipal waste biosolids and the land application of swine waste effluent; two processes which both contribute nitrogen to the ecosystem. The first of these processes involves the land application of municipal waste biosolids as a cost effective way to dispose of these nutrient rich byproducts of the wastewater treatment process. During the last three decades extensive research has been conducted on nitric oxide emissions from agricultural soils and consequently an extensive database has been developed which is used to relate these emissions to various environmental parameters. Biosolid amended soils, however remain a land-use type which are comparatively much less studied.

Therefore, models used to estimate nitric oxide inventories often treat the biosolid amended soils the same as agricultural soils amended with commercially derived fertilizers.

A controlled experiment involving the application of municipal waste biosolids to agricultural soils was shown to enhance NO emissions. A more detailed analysis throughout several seasons found the nitric oxide emissions from biosolid amended soils to have a strong temperature dependence and that their source strength is much larger relative to soils amended with chemically derived fertilizers. Modeling of this source strength using the MultiScale Air Quality Simulation Platform (MAQSIP) indicated that when the biosolids are assumed to be spread evenly throughout the counties, no changes in the model output are evident during daylight hours, however it is possible to discern slight decreases of ozone during the evening. When the same biosolids are concentrated in one area of the county, as opposed to being evenly distributed, the changes are more pronounced with decreases in ozone concentration reaching as high as approximately 12% and slight increases appearing (approximately 2%) during the afternoon hours.

The second process which is contributing nitrogen to the ecosystem is the land application of swine effluent to agricultural soils. This ammonia-rich effluent has gained wide spread attention in North Carolina, due to the explosive growth of the swine industry during the past decade. This study revealed that while the average source strength of ammonia from soils is significantly smaller than that of the lagoons, the much larger surface area of the soils causes them to also be an important emissions source. Additionally, it was observed that for time periods immediately following slurry

application, the NH_3 flux increased significantly and remained elevated for at least four days after application. Temperature explained over 70% of the variability in NH_3 emissions prior to being amended with the lagoon effluent and approximately 40% of the NH_3 emissions for time periods after being amended with the lagoon effluent. A fundamental mechanistic mass transfer model is presented and discussed in terms of its applicability for estimating NH_3 flux and was found to be an effective predictor of the NH_3 emissions for time periods immediately following slurry application.

CHAPTER I. INTRODUCTION

Nitrogen is perhaps the most important nutrient governing the growth and reproduction of living organisms. Nitrogen compound emissions also have a profound effect on air quality. Two major needs that drive the contemporary perturbations of the nitrogen cycle are the seemingly insatiable human appetite for energy, leading to the emission of nitrogen oxides into the atmosphere, and the need for food to sustain growing numbers of people all over the world, leading to the agricultural emission of ammonia. Once released into the atmosphere by either man-made (anthropogenic) or natural sources, these nitrogen compounds can undergo several different processes such as transformation due to atmospheric reactions (e.g. gas-to-particle conversion), transport associated with wind, and finally wet and dry deposition (Figure 1.1). All of these processes can perturb the environment with a host of beneficial and detrimental effects, such as increased crop yields from nitrogen loading or decreased visibility from increased aerosol production.

Scientists have focused recently on the oxidized species of nitrogen (NO_x=NO+NO_2) and their role as precursors to ozone (O_3) formation, and the reduced species (NH_x=ammonia+ammonium+amines) and their role in nitrogen enrichment and eutrophication of aquatic ecosystems. Nitrous oxide (N_2O), while contributing to ozone destruction in the stratosphere and to climate change as a greenhouse gas, is relatively inert in the troposphere and therefore has negligible consequences in tropospheric photochemistry (Warneck, 2000). The concentrations of these trace species in the

atmosphere are small (0.01 – 400 ppbV), however they have been shown to have significant impacts on chemical and physical processes in the atmosphere (Conrad, 2001).

Although nitrogen is a critical nutrient for the survival of micro-organisms, plants, humans and animals, it can cause detrimental effects when concentrations reach excessive levels (Paerl, 1997; Erisman et al., 1998). Figure 1.2 (Gunderson et al., 1992) illustrates this point by showing how an ecosystem responds to increased N loadings. The horizontal line is a crop which receives no atmospheric N deposition, and as indicated by the vertical axis, has a stable index of productivity. However, as N is initially added to the system, the index of productivity steadily increases to the point of diminishing returns, where any additional N loading actually reduces productivity (Schlesinger, 1997). In addition to the productivity concerns of aquatic and terrestrial ecosystems, oxidized and reduced N compounds each play a specialized role in degrading human health and its welfare. Some of the consequences associated with elevated concentrations and depositions of both oxidized and reduced N species are:

1. Respiratory disease caused by exposures to high concentrations of:
    - Tropospheric ozone
    - Other photochemical oxidants
    - Fine particulate aerosol (e.g. PM 2.5)
    - Direct toxicity of NO_2 (on rare occasions)
2. Nitrate contamination of drinking water

3. Eutrophication, harmful algal blooms and decreased surface water quality
4. Climatic changes associated with increases in nitrous oxide (greenhouse gas)
5. Nitrogen saturation of forest soils

(Erisman et al., 1998).

Nitric Oxide

Nitric Oxide (NO), which is estimated to have a global source strength of approximately 44 Tg yr^{-1} (Table 1.1), plays an important role in tropospheric photochemistry. Increasing NO emissions, in the presence of hydrocarbons and sunlight, are thought to be the cause of increased regional levels of tropospheric ozone and other photochemical oxidants (Logan, 1983; Penkett, 1988). Ozone photochemistry in the troposphere is regulated by oxides of nitrogen ($NO_X = NO + NO_2$). Currently, the only known pathway for the production of ozone is the photolysis of NO_2 ($NO_2 \rightarrow NO + O(^3P)$), which further reacts with O_2 to produce ozone (O_3) by the reaction $O(^3P) + O_2 \rightarrow O_3$. In a pseudo-photostationary environment, the O_3 produced would react with the NO that was generated via the photolysis of NO_2 in the following reaction: $NO + O_3 \rightarrow NO_2 + O_2$. Hence, there is no net production of O_3. However, in the real atmosphere, hydroxyl radicals combine with volatile organic compounds (VOC's) to produce new radicals which preferentially react with NO, allowing a net O_3 accumulation. The auto catalytic role of NO in the cycle for ozone formation can be seen in Figure 1.3.

Yienger and Levy (1995) developed an empirically based model to estimate soil NO_X emissions on a global scale. They have reported that anthropogenic land use is having a significant impact on global soil NO_X emissions and that soil emissions can account for up to 75% of the total NO_X budget depending on location and time of year. In the Southeast U.S., which is NO_X limited, an increase in NO_X emissions is believed to produce a corresponding increase in O_3 levels (Southern Oxidant Study, 1993). O_3 negatively affects human health, as well as ecological systems, such as crop yield. Studies show that prolonged exposure to high ozone levels causes persistent functional changes in the gas exchange region of the lungs. Additionally, ozone plays a critical role in controlling the chemical lifetimes and the reaction products of many atmospheric species (National Research Council, 1991). Gaseous nitric acid (HNO_3), the end product of NO reactions in the atmosphere, combines with either aerosols or water in the atmosphere, and is removed via rain, snow, or other deposition processes, as acidic deposition.

Ammonia

Ammonia (NH_3) emissions are estimated to have a global source strength of approximately 75 Tg yr^{-1} (Table 1.2). These emissions have garnered increased interest in the past few years, due in part to the detrimental effects of excess nitrogen deposition to nutrient sensitive ecosystems (Aneja et al., 1998a; Nihlgard, 1985; van Breemen, 1982). Moreover, NH_3 is the most prevalent gaseous base found in the atmosphere, and is therefore fundamental in determining the overall acidity of precipitation (Warneck,

2000), cloudwater (Li and Aneja, 1992), and atmospheric aerosols (Lefer et al., 1999). The ecological impact of atmospheric NH_3 deposition may be substantial as reduced nitrogen species are thought to be the most biologically available of nitrogen species in N-limited coastal and estuarine ecosystems (Paerl, 1997). In the atmosphere, NH_3 reacts primarily with acidic species to form ammonium sulfate, ammonium nitrate or ammonium chloride, or it may be deposited to the earth's surface by either dry or wet deposition processes.

The spatial scale of a particular NH_3 source's contribution to atmospheric nitrogen deposition is governed in part by the gas to particle conversion rate of NH_3 to NH_4^+. Because of the short lifetime of NH_3 in the atmosphere (τ = 1-5 days or less) (Warneck, 2000), low source height, and relatively high dry deposition velocity (Asman and van Jaarsveld, 1992), a substantial fraction (20-40%) will likely deposit near its source. However, ammonium (NH_4^+) aerosols, with atmospheric lifetimes on the order of τ = 1-15 days (Aneja et al., 1998b) will tend to deposit at larger distances downwind of sources. Ammonia emissions from animal operations contribute substantially to atmospheric nitrogen loading and may contribute the same order of magnitude as emissions of NO in some parts of the world (Steingröver and Boxman, 1996).

Trends

Over the course of the past century fossil fuel combustion has increased to meet growing energy demands. The global amount of fossil fuel use per person (Figure 1.4) has increased by more than a factor of 6 over the last 75 years. At the same time,

scientists have synthesized nitrogen-based fertilizers to enhance crop development and to maximize production on limited land space. Before the mass production of fertilizers, it can be assumed that there was an approximate balance between the relatively unreactive molecular nitrogen (N_2-comprises approximately 79% of air) in the atmosphere, which was naturally converted to forms used by plants and animals, and the amount of nitrogen returned to the atmosphere via natural processes (Delwiche, 1970). Currently, however, the global production of fertilizer is approximately 100 million metric tons of nitrogen per year, compared to approximately one million metric tons only 40 years ago (The Fertilizer Institute, 2000).

Coal combustion was once believed to be the dominant source of ammonia in the atmosphere (Warneck, 2000). Healey et al., (1970) showed that the NH_3 contribution from coal was small compared to NH_3 emitted from animal waste where the mechanism responsible for the NH_3 release is the bacterial decomposition of urea to NH_3 and CO_2 (Warneck, 2000). The growth of the intensively managed animal operations in some areas of the country has resulted in areas with elevated ambient NH_3 concentrations (Nelson, 2000). In the US, for example, the swine population accounts for approximately 10% of the NH_3-N budget (Figure 1.6a). In NC, however, which has experienced an explosive growth in the swine population (Figure 1.5) and is currently the second largest swine producing state in the nation, the swine population is estimated to account for approximately 46% of the NH_3-N emissions (Figure 1.6b). The combined effects of increased fertilizer use, intensively managed animal operations and increased power

production have reached a point where the scientific community has major concerns about the fate of the nitrogen produced.

Nitrogen Cycle

Although the atmosphere is made up of approximately 79% N, plants and animals can only benefit from that portion which is first fixed, meaning the nitrogen is converted into a form which plants or animals can utilize (Delwiche, 1970). Referring to Figure 1.7, the nitrogen present in the atmosphere can be traced through the various pathways in the atmosphere-soil system. Under aerobic conditions, certain bacteria present in the soil can satisfy their energy needs through the oxidation of ammonia to nitrate, or nitrification. During anaerobic conditions, the nitrogen fixation process is reversed and N_2 is returned to the atmosphere. As shown in Figure 1.7, NH_4^+ first appears in the soil through a process called mineralization, and then depending on soil conditions can be released as NH_3 gas to the atmosphere. NO can be released to the atmosphere through both nitrification and denitrification, each of which will be discussed in turn (Warneck, 2000).

Nitrification is defined as an aerobic process in which chemoautotrophic nitrifying bacteria satisfy their energy needs via the oxidation of ammonium (NH_4^+) to nitrite with the end product being nitrate (NO_3^-) (Davidson, 1991). Among this chemoautotrophic group of bacteria are the nitrosomonas which oxidize NH_4^+ to NO_2^- and nitrobacter which oxidize NO_2^- to NO_3^- (Delwiche, 1970). While not apparent in Figure 1.7, several researchers have used laboratory experiments to show that chemoautotrophic nitrifiers

can produce NO in the soil (Firestone and Davidson, 1989). These studies have consisted of acetylene or nitrapyrin being used to inhibit NH_4^+ oxidation and chlorate to inhibit NO_2^- oxidation which have shown that NO is produced as a result of the organisms responsible for the oxidation of NH_4^+ to NO_2^- (Davidson, 1992; Tortoso and Hutchinson, 1990; Holbrook, 1994).

Referring to Figure 1.7, dentrification is defined as the reduction of NO_3^- to NO_2^- and further to N_2. This process, which occurs when the soil is almost, but not completely anaerobic, serves as the N_2 regeneration portion of the N cycle (Warneck, 2000). Unlike the relatively fewer types of bacteria responsible for nitrification, there are several different types of bacteria which carry out the dentrification process. These denitrifiers, pseudomonas denitrificanas for example, are aerobic species which have the ability to use the oxides of nitrogen as an O_2 source (Delwiche, 1970). Anaerobic conditions in the soil are typically found to be the result of increased soil moisture, or waterlogging of the soil pores (Warneck, 2000). The water-logging of the soil pores acts to restrict the diffusion of gases through the soil and to increase the time for NO to diffuse to the soil surface. The slowed transfer results in further reduction and hence less NO is emitted from the soil. The effect of decreased NO emissions as % WFPS reaches a critical value can be seen in Figure 1.8 which depicts Davidson's (1991) model of N production versus different values of % WFPS. Although Figure 1.7 does show NO produced via denitrification, it is not commonly found to be a large contribution to the total flux in field studies. Most studies, in fact, find the chemoautotrophic nitrifying bacteria to be the

predominant source of the NO emitted from the soils (Anderson and Levine, 1986; Tortoso and Hutchinson, 1990; Hutchinson et al., 1993).

Methods and Materials

Dynamic Flow-Through Chamber

A dynamic flow-through chamber lined with five-mil thick fluorinated ethylene propylene (FEP) Teflon was used to measure NO and/or NH_3 concentrations emitted from the soil. The translucent chamber, 26.5 cm in diameter, and 47.2 cm high (volume=26.0 liters), fits inside a stainless steel metal ring, which is driven into the ground to a depth of ~10 cm (Figure 1.9). Zero grade air, which is used as a carrier gas, is passed through the chamber at a constant flow rate (approximately 5 lpm), via a flow controller located on top of the chamber (Gilmont Shielded Industrial Flowmeter, Accuracy ± 5%). The air inside the chamber is mixed by a variable-speed, motor driven Teflon impeller. The sample exiting the chamber travels through Teflon tubing (1/4" outside diameter, 5/32" inside diameter) to the detection instruments. The entire measuring system, from the inlet port on the chamber to the point where the stream is analyzed in the instrument, is coated by Teflon, stainless steel or gold to minimize further chemical reactions with the sample stream. The sample lines do not exceed 10 meters. The NO detection instruments draw approximately 1.5 lpm, which resulted in a sample residence time in the sample lines of approximately 5 seconds.

Chamber Effects

The techniques currently employed to measure fluxes of trace gases from soil and water surfaces can be divided into micrometeorological and chamber techniques. The micrometeorological techniques consist of the gradient and eddy correlation methods while the chamber techniques can be divided in to the static and dynamic methods. Each system has its benefits and drawbacks. However as part of National Science Foundation (ATM-9420610) "NO_X Emissions from Agricultural Soils: Intercomparison of Micrometeorological and Dynamic Chamber Techniques" project, these differences were analyzed and determined not to be statistically significant (Li et al., 1999; Roelle et al., 1999). Nevertheless a major concern with the chamber method is that it is intrusive and could possibly alter the microclimate and therefore is not representative of the real conditions. To as great an extent as possible, this concern has been examined.

Two of the principle concerns with the chamber design are increased temperature ("greenhouse effect") and increased humidity in the chamber and sample lines. Experiments were conducted by previous researchers and as part of this study. Sullivan (1996) reported that the average temperature difference of the soil inside and outside the chamber was 0.23±1.0°C and that air temperature difference inside and outside the chamber was 3.77 ± 2.52 °C. The average of five experiments at various research sites were conducted to verify previous results and found that the average temperature difference between the soil inside and the soil outside the chamber was 0.03 ± 0.65 °C (Figure 1.10). The days selected for these experiments were during the summer to

determine the temperature difference at maximum heating and all days were either clear or partly cloudy with daytime highs of 32 °C ± 3 °C.

Excess humidity in the chamber and sample lines is a problem when using ambient air as the carrier gas. This problem was addressed by periodically blowing out any condensation in the lines and chamber with zero grade air, and/or creating a water trap to help collect any moisture prior to the carrier gas entering the chamber. During all measurement campaigns presented here, the carrier gas used was zero grade air, which virtually eliminated the issue of moisture in the chamber and sample lines. Occasionally, if the soil is sufficiently moist, there was still moisture that developed every few hours in the sample lines even with the zero grade air. To analyze the effect of moisture, the analyzer was spanned with known concentrations of NO and NH_3 with a short (<2 m) section of Teflon tubing and then this piece of tubing was replaced with a 10 m length of tubing containing visible moisture droplets. There was no detectable loss of either NO or NH_3 after 40 minutes of sampling. In another study, the chamber lining was wetted so that there were visible droplets on the chamber walls and a petri dish filled with water was placed on the bottom of a sealed chamber. A known concentration of NH_3 was delivered to the chamber and losses in the chamber ranged from 6-7%.

Experiments were conducted to determine if the mixing speed of the Teflon impeller altered soil NO flux measurements. Varying the speed between 20 and 100 revolutions per minute (rpm) did not produce any significant changes in the calculated NO flux. The impeller was set to 50 rpm for the remainder of the experiment. Outlets in

the chamber ensured that there were no substantial pressure differences between the outside atmosphere and the air within the chamber. Research conducted on similar chambers using a tilting water manometer indicate that pressure differences were below detection limits (0.2 mm H_2O) (Johansson and Granat, 1984).

The dynamic chamber system, with the continuous stirring provided by the impeller, meets the necessary criteria for performance as a Continuously Stirred Tank Reactor (CSTR). For performance as a CSTR, the chamber needs to be "ideally" mixed (Aneja, 1976). In ideal mixing, the composition of any elemental volume within the chamber is assumed to be the same as that of any other volume within the chamber. Trace experiments (Residence Time Distribution) were used to test the flow and mixing characteristics of the system. The results of these mixing studies indicated that the dynamic chamber behaved as a "perfect" mixer with negligible stagnancy or channeling (Aneja et al., 2000). NH_3 fluxes were calculated using a mass balance approach as described in Roelle et al. (1999) and Aneja et al. (2000).

Utilizing the power law profile, which is frequently used in air pollution applications (Arya, 1999), we are able to estimate the wind velocities at a height of 0.1 m (the approximate height of the impeller above the soil air interface), when the 10 m wind heights are known. The power law profile is given by:

$$\frac{V}{V_r} = \left(\frac{Z}{Z_r}\right)^m \qquad (1)$$

where V_r is the wind velocity at a reference height Z_r and m is taken to be 0.1 for this smooth surface (Arya, 1988). Mean wind velocities were between 1 and 4 m s^{-1} (at a height of 10 m) throughout this measurement period. Using the power law profile (Equation 1), and the measured 10 m wind velocities, equates to wind speeds between 0.6 and 2.4 m s^{-1} at a height if 10 cm (approximate height of impeller). This calculated 10 cm wind speed approximates the wind speeds measured inside of the chamber (~ 1 to 2.5 m s^{-1}) using a hot wire anemometer. However, it should be noted that equality of the horizontal winds does not ensure equality of the emissions between the inside and outside of the chamber.

While the different flux methodologies have been intercompared and found to produce reasonable agreement in emission estimates, some comparison of the factors effecting diffusivity should be examined. For example, in the neutral surface layer the mixing length and eddy viscosity can be shown to vary linearly with height and depend on the friction velocity as described in Arya, 1999. Evaluation of this parameter was outside the scope of this research, however future work to verify equality between conditions inside and outside the chamber should attempt to specify eddy length scales and viscosity.

Sampling Scheme

The daily sampling scheme consisted of measuring concentrations of NO and/or NH_3 after the sample exited the dynamic flow-through chamber. A daily experiment consisted of placing the chamber on the stainless steel collar, which had been inserted

into the soil the previous evening. Typically, all experiments were conducted a minimum of 50 meters from any field edges to avoid any boundary effects. The chamber was placed on the collar at approximately 8:00 AM and flushed with zero grade air for at least one hour before data collection began at 9:00 AM. This technique ensured that the concentrations within the chamber reached steady state prior to any data acquisition and allowed for the instruments to undergo their daily calibrations. Daily experiments ended at approximately 5:00 PM and the stainless steel collar was relocated to a random location within a 10m radius of the mobile laboratory, in preparation for the next days experiment. This procedure allowed a minimum of 16 hours for any effect on soil NO flux, due to soil disturbances caused by the insertion of the stainless steel collar, to dissipate. Depending on research objectives, 24 hour diurnal experiments were, on occasion, also conducted.

Nitric Oxide and Ammonia Analyzers

Nitric Oxide (NO) concentrations were measured using a Thermo Environmental Instruments Incorporated (TECO) Model 42S chemiluminescence, low level NO analyzer (Thermo Environmental Instruments, Inc., 1992). The principle behind the operation of the NO instrument is the gas phase reaction between ozone (O_3) and NO, given by:

$$NO + O_3 \rightarrow NO_2 + O_2 + h\nu \qquad (2)$$

Light emissions from the decay of NO_2 to lower energy states is proportional to the concentration of nitric oxide. This decay is detected in a photomultiplier tube and converted to a concentration measurement after calibration with known standards.

The TECO model 42S, in its standard configuration, does not measure NH_3. Therefore, the instrument had to be modified so that we could also calculate the ammonia emissions from agricultural soils. The modified instrument is still based on the gas phase reaction between O_3 and NO, and the detection of the decay of the excited NO_2 molecule as previously described (a schematic of the modified 42S is given in Figure 1.11). In flow path 1, the sample stream is mixed with high concentrations of O_3 to produce an NO reading. In flow path 2, the sample stream bypasses the stainless steel converter, and passes through the molybdenum converter (325 °C) which effectively converts the oxides of N to NO, while allowing the NH_3 to pass through, producing an NO_Y reading. In flow path 3, the sample passes through the stainless steel converter (775 °C), effectively converting the oxides of N and NH_3 to N, producing a value referred to as N_T. The instrument is designed to alternate between flow paths, and by subtracting the NO_Y signal from N_T, the concentration of NH_3 in the sample stream can be determined.

Calibrations of the instruments were conducted following protocols using a TECO 146 dilution/titration instrument in conjunction with a cylinder of 3.82 ppmV NO in N_2 (National/Specialty gases) and zero grade air (National Welders). The TECO 146 was serviced and calibrated to specifications by the manufacturer prior to the Summer 1999 measurement campaign. A multipoint calibration was conducted prior to, and at the midpoint of, the measurement period. Each day, zero and span checks were conducted according to the operator manuals.

Meteorological data were collected via a Campbell Scientific meteorological package. Air Temperature and % Relative Humidity (%RH) are measured inside of a radiation shield at a height of 1.5 m. The accuracy of both the RH and temperature probe is (±) 3%. A LI-Cor 200SZ pyranometer is used for measuring sun plus sky radiation (accuracy ± 3%).

Data Acquisition System and Mobile Laboratory

All of the gas detection and data acquisition instrumentation is housed in a temperature controlled mobile laboratory. The mobile system consists of a modified Ford Aerostar van with a 13,500 BTU air conditioning unit. The temperature inside the van is maintained within the operating range of the instruments. The data acquisition system is a Campbell Scientific 21X Micrologger used in conjunction with a Toshiba laptop computer. Power for the air conditioning and all of the detection instruments was standard 110 volt AC commercial power.

Flux Calculation

The NO fluxes were calculated from a mass balance equation (Kaplan et al., 1988; Kim et al., 1994). The mass balance equation is:

Accumulation = Flow in - Flow out - Reactions

$$\frac{dC}{dt} = \left(\frac{q[C_{air}]}{V} + \frac{JA}{V}\right) - \left(\frac{LA'}{V} + \frac{q}{V}\right)[C] - R \qquad (3)$$

where

J = emission flux per unit area

L = loss term by chamber wall per unit area assumed first order in [NO]

q = flow rate through the chamber

V = volume of the chamber

C = NO concentration in the chamber

C_{air} = NO concentration in the ambient air immediately adjacent to the chamber (the inlet of the chamber)

R = chemical production/destruction rate in the chamber

A = surface area covered by the chamber

A' = surface area of the chamber walls

Assuming the chamber is well mixed, the concentration [C] measured can be assumed to be the same everywhere within the chamber. Using zero grade air as the carrier gas, the initial concentration or $[C_{air}]$ is 0. Additionally, at steady state conditions, the change of concentration, with respect to time, will be zero. Equation (3) reduces to:

$$\frac{JA}{V} = (\frac{L'A'}{V} + \frac{q}{V})[C] \tag{4}$$

where $[C]$ is the concentration measured at the outlet of the chamber.

In equation (4), the new loss term (L') is the sum of the loss of NO through reactions with the chamber walls and chemical reactions of NO with existing oxidants in the carrier gas (R), such as ozone and peroxy radicals (Kim et al., 1994; Aneja et al., 1995). The total loss term (L') was determined empirically (five experiments were conducted throughout the day and night) utilizing a method developed by Kaplan et al. (1988). Kaplan's technique uses the modified form of equation (3):

$$\frac{dC}{dt} = \frac{JA}{V} - \left(\frac{L'A'}{V} + \frac{q}{V}\right)[C] \tag{5}$$

and introduces an equilibrium value for NO, given by C_{eq}. Utilizing the equilibrium value, and plugging in for $\frac{JA}{V}$ yields:

$$\frac{dC}{dt} = (C_{eq} - C)\left(\frac{L'A'}{V} + \frac{q}{V}\right) \tag{6}$$

The solution to (6) is given by:

$$-\ln\frac{C_{eq} - C}{C_{eq} - C_o} = \left(\frac{L'A'}{V} + \frac{q}{V}\right)t \tag{7}$$

C_o is the NO concentration in the chamber when NO reaches the first equilibrium state at an initial flow rate and C_{eq} is the NO concentration in the chamber after the flow rate is reduced and allowed to reach a second equilibrium. From the linear relationship

between the value of $-\ln\frac{C_{eq}-C}{C_{eq}-C_o}$ and time during the experiment, the slope is found to represent $\left(\frac{L'A'}{V}+\frac{q}{V}\right)$. The graphs of $-\ln\frac{C_{eq}-C}{C_{eq}-C_o}$ plotted versus time for the 5 different Kaplan experiments is shown in Figure 1.12. The total loss in the chamber was estimated to be 0.02 ± 0.007 cm second^{-1} from the average of 5 experiments conducted at different times throughout the measurement period. This value of (L') (=.02 cm second^{-1}) agrees with that found by Kim et al. (1994), and is directly used in equation (4) to calculate the NO flux during this measurement period.

Soil Analysis

Soil temperature was recorded every minute, and these values were binned and averaged every 15 minutes using a Campbell Scientific soil temperature probe (accuracy ± 3%) inserted 5 cm into the soil, adjacent to the chamber. A soil sample was taken from the center of the dynamic flow-through chamber footprint at the end of each measurement period (approximately 1 sample per day) and analyzed for soil pH, and percent Water Filled Pore Space (%WFPS) by the Duke University Department of Civil and Environmental Engineering and/or the North Carolina State University Department of Biological and Agricultural Engineering. Samples were taken with a bucket auger which removed a soil core to a depth of approximately 20 cm.

Soil bulk density, which is the weight of the soil solids per unit volume of total soil, and soil particle density, are used to determine the %WFPS of the soil (Troeh and Thompson, 1993). The core method (345 cm^3) was used to determine the soil bulk

density for the research site (Blake and Harge, 1986). The standard particle density is 2.65 g/cm^3 for most soils, however particle densities will differ from this value if the soils have high organic matter content or are high in heavy minerals such as hydrous oxides of iron. The expression, % WFPS, is a measure of soil water content and can be expressed as the percentage of pore spaces in the soil filled with water. The %WFPS is a convenient expression to describe soil moisture because it accounts for the differing bulk and particle densities of soils and therefore allows for the comparison of soil moisture from different soil types.

The total extractable nitrogen was calculated by summing the extractable fractions of ammonium (NH_4^+) and nitrate (NO_3^-) determined from the soil samples. Extractable NH_4^+ and NO_3^- were determined using a 1 M KCL soil extract (expressed on a weight basis) (Keeney and Nelson, 1982) and standard autoanalyzer techniques (Lachat Instruments, 1990). The Total Kjeldahl Nitrogen (TKN) was determined using a digestion procedure, which converts all the N in the sample to NH_4^+ whose concentration is then determined using colorimetry. The total soil water content was calculated as:

[initial weight - oven dry weight (105 °C)] / oven dry weight (105 °C) (8)

Objectives

The objectives of this study can be stated as follows:

1. Design a field study to measure nitric oxide emissions from biosolid amended soils.
2. Evaluate nitric oxide emissions from soils amended with biosolids and develop an algorithm for predicting its source strength in North Carolina.
3. Include biosolid amended soils as a new land-use class in biogenic NO emission inventories. Compare and contrast inventories with and without this new land-use class.
4. Use an air quality model to analyze effects of including this new land-use class.
5. Design a field study to measure ammonia emissions from agricultural soils, before and after they have been sprayed with swine waste effluent.
6. Develop an observationally based model relating ammonia emissions to soil parameters as well as present a fundamental mechanistic mass transport model. Assess both models with field data.

References

Anderson I. C. and J.S. Levine, Relative rates of nitric oxide and nitrous oxide production by nitrifiers, denitrifiers, and nitrate respirers, Applied and environmental microbiology, 51, 938-945, 1986.

Aneja, V.P., Dynamic studies of ammonia uptake by selected plant species under flow reactor conditions, PhD thesis, p. 216, NC State University, Raleigh, NC, 1976.

Aneja V.P., W.P. Robarge and B.D. Holbrook, Measurements of nitric oxide flux from an upper coastal plain, North Carolina agricultural soil. Atmospheric Environment, 21, 3037-3042, 1995.

Aneja, V.P., G. Murray and J. Southerland, Atmospheric Nitrogen Compounds: Emissions, Transport, Transformation, Deposition and Assessment; EM, 22-25, April 1998a.

Aneja, V.P. and G. Murray, An overview of Program GNATS (GEOPONIC Nutrient and Trace Gas Study), Proceedings of the First International Nitrogen Conference, Noordwijkerhout, The Netherlands, 23-27, March, 1998b.

Aneja, V.P., J.P. Chauhan and J.T. Walker, Charaterization of atmospheric ammonia emissions from swine waste storage and treatment lagoons, Journal of Geophysical Research, 105, 11,535-11,545, 2000.

Aneja, V.P., P.A. Roelle, G.C. Murray, J. Southerland, J.W. Erisman, D. Fowler, W. Asman and N. Patni, Atmospheric nitrogen compounds II: emissions, transport, transformation, deposition and assessment, Atmospheric Environment, 35, 1903-1911, 2001.

Arya, S.P., Introduction to Micrometeorology, Academic Press, Inc., New York, NY, pp. 141-143, 1988.

Arya, S.P., Air Pollution Meteorology and Dispersion, Oxford University Press, New York, NY, p. 90-91, 98-100, 1999.

Asman, W.A.H. and J.A. van Jaarsveld, A variable-resolution transport model applied for NH_x in Europe, Atmospheric Environment, 26A, 445-464, 1992.

Battye, R., W. Battye, C. Overcash, S. Fudge and W.G. Benjey, Development and selection of ammonia emission factors, Final Report, prepared for: U.S. Environmental Protection Agency Office of Research and Development, Washington, DC, 1994.

Blake, G.R. and K.H. Hartge, Particle Density. In Methods of Soil Analysis, Part 1 (edited by Klute A.), ASA Monograph No. 9, American Society of Agronomy, Madison, WI, Chap 14, 1986.

Bouwman, A.F., D.S. Lee, W.A.H. Asman, F.J. Dentener, K.W. van der Hoek and J.G.J. Olivier, A global high-resolution emission inventory for ammonia, Global Biogeochemical Cycles, 11, 561-587, 1997.

Conrad, R., Evaluation of data on the turnover of NO and N_2O by oxidative versus reductive microbial processes in different soils, Phyton, in press, 2001.

Davidson, E.A., Fluxes of nitrous oxide and nitric oxide from terrestrial ecosystems, Microbial Production and Consumption of Greenhouse Gases: Methane, Nitrogen Oxides, and Halomethanes, (edited by Rogers, J.E., and Whitman, W.B.), pp. 219-235. American Society for Microbiology, Washington, D.C 20005, 1991.

Davidson, E.A., Sources of nitric oxide and nitrous oxide following wetting of dry soil, Soil Science Society of America Journal, 56, 95-102, 1992.

Delwiche, C.C., The nitrogen cycle, Scientific American, 223, 137-146, 1970.

Erisman, J.W., T. Brydges, K. Bull, E. Cowling, P. Grennfelt, L. Nordberg, K. Satake, T. Schneider, S. Smeulders, K. W. Van der Hoek, J.R. Wisniewski and J. Wisniewski, Summary statement, Proceedings of the First International Nitrogen Conference, Noordwijkerhout, The Netherlands, 23-27 March, 1998.

Fehsenfeld, F., J. Meagher and E. Cowling (Eds.), Southern Oxidants Study Annual Report, pp. 47-61, 1993.

Firestone, M.K. and E.A. Davidson, Microbiological basis of NO and N_2O production and consumption. Exchange of Trace Gases Between Terrestrial Ecosystems and the Atmosphere, (edited by M.O. Andreae and D.S. Schimmel), pp.7-21, John Wiley, New York, 1989.

Fourth Report of the Photochemical Oxidants Review Group, Ozone in the United Kingdom, ISBN 1-870393-30-9, 1997.

Gundersen, P., Mass balance approaches for establishing critical loads for nitrogen in terrestrial ecosystems. In: P. Grennfelt and E. Thörnelöf (eds.), Critical loads for nitrogen. Report No. Nord 1992: 41, Nordic Council of Ministers, Copenhagen, Denmark, 1992.

Healey, T.V., H.A.C. McKay, A. Pilbeam and D. Scargill, Ammonia and ammonium sulfate in the troposphere over the United Kingdom, Journal of Geophysical Research, 75, 2317-2321, 1970.

Holbrook, B.D., Characterization and graphical visualization of fluxes of oxides of nitrogen from agricultural soils in North Carolina, MS Thesis, NC State University, Dept MEAS, 1994.

Hutchinson, G.L., W.D. Guenzi and G.P. Livingston, Soil water controls on aerobic soil emission of gaseous nitrogen oxides, Soil Biology and Biochemistry, 25, 1-9, 1993.

Johansson, C. and L. Granat, Emission of nitric oxide from arable land. Tellus, 36B, 25-37, 1984.

Kaplan, W.A., S.C. Wofsy, M. Keller and J.M.D. Costa, Emission of NO and deposition of O_3 in a tropical forest system, Journal of Geophysical Research, 93, 1389-1395, 1988.

Kim, D.S., V.P. Aneja and W.P. Robarge, Characterization of nitrogen oxide fluxes from soil of a fallow field in the central piedmont of North Carolina, Atmospheric Environment, 28, 1129-1137, 1994.

Lachat Instruments Company, Methods Manual for the Quik Chem Automated Ion Anlayzer. Lachat Instruments, 6645 West Mill Road, Milwaukee, WI 53218, 1990.

Lee, D.S., I. Köhler, E. Grobler, F. Rohrer, R. Sausen, L. Gallardo-Klenner, J.G.J. Oliver, F.J. Dentener and A.F. Bouwman, Estimates of global NO_x emissions and their uncertainties, Atmospheric Environment, 31, 1735-1749, 1997.

Lefer, B.L., R.W. Talbot and J.W. Munger, Nitric acid and ammonia at a rural northeastern US site, Journal of Geophysical Research, 104, 1645-1661, 1999.

Li, Z. and V.P. Aneja, Regional analysis of cloud chemistry at high elevations in the eastern United States. Atmospheric Environment, 26A, 2001-2017, 1992.

Li,Y., V.P.Aneja, S.P. Arya, J.Rickman, J.Brittig, P.A. Roelle and D.S. Kim, Nitric oxide emission from intensively managed agricultural soil in North Carolina, Journal of Geophysical Research, 104, 26,115 – 26,123, 1999.

Linn, D.M. and J.W. Doran, Effect of water-filled pore space on carbon dioxide and nitrous oxide production in tilled and nontilled soils, Soil Science. Society of America Journal, 48, 1267-1272, 1984.

Logan, J.A., Nitrogen oxides in the troposphere; Global and regional budgets, Journal of Geophysical Research, 88, 10785-10807, 1983.

National Research Council, Rethinking the Ozone Problem in Urban and Regional Air Pollution, National Academy Press, pp. 1-39, 351-379, Washington, D.C., 1991

Nelson, D.R., Analysis of ammonia emissions from agriculture and ammonium concentrations in the southeast United States, MS Thesis, NC State University, Dept MEAS, 2000.

Nihlgard, B, The ammonium hypothesis-An additional explanation to the forest dieback in Europe, Ambio, 14, 2-8, 1985.

Penkett, S.A., Indications and causes of ozone increase in the troposphere, in The Changing Atmosphere, edited by F.S. Rowland and I.S.A. Isaksen, pp. 91-103, John Wiley, New York, 1988.

Roelle, P.A., V.P. Aneja, J. O'Connor, W. Robarge, D.S. Kim and J.S. Levine, Measurement of nitrogen oxide emissions from an agricultural soil with a dynamic chamber system, Journal of Geophysical Research, 104, 1609-1619, 1999.

Schlesinger, W.H., Biogeochemistry, An analysis of global change, Second Edition, Academic Press, New York, 1997.

Schlesinger, W.H. and A.E. Hartley, A global budget for atmospheric NH_3, Biogeochemistry, 15, 191-211, 1992.

Steingröver, E. and A.W. Boxman, Nutrients and growth of forest trees as affected by nitrogen deposition, In Atmospheric Ammonia: Emissions, Deposition and Environmental Impacts, Poster Proceedings, 109-111, Sponsored by the UK Department of Environment, Culham, Oxford, 1996.

Sullivan, L.J., T.C. Moore, V.P. Aneja and W.P. Robarge, Environmental variables controlling nitric oxide emissions from agricultural soils in the southeast United States, Atmospheric Environment, 30, 3573-3582, 1996.

The Fertilizer Institute, http://tfi.org/worconch.pdf

Thermo Environmental Instruments, Inc., Instruction Manual Model 42S: Chemiluminescence NO-NO_2-NO_X analyzer, Designated reference method number RFNA-1289-074, Franklin, Mass., 1992.

Tortoso, A.C. and G.L. Hutchinson, Contributions of autotrophic and heterotrophic nitrifiers to soil NO and N2O emissions, Applied and Environmental Microbiology, 56, 1799-1805, 1990.

Troeh, F.R. and L.M. Thompson, Soils and Soil Fertility. Oxford University Press, pp. 193-215, New York, 1993.

van Breemen, N., P.A. Burrough, E.J. Velthorst, H.F. van Dobben, T. de Wit, T.B. Ridder and H.F.R. Reijnders, Soil acidification from atmospheric ammonium sulphate in forest canopy throughfall, Nature, 299, 548-550, 1982.

Warneck, P., Chemistry of the natural atmosphere, second edition, Academic Press, Inc., New York, NY, pp. 511-530, 2000.

Yienger J.J. and H. Levy II, Empirical model of global soil-biogenic NO_X emissions, Journal of Geophysical Research, 100, 11,447-11,464, 1995.

Source	NO_x[†]
Fossil Fuel Combustion	22
Biomass Burning	7.9
Lightening Discharges	5.0
Release from Soils	7.0
NH_3 Oxidation	0.9
Statosphere	0.64
High-flying aircraft	0.85
Total Sources*	**44**

Sink	NO_x[‡]
Wet deposition, land	19
Wet deposition, oceans	8
Wet deposition, combined	27
Dry deposition	16
Total Sinks	**43**

(1 Tg = 10^{12} g).

Source:

† Lee et al., 1997

‡ Logan, 1983

Table 1.1. Global tropospheric NO_x budget. Source: modified from Warneck, 2000.

Source	NH_3[†]	Sink	NH_3[†]
Coal Combustion	2	Wet deposition	46
Automobiles	0.2	Dry deposition	10
Biomass Burning	5	Reaction with OH	1
Domestic animals	32		
Wild animals	–		
Human excrements	4		
Soil/plant emissions	10		
Fertilizer losses	9		
Oceans	13		
Total Sources*	**75**	**Total Sinks**	**57**

* It is accepted that the apparent difference between total NH_3 sources and sinks represents uncertainties in identified budget terms, not atmospheric accumulation.

[–] Indicates insignificant or unavailable terms.

(1 Tg = 10^{12} g).

Source:

† Schlesinger and Hartley, 1992

Table 1.2. Global tropospheric NH_3 budget. Source: modified from Warneck, 2000.

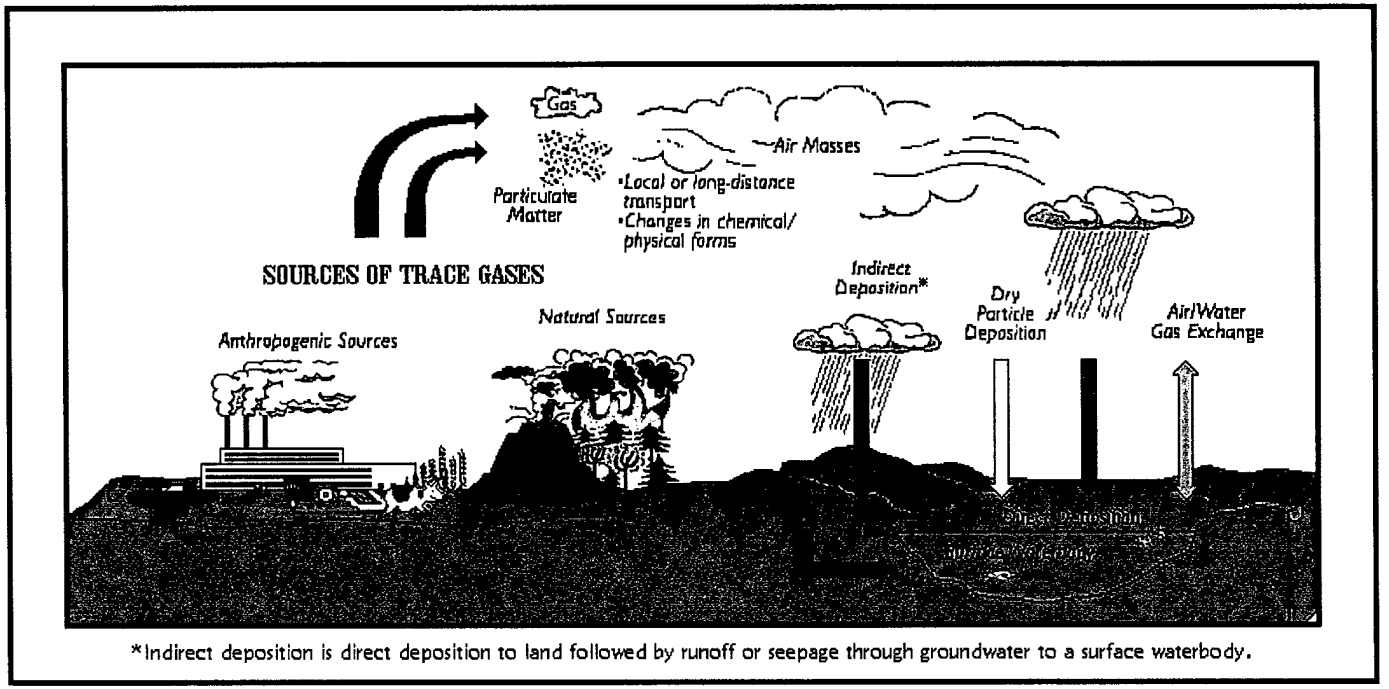

Figure 1.1. Atmospheric emissions, transport, transformation and deposition of trace gases.

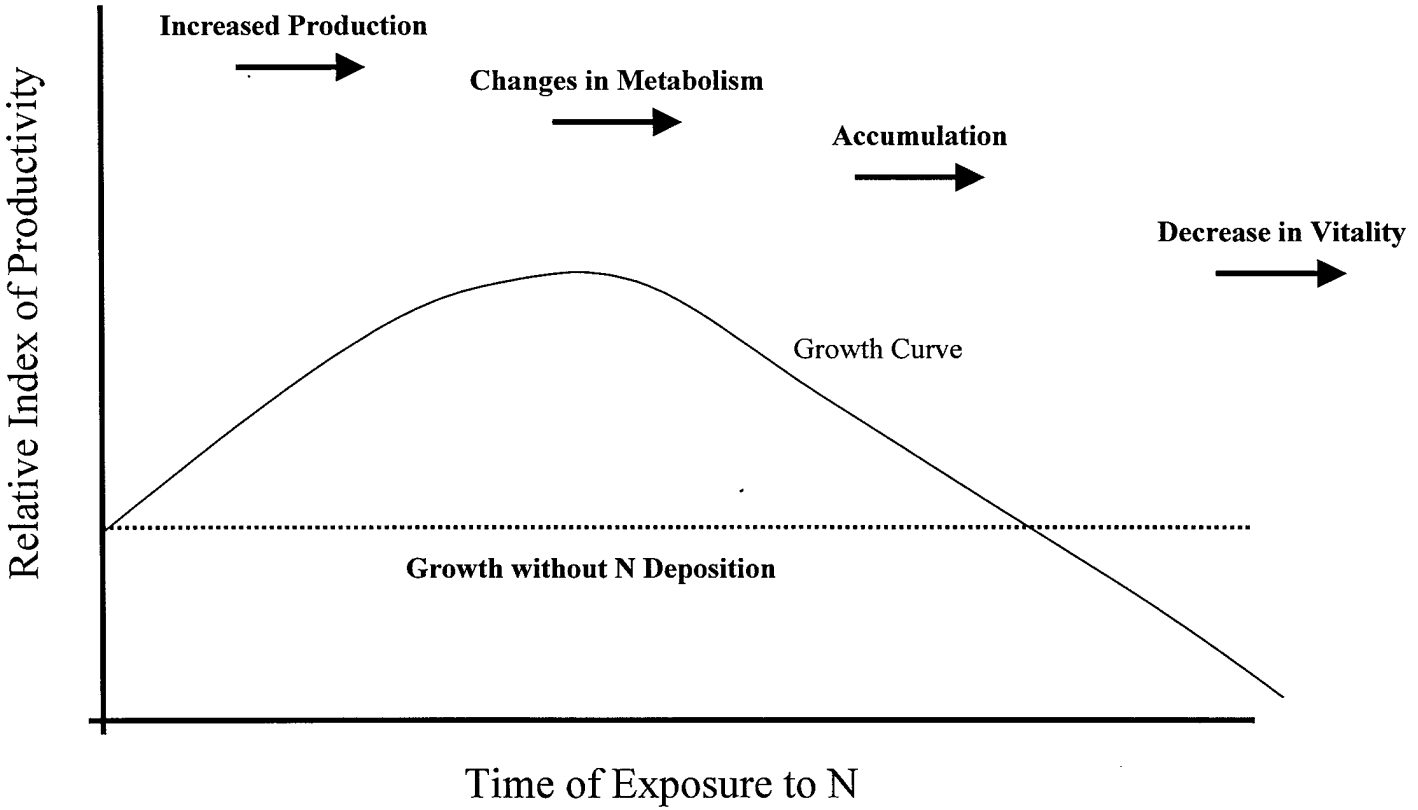

Figure 1.2. Hypothetical growth curve for an ecosystem, given different lengths of exposure to nitrogen. Source: Gundersen, 1992.

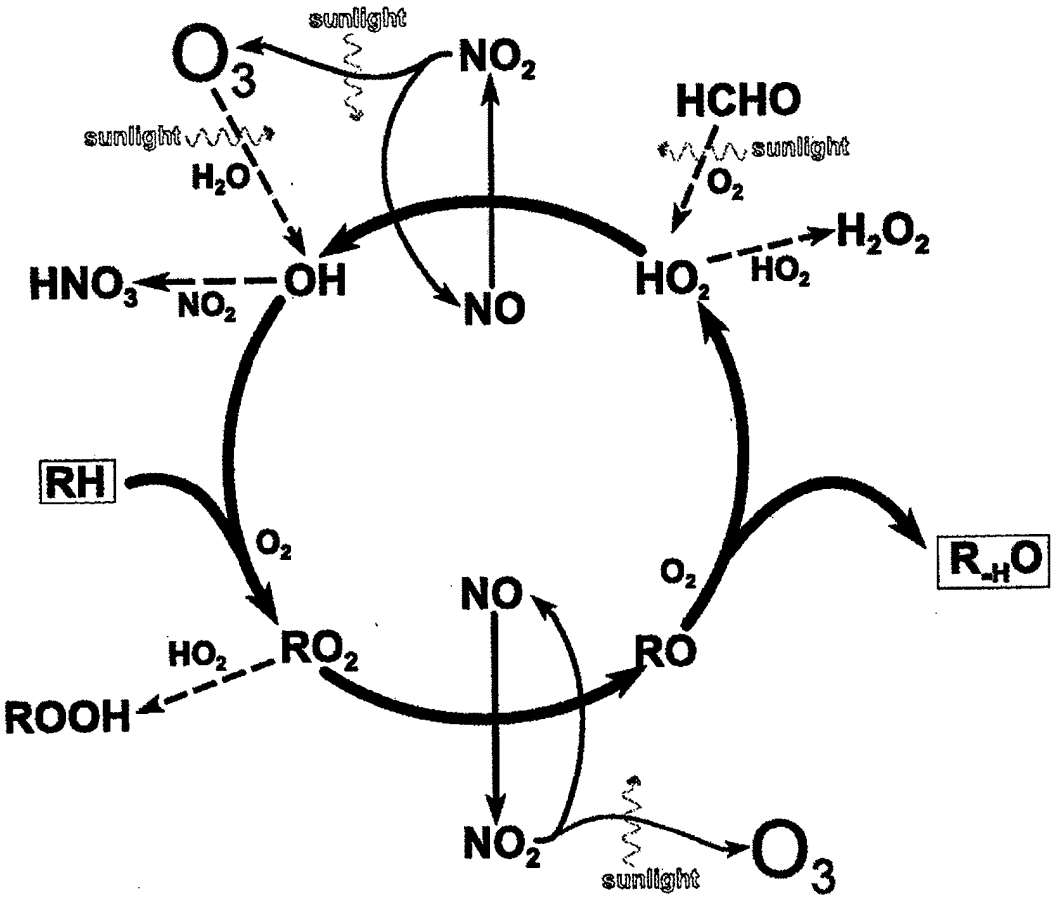

Figure 1.3. Nitric Oxide cycle for ozone formation. Source: Fourth Report of the Photochemical Oxidants Review Group, 1997.

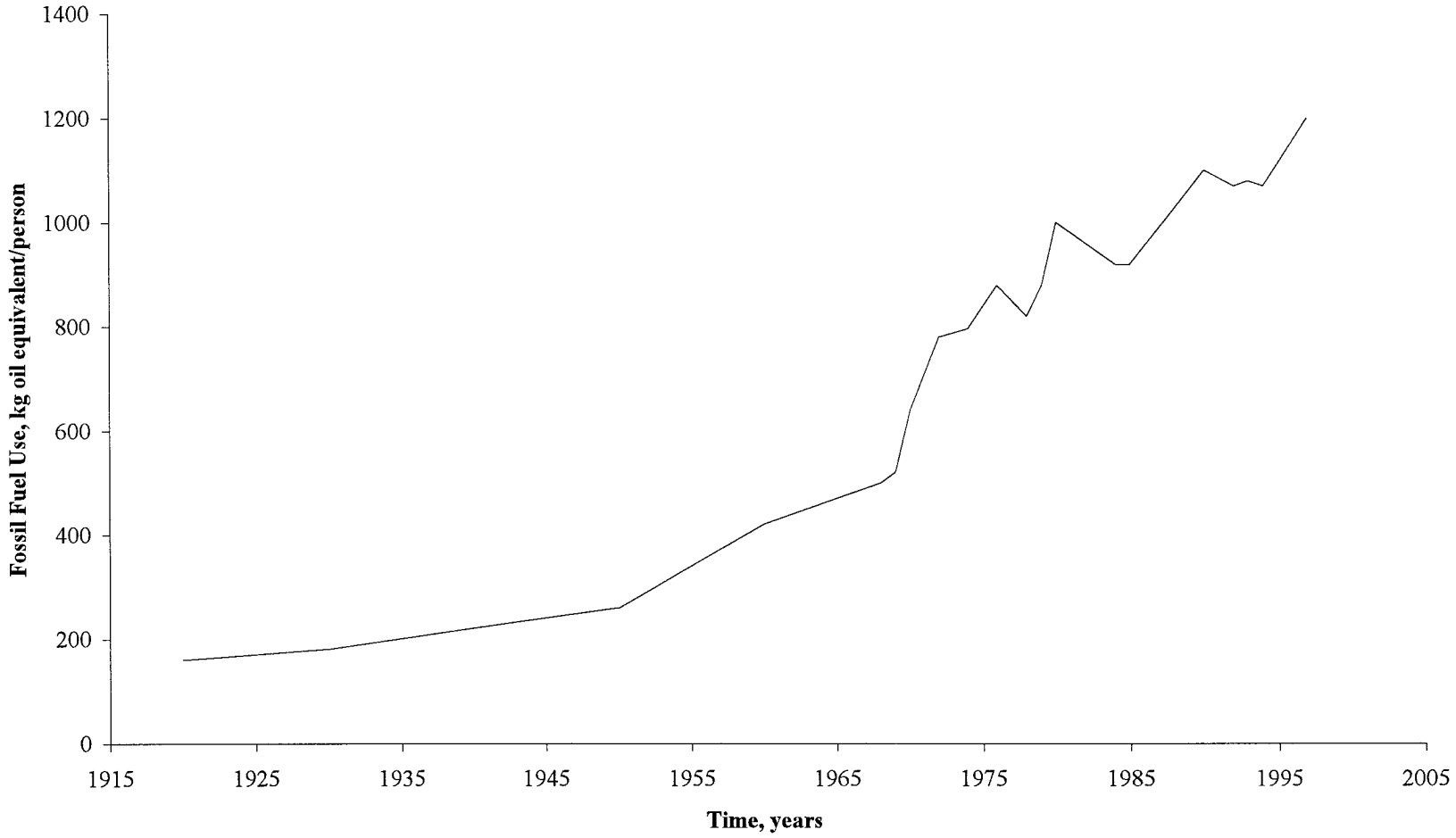

Figure 1.4. Trends in global fossil fuel use per person. Source: Galloway, 1998.

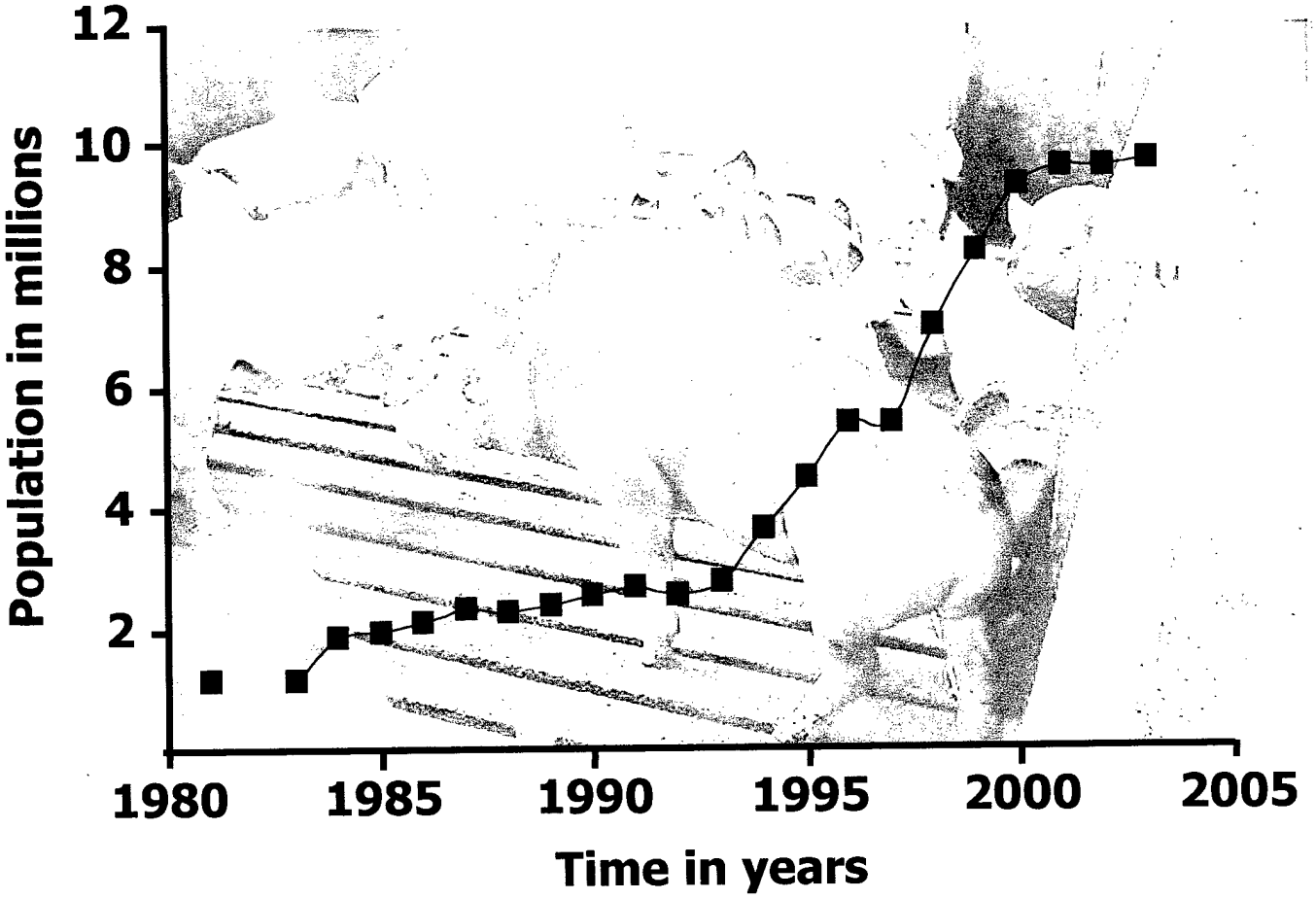

Figure 1.5. Swine population in North Carolina. Source: North Carolina Agricultural Statistics, 2001.

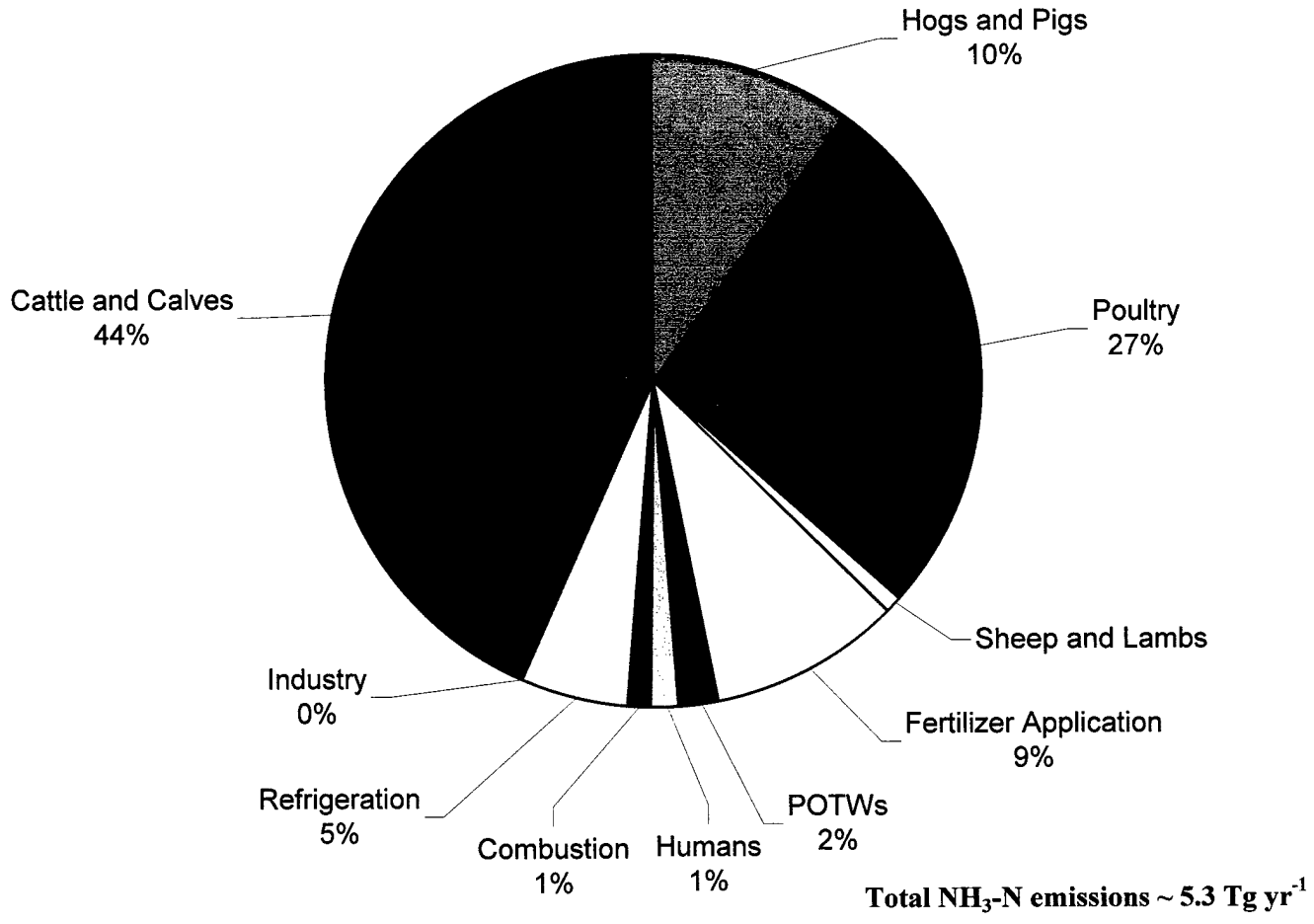

Figure 1.6a. Percent of Ammonia-Nitrogen from various sources in the US for 1994. Source: Battye et al., 1994.

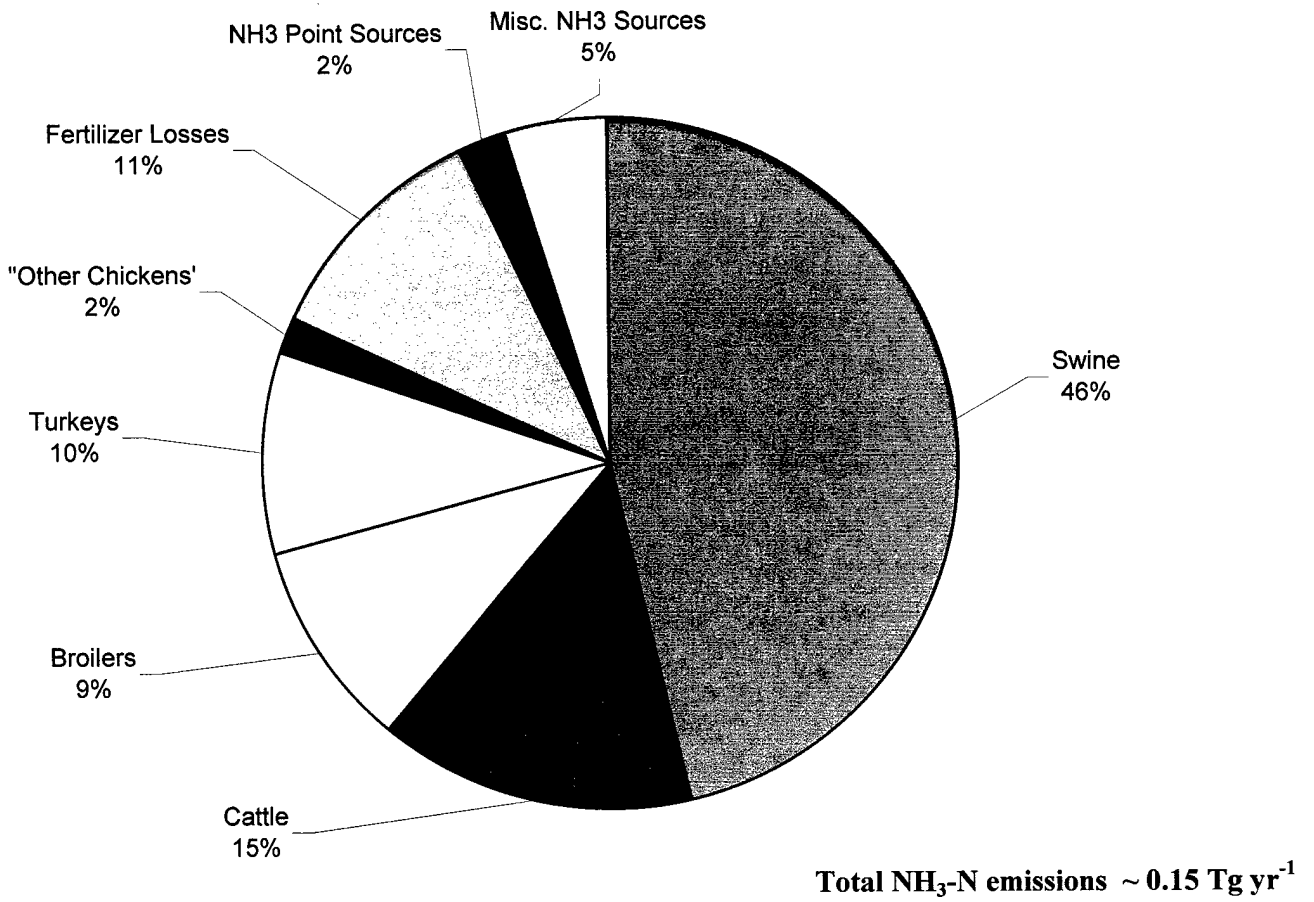

Figure 1.6b. Percent of Ammonia-Nitrogen from various sources in North Carolina for 1996. Source: Aneja et al., 1998a.

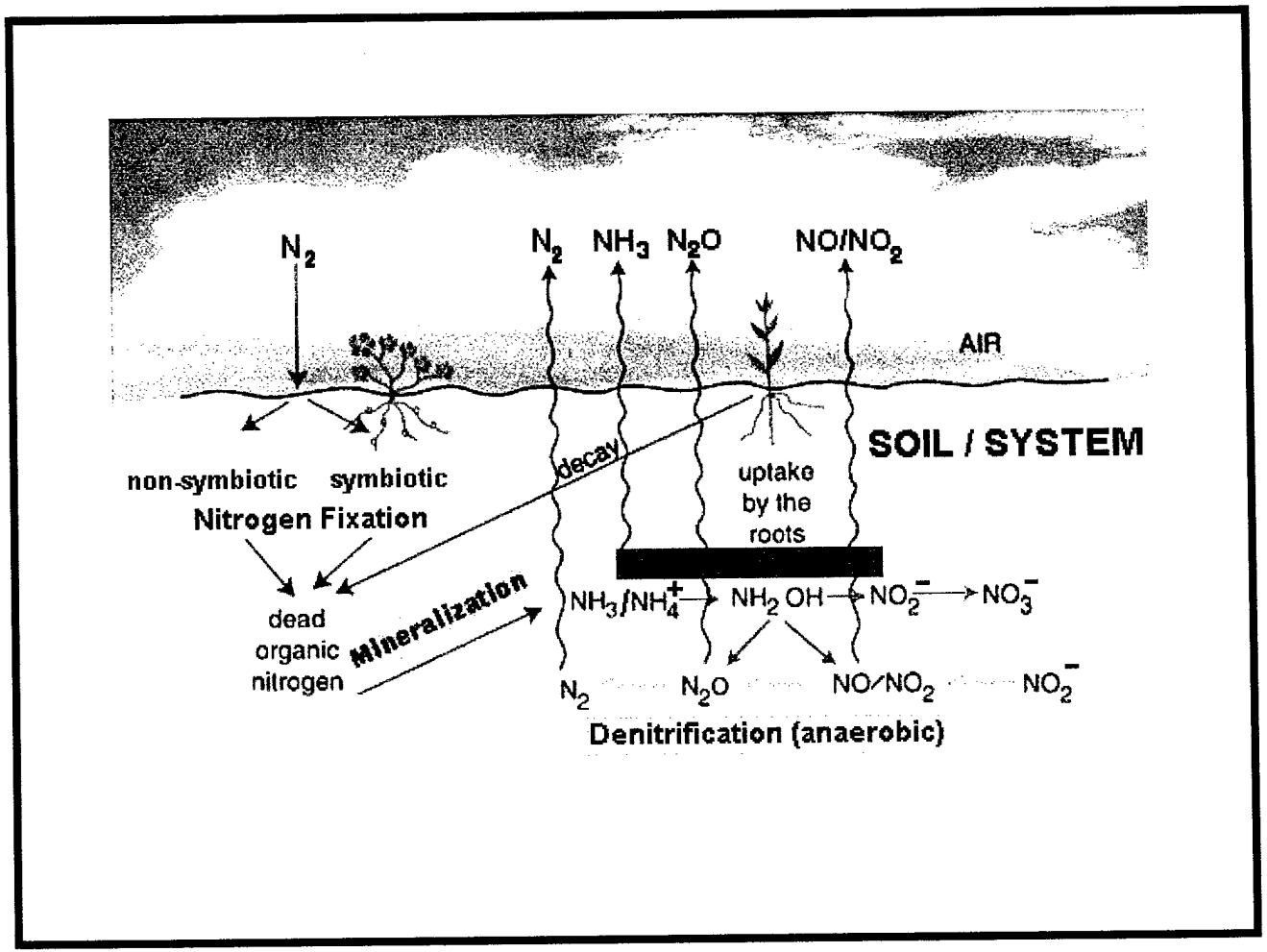

Figure 1.7. Biological nitrogen cycle in the atmosphere-soil system. Source: Warneck, 2000.

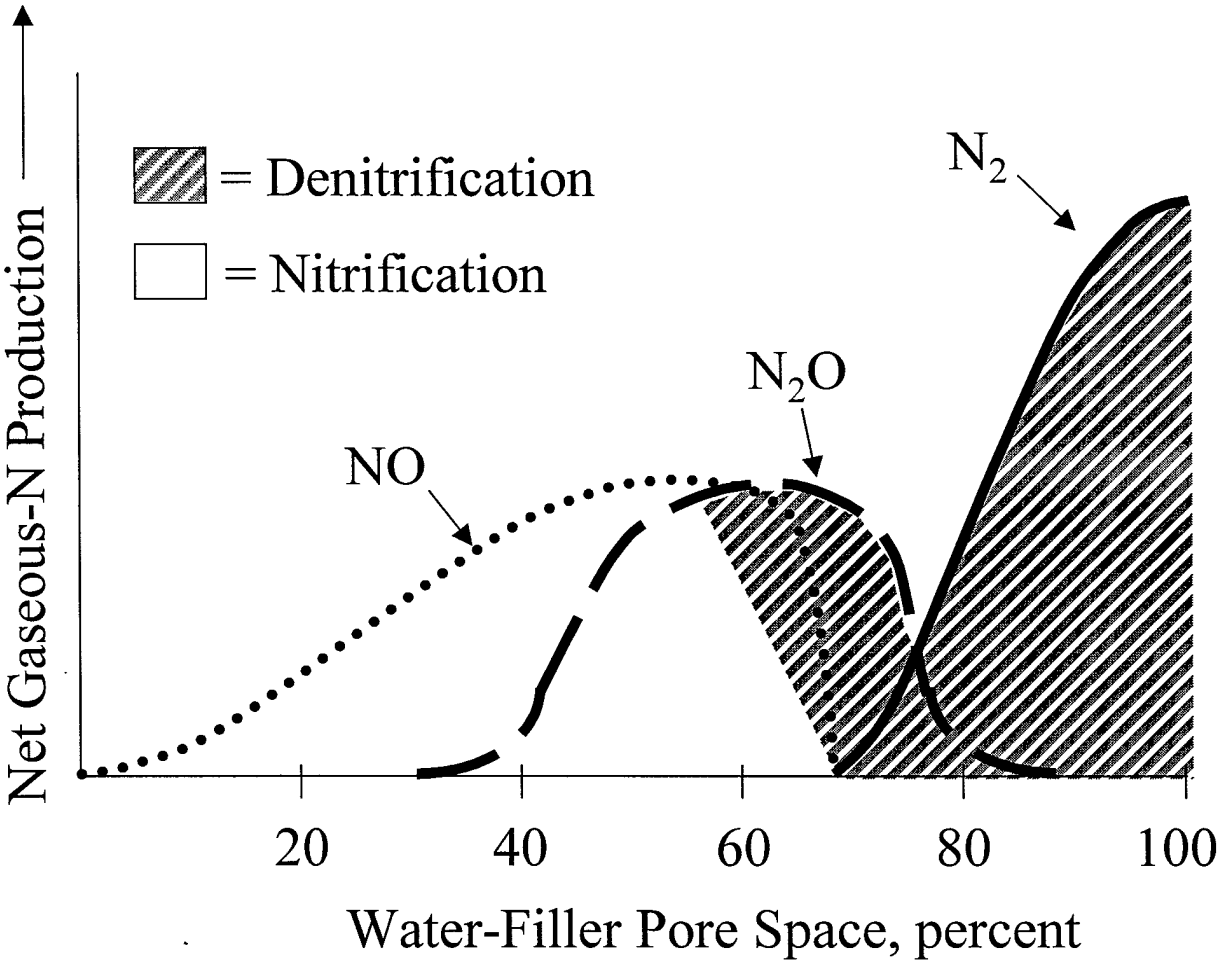

Figure 1.8. Model of N production versus %WFPS. Source: Davidson, 1991.

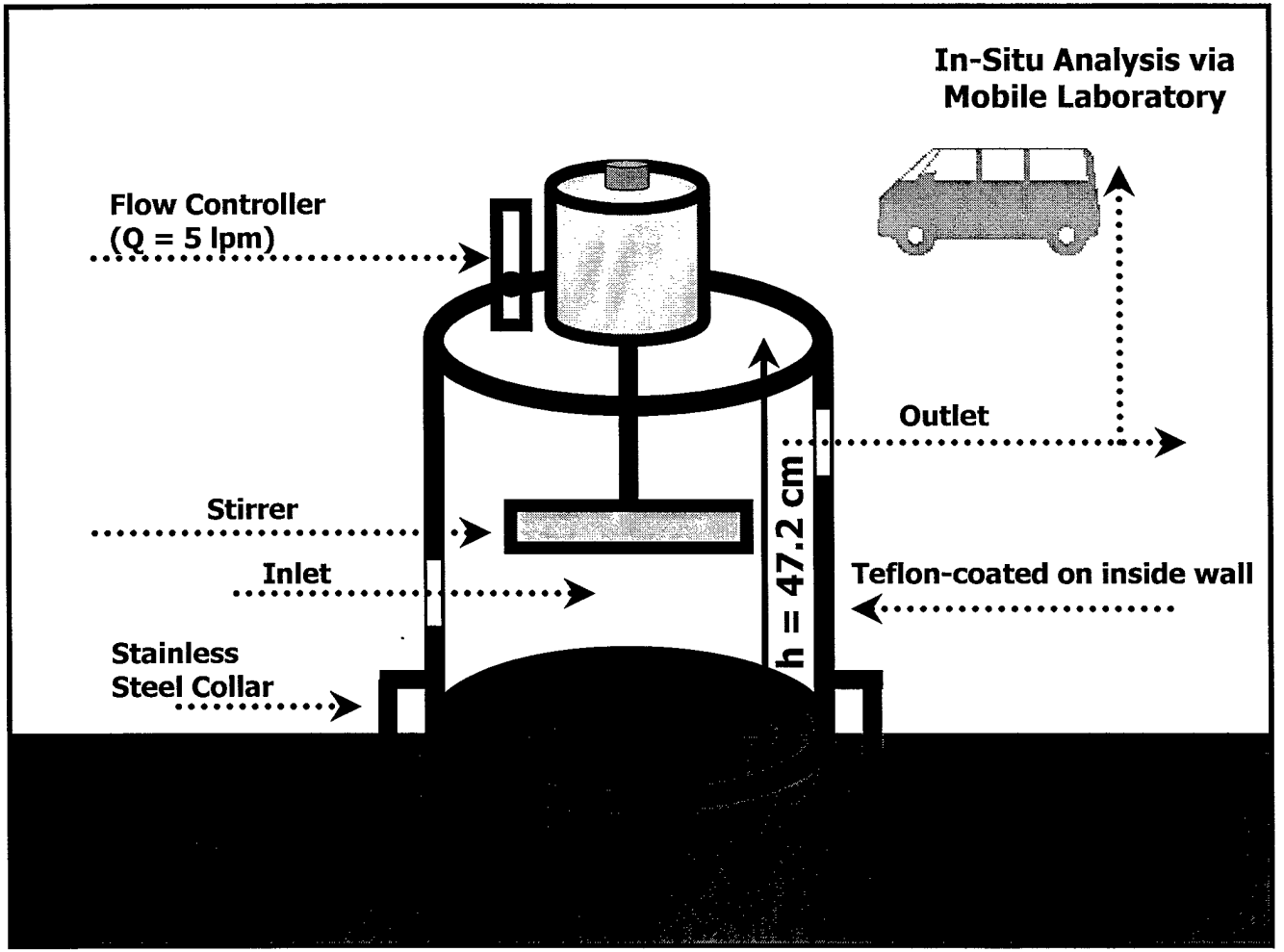

Figure 1.9. Schematic of Dynamic Flow-Through Chamber.

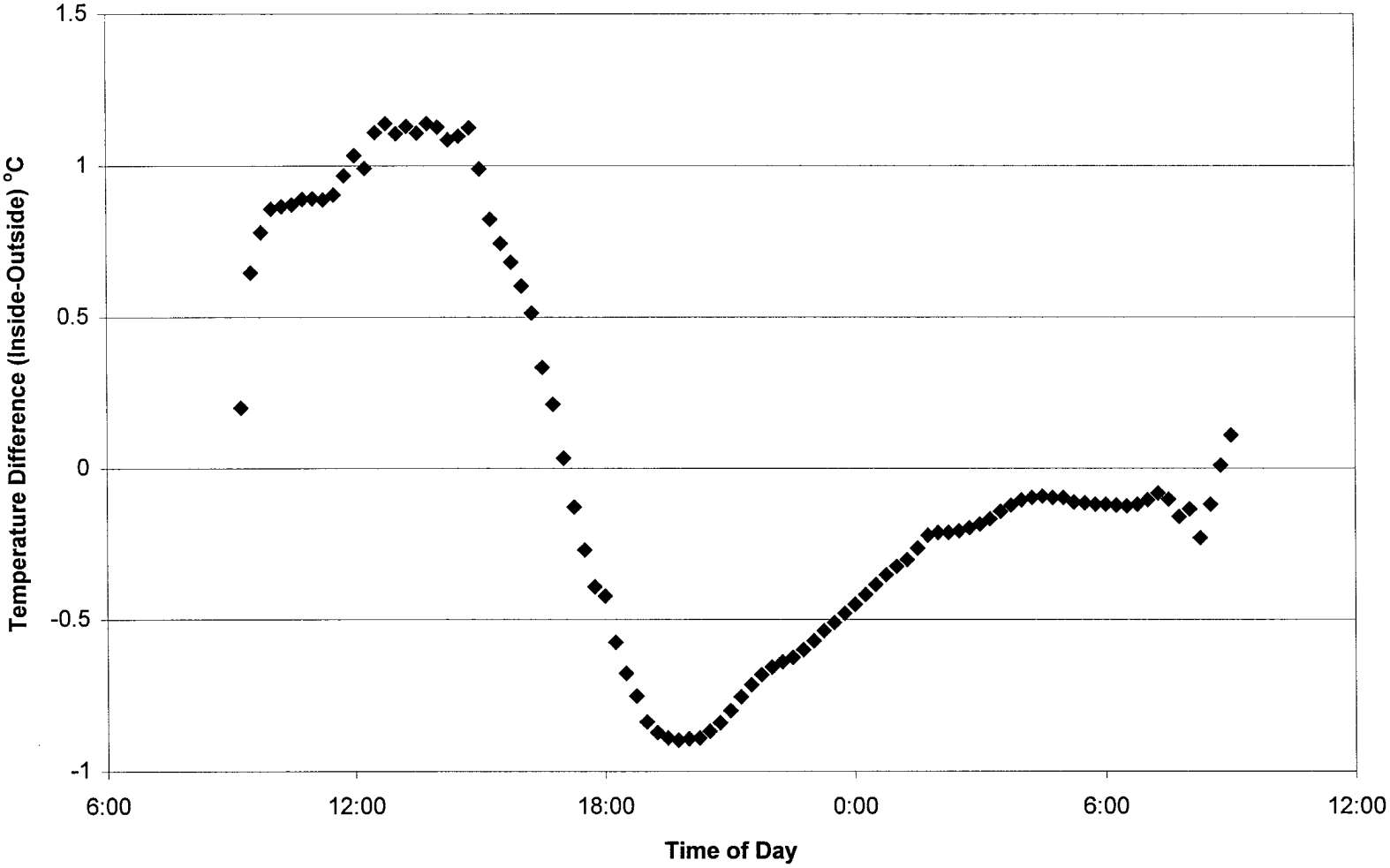

Figure 1.10. Temperature Difference between the inside and outside of the dynamic flow-through chamber. This data represents the average of 5 experiments measured at a depth of approximately 5 cm.

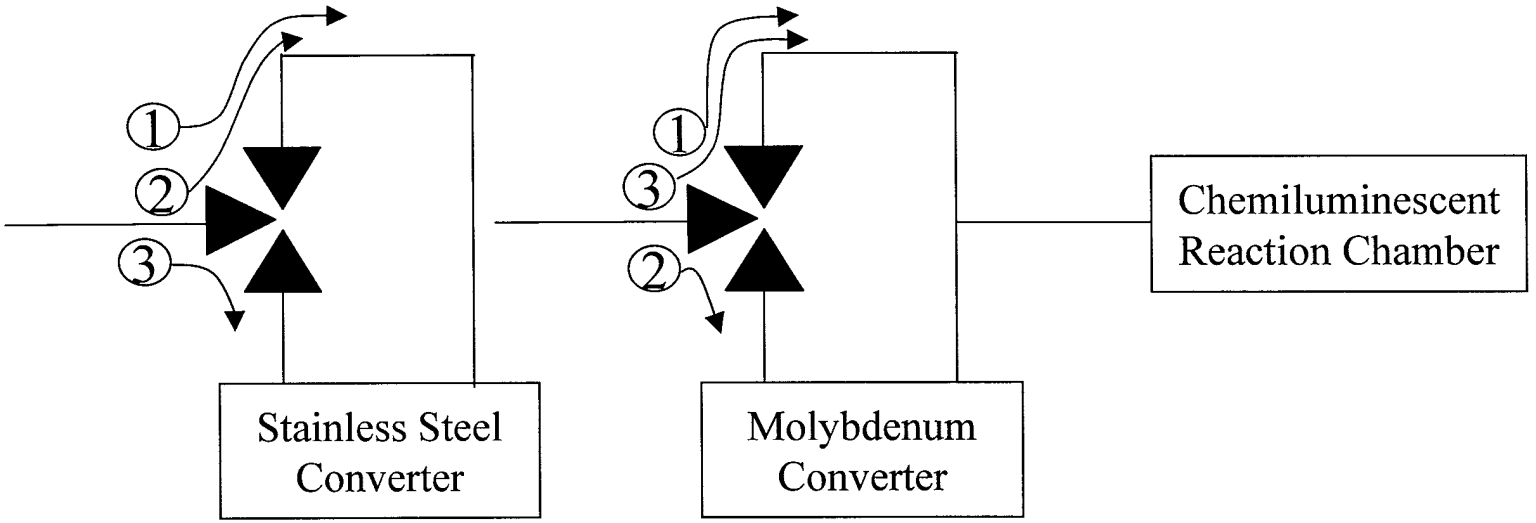

FLOW PATH	MODE	INSTRUMENT READING
1	Both Converters Bypassed	NO
2	Stainless Steel Converter Bypassed Molybdenum Converter Flow-Through	NO_Y
3	Stainless Steel Converter Flow-Through Molybdenum Converter By-passed	N_T

$$N_T - NO_Y = NH_3$$

Figure 1.11. Schematic of modified Thermo Environmental Instruments Incorporated (TECO) Model 42S chemiluminescence analyzer. Instrument is now capable of also measuring ammonia.

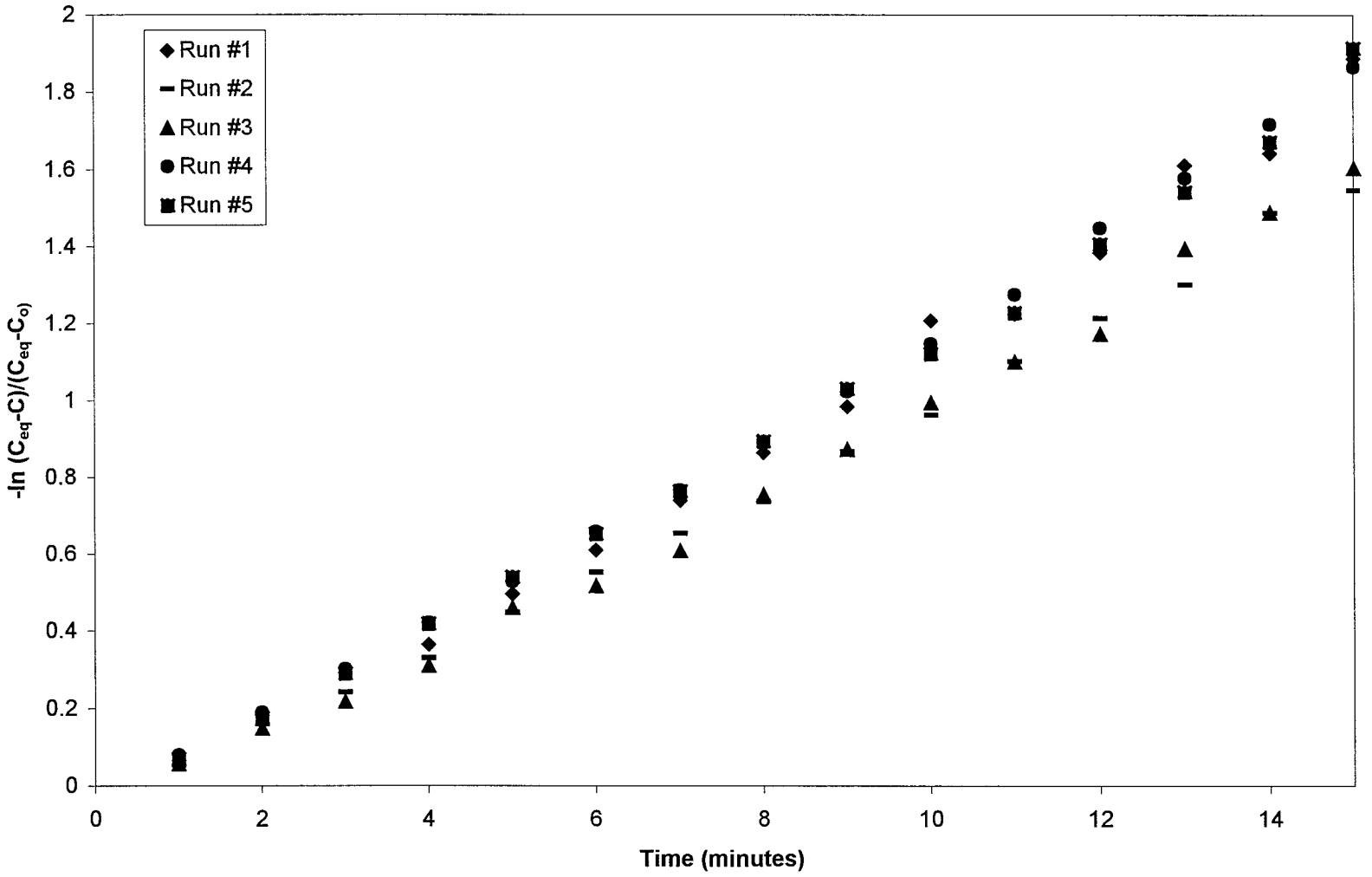

Figure 1.12. Summary of 5 Kaplan experiments conducted during Summer 1999 study. Average loss term (L')=0.02cm s^{-1}.

CHAPTER II. BIOGENIC NITRIC OXIDE EMISSIONS FROM CROPLAND SOILS

by

Paul A. Roelle and Viney P. Aneja

Department of Marine, Earth, and Atmospheric Sciences
North Carolina State University
Raleigh, NC 27695-8208

and

B. Gay, C. Geron and T. Pierce
U.S. Environmental Protection Agency
Research Triangle Park, NC 27711

Published in: Atmospheric Environment, 35, 115-124, 2001.

Abstract

Emissions of nitric oxide (NO) were determined during late spring and summer 1995 and the spring of 1996 from four agricultural soils on which four different crops were grown. These agricultural soils were located at four different sites throughout North Carolina. Emission rates were calculated using a dynamic flow-through chamber system coupled to a mobile laboratory for in-situ analysis. Average NO fluxes during late spring 1995 were: 50.9 ± 47.7 ng N m^{-2} s^{-1} from soil planted with corn in the lower coastal plain. Average NO fluxes during summer 1995 were: 6.4 ± 4.6 and 20.2 ± 19.0 ng N m^{-2} s^{-1} respectively from soils planted with corn and soybean in the coastal region; 4.2 ± 1.7 ng N m^{-2} s^{-1} from soils planted with tobacco in the piedmont region; and 8.5 ± 4.9 ng N m^{-2} s^{-1} from soils planted with corn in the upper piedmont region. Average NO fluxes for spring 1996 were: 66.7 ± 60.7 ng N m^{-2} s^{-1} from soils planted with wheat in the lower

coastal plain; 9.5 ± 2.9 ng N m^{-2} s^{-1} from soils planted with wheat in the coastal plain; 2.7 ± 3.4 ng N m^{-2} s^{-1} from soils planted with wheat in the piedmont region; and 56.1 ± 53.7 ng N m^{-2} s^{-1} from soils planted with corn in the upper piedmont region. An apparent increase in NO flux with soil temperature was present at all of the locations. The composite data from all the research sites revealed a general positive trend of increasing NO flux with soil water content. In general, increases in total extractable nitrogen (TEN) appeared to be related to increased NO emissions within each site, however a consistent trend was not evident across all sites.

Introduction

Ozone is produced in the troposphere through photochemical processes involving oxides of nitrogen ($NO_X = NO + NO_2$) and volatile organic compounds (VOCs). Tropospheric ozone is an important photochemical air pollutant which increases respiratory illness, damages crops, and causes other environmental problems. Currently, the only known pathway for the production of ozone is the photolysis of NO_2 ($NO_2 \rightarrow NO + O(^3P)$), which further reacts with O_2 to produce ozone (O_3) by the reaction $O(^3P) + O_2 \rightarrow O_3$. In a pseudo-photostationary environment, the O_3 produced would react with the NO that was generated via the photolysis of NO_2 in the following reaction: $NO + O_3 \rightarrow NO_2 + O_2$. Hence, there is no net production of O_3. However, in the real atmosphere, hydroxyl radicals combine with VOC's to produce new radicals which preferentially react with NO, allowing a net O_3 accumulation.

Recent estimates report that on a global scale biogenic emissions of NO are comparable to anthropogenic sources (~ 20 Tg NO-N $year^{-1}$) (Li et al., 2000). Regions such as the southeast U.S., which comprise approximately 40% of the US non-attainment areas, are classified as NO_X limited and increased emissions of NO into the troposphere are likely to produce increased O_3 concentrations (Fehsenfeld et al., 1993). Over 40% of the ozone non-attainment areas of the U.S. are in the Southeast. Therefore, in order to formulate more successful ozone control strategies in the southeast U.S., the source strength of ozone precursors (i.e., NO) and the parameters which control their release must be better understood. An estimate of the global source of biogenic NO emissions conducted by Davidson and Kingerlee (1997) reports a slight improvement over

estimates made by Galbally and Roy (1978). In their paper, Davidson and Kingerlee report that further improvements to their estimate will most likely come from an increased biogenic NO dataset and by gaining a greater understanding of the processes which govern the release of NO from the soil. To these ends, the objectives of this study were to increase the NO dataset and to attempt to verify previously reported relationships between NO and environmental variables (i.e., soil temperature, soil water content, applied N fertilizer).

Methods and Materials

Field Sites and Sampling Scheme

NO concentration measurements were made from four different agricultural soils (on which corn, soybean, tobacco and wheat were cultivated) during late spring and summer 1995 and spring 1996 (refer to Tables 2.1 & 2.2 for research sites, dates, soil parameters and NO flux values). All of the sites, except for Plymouth were operated by the North Carolina State University in conjunction with the North Carolina Agricultural Research Service. All of the sites were managed using practices typical for their respective crops and physiographic locations.

The design of this experiment was to measure soil emissions of NO at four different locations in North Carolina during two different times of the year. Each site was sampled twice, once in the late spring/summer and again the following year in the spring. The measurement locations at each site were essentially the same as the previous season (within a distance of 5 m). The daily sampling scheme consisted of measuring ambient NO concentrations at ground level before entering the dynamic flow-through

chamber and immediately after exiting the chamber. A Toshiba laptop computer using Labview software (National Instruments) was utilized as the data acquisition system. The system produced 60 second rolling average concentrations, which were then binned and averaged every 15 minutes. A daily experiment consisted of placing the chamber on the stainless steel collar approximately one hour prior to data acquisition. At the conclusion of each daily experiment, the collar was relocated to a random position within a 10m radius of the mobile laboratory, allowing a minimum of 12 hours for any effect on the soil, due to insertion of the collar, to dissipate. The randomization of the collar and chamber system placement resulted in it being located both in and between the rows of the row crops (corn, soybean, tobacco), however, plants were never inside the enclosure.

Instrumentation and Flux Calculation

The chamber design, associated mass balance equation and calibration procedures are described in full in Chapter I.

Soil Analysis

Soil samples and soil analyses are described in full in Chapter I.

Results and Discussion

Soil Temperature

Figure 2.1 is an hourly averaged diurnal profile of NO flux versus time of day for each site and crop type. This graph has been split to reflect 2 different ranges in NO flux so that diurnal variations can be better discerned. In general, both graphs reveal that maximum NO emissions occur in the afternoon when soil temperatures are typically at a maximum and reduce to lower values in the late afternoon hours when soil temperatures are typically lower. The bottom graph also reveals that several sites have a local

maximum of NO emissions in the morning. This morning peak has been observed by other researchers (Johansson and Granat, 1984; Roelle, 1996), however a solid understanding as to the cause of this phenomenon has yet to be determined. It has been hypothesized that this morning peak is a result of plant roots which may exude organic substances in the morning hours which denitrifying bacteria can utilize to produce NO (Johansson and Granat, 1984). Aneja et al. (1995) reported a negative correlation between NO flux and soil temperature, which was explained by a combination of moisture and heat stress on the soil microorganisms in the top 20 cm of soil. This explanation is not sufficient in this study, because although there was a brief period when the correlation was negative, the greatest values of NO flux were in the afternoon, when soil temperatures were at a maximum.

It is generally found that in the range of temperatures between 288-308 ^{o}K, biochemical reactions will rise exponentially with temperature (Warneck, 2000). Several researchers have investigated this relationship, and in fact have observed there to be an exponential dependence of NO flux on soil temperature (Williams and Fehsenfeld, 1991; Sullivan et al., 1996; Thornton et al., 1997; Roelle et al., 1999). The research conducted during this experiment revealed similar results, however, the exponential dependence of NO flux on soil temperature was not consistent at all sites.

Plymouth, NC, during the late spring 1995 experiment displayed some dependence of NO flux on soil temperature [log (NO flux) = 0.083(Soil T) - 0.41; R^2 =0.27] for the entire 16 day period. However, this research site was characterized by an additional application of N fertilizer midway through the experiment allowing the data to

be segregated into periods 'before' and 'after' fertilization. For the period before the additional N fertilization, there was virtually no relationship between temperature and flux [Log (NO flux) = 0.023(Soil T) + 0.89; R^2 =0.10]. However, for the period after the additional N fertilization (Excluding one day due to the remnants of Hurricane Allison flooding the field), the relationship increased [Log (NO flux) = 0.23(Soil T) - 3.823; R^2 =0.58]. Additionally there was some dependence of NO flux on soil temperature observed at a soybean crop located in Kinston, NC during the summer 1995 research period when one day was excluded due to heavy rains the previous day [Log (NO flux) = 0.45(Soil T) - 11.33; R^2 =.35]. There was also some dependence observed at the tobacco crop in Oxford, NC [Log (NO flux) = 0.09(Soil T) - 2.00; R^2 =.56]. At the remainder of the research sites, this same exponential dependence on soil temperature was difficult to detect.

Figure 2.2 is a composite of the data from each site with hourly averaged soil temperature plotted versus hourly averaged NO flux. This graph and regression analysis reveals a significant improvement in R^2 values for data which was collected at Plymouth and Reidsville, which were being cultivated with corn during approximately 86% of the measurement period. These results are more in line with similar analyses conducted by Thornton et al., 1997, who reported R^2 values of 0.87 for a dataset comprised of approximately 9900 observations, of which 94% were from soils where corn was being cultivated. This deviation from the often-cited relationship between NO flux and soil temperature at Kinston and Oxford suggests that factors other than soil temperature are acting to control the flux of NO. Researchers in California conducting extensive research

on a very robust NO data set report that depending on location and time, other variables (i.e. crop type, soil type, water filled pore space, N content) can have stronger influences than soil temperature on NO flux (Matson et al., 1997). Additionally, Sullivan et al. (1996) reported that differences in a crops growth stage and the age and amount of root biomass further act to influence the NO flux/temperature dependence.

Total Extractable Nitrogen

Another variable, which has also been found to control the NO flux, is total extractable nitrogen (TEN) ($NH_4^+ + NO_3^-$). Figure 2.3 is a graph of the total average NO flux (stippled bar) (0900-1700) and TEN on the secondary axis plotted for each research site. Three sampling days were removed from this analysis, which occurred during or immediately after rain events at the site. This graph does reveal a trend of NO emissions responding to increasing and decreasing amounts of TEN, however a consistent relationship was unable to be detected. Researchers conducting similar studies have reported on the effects of organic and inorganic nitrogen content in soils on NO emissions and in general have found that soils with higher N content produce higher NO emissions (Davidson, 1991 a,b; Cardenas et al., 1993; Potter et al., 1996; Sullivan et al., 1996; Roelle et al., 1999). If the research conducted in spring 1995 at Plymouth, NC is taken as an example, it is evident that TEN alone is not controlling the release of NO from the soil. At this site, a small increase in TEN was associated with a much larger increase in NO emissions. A plausible explanation as to the lack of a consistent relationship in our data between TEN and NO emissions could be the result of our soil sampling method. One method of N fertilizer application is to use applicator nozzles

which drag across the soil surface (2 cm wide strip of concentrated liquid fertilizer). This application method was used on the corn crop at the Plymouth site. Upon drying, there is no way to discern where exactly this fertilizer band is in the interrow (1 m width). It is possible that the fertilized strip was in the chamber footprint (diameter 27 cm) but our soil core sample (diameter 8.3 cm) missed the band. Further, it is possible that a soil sample, which occurred immediately following fertilization, collected the fertilized strip which had yet to penetrate the soil surface.

Statistical analysis relating TEN with NO in Figure 2.3 reveals a noisy data set with an R-squared value of only 0.15. However, this relationship does improve and becomes highly significant ($p<0.0001$) when those flux values greater than 100 ng N m^{-2} s^{-1} are removed from the regression. The justification for removing 3 (from Spring 95 data set) of the 5 data points greater than 100 ng N m^{-2} s^{-1} is that the data were collected immediately (within 2 weeks) after fertilization. In contrast, at all the remaining measurement sites, there were no data collected within at least one month of fertilization. These results suggest that TEN can be used effectively in NO flux models, although further research will be needed to determine under what physiological and environmental conditions this relationship can be best applied. Sullivan et al. (1996), during a field study with an equivalent experimental design, experienced similar results and reported that the differences in a plants physiological growth stages, during which nitrogen demands of the plants will vary, confound the relationship between NO flux and TEN.

Soil Moisture

The role of soil moisture on NO flux has been examined by several researchers (Cardenas et al., 1993; Valente and Thornton, 1993; Ormeci et al., 1999). Typically, each soil type will have a range of soil moisture which optimizes NO flux. For example, Cardenas et al. (1993) reported that the optimum range of soil water content for sandy loam soils was between 9-18%. Moisture values above a soil's optimum zone will generally decrease NO flux due to pore spaces filling with water and inhibiting gas transport. Moisture values below a soils optimum zone will generally lead to decreased NO emissions as a result of moisture stress to the soil microbes. Figure 2.4 is a graph of the daily averaged (0900-1700) NO flux values versus % soil moisture for the four research sites where the experiments were conducted. These results partially support Cardenas' et al. (1993) research in that NO flux tends to respond positively to increased moisture, and then begins to decrease again at moisture levels greater than 20%. However, it is also evident that with R-squared values of 0.2, this variable alone cannot adequately predict NO emissions from biogenic processes. Using the same rationale as in Figure 3, the data points greater than 100 ng N m^{-2} s^{-1} were removed from the data set and then reanalyzed. However unlike Figure 2.3, this approach only resulted in a slightly better model prediction (R^2=.3).

NO Response to Soil Parameters

Chameides et al. (1988 and 1994) have reported on the importance of including both anthropogenic and biogenic NO emissions when attempting to predict the concentrations of tropospheric ozone. One of the methods used in air quality models for estimating soil NO emissions is the Biogenic Emissions Inventory System (BEIS2)

model. This model utilizes soil temperature data and an emission factor which is based on crop type, the type and amount of fertilizer applied, and other chemicals applied to the soil (Birth et al., 1995). The NO flux is then calculated by:

$$\text{NO Flux (ng N m}^{-2}\text{ s}^{-1}) = A * EXP(0.71*T_s)$$

where

A = experimentally-derived coefficient which is dependent on the land use category

T_s = soil temperature

(Williams et al., 1992).

This temperature dependence model has been questioned by several researchers who have found that temperature alone does not adequately explain the flux of NO in their measurements (Matson et al., 1997; Roelle et al., 1999; Li et al., 1999). In fact, Matson et al. (1997) reported that for most crops in their research, percent water-filled pore space (WFPS) was equally as important as temperature in predicting NO emissions.

Table 2.3 lists Williams' values for A as well as those calculated for this study. The range of soil temperatures (T_s) with the corresponding fluxes produced using the BEIS2 model versus the actual data measured during this study is also on this table. There was reasonable agreement between A factors for the corn crop, where Williams' A value is 9 ng N m^{-2} s^{-1} and the A value from this study is 7 ng N m^{-2} s^{-1}. However, the remaining crops, (soybean, tobacco, and wheat) varied from Williams' model by factors of 15, 6.7, and 3.7 respectively. Research conducted in the San Joaquin Valley in California produced even larger deviations from Williams' model, where these researchers calculated A values for corn between 0.0001 and 0.0005 ng N m^{-2} s^{-1} (Matson et al., 1997). As the table indicates, using the BEIS2 model to estimate NO emissions

can produce values different by up to an order of magnitude than the NO emissions that were calculated during this study.

Conclusions and Recommendations

NO emissions and soil properties were studied from several croplands in order to gain a better understanding of the chemical and physical properties of soil which influence NO flux, and to provide much needed data to the biogenic NO emission dataset. Utilizing a dynamic flow-through chamber, the flux of NO from soil was determined for four different regions and crop types during both spring and summer. NO flux was generally found to follow a diurnal profile with maximum emissions coinciding with maximum soil temperatures. Additionally, several sites displayed a morning peak in NO emissions, which is occasionally observed by some researchers but has yet to be explained. The exponential dependence of NO flux on soil temperature existed at all sites, but to different levels of significance. It was also observed that NO flux did respond to varying amounts of both total extractable nitrogen (TEN) in the soil and soil moisture content.

Although relationships between soil parameters (soil moisture, TEN, soil temperature) were evident, no one variable or combination of variables has yet been found to adequately model the flux of NO from agricultural soils. Parkin (1993) addressed the difficulty in modeling a system with such high variability, yet stressed the importance of continued research, as improved estimates will only be achieved as we gain a greater understanding of the processes causing the variability. The data from this observationally based study raise concerns about the current practice of basing emission

estimates solely on temperature and land cover type. Errors in soil emission estimates caused by ignoring the influence of parameters such as soil moisture and TEN, which was pointed out in the comparison of BEIS2 model estimates to actual calculated fluxes, may also hinder the ability of ozone models to simulate VOC/NO_x emission control scenarios. With the addition of this data set reported here, and with data such as reported by Thornton et al. (1997), the scientific community should combine other observational data to build a model which includes a broader set of environmental parameters (i.e., %WFPS, TEN, soil type), which will likely lead to better estimates of NO emissions from agricultural soils.

References

Aneja V.P., W.P. Robarge and B.D. Holbrook, Measurements of nitric oxide flux from an upper coastal plain, North Carolina agricultural soil. Atmospheric Environment, 21, 3037-3042, 1995.

Birth, T.L. and C.D. Geron, Users guide to the personal computer version of the biogenic emissions inventory system (PC-Beis2), EPA-600/R-95-091, July 1995.

Cardenas L., A. Rondon, C. Johannson and E. Sanhueza, Effects of soil moisture, temperature, and inorganic nitrogen on nitric oxide emissions from acidic tropical savannah soils, Journal of Geophysical Research, 98, 14,783-14,790, 1993.

Chameides, W., R. Lindsay, J. Richardson and C. Kiang, The role of biogenic hydrocarbons in urban photochemical smog: Atlanta as a case study, Science, 241, 1473-1475, 1988.

Chameides, W., P. Kasibhatla, J. Yienger and H. Levy, Growth of continental-scale metro-agro-plexes, regional ozone pollution, and world food production, Science, 264, 74-77, 1994.

Davidson, E.A., Sources of nitric oxide and nitrous oxide following wetting of dry soil, Soil Science Society of America Journal, 56, 95-102, 1992.

Davidson E.A., Fluxes of nitrous and nitric oxide from terrestrial ecosystems, in Microbial Production and Consumption of Greenhouse Gases, Methane, Nitrogen Oxides and Halomethanes, edited by J.E. Rogers and W.B. Whitman, pp. 219-235, American Society for Microbiology, Washington, D.C., 1991.

Davidson, E.A. and W. Kingerlee, A global inventory of nitric oxide emissions from soils, Nutrient Cycling in Agroecosystems, 48, 37-50, 1997.

Fehsenfeld, F., J. Meagher and E. Cowling (Eds.), Southern Oxidants Study Annual Report, pp. 47-61, 1993.

Galbally, I.E., and C.R. Roy, Loss of fixed nitrogen from soils by nitric oxide exhalation, Nature, 734-735, 1978.

Johansson C. and L. Granat, Emission of nitric oxide from arable land, Tellus, 36B, 25-37, 1984.

Li, Y., V.P., Aneja, S.P., Arya, J. Rickman, J. Brittig, P. Roelle and D.S. Kim, Nitric oxide emission from intensively managed agricultural soil in North Carolina, Journal of Geophysical Research, 104, 26,115-26,123, 1999.

Matson, P., M. Firestone, D. Herman, T. Billow, N. Kiang, T. Benning and J. Burns, Agricultural systems in the San Juaquin Valley: Development of Emission Estimates for Nitrogen Oxides, Technical Report, University of Califrnia, Berkeley, Contract Number 94-732, 1997.

Ormeci, B., S.L. Sanin and J. Peirce, Laboratory study of NO flux from agricultural soil: Effects of soil moisture, pH and temperature, Journal of Geophysical Research, 104, 1621-1629, 1999.

Parkin, T.B., Spatial variability of microbial processes in soil-A review, Journal of Environmental Quality, 22, 409-417, 1993.

Parrish, D.D., E.J. Williams, D.W. Fahey, S.C. Liu and F.C. Fehsenfeld, Measurement of nitrogen oxide fluxes from soils: intercomparison of enclosure and gradient techniques, Journal of Geophysical Research, 92, 2165-2171, 1987.

Potter, C.S., P.A. Matson, P.M. Vitousek and E.A. Davidson, Process modeling of controls on nitrogen trace gas emissions from soils worldwide, Journal of Geophysical Research, 101, 1361-1377, 1996.

Roelle, P.A., Chemically reactive nitrogen trace species in the Planetary Boundary Layer, MS Thesis, NC State University, Dept of Marine, Earth and Atmospheric Sciences, p. 73, 1996.

Roelle, P.A., V.P. Aneja, J. O'Connor, W. Robarge, D.S. Kim and J.S. Levine, Measurement of nitrogen oxide emissions from an agricultural soil with a dynamic chamber system, Journal of Geophysical Research, 104, 1609-1619, 1999.

Sullivan L.J., T.C. Moore, V.P. Aneja and W.P. Robarge, Environmental variables controlling nitric oxide emissions from agricultural soils in the southeast United States, Atmospheric Environment, 30, 3573-3582, 1996.

Thornton, F., P. Pier and R. Valente, NO emissions from soils in the southeastern United States, Journal of Geophysical Research, 102, 21,189-21,195, 1997.

Valente, R.J. and Thorton F.C., Emissions of NO from soil at a rural site in Central Tennessee, Journal of Geophysical Research, 98, 16,745-16,753, 1993.

Warneck, P., Chemistry of the Natural Atmosphere, Second edition, pp. 514-515, New York, 2000.

Williams E.J. and Fehsenfeld F.C., Measurement of soil nitrogen oxide emissions at three North American ecosystems, Journal of Geophysical Research, 96, 1033-1042, 1991.

Williams E., A. Guenther and F. Fehsenfeld, An inventory of nitric oxide emissions from the soil in the United States, Journal of Geophysical Research, 97, 751-7519, 1992.

Crop	Location / Measurement Dates	Fertilization Dates	N Applied (amount and how applied)	Soil
Corn	Plymouth, NC N Latitude: 35° 43' W Longitude: 76° 42' May 15- Jun 9, 1995	April 12 May 20	9 kg N/ha as 10-20-20/soil injection 64 kg N.ha as 30% N soln†/broadcast 102 kg N/ha as 30% N soln†/side-dressed	Portsmouth Fine Sandy Loam
Corn	Kinston, NC N Latitude: 35° 18' W Longitude: 77° 34' Jun 30-5 Jul, 1995	April (pre-plant) mid-May	33 kg/ha as 10-20-20/soil-injection 157 kg/ha as 30% N soln†/side-dressed	Rains Fine Sandy Loam
Corn	Reidsville, NC N Latitude: 36° 23' W Longitude: 79° 42' Aug 3 – Aug 10, 1995	April (at-planting) mid-May	56 kg/ha as 10-20-20/soil-injection 141 kg N/ha as NH_4NO_3/side-dressed	Pacolet Sandy Loam
Corn	Reidsville, NC May 14-18 May, 1996	April (at-planting)	45 kg N/ha as 10-20-20/soil injection	Pacolet Sandy Loam
Soybean	Kinston, NC Jul 10-Jul 13 1995	none		Rains Fine Sandy Loam
Tobacco	Oxford, NC N Latitude: 36° 17' W Longitude: 78° 37' Jul 20-Jul 27, 1995	mid-May (1 week after transplanting) late-May (2weeks after transplanting)	45 kg N/ha as 8-8-24/soil injection 25 kg/ha as 15-0-14/side-dressed	Vance Sandy Loam
Wheat	Plymouth, NC Apr 11-Apr 14, 1996	Oct (at-planting) Feb	50 kg N/ha as 10-20-20/soil injection 100 kg N/ha as NH_4NO_3/broadcast	Portsmouth Fine Sandy Loam
Wheat	Kinston, NC Apr 17-Apr 20, 1996	Oct (pre-planting) Feb	30 kg N/ha as 10-20-20/soil injection 120 kg/ha as 30% N soln†/side-dressed	Portsmouth Fine Sandy Loam
Wheat	Oxford, NC Apr 24 – Apr 28, 1996	Oct (at-planting) Feb	45 kg N/ha as 10-10-10/broadcast 95 kg/ha as NH_4NO_3/broadcast	Vance Sandy Loam

† = 30% N solution contains equal parts urea, ammonia and nitrate

Table 2.1. Location, dates, fertilizer application and soil types of the sites where the research was conducted.

Location	Crop		Soil Temp (°C)	TEN mg N / (Kg dry Soil)	% Soil Moisture	NO (ng N m^{-2} s^{-1})
Plymouth	Corn	Avg	24.1	51.0	21.1	50.9
N=16		Std Dev	3.2	26.2	2.8	47.7
n=759		Min	16.4	24.0	17.7	4.2
		Max	32.7	116.0	27.7	264.7
Kinston	Corn	Avg	25.6	9.8	12.4	6.4
N=5		Std Dev	2.6	1.7	1.4	4.6
n=203		Min	21.1	8.0	10.7	2.1
		Max	32.6	12.1	14.0	37.2
Kinston	Soybean	Avg	25.8	14.2	12.8	20.2
N=4		Std Dev	3.2	3.4	0.8	19.0
n=276		Min	21.5	11.0	11.6	1.7
		Max	31.9	19.0	13.4	96.8
Oxford	Tobacco	Avg	27.4	8.0	5.6	4.2
N=6		Std Dev	2.2	2.5	2.3	1.7
n=285		Min	23.5	6.0	2.7	1.0
		Max	32.5	13.0	8.1	13.0
Reidsville	Corn	Avg	23.0	12.8	11.3	8.5
N=4		Std Dev	2.5	11.9	2.4	4.9
n=289		Min	19.7	4.0	10.0	1.4
		Max	29.0	32.0	15.6	20.5
Plymouth	Wheat	Avg	14.3	9.4	22.7	66.7
N=4		Std Dev	3.2	4.4	1.2	60.7
n=229		Min	5.5	5.3	21.3	2.7
		Max	19.2	13.9	23.8	175.6
Kinston	Wheat	Avg	17.1	3.2	9.4	9.5
N=4		Std Dev	2.9	0.8	2.5	2.9
n=166		Min	9.5	2.2	6.3	4.3
		Max	21.5	4.0	11.7	19.9
Oxford	Wheat	Avg	15.4	1.8	6.9	2.7
N=4		Std Dev	2.4	0.5	1.3	3.4
n=187		Min	10.7	1.3	5.8	0.0
		Max	19.3	2.4	8.7	25.5
Reidsville	Corn	Avg	19.1	19.7	21.7	56.1
N=4		Std Dev	4.9	13.0	2.4	53.7
n=161		Min	11.0	8.6	19.8	4.5
		Max	28.4	36.5	24.9	191.9

Table 2.2. Soil parameters and NO flux for various agricultural soils on which different crops were grown. N=number of sampling days; n=number of NO concentration measurements. TEN=total extractable nitrogen

	Corn	Soybean	Tobacco	Wheat
Emission Factor (A) [this study] **(ng N m^{-2} s^{-1})**	7.0	3.0	0.6	11.0
Williams' Emission Factor (A) (ng N m^{-2} s^{-1})	9.0	0.2	4.0	3.0
T_{soil} Range (^{o}C)	11.0 – 32.7	21.5 – 31.9	23.5 – 32.5	5.5 – 21.5
NO Flux [using BEIS2] **(ng N m^{-2} s^{-1})**	20.0 – 92.0	1.0 – 2.1	21.0 – 40.0	4.0 – 14.0
NO Flux [this study] **(ng N m^{-2} s^{-1})**	Range: 2.0 – 265.0 Average: 30.0	Range: 2.0 – 97.0 Average: 30.0	Range: 1.0 – 13.0 Average: 4.0	Range: 0.0 – 176.0 Average: 26.0

Table 2.3. NO emissions for this study and the results using the BEIS2 model for the corresponding range of soil temperatures observed during the study.

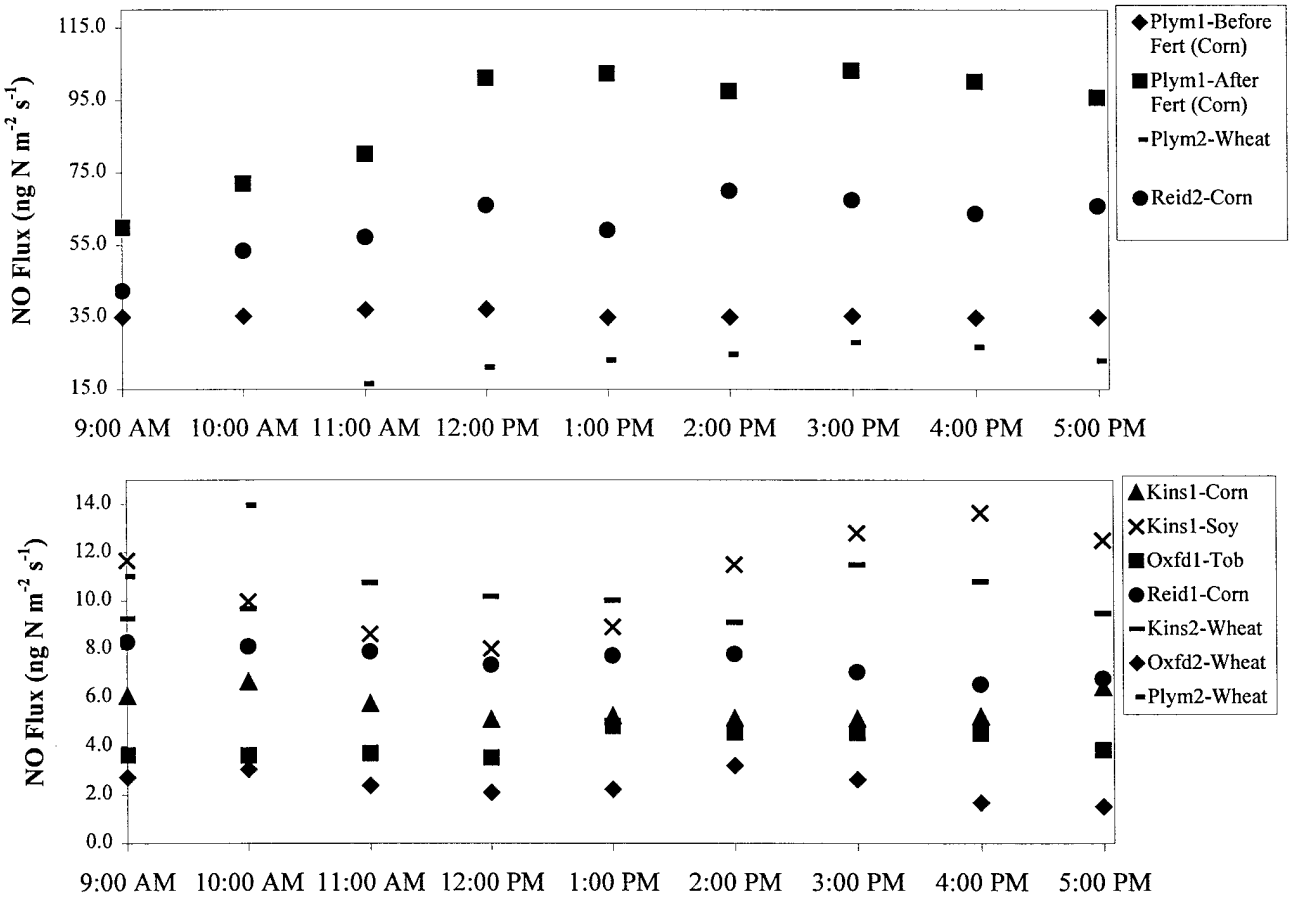

Figure 2.1. Hourly averaged NO flux (0900-1700) for each measurement site and crop type. Note the change in scale on the vertical axes-graphs have been split so that diurnal trends would be easier to discern. The 1 & 2 attached to each site name indicates the season the site was sampled, 1=late spring/summer 95; 2=spring 96.

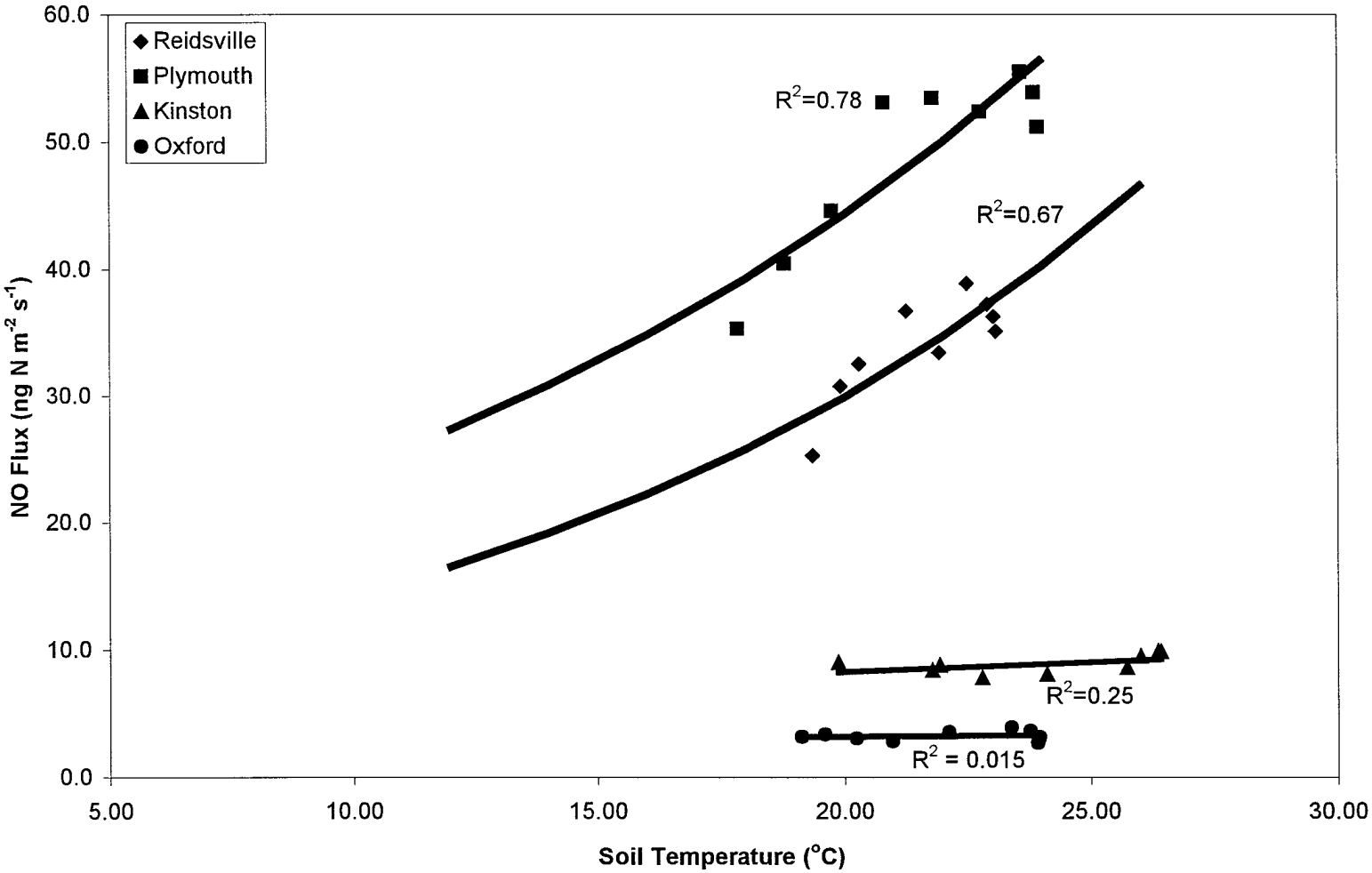

Figure 2.2. Hourly averaged NO flux plotted versus hourly averaged soil temperature (at 5 cm depth) for the composite data from the four sites where the data was collected.

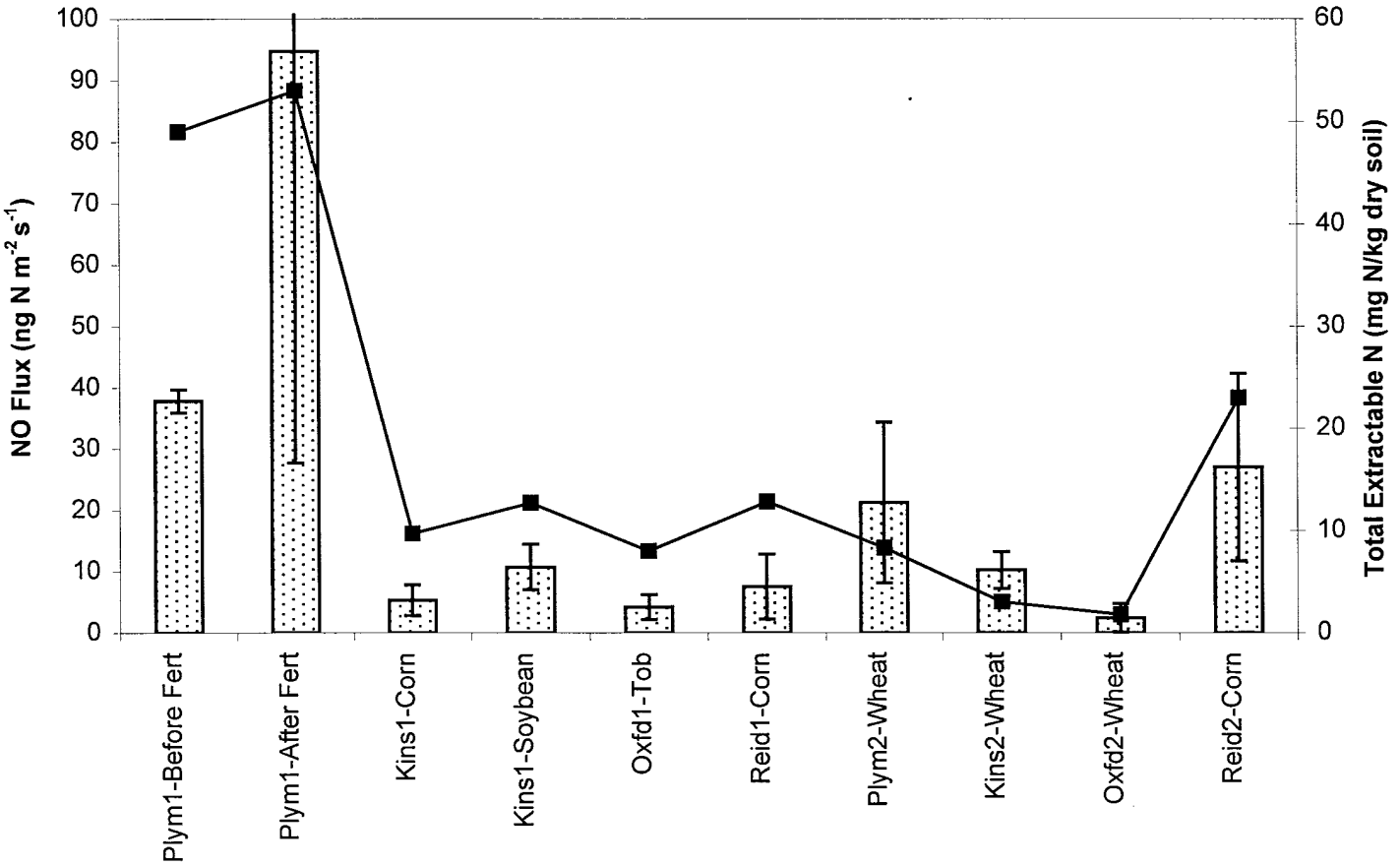

Figure 2.3. NO flux between 0900-1700 (stippled bars) and total extractable N (on secondary axis) plotted for each site. The 1 & 2 attached to each site name indicates the season the site was sampled, 1=late spring/summer 95; 2=spring 96. Error bars represent one standard deviation. One sampling day at Kinston1-Soybean, Plymouth2-Wheat, and Reidsville2-Corn, were not included in this dataset due to rainshowers occurring at the site.

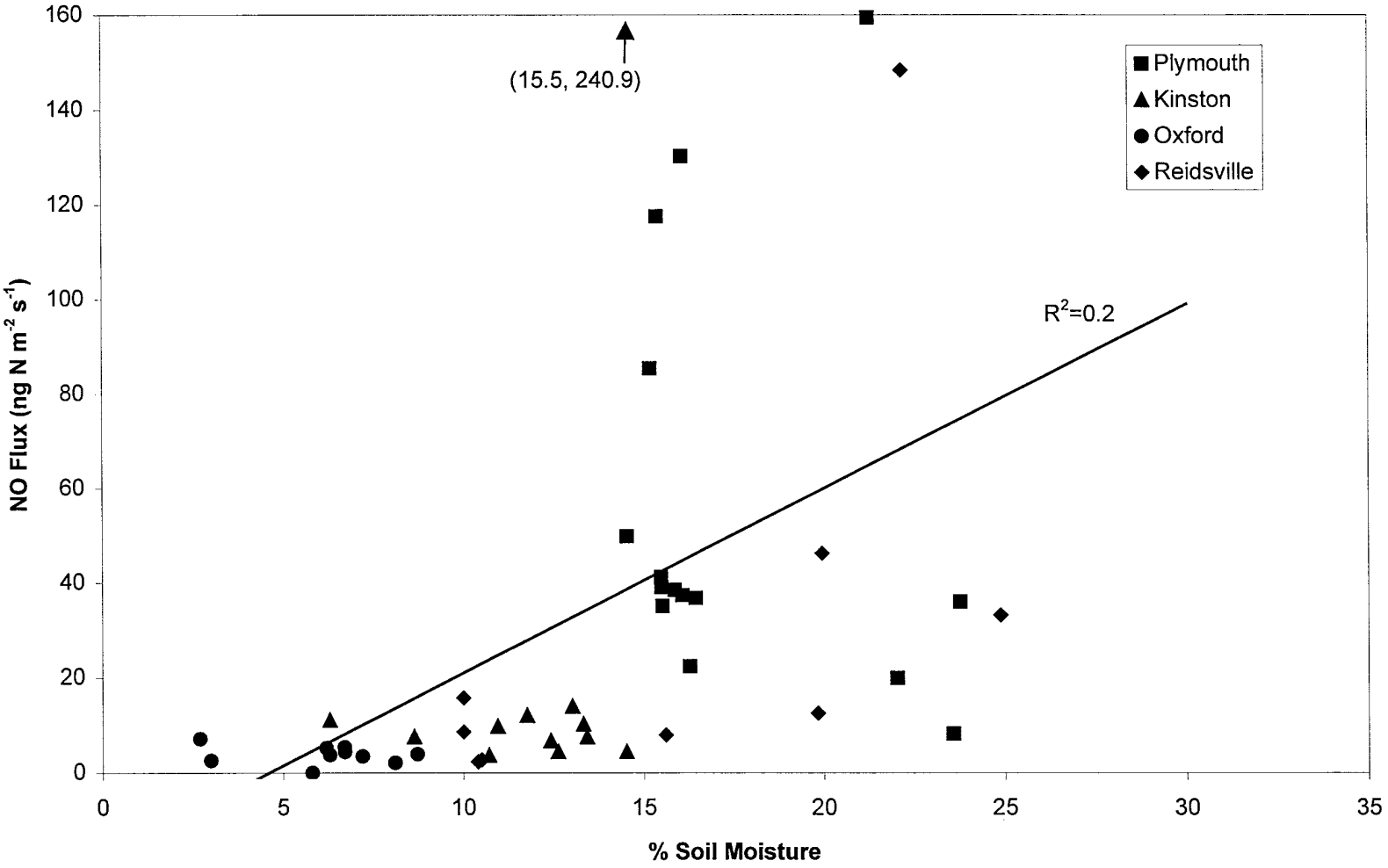

Figure 2.4. Average NO flux (0900-1700) vs % Soil Moisture. Percent soil moisture was determined from a soil sample taken from the center of the chamber footprint at the end of each measurement period. Data have been segregated into sites.

CHAPTER III. NITRIC OXIDE EMISSIONS FROM SOILS AMENDED WITH MUNICIPAL-WASTE BIOSOLIDS

by

Paul A. Roelle and Viney P. Aneja

Department of Marine, Earth, and Atmospheric Sciences
North Carolina State University
Raleigh, NC 27695-8208

Published in: Atmospheric Environment, in press, 2001.

Abstract

Spreading of nitrogen-rich municipal waste biosolids (NO_3^--N < 256 mg-N/kg dry weight, NH_3-N ~23,080 mg-N/kg dry weight, Total Kjeldahl N ~ 41,700 mg-N/kg dry weight) to human food and non-food chain land is a practice followed throughout the US. This practice may lead to the recovery and utilization of the nitrogen by vegetation, but it may also lead to emissions of biogenic nitric oxide (NO), which may enhance ozone pollution in the lower levels of the troposphere. Recent global estimates of biogenic NO emissions from soils are cited in the literature, which are based on field measurements of NO emissions from various agricultural and non-agricultural fields. However, measurements of biogenic emissions of NO from soils amended with biosolids are lacking. Utilizing a state-of-the-art mobile laboratory and a dynamic flow-through chamber system, in-situ concentrations of nitric oxide (NO) were measured during the Summer/Fall of 1999 and Winter/Spring of 2000 from an agricultural soil which is routinely amended with municipal waste biosolids. The average NO flux for the

Summer/Fall time period (9 June 1999- 3 September 1999) was 57.8 ± 34.6 ng NO-N m^{-2} s^{-1}. Biosolids were applied during September 1999 and the field site was sampled again during Winter/Spring 2000 (28 February - 9 March 2000), during which the average flux was 3.6 ± 3.9 ng NO-N m^{-2} s^{-1}. Summer accounted for 60% of the yearly emission while fall, winter and spring accounted for 20%, 4% and 16% respectively. Field experiments were conducted which indicated that the application of biosolids increases the emissions of NO and current techniques to estimate biogenic NO emissions would have underestimated the NO flux from this field by a factor of 26. Soil temperature and % Water Filled Pore Space (%WFPS) were observed to be significant variables for predicting NO emissions, however %WFPS was found to be most significant during high soil temperature conditions. In the range of pH values found at this site (5.8 ± 0.3), pH was not observed to be a significant parameter in predicting NO emissions.

Introduction

Although there have been many experiments conducted that have measured NO emissions from various soil types (Johansson and Granat, 1984; Kaplan et al., 1988; Aneja et al., 1995; Williams and Fehsenfeld, 1991; Kim et al., 1994, Roelle et al., 2001), relatively few have included intensively managed agricultural soils, or continued measurements for substantial periods of time (Anderson and Levine, 1987; Sullivan et al., 1996). In the Southeast U.S., which is NO_X limited, an increase in NO_X emissions is believed to produce a corresponding increase in O_3 levels (Fehsenfeld et al., 1993). Ozone adversely affects human health and has also been shown to reduce crop yield. Studies show that prolonged exposure to high ozone levels causes persistent functional changes in the gas exchange region of the lungs. Additionally, ozone plays a critical role in controlling the chemical lifetimes and the reaction products of many atmospheric species (National Research Council, 1991). Gaseous nitric acid (HNO_3), the end product of NO reactions in the atmosphere, combines with either aerosols or water in the atmosphere, and is removed via rain, snow, or other deposition processes, as acidic deposition.

Davidson and Kingerlee (1997) reviewed over 60 papers in order to develop a global inventory of NO emissions from soils. Their revised estimate included emissions from grasslands, desert, marshlands, tundra, forests, fertilized and unfertilized croplands. However none of the papers addressed NO emissions from land treated with biosolids from wastewater treatment facilities. A sample of the 112 different NO flux values reported by Davidson and Kingerlee (1997) is presented in Table 3.1. Although eight of

the sixty papers had larger emissions than this field study, most of the sites reported lower NO emissions. In fact, the overall average of 112 reported NO flux averages was 17.4 ng N-NO yr^{-1}, while the average from this field study was 57.8 ng N-NO yr^{-1}. In the U.S. alone, more than 6 million dry metric tons of biosolids are generated annually, and approximately 30% is spread or injected into the land (Peirce and Aneja, 2000). Given that there is a lack of field data from soils amended with biosolids may indicate a possible error in the global estimates of NO.

Methods and Materials

Biosolids

The biosolids applied to the field in this study were from a wastewater treatment facility located in North Carolina. The population which this facility serves is approximately sixty thousand people. The flow of wastewater through the plant is approximately 30.3 x 10^6 liters day^{-1}. The wastewater treatment facility consists of preliminary treatment, primary treatment, secondary treatment, disinfection and sludge treatment and disposal (Figure 3.1). Preliminary treatment is the part of the process where the wastewater is first screened for large objects via mechanical filters and then enters grit chambers where sand and inorganic solids settle out. During primary treatment, the heavier solids, which have settled to the bottom, and the lighter solids which have risen to the top, are removed from the tanks by skimming/scraping processes. The wastewater emitted from the primary treatment then enters the secondary treatment. During this step, the liquid is aerated and microbial biomass is introduced to induce nitrification. At the conclusion of the secondary treatment, the liquid is treated with

chlorine to remove any infectious organisms and then the water is released to a local stream. The heavier and lighter solids combined together, called biosolids or sludge, are then sent to the treatment part of the facility where it is prepared for land application. At this stage the biosolids are then transported, via tanker trucks, to facilities where it is stored until it can be applied to various fields. The biosolids that were used for simulated fertilization experiments were collected from the purging faucet of a digested sludge storage tank outlet. The biosolids were discarded within two weeks of being collected to avoid possible changes in their biological and chemical composition (Droste 1997). Table 3.2 is a description of the chemical composition of the biosolids. The biosolids were also analyzed for metals with the results on a dry weight basis as follows: arsenic (2.8 mg/kg), cadmium (1.8 mg/kg), chromium (29.5 mg/kg), copper (342 mg/kg), lead (48.5 mg/kg), mercury (2.9 mg/kg), molybdenum (5.7 mg/kg), nickel (8.4 mg/kg), selenium (2.0 mg/kg), and zinc (509 mg/kg). No biosolids were applied to the crop during the in-situ measurement period, therefore fertilization was simulated by applying approximately 400 ml of biosolids (an amount equivalent to what the dynamic chambers footprint area would typically receive) onto the soil surface 30 minutes prior to any measurements. Field measurements were made during summer 1999 (June-August), winter 2000 (February-March) and spring 2000 (May-June). The field studies on the biosolid amended soils were conducted during the spring and summer measurement campaigns to represent the actual times when the crop would receive biosolid applications.

Instrumentation and Flux Calculation

The chamber design, associated mass balance equation and calibration procedures are described in full in Chapter I.

Physiographic Location

NO concentration measurements were made on a property which is owned by a municipal water and sewer authority located in central North Carolina. Through a cooperative agreement, a local farmer cultivates the field and the water/sewer authority applies nutrients in the form of biosolids and limes as necessary. The crop grown during our measurement campaign was a small grain including Kenland Red Clover and Hallmark Orchard Grass, which was planted in fall 1998 and amended with biosolids in January 1999 with approximately 80 kg N/ha. (Note: this year's fertilizer data was not available and these values are from fertilizer records of the preceding year). The measurements at this field site occurred 9 June – 3 September 1999 and 28 February-9 March 2000). The field site was mowed on July 27, limed at the end of August and then received another application of biosolids in mid September (~80 kg N/ha).

Sampling Scheme

For a complete description of the sampling method used see Chapter I (Sampling Scheme).

Soil Analysis

The mineral soils at this research site are classified in the soil survey as Lignum silty loam, which is described as a moderately well drained, slowly permeable soil on the uplands with slopes of 0 to 3% (Dunn, 1977). However, soil surveys generally cover

broad areas, and a soil texture determination of our specific soil cores within the larger research site identified our samples soils as a sandy loam (Tabachow, 2000). Soil temperature was recorded every minute, and these values were binned and averaged every 15 minutes using a Campbell Scientific soil temperature probe (accuracy ± 3%) inserted 5 cm into the soil, adjacent to the chamber.

Results and Discussion

Effects of Soil Nitrogen Content and pH

The data set plotted in Figures 3.2 (a-c) represent daily average NO flux values (0900-1700) versus the daily sampled nitrogen content as Total Kjeldahl Nitrogen, NH_3 and NO_3^- respectively. As indicated by the data in Figure 3.2a, TKN is not found to be a significant variable in predicting NO emissions. However, Figures 3.2b and 3.2c reveal that the addition of ammonia or nitrate to the soil produces a corresponding increase in NO emissions. These results are to be expected based on the predominant NO production pathways, namely nitrification and denitrification processes, and the fact that the organic-N must first be converted to inorganic forms prior to nitrification or denitrification processes to occur (Warneck, 2000; Troeh and Thompson, 1993). The fact that NO increases in response to both NH_3 and NO_3^- indicates that both nitrifiers and denitirifiers are present in the soil. However, the steeper slope in Figure 3.2c may indicate that denitrification is a slightly more significant process in this biosolid amended soil system.

This field site is typically amended with biosolids twice per year and the last application prior to the summer 1999 measurement campaign was in January 1999. In order to examine how biosolid applications immediately affect NO emissions, three

experiments were conducted in which one served as a control and two experiments had biosolids applied to the soil. Previous experiments, both by the North Carolina State University Air Quality Research Group and other researchers have shown that adjacent plots with seemingly homogeneous soils can differ in NO emissions by more that an order of magnitude (Williams and Fehsenfeld, 1991; Valente et al., 1995). In order to make the experimental plot as homogeneous as possible, a depression was dug (13" x 38") large enough to accommodate two chambers side-by-side, and deep enough to simulate the depth to which the soil is tilled. Each time an experiment was conducted on this plot, the soil was removed, thoroughly mixed and then returned where it was left undisturbed for 48 hours prior to any measurements. On both biosolid-amended experiments, the biosolids were collected directly from the purging spigot of the biosolid storage tank outlet which fills the tankers used to transport the biosolids to the field sites. The biosolids were applied to the experimental plots by pouring the biosolids (~80 kg N/ha - an amount equivalent to what this size plot would typically receive) onto the soil surface 30 minutes prior to any measurements.

Figure 3.3a represents the first experiment in which no biosolids were applied to either plot. The purpose of this experiment was to see if mixing the soil had, in fact, produced a fairly homogeneous environment. Although the graph does show a slight divergence between 12:00 – 2:00 pm, in general the NO emissions measured in the two plots shows similar trends. For example, relative peaks appeared at both plots at approximately the same time (12:00, 2:30, 4:15). Further similarities were that emissions from both plots decreased during the first 2 hours of measurements which is surprising

because soil temperatures were actually increasing during this time period. Given the fact that adjacent soils can differ by orders of magnitude, and that the largest difference between these two plots never exceeded 45%, we believed that we had created an environment similar enough to examine differences between two side-by-side chambers.

Figure 3.3b represents the first of 2 experiments conducted on a plot amended with biosolids. The experiment started similarly to the unamended experiment (Figure 3.3a) in that both plots began with fluxes of NO that were within 45% difference of each other. However, unlike Figure 3.3a, the emission from the amended plot immediately began to increase while that in the unamended plot maintained a fairly steady value. From the results of this one experiment, it appears as if the plot amended with biosolids did affect the NO emissions. Figure 3.3c is a graph of the second experiment in which one of the plots was amended with biosolids. This experiment began with NO emissions at almost the same exact NO flux value. Similarly to Figure 3.3a, both plots follow very similar diurnal profiles, with relative minimum and maximum emissions occurring at approximately the same time throughout the profile. The amended plot, however, appears to respond to the biosolids application with a greater amplitude in emissions than the non-amended plot, especially in the late afternoon when the biosolids have had a chance to permeate into the top layer of the soil and come into contact with more of the bacteria which are presumed to be responsible for the production of NO.

Relationships between soil pH and NO flux in field studies have been investigated in the past and have proven difficult to discern due to the fact that pH values remain in a fairly tight range in intensively managed agricultural fields (Roelle et al., 1999). Average

pH values for this measurement period were 5.8 ± 0.30. Statistical analysis of the data measured during this campaign revealed no apparent relationship and that pH was not a predictor of NO flux at this field site. These results are corroborated by the findings of both the Ormeci et al. (1999) and Matson et al. (1997) for similar ranges of pH. Ormeci et al. (1999) reported that NO emissions reach maximum values for near neutral to lower soil pH values. Under more acidic conditions, the chemical decomposition of NO_2 and HONO, otherwise known as chemodenitrification, has been suggested to be responsible for the increased availability of NO in the soil (Galbally, 1989). Controlled laboratory experiments, in which pH was varied while maintaining constant soil temperature and soil moisture resulted in highest NO emissions when soil pH was at its lowest value (4.3) (Ormeci et al., 1999). In an extensive field study conducted in the San Juaquin Valley, CA, Matson et al. (1997) found the highest NO emissions occurring for pH< 4.0. Both studies found NO emissions to be unaffected by changes in pH in the range between 5 and 8.

Effects of Soil Temperature and Soil Water Content

An important parameter controlling NO emissions, which has been studied by many investigators, is soil temperature (Williams et al., 1992; Kim et al., 1994; Sullivan et al., 1996; Roelle et al., 1999). Biochemical rates in the soil have been shown to rise exponentially with soil temperature in the range between 15-35 °C (Warneck, 2000). The relationship most cited in the literature, and which is also used in the Environmental Protection Agencies' (EPA) Biogenic Emissions Inventory System 2 (BEIS2) is the model proposed by Williams et al. (1992) which is given by:

$$\text{Flux (ng N m}^{-2}\text{ s}^{-1}) = A*\text{Exp}(0.071*T_s) \quad (1)$$

where A = experimentally derived coefficient associated with land use categories

T_s = soil temperature (°C)

In order to examine similar exponential relationships with this dataset, the protocol used by Thornton et al. (1997) was adopted. Soil temperatures were segregated into 1.5 °C spans and the corresponding fluxes were averaged to produce one mean NO flux for each temperature span. The results of this procedure are plotted in Figure 3.4, with the corresponding regression equation and R^2 values. Because of the strong dependence of NO flux on soil temperature, the highest emissions are found during the summer. Utilizing the regression equation in Figure 3.4, and the air-to-soil temperature conversion factors described in Williams et al. (1992), we estimate that Summer (June-August) accounts for 60% of the yearly emissions, while Fall (September-November), Winter (December-February), and Spring (March-May) account for 20%, 4%, and 16% respectively. The use of the BEIS2 model would yield a different distribution of NO emissions of 44%, 24%, 10% and 22% for Summer, Fall, Winter and Spring respectively. The BEIS2 could underestimate the yearly NO emissions from biosolid-amended soils (Figure 4.4) by a factor of 26.

The relationship between emissions of NO and soil temperature discussed previously, is further confounded by the dependence of NO emissions on soil moisture content. Researchers have found that nitrification is optimized for moisture contents between 30 and 65% WFPS (Davidson and Swank, 1986; Parton et al., 1988). Recent

laboratory experiments conducted by Ormeci et al., (1999) found that the range for maximum NO emissions occurred between 20-45%.

In Figure 3.5, the data are binned into values of % WFPS of 25, 35 and 45 and soil temperatures of 15, 25, 35 °C. NO flux follows a general trend of increasing emissions as % WFPS increases within a given soil temperature, except at 25 °C. Likewise, within a given % WFPS, NO emissions increase as soil temperatures increase except at 35% WFPS. Soil temperature and %WFPS were both found to be statistically significant parameters for predicting NO emissions, however %WFPS was only significant during high (T=35 °C; R^2=0.46) and low (T=15 °C; R^2=.21) soil temperatures. The highest average NO flux occurred at 45% WFPS and 35 °C soil temperature (119.3 ng N m^{-2} s^{-1}), which is expected when considering the temperature dependence alone. However, relatively equivalent NO flux values occurring at 35% WFPS and 25 °C (114.3 ng N m^{-2} s^{-1}) seems to indicate that these conditions may also be optimum for maximizing NO production from this biosolid amended field site.

Conclusions and Recommendations

NO emissions from fields amended with biosolids were studied during Summer/Fall 1999 and Winter/Spring 2000, in order to examine what environmental parameters might control these emissions and to determine the impact of biosolids applications on soil NO emissions. Soil temperature and %WFPS are both found to be significant parameters for predicting NO emissions, however %WFPS is only significant during high (T=35 °C; R^2=0.46) and low (T=15 °C; R^2=.21) soil temperatures. When NO was modeled versus Total Kjeldahl Nitrogen and the inorganic components, NO

emissions were found to be dependent only on the inorganic N species. Further, at this field site, denitrification appeared to be the dominant process for NO production. The average NO emissions from this small grain field were up to a factor of 26 higher than what the EPA's currently used biogenic emissions model would predict for similar crop types. This leads to the conclusion that NO emissions are currently being underestimated for these biosolid-amended fields. Further, the use of the BEIS2 model estimated NO emissions in photochemical models may also be erroneous.

The practice of land applying biosolids not only serves as an economical means of disposal but also saves farmers the expense of purchasing chemically-derived fertilizers. In North Carolina, biosolid amended soils are applied in localized areas and represent a small fraction of total crop land soils (<1%), and therefore will likely represent only a small fraction of the total biogenic NO budget. However, these biosolid amended soils may act as significant sources of localized O_3 production, especially during the hot and stagnant periods of the summer when biogenic NO emissions and photochemical activity are at a maximum. Therefore future work should consist of a modeling study to examine the localized effects biosolid amended soils have on O_3 production.

References

Anderson I. C. and J.S. Levine, Simultaneous field measurements of biogenic emissions of nitric oxide and nitrous oxide, Journal of Geophysical Research, 92, 965-976, 1987.

Aneja V.P., W.P. Robarge and B.D. Holbrook, Measurements of nitric oxide flux from an upper coastal plain, North Carolina agricultural soil, Atmospheric Environment, 21, 3037-3042, 1995.

Davidson, E.A. and W.T. Swank, Environmental parameters regulating gaseous-N losses from two forested ecosystems via nitrification and denitrification, Applied and Environmental Microbiology, 52, 1287-1292, 1986.

Davidson E.A. and W. Kingerlee, A global inventory of nitric oxide emissions from soils, Nutrient Cycling in Agroecosystems, 48, 37-50, 1997.

Delany, A.C., D.R. Fitzjarrald, D.H. Lenschow, R.J. Pearson, G.J. Wendel and B. Woodruff, Direct measurements of nitrogen oxides and ozone fluxes over grassland, Journal of Atmospheric Chemistry, 4, 429-444, 1986.

Droste, R.L., Theory and practice of water and wastewater treatment, John Wiley and Sons, Inc. New York, pp. 800, 1997.

Dunn, J. Soil survey of Orange County, North Carolina, Department of Agriculture, Soil Conservation Service, in cooperation with the North Carolina Agricultural Experiment Station and the Orange County Board of Commissioners, 1977.

Fehsenfeld, F., J. Meagher and E. Cowling (Eds.), Southern Oxidants Study Annual Report, pp. 47-61, 1993.

Galbally, I.E., Factors controlling NO emissions from soils, in Exchange of Trace Gases Between Terrestrial Ecosystems and the Atmosphere: The Dahlem Conference, edited by M.O. Andreae and D.S. Schimel, 343-365. John Wiley, New York, 1989.

Johansson C. and Granat L., Emission of nitric oxide from arable land. Tellus, 36B, 25-37, 1984.

Kaplan, W.A., S.C. Wofsy, M. Keller and J.M.D. Costa, Emission of NO and deposition of O3 in a tropical forest system, Journal of Geophysical Research, 93, 1389-1395, 1988.

Kessel, M., J. Grieser, W. Wobrock, W. Jaeschke, S. Fuzzi, M.C. Facchini and G. Orsi, Nitrogen oxide concentrations and soil emission fluxes in the Po Valley, Tellus, 44B, 522-532, 1992.

Kim D.S., V.P. Aneja and W.P. Robarge, Characterization of nitrogen oxide fluxes from soil of a fallow field in the central piedmont of North Carolina, Atmospheric Environment, 28, 1129-1137, 1994.

Matson, P., M. Firestone, D. Herman, T. Billow, N. Kiang, T. Benning and J. Burns, Agricultural systems in the San Juaquin Valley: Development of Emission Estimates for Nitrogen Oxides, Technical Report, Prepared by: Department of Environmental Policy, Policy and Management, U. of Ca, Berkeley, Contract Numb: 94-732, 1997.

National Research Council, Rethinking the Ozone Problem in Urban and Regional Air Pollution, National Academy Press, pp. 1-39, 351-379, Washington, D.C., 1991

Ormeci, B, S.L. Sanin and J.J. Peirce, Laboratory study of NO flux from agricultural soil: Effects of soil moisture, pH, and temperature, Journal of Geophysical Research, 104, 1621-1629, 1999.

Parton, W.J., A.R. Mosier and D.S. Schimel, Rates and pathways of nitrous oxide production in a shortgrass steppe, Biogeochemistry, 6, 45-58, 1988.

Peirce, J.J. and V.P. Aneja, Nitric oxide emissions from engineered soil systems, Journal of Environmental Engineering, ASCE, 126(3), 225-232, 2000.

Roelle, P.A., V.P. Aneja, J. O'Connor, W. Robarge, D.S. Kim and J.S. Levine, Measurement of nitrogen oxide emissions from an agricultural soil with a dynamic chamber system, Journal of Geophysical Research, 104, 1609-1619, 1999.

Roelle, P.A., V.P. Aneja, B. Gay, C. Geron and T. Pierce, Biogenic nitric oxide emissions from cropland soils, Atmospheric Environment, 35, 115-124, 2001.

Sullivan L.J., T.C. Moore, V.P. Aneja and W.P. Robarge, Environmental variables controlling nitric oxide emissions from agricultural soils in the southeast United States, Atmospheric Environment, 30, 3573-3582, 1996.

Tabachow, R.M., Nitric oxide emissions from unamended, biosolids amended, and mineral fertilizer amended agricultural soil, MS Thesis, Department of Civil and Environmental Engineering, Duke University, 2000.

Thornton, F.C., B.R. Bock and D.D. Tyler, Soil emissions of nitric oxide and nitrous oxide from injected anhydrous ammonium and urea, Journal of Environmental Quality, 25, 1378-1383, 1996.

Thornton, F.C., P.A. Pier and R.J. Valente, NO emissions from soils in the southeastern United States, Journal of Geophysical Research, 102, 21,189-21,195, 1997.

Troeh, F.R. and L.M. Thompson, Soils and Soil Fertility, Fifth Edition, Oxford University Press, pp. 193-213, New York, 1993.

Valente, R.J. and F.C. Thornton, Emissions of NO from soil at a rural site in central Tennessee, Journal of Geophysical Research, 98, 16,745-16,753, 1993.

Valente, R.J., F.C. Thornton and E.J. Williams, Field comparison of static and flow-through chamber techniques for measurement of soil NO emission, Journal of Geophysical Research, 100, 21,147-21,152, 1995.

Warneck, P., Chemistry of the natural atmosphere, second edition, Academic Press, Inc., New York, NY, pp. 511-517, 2000.

Williams, E.J., D.D. Parrish and FC Fehsenfeld, Determination of nitrogen oxide emissions from soils: results from a grassland site in Colorado, United States, Journal of Geophysical Research, 92, 2173-2179, 1987.

Williams, E.J. and Fehsenfeld F.C., Measurement of soil nitrogen oxide emissions at three North American ecosystems, Journal of Geophysical Research, 96, 1033-1042, 1991.

Williams, E., A. Guenther and F. Fehsenfeld, An inventory of nitric oxide emissions from soils in the United States, Journal of Geophysical Research, 97, 7511-7519, 1992.

Cultivated Land – Temperate			
Location	**Description**	**Mean Flux (ng N m^{-2} s^{-1})**	**Source**
TN, USA	Corn – unfertilized	3.06	Thornton et al., 1996
TN, USA	Corn – fertilized, 111 kg N/ha	44.4	Valente and Thornton, 1993
NC, USA	Cotton – fertilized 84 kg N/ha	3.9	Aneja et al., 1995
NC, USA	Corn – fertilized, 173 kg N/ha	8.1	Aneja et al., 1995
Italy	Agricultural area, heavily fertilized with urea	91.7	Kessel et al., 1992
VA, USA	Corn and Barley – fertilized, 196.4 kg N/ha	6.9	Anderson and Levine, 1987
NC, USA	Sludge Amended soil	57.8	This Study
Grassland / Woodland – Temperate			
CO, USA	Wheat grass	8.9	Delany et al, 1986
CO, USA	Grassland	3.1	Williams et al., 1987

Table 3.1. NO emission data from different land classes. Source: Davidson and Kingerlee, 1997.

Soil, Grab Sample		Biosolids, Grab Sample	
Parameter	**Quantity**	**Parameter**	**Quantity**
Ammonia Nitrogen (NH_3-N)	< 28.6 mg-N/kg dry weight	Ammonia Nitrogen (NH_3-N)	23,080 mg-N/kg dry weight
Nitrate Nitrogen (NO_3^--N)	< 5.7 mg-N/kg dry weight	Nitrate Nitrogen (NO_3^--N)	< 256 mg-N/kg dry weight
Nitrite Nitrogen (NO_2^--N)	< 5.7 mg-N/kg dry weight	Nitrite Nitrogen (NO_2^--N)	< 443 mg-N/kg dry weight
Total Kjeldahl Nitrogen	753 mg-N/kg dry weight	Total Kjeldahl Nitrogen	41,700 mg-N/kg dry weight
pH	5.83	Phosphorus	37,350 mg-N/kg dry weight
Soil Class	Mineral	Percent Solids	3.4%
Bulk Density	1.27 g/cm^3		
Particle Density	2.44 g/cm^3		

Total Kjeldahl Nitrogen = organic N + NH_3-N + NH_4^+-N

Table 3.2. Characteristics of grab samples of the soil at the research site and of the biosolids which are applied to the field.

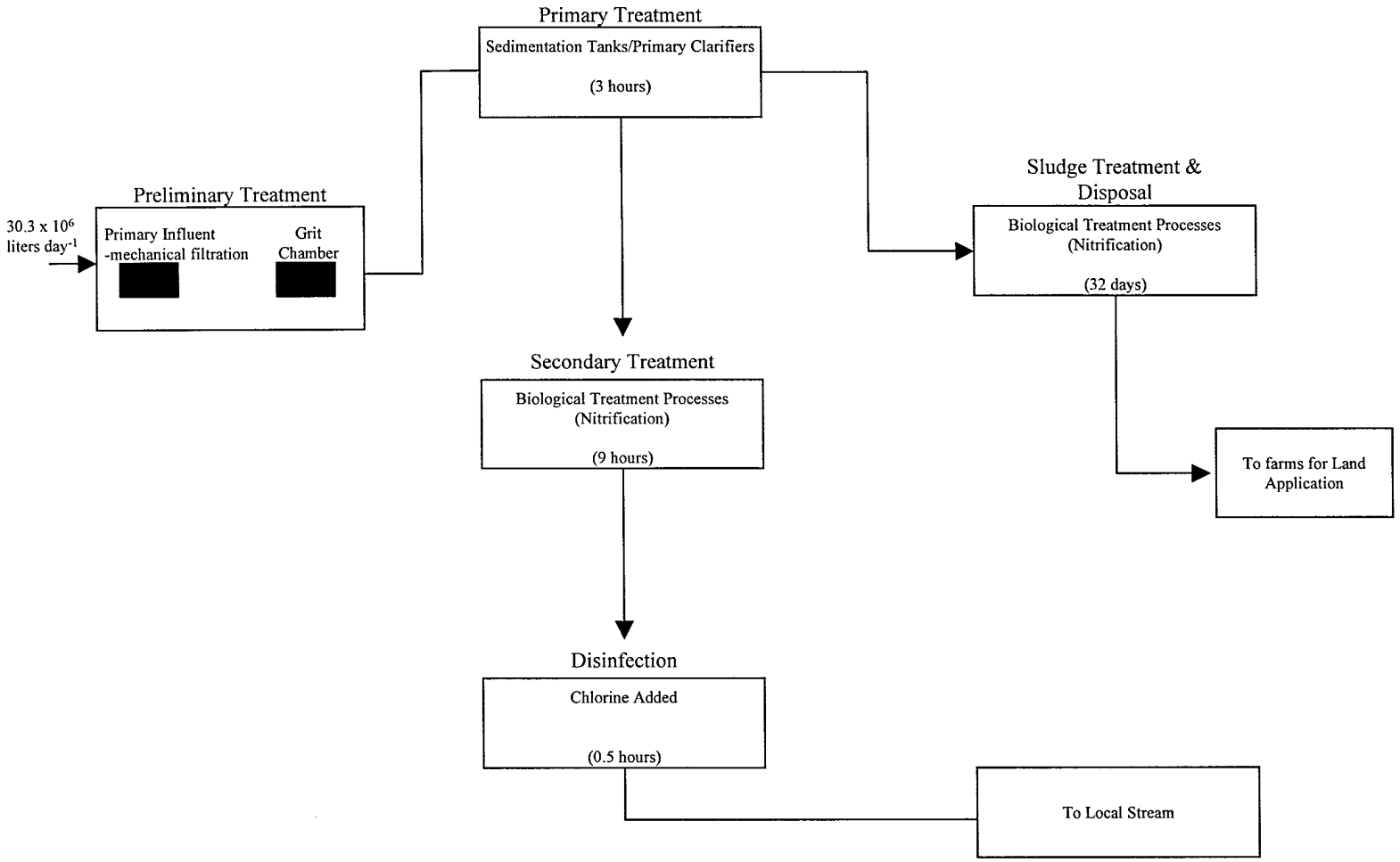

Figure 3.1. Schematic of Waste-Water Treatment Facility.

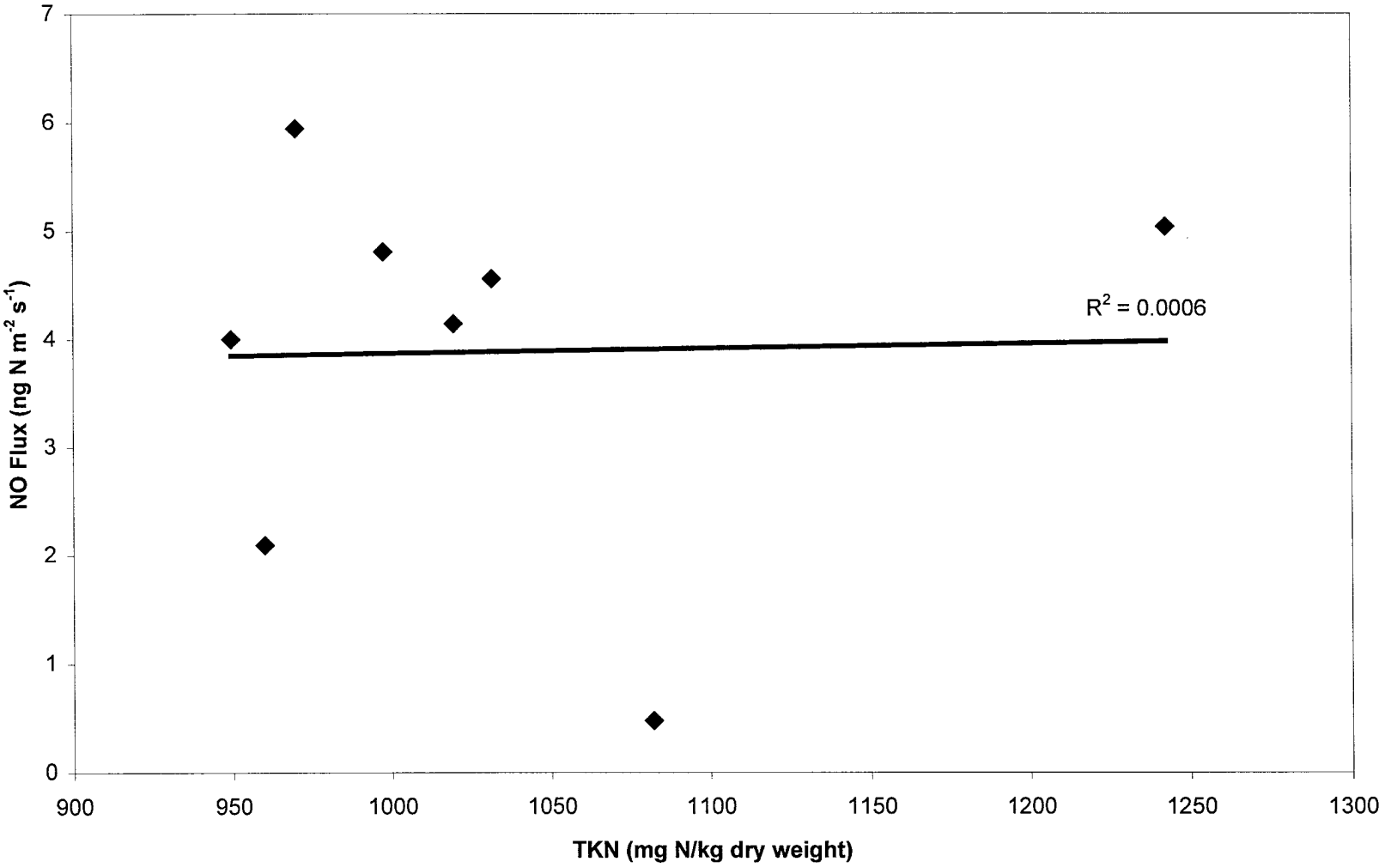

Figure 3.2a. NO Flux (ng N m^{-2} s^{-1}) plotted versus Total Kjeldahl Nitrogen. TKN=organic N+NH_3-N+NH_4^+-N.

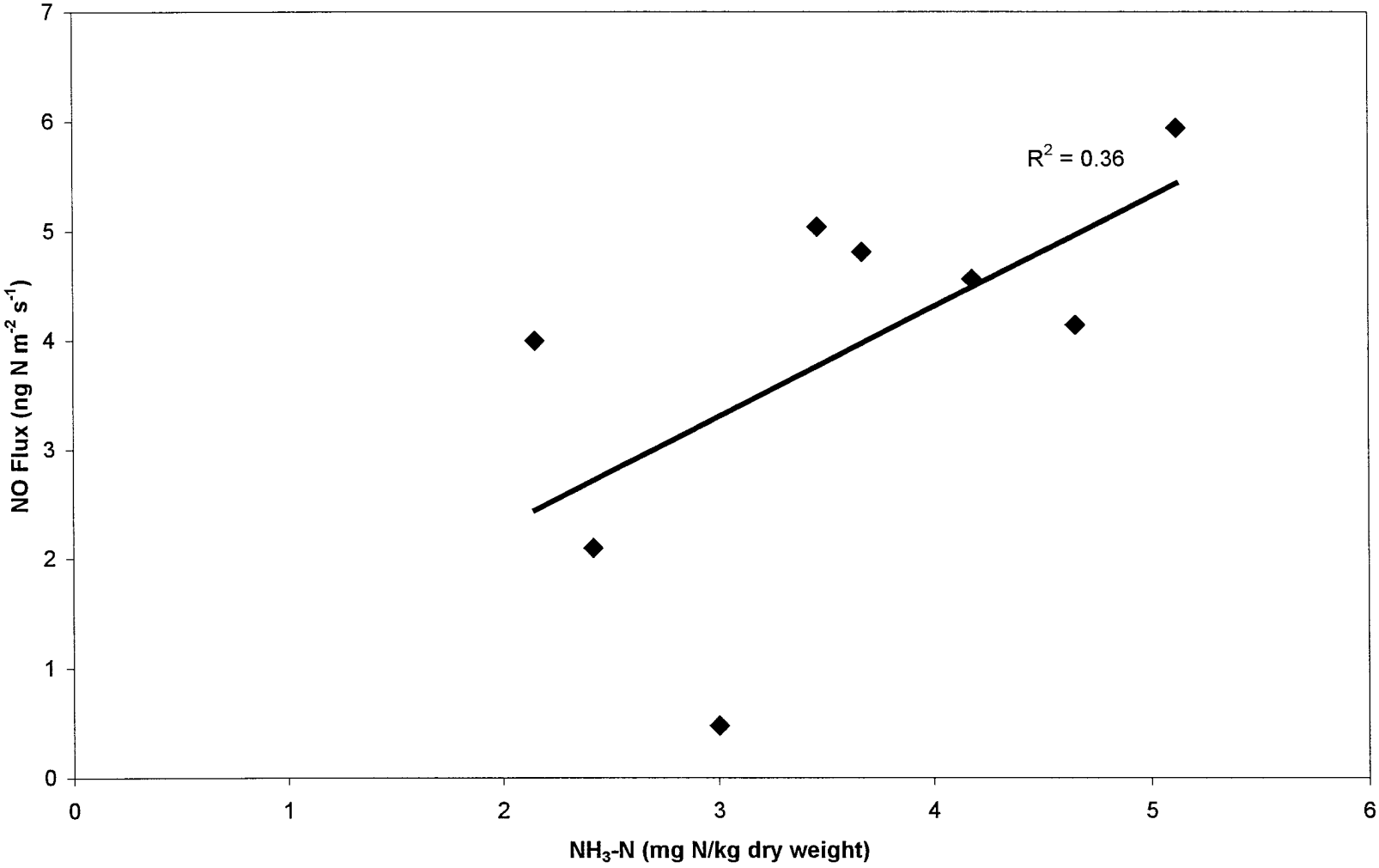

Figure 3.2b. NO Flux (ng N m^{-2} s^{-1}) plotted versus NH_3.

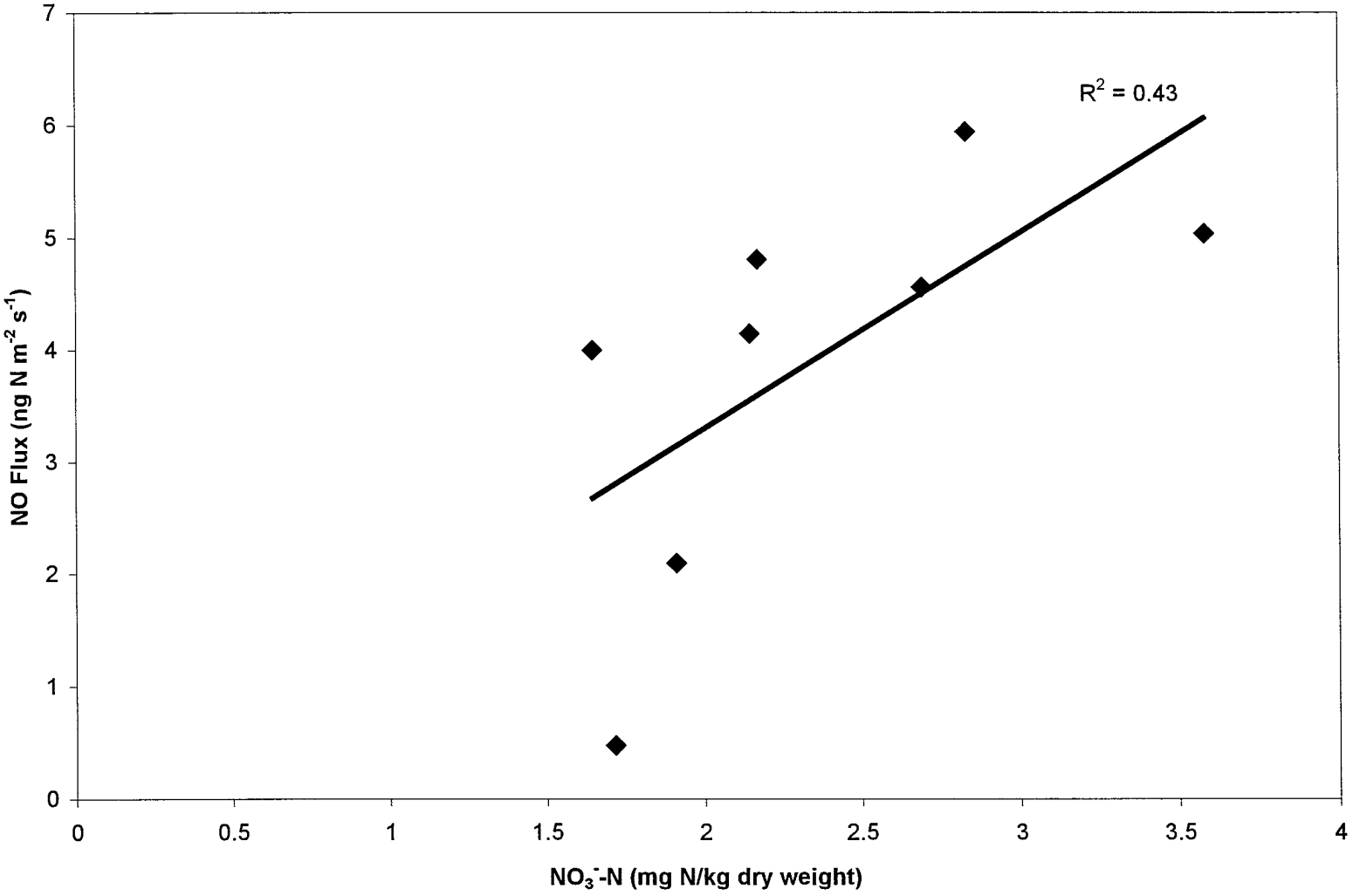

Figure 3.2c. NO Flux (ng N m^{-2} s^{-1}) plotted versus NO_3^-.

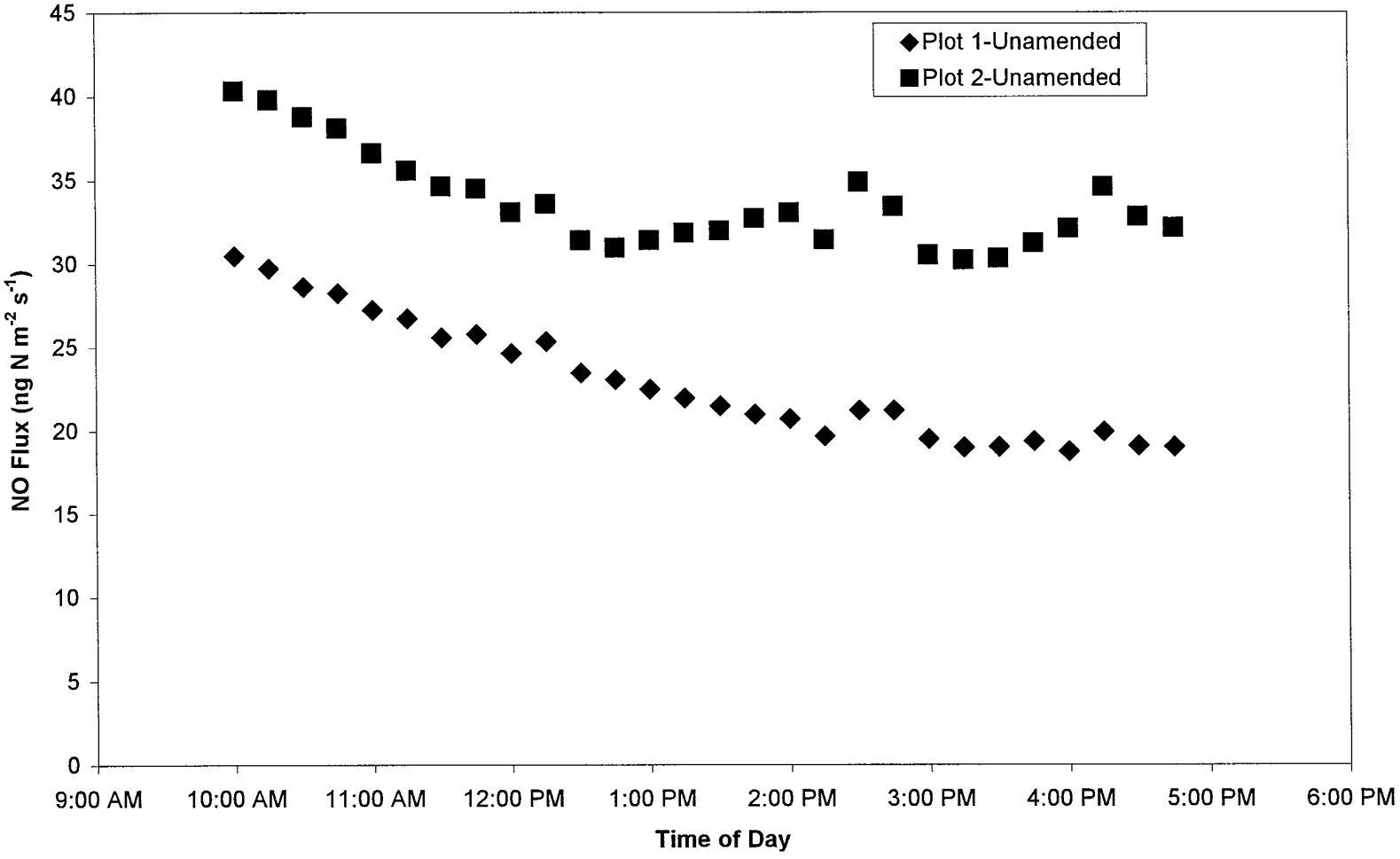

Figure 3.3a. Plot of NO Flux vs Time of Day on an unamended experimental plot (July 21, 1999).

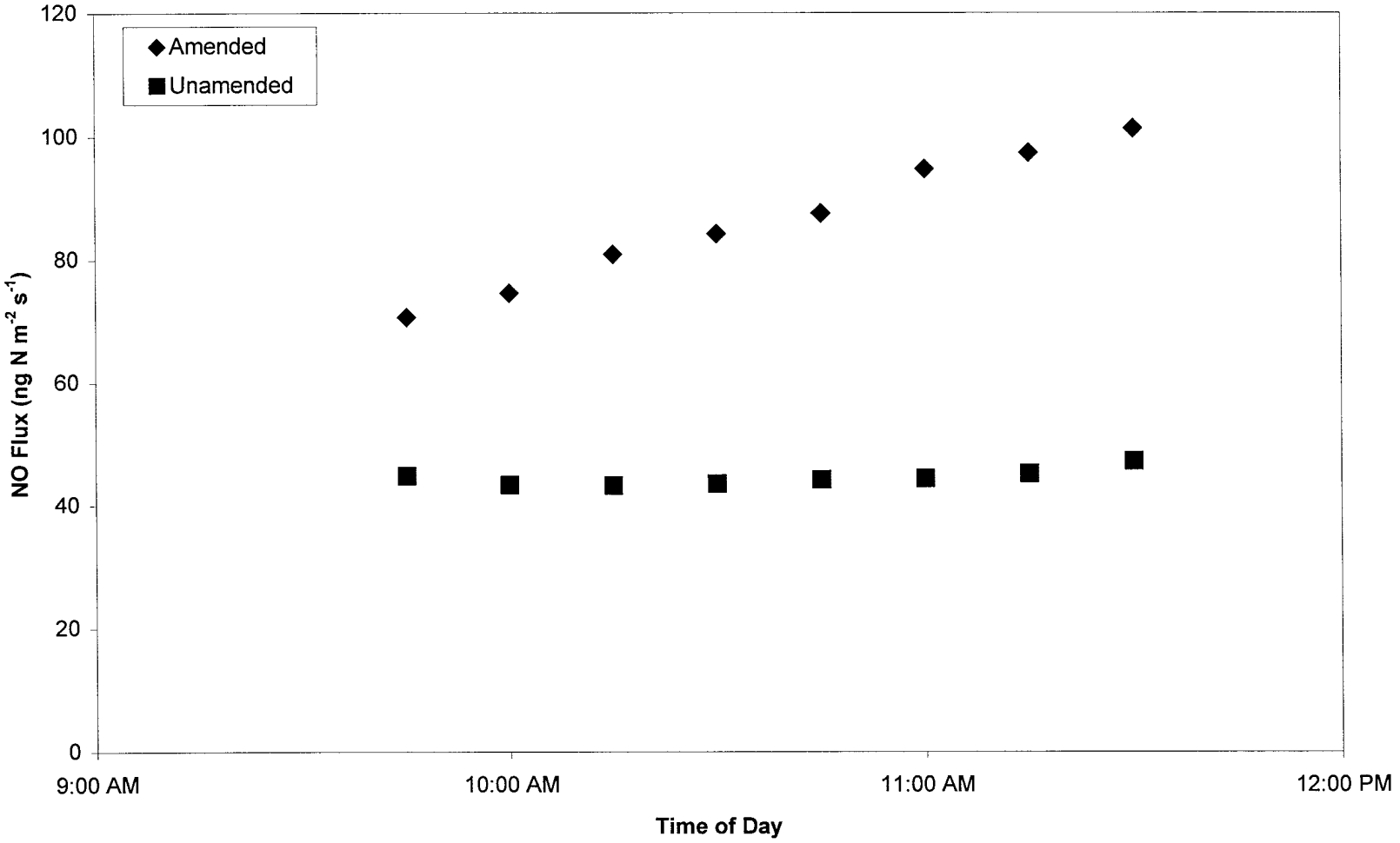

Figure 3.3b. Plot of NO Flux vs Time of Day on an amended (~ 75 ml of biosolids) experimental plot (July 23, 1999). One plot was amended with biosolids approximately 30 minutes prior to sampling. The other plot did not receive any additional biosolids.

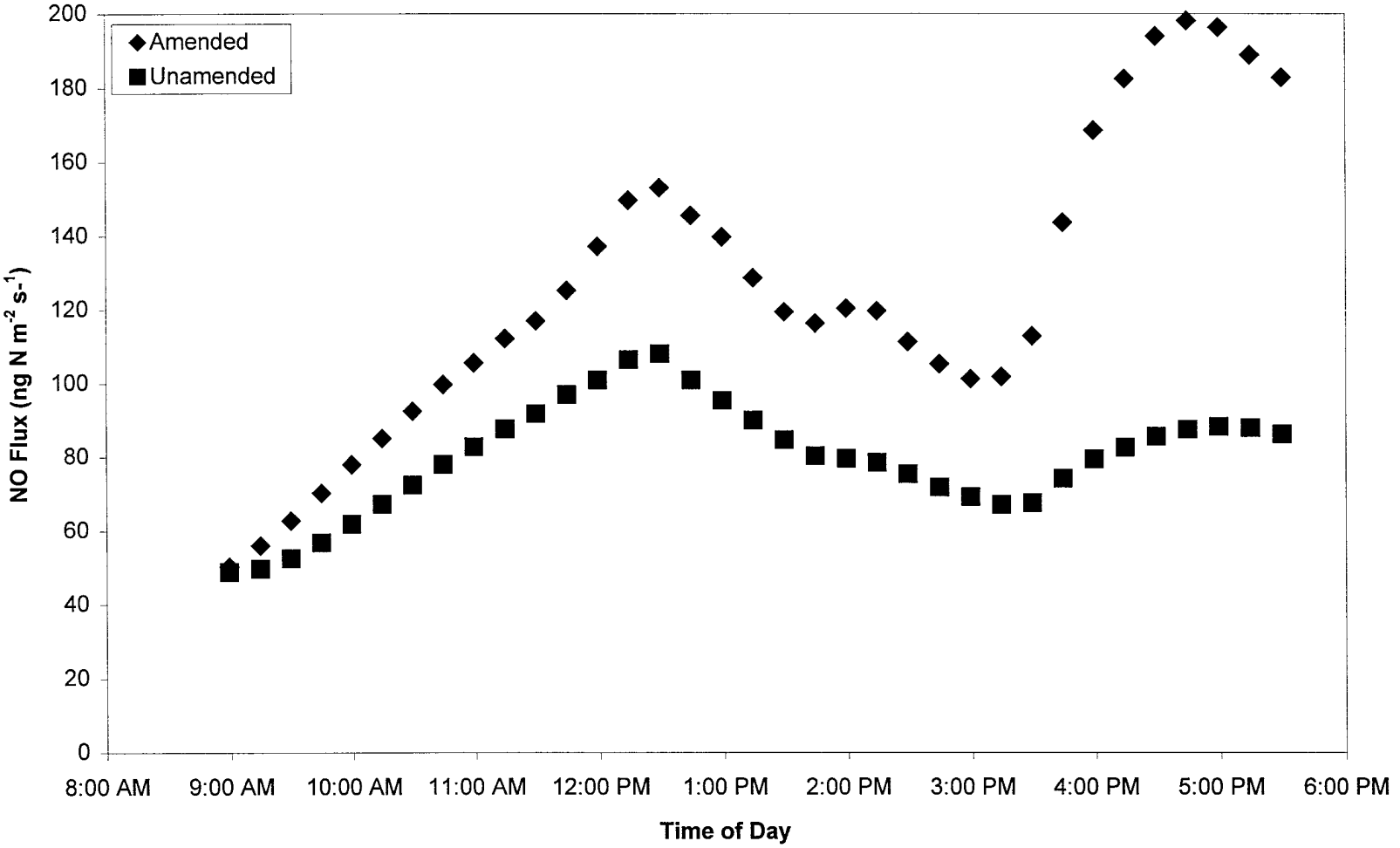

Figure 3.3c. Plot of NO Flux vs Time of Day on an amended (~ 75 ml of biosolids) experimental plot (July 29, 1999). One plot was amended with biosolids approximately 30 minutes prior to sampling. The other plot did not receive any additional biosolids.

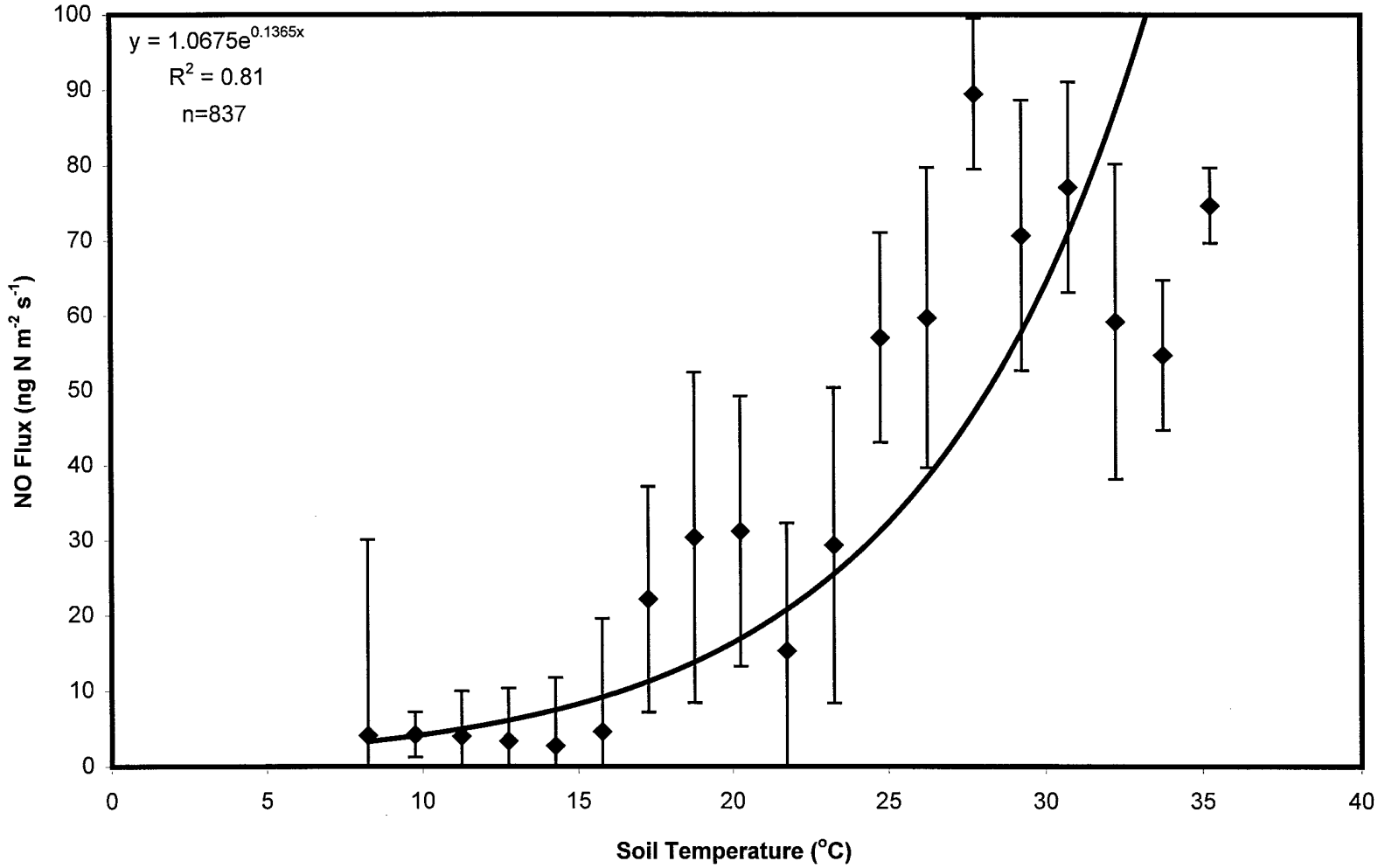

Figure 3.4. NO flux plotted versus soil temperature. NO flux has been binned into 1.5 °C temperature spans and the average flux for each temperature span is plotted.

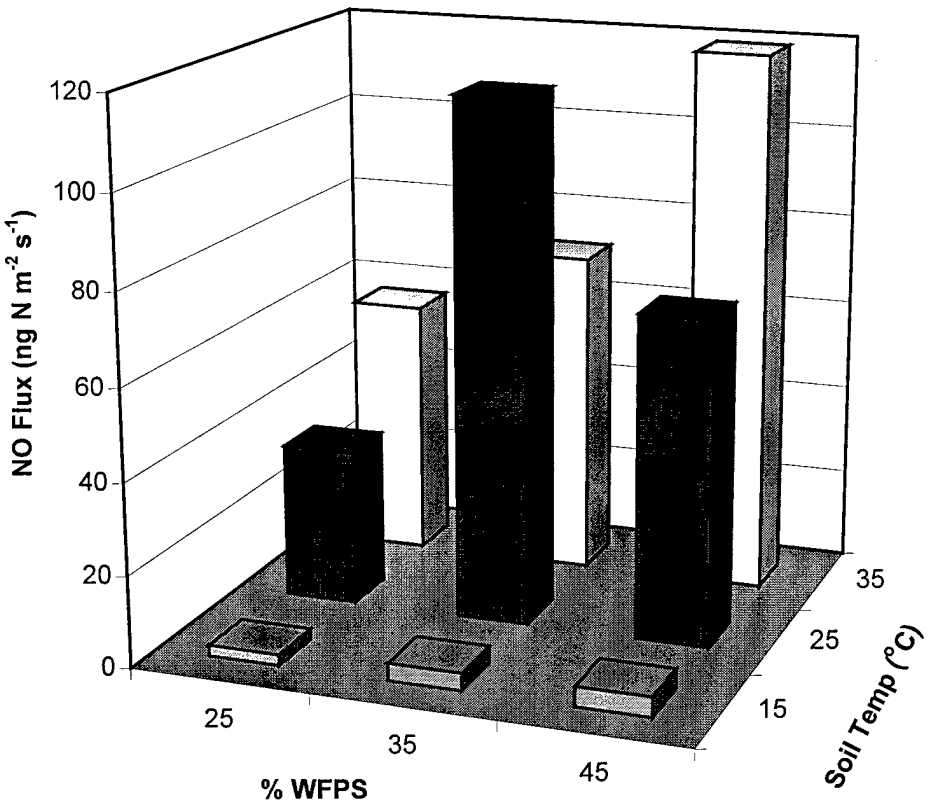

Figure 3.5. NO flux plotted versus %WFPS and soil temperature. %WFPS has been binned into values of 25, 35 and 45% and soil temperature has been binned into values of 15, 25 and 35 °C.

CHAPTER IV. MODELING OF NITRIC OXIDE EMISSIONS FROM BIOSOLID AMENDED SOILS

Abstract

Utilizing a state-of-the-art mobile laboratory in conjunction with a dynamic flow-through chamber system, in-situ concentrations of nitric oxide (NO) were measured during the summer, winter and spring of 1999/2000. The field site where these measurements were conducted was an agricultural soil amended with biosolids from a municipal wastewater treatment facility. The average NO flux from this biosolid amended soil was found to be exponentially dependent on soil temperature [NO Flux = 1.07 $\exp(0.14*T_{soil})$; R^2=0.81]. Comparing this relationship to results of the widely applied Biogenic Emissions Inventory System (BEIS) model revealed that for this field site, if the BEIS model was used, the NO emissions would have been underestimated by a factor of 26. Using this newly developed NO flux algorithm, combined with North Carolina Division of Water Quality statistics on how many biosolid amended acres are permitted per county, county-based NO inventories from these biosolid amended soils were calculated. Results from this study indicate that when the majority of North Carolina is taken into consideration, NO emissions from biosolid amended soils represent approximately 1% of the total biogenic NO emissions. However, county-level biogenic NO emissions can increase by as much as 18% when biosolid amended soils are included and depending on location and time of day the biogenic emissions can be larger than the anthropogenic NO emissions. The Multiscale Air Quality Simulation Platform (MAQSIP) was then used to model differences in ozone (O_3) and odd-reactive nitrogen (N) products (NO_y) which might be caused by differences in the estimated NO

emissions. Results showed that during the daytime, when mixing heights are typically at their greatest, any changes in O_3 or NO_y concentrations predicted by the model were insignificant and unrecognizable. However, in some locations during late evening/early morning hours and depending on how the acreages of biosolid-amended soil are dispersed throughout the model, the changes in concentration of these species can be as large as 10%.

Introduction

Although it is well established that the primary source of nitric oxide (NO) emissions into the troposphere is anthropogenic activity, soil emissions can also make a significant contribution to the NO budget (Warneck, 2000). Depending on which NO budget is considered, soil emissions and biomass burning rank either second or third behind fossil fuel combustion as the largest source of NO emissions (Table 1.1). In fact, in some regions the soil contribution has been reported to be approximately equal to the emissions from anthropogenic sources (Yienger and Levy, 1995). Because of its role in tropospheric ozone (O_3) formation, accurate inventories of NO are required to confidently run air quality models and to design and implement O_3 control strategies.

Williams et al. (1992) reported on the strong dependence of biogenic NO emissions on soil temperature and land use type. The algorithm which Williams et al. (1992) developed is one of the principal methods which researchers currently use to derive global inventories of soil NO emissions (Yienger and Levy, 1995; Thornton et al., 1997). In fact, many current air quality models derive the biogenic NO input data from the Biogenic Emissions Inventory System (BEIS2) model which is based on a temperature and land-use algorithm proposed by Williams et al. (1992). While many studies have been conducted on fallow soils, forested soils, grassland, golf course soils, agricultural soils, etc., there are comparatively fewer studies on emissions from biosolid amended soils and therefore no land-use type for this category currently exists in the BEIS2 model.

Biosolids are often applied to the soil for their beneficial nutrient content and as a cost effective way to dispose of this byproduct of the wastewater treatment process (See Chapter III for detailed discussion of biosolids). Currently in the United States, approximately 6,000,000 metric tons are generated annually (Peirce and Aneja, 2000). In this paper, a flux algorithm which has been previously developed (Chapter III) to estimate NO emissions from biosolid amended soils, will be applied to those acreages in North Carolina which receive biosolid applications. This updated NO inventory will then be used in the Multi Scale Air Quality Simulation Platform (MAQSIP) to model ozone (O_3) production on a 4 x 4 km grid scale resolution (modified case). These results will then be compared to estimated O_3 concentrations using the existing NO inventory (base case). The oxidized nitrogen species (NO_Y = $NO+NO_2+HNO_3+HONO+NO_3+N_2O_5+HNO_4+PAN+RONO_2+ROONO_2$) and ratios of these species will also be analyzed to help determine the end products of the increased NO emissions. This comparison will help to determine whether a significant error may exist in air quality models by neglecting biosolid-amended soils as a land-use class when developing the NO emission inventories.

Methods and Materials

Instrumentation and Flux Calculation

The chamber design, associated mass balance equation and calibration procedures are described in full in Chapter I.

Model

MAQSIP is a publicly available, fully modularized, three dimensional modeling framework which has been developed through a cooperative agreement between the North Carolina Supercomputing Center and the US Environmental Protection Agency's (EPA) National Exposure Research Laboratory (NERL). The current MAQSIP model was developed with various options for describing regional and urban-scale air quality through physical and chemical processes. MAQSIP was, in part, developed as a result of the dissatisfaction with the black-box type models, which only allowed the user to modify the inputs or adjust a few of the model parameterizations to optimize the performance of the model (MAQSIP Users Manual, 1998). The open approach of MAQSIP allows scientists to develop subroutines as new science becomes available, apply them in the model and then evaluate their effectiveness. In "open" type models, the rate constants and chemical mechanisms are evaluated with environmental chamber data. Different, or improved chemical mechanisms can be substituted into the model after evaluation. However the mechanisms themselves are not adjusted once they are placed within the modeling framework.

The model is designed so that fine grids (2-6 km) for urban scale simulations can be nested within coarser grids (18-80 km) for regional scale simulations, and consists of a vertical domain of up to 30 layers. The spatial resolution used in this study was a 4 x 4 km grid cell, 38 m high, where one concentration per species was calculated for each grid cell. The episode being examined is a 13-day period from June 19 – July 1, 1996, and the model domain (480 km x 276 km) covers the majority of North Carolina (see Figure 4.1).

Mixing ratios of species are determined in the model by solving the mass conservation equation for a given volume. The equation can be represented as:

$$\frac{\partial C}{\partial t} = -\nabla \cdot (VC) + \nabla \cdot (K\nabla C) + R + S \qquad (1)$$

where

C : mixing ratio of species of interest

V : velocity vector (3-Dimensional at each point in model domain)

K : eddy diffusivity used to parameterize fluxes of tracer species at subgrid-scale

S : losses due to sources and sinks (to include dry deposition)

R : changes in concentration due to chemical reactions

(MCNC, 2001; Arya, 1999)

For this simulation MAQSIP was configured to predict lower tropospheric ozone and NO_y species using: Carbon Bond IV chemical mechanism, K-Theory for turbulent redistributions of pollutants in the vertical and a dry deposition scheme (McHenry et al., 1999).

Carbon Bond IV Mechanism (CBM IV)

Computational power currently limits the ability to explicitly represent the chemistry of the hundreds of organic species in the troposphere (Gery et al., 1989). Therefore, to be able to represent these reactions, the common chemistry of the reactive hydrocarbons are grouped together. Two different grouping approaches have been attempted, namely structural and molecular grouping, where the former involves grouping according to the type of bond (ie, single carbon bond, double carbon bond, etc.),

and the latter groups common reactions of entire molecules (Gery et al., 1989). Grouping by bond type has been found to be a favorable approach as there are many fewer categories to consider as opposed to the large number of organic species in the atmosphere. The carbon bond approach categorizes the species as follows:

1) inorganic species
2) organic species that, because of their unique chemistry, are treated explicitly
3) organic species that are represented by carbon bond surrogates
4) organic species that are represented by molecular surrogates

(Gery et al., 1989).

This approach, which contains over 200 chemical reactions, was found to be too computationally extensive and was paired down to the approximately 80 reactions now present in CB IV. Both the larger mechanism and CB IV were tested in smog chamber studies and both performed well without any consistent bias between the two models. The current Carbon Bond IV principle mechanism is listed in Table 4.1.

K Theory Scheme for Turbulent Vertical Re-Distribution of Pollutants:

Accurate representation of the atmospheric boundary layer is important to air quality modelers, as conditions in this layer dictate the vertical extent to which the pollutants can be mixed. The model uses the general form of the following dynamic and thermodynamic equations:

$$\frac{\partial u}{\partial t} = -u\frac{\partial u}{\partial x} - v\frac{\partial u}{\partial y} - \frac{\partial}{\partial z}\left(\overline{u'w'}\right) - f\left(v_g - v\right) \qquad (2)$$

$$\frac{\partial v}{\partial t} = -u\frac{\partial v}{\partial x} - v\frac{\partial v}{\partial y} - \frac{\partial}{\partial z}\left(\overline{v'w'}\right) + f\left(u_g - u\right) \qquad (3)$$

$$\frac{\partial T}{\partial t} = -u\frac{\partial T}{\partial x} - v\frac{\partial T}{\partial y} - \frac{\partial}{\partial z}\left(\overline{w'T'}\right) \tag{4}$$

$$\frac{\partial q_v}{\partial t} = -u\frac{\partial q_v}{\partial x} - v\frac{\partial q_v}{\partial y} - \frac{\partial}{\partial z}\left(\overline{w'q_v'}\right) \tag{5}$$

u: eastward component of the wind

v: northward component of the wind

u_g: eastward component of the geostrophic wind

v_g: northward component of the geostrophic wind

$(\overline{\quad})$: turbulent fluxes

z: altitude

f: coriolis parameter

q_v: mixing ratio of water vapor

T: temperature

Explicitly solving for the turbulent fluxes is both computationally expensive and time consuming, making it impractical for real-time air quality forecasting. Therefore to solve for these turbulent fluxes, they are assumed to be related to the mean gradients, as initially proposed by J. Boussinesq in 1877 (Arya, 1999), and solved using gradient theory.

Dry Deposition Scheme

Dry deposition is defined as airborne gaseous and particulate matter being transferred to the earth's surface (Arya, 1999). Early air quality models used constant deposition velocities (V_d) in either time or space, which various researchers have shown

to be a poor assumption (Hicks et al., 1982; Wesely et al., 1985). These researchers have shown that deposition of various trace gases and particulates have considerable variability depending on meteorology, land-use type, insolation and season, particulate size, etc. Deposition velocity is used to calculate the flux of the pollutant in question to a surface through the following expression:

$$V_d = \frac{\text{Flux}}{[C]_{\text{pollutant}}} \tag{6}$$

The constant (V_d) approach led to inaccurate deposition estimates of trace gases and particulates when applied to large regions with different topography and meteorological conditions. Walcek et al., (1986) have described a method for computing maps of deposition velocities which account for meteorology and land use type. In their model, they use fine resolution meteorological model output and land use data from the United States Environmental Protection Agency to adjust the deposition velocities that are then used in the MAQSIP model.

Emissions Data

Emission inputs into MAQSIP are provided by the Sparse Matrix Operator Kernel Emissions (SMOKE) modeling system. The submodels for SMOKE are biogenic, mobile, area and point emissions (Figure 4.2), which eventually are merged to produce emissions that are ready for input into the models timeline and grid system. The biogenic emissions processing submodel is essentially the Biogenics Emissions Inventory System 2 (BEIS2) model which has been slightly modified to be compatible with SMOKE. The

biogenic sources include Volatile Organic Compounds (VOCs) from plants and trees and NO_x emissions from soil processes.

Prior to any emission inventories being produced, accurate representation of the meteorological conditions must be produced as many of the emission processes are dependent on the temperature fields. Meteorological files for MAQSIP are provided by the Pennsylvania State University (PSU) and National Center for Atmospheric Research (NCAR) mesoscale model 5 (PSU/NCAR MM5). A schematic of the inputs and outputs of MAQSIP can be seen in Figure 4.3.

Currently, biogenic nitric oxide emissions are estimated in BEIS2 through a temperature and land-use relationship described in Williams et al. (1992), where

$$\text{NO Flux (ng N m}^{-2}\text{ s}^{-1}) = A*\text{Exp}(0.071*T_s) \quad (7)$$

The coefficient, A, is an emission factor that is experimentally derived and based on land use. T_s (°C) is soil temperature which is computed via air temperature (T_a in °C) through the following algorithm, given by Williams et al. (1992):

Grasslands	$T_s=0.66T_a+8.8$	(8)
Forests	$T_s=0.84T_a+3.6$	(9)
Wetlands	$T_s=0.92T_a+4.4$	(10)
Agriculture	$T_s=0.72T_a+5.8$	(11)

For each of the 4 x 4 km grid cells (=1600 ha) in the model domain, statistics are available which describe the land-use in that grid cell. An example of these statistics are shown in Table 4.2. Each 4 letter code corresponds to a crop, tree or land use type and has an associated acreage and an emissions factor that is used for calculating the NO flux.

In general, the emission factors will be highest for those crops which receive the highest applications of nitrogen fertilizer (ie, corn, cotton, wheat), as increased N fertilization has been shown to increase NO emissions (Sullivan et al., 1996; Roelle et al., 1999). While this land use approach is a significant improvement over the earlier methods which assumed constant NO emissions across all crops or forest types, it still fails to capture the emissions from all land-use types. For example, if a rye crop were fertilized with biosolids, it would be treated in the model as having an NO factor of 12.8 $\mu g\ m^{-2}\ h^{-1}$. An earlier study (Chapter III) showed that a rye crop amended with biosolids generates an NO emission factor closer to the value for corn (550.5 $\mu g\ m^{-2}\ h^{-1}$). Using daily averaged temperatures, Figure 4.4 shows how the BEIS2 model would have underestimated the NO emissions during all seasons. Therefore this study proposes to modify the current NO inventory (base case) so that these biosolid amended acreages are represented in the biogenic NO inventory (modified case).

Source Apportionment

The process of applying biosolids to soils in North Carolina requires a permit from the North Carolina Division of Water Quality. The Division of Water Quality maintains a database of all existing permits on a county-basis and although restrictions do exist that dictate where and when the biosolids can be applied, there is no restriction upon which crop they are applied (Barnett, 2000). For the purposes of this study, the acreages of biosolid amended soils within each county are assumed to be equal to the existing permits issued. Figure 4.5 represents the area of North Carolina within the model domain and the respective acreages of biosolid amended soils within each county.

It is not possible to ascertain where within each county the biosolids are applied, therefore the procedure used to apportion the biosolids within a county was to distribute them so that each 4 x 4 km grid cell within the county had the same percentage of biosolid amended soil in its respective cell. County boundaries do not follow the same boundaries as the grid cells, and therefore there were often cells that contained acreages in two counties. In these instances, the county surrogate data, which identifies the fraction of a grid cell within a county, were used to apportion the biosolids accordingly. It is estimated that ½ of the total cost of wastewater treatment is tied to disposal (Viessman and Hammer, 1993). Consequently, transporting distances will, in part, dictate where these biosolids are applied and evenly distributing the biosolids throughout the county may not be the most likely scenario. Therefore, in another scenario we have also analyzed the impact of concentrating the biosolids in only one area of the county. These two scenarios should be viewed as bounds which can be used to assess the significance of biosolid application in terms of changes in ozone or NO_y concentrations.

The new biosolid amended acreage for each grid cell could not simply be added back into Table 4.2, because this would cause the total acreages within each grid cell to be too large (ie, total acreages in each cell would now be 1600 ha + biosolid amended acres). Because the crops or land-use types receiving the biosolids could not be identified, the biosolid category was substituted for the Mscp (Miscellaneous Crop) category in all instances. For example (in Table 4.2), if grid cell 001 001 was determined to contain 50 ha of biosolid amended soils, then category Mscp would be reduced to 484.8 ha and a new category of biosolid amended soils would be added with an acreage

of 50 and the emission factor for the biosolid amended soil (calculated previously) would be applied to this acreage. It was now possible to account for the biosolid amended soil and determine a new NO inventory for each grid cell in the model domain.

The increase in biogenic emissions of NO resulting from the biosolids applications was determined for each of the counties in the model domain to produce a modified NO inventory. The average increase of biogenic NO in each of the North Carolina counties in the model domain can be seen in Figure 4.6. For example, in Gaston County NC, approximately 18% of the biogenic NO is due to these biosolid amended soils, and in Brunswick County, Forsyth County, Granville County and Wake County, the contribution from biosolid amended soils is 10%, 14%, 9% and 7% respectively. Similarly, applying all the biosolids in concentrated areas resulted in 1-2 grid cells being modified in each of the 5 counties with the highest biosolid land application rate. The cells which were selected and the factors by which the biogenic NO emissions increased in each of these cells can be seen in Figure 4.7.

Results and Discussion

Figure 4.8 shows the relative contributions to the NO inventory from biogenic and anthropogenic sources for the entire model domain and for the 5 counties with the largest application rates of biosolids. Over the entire model domain, the biogenic emissions represent approximately 5% of the anthropogenic emissions. Surprisingly, for the 5 counties with the greatest applications of biosolids (with the exception of Granville County) the biogenic emissions make up an even smaller fraction than the overall model average of 5% (Brunswick County~1%; Gaston County<1%; Granville

County~11%;Wake County~2.5%; Forsyth County~1%). While this may at first seem contradictory, this relationship can be explained by a combination of population centers and power generation locations (Figure 4.9).

Biosolids are produced as a byproduct of the municipal waste-water treatment process (Chapter III), therefore those areas with the densest populations will produce the greatest quantity of biosolids. In these more densely populated counties (or adjacent counties), if land application is the chosen method of handling (as opposed to the costlier methods of land-filling or incineration), there will be greater land application rates (ie, Gaston County and Wake County, Forsythe County). These densely populated urban areas have greater vehicular activity, and in some instances have large power production facilities and therefore have NO budgets dominated by anthropogenic sources. This effect can clearly be seen in Figure 4.10, which shows the strong mobile NO_x source strength near Gaston County, Wake and Forsyth Counties, and to a lesser extent, Brunswick and Granville Counties. Although Brunswick County is less affected by mobile sources, the biogenic NO contribution is still overshadowed by the utility sources (Figure 4.9).

When the data from Figure 4.8 is hourly averaged over the entire model domain (Figure 4.11), several interesting observations become apparent. First, the peaks in both curves are in phase, occurring in the late afternoon, which is to be expected based on the biogenic temperature dependence and vehicle driving patterns which reach a maximum during the late afternoon. The two relatively lower peaks in anthropogenic emissions which occur at approximately 75,100, 250 and 270 hours are during weekends when

vehicular traffic is generally at a minimum (Figure 4.12). What is most revealing in Figure 4.11 is the large standard deviation in anthropogenic emissions indicating that relatively few of the grid cells in the model domain are responsible for the majority of the emissions. Upon inspection of the individual grid cells it was found, as expected, that those grid cells responsible for the majority of the emissions were located in and around where the power plants were located (Figure 4.9). Furthermore, the anthropogenic emissions vary by as much as a factor of four throughout the diurnal profile, whereas the biogenic emissions vary by only 30%. The combination of these two effects (location within the model domain and time) indicates that on a localized scale, the biogenics could represent a significant fraction of the total NO emissions and may therefore be important in terms of developing accurate air quality models.

An example of the temporal and spatial relationship can be seen in Figure 4.13 (a-b) which shows the variation in the ratio of biogenic NO emissions to the anthropogenic emissions. In Figure 4.13a (weekday, mid-afternoon), the biogenics in Granville County are at most 40% of the anthropogenic source strength, and only in a few remote locations. The white line extending from the southwest corner of the county to the northeast reflects Interstate 85 and the dominance of mobile sources. Figure 4.13b represents a weekend early-morning episode which shows how the biogenics now begin to dominate the anthropogenics, in some instances by an order of magnitude, throughout the more rural portions of the county. Similar analyses were conducted for other counties with the same results and therefore in the analysis of the MAQSIP model runs, those areas and time

periods in which biogenics make the most significant contribution to the total NO budget will be most closely scrutinized.

In Figure 4.14 (a-c), the change in O_3 concentration ($\Delta[O_3]$) (Modified Case - Base Case) in pptV is plotted beginning the evening (8:00 pm) of Wednesday, June 26 and ending after sunrise (8:00 am) on the following day. In Figure 4.14a, the areas of greatest $\Delta[O_3]$ are observed to coincide with the areas of greatest biosolid application (Figure 4.5). Furthermore these areas are all negative in value, as shown by the scale to the side of the figure, indicating ozone depletion. During the early morning (Figure 4.14b), the same pattern of O_3 depletion occurs but in greater magnitude. As daylight approaches (Figure 4.14c), the same regions of maximum biosolid application continue to have the largest $-\Delta[O_3]$, however the magnitudes begin to get smaller.

Similarly to the weekday episode, a weekend morning (Figure 4.15a) shows O_3 being consumed in the largest quantities where the biosolid application is the greatest. Interestingly, while the large urban centers continue to indicate ozone depletion, some of the more rural areas which also had high biosolid application rates are beginning to show modest increases in O_3 production. This relationship could confirm that some areas in North Carolina may be NO_x limited, meaning an increase in the NO_x emissions results in increased $[O_3]$. The early morning plot (Figure 4.15b) shows approximately the same trends as the weekday plot, where regions of greatest biosolid application contribute the most to the O_3 depletion. Throughout the daylight hours (~ 8:00 am – 8:00 pm), no consistent changes in $[O_3]$ (other than patterns similar to the one shown in Figure 4.15a) were observed on any of the modeled days. This same diurnal pattern of decreasing $[O_3]$

throughout the evening, reaching a maximum $-\Delta[O_3]$ before sunrise and then gradually returning to unrecognizable changes throughout the daylight hours was evident during all of the modeled days and can be explained by the combined effects of meteorology and chemistry.

Figure 4.16 shows the diurnal variation of the mixed layer, depicting how it grows to its maximum in the afternoon coinciding with the maximum daytime heating. It is therefore expected that the greatest impact of any increased NO emissions would occur during the morning/evening hours when they are confined to the smallest mixing volume. Any increased emissions during the daytime would be rapidly diluted as the species mix through a significantly greater volume of the troposphere. The influence of chemistry is based on the following equation: $NO + O_3 \rightarrow NO_2 + O_2$, which acts to remove O_3 throughout the night. During the evening when the boundary layer is confined, and the biogenic NO source strength is increased as a result of the biosolids, ozone consumption is increased and most evident in areas of greatest biosolid application, as shown in Figures 4.14 and 4.15. However, as was shown in Figure 4.15a, there may be a few hours prior to the boundary layer reaching its maximum that the increased NO results in slight increases of $[O_3]$.

It should be pointed out that all of the $\Delta[O_3]$ data presented in Figures 4.14 and 4.15 are in units of pptV whereas ambient concentrations of O_3 during this same time period are typically on the order of 1-100 ppbV. At no time during the daylight hours does the $\Delta[O_3]$ approach the same order of magnitude as the ambient concentrations and is typically several orders of magnitude smaller indicating that during periods of greatest

mixing the increase in NO has negligible consequences on overall ozone formation. The simulation with the overall greatest change in [O_3] is plotted in Figure 4.17 along with a time series of the data throughout a diurnal cycle. This relationship highlights that daytime ozone concentrations are unaffected by the increased biogenic NO emissions and that any change at night consists of slight ozone depletion (<1%).

Applying all biosolids in a concentrated region of the county, as described in Figure 4.7, produces more pronounced results. Figure 4.18 shows the percentage change in [O_3] and the corresponding time series of this change throughout a diurnal cycle at a Gaston County location. Like the other plots, the biggest change in [O_3] occurs at night and consists of ozone depletion. Whereas in the earlier method of evenly distributing the biosolids throughout the county resulted in changes of less than 1%, the highly concentrated biosolid areas now see ozone being depleted by as much as 11%. Further, for the first time, consistent trends of increased ozone production (>1%) during afternoon hours were evident, albeit at values less than 3%.

In addition to O_3 production, as NO is oxidized it also gives rise to new compounds which are often grouped together in the family called NO_y. This family of odd-reactive nitrogen species consists of NO_x ($NO+NO_2$), nitric acid (HNO_3), nitrous acid (HONO), the nitrate radical (NO_3), dinitrogen pentoxide (N_2O_5), peroxynitric acid (HNO_4), peroxyacetyl nitrate (PAN) ($RC(O)OONO_2$), alkyl nitrates ($RONO_2$) and peroxyalkyl nitrates ($ROONO_2$). Figure 4.19 shows the percentage increase in NO_y concentrations between the modified case and the base case where the bioslids have been evenly distributed throughout all grid cells in the county. Also included in Figure 4.19 is

the time series of the data with the greatest percentage increase throughout a diurnal cycle which was observed to be in Brunswick County. As shown in the graph, any change in [NO_y] during daylight hours was imperceptible within several orders of magnitude, and the maximum change throughout the evening was an increase in [NO_y] of ~ 2%.

NO_y, which is a quasi-conserved quantity, is of significant atmospheric interest because through ratio analysis it is possible to examine the fate of the increased nitrogen and also to determine relative aging of an airmass (Roberts, 1995). For example, Figure 4.20 is a plot of the ratio of NO_x/NO_y which shows that near the large urban centers, the majority of NO_y exists as NO_x. However, in more rural areas, the NO_x emitted into the atmosphere upstream begins to be converted into organic and inorganic nitrates and therefore makes up a smaller fraction of the NO_y. During the nighttime, the increase in [NO_y] observed in Figure 4.19 can almost solely be attributed to the increased NO, as investigation of the changes in the ratios of all the individual species to NO_y resulted in changes of less than .01%.

Conclusions and Recommendations

Comparing the NO flux algorithm developed in an earlier study (Chapter III) to results using the BEIS2 algorithm (Base case) revealed that, for one particular field site the BEIS2 model would have underestimated NO emissions, on a yearly average, by a factor of 26. Applying this new flux algorithm to the biosolid acreage data, a modified NO inventory was developed (Modified case). It should be noted that the data used to produce this revised inventory was from only one field site and has been extended to all soils throughout the model domain receiving the biosolids. The exponential temperature

relationship reported here, however has been consistently reported throughout the literature and therefore provides some basis for this study to be extended to these various soil and crop types throughout North Carolina. It should not be assumed, however that this temperature dependence can be extended to all temperatures, as temperatures outside the range of 15-35 °C are often found to alter the often-cited exponential relationship.

The results of this research indicate that on a broad scale (entire model domain ~ 132,000 km^2), the contribution of NO from biosolid amended soils to the total biogenic emissions inventory in North Carolina is approximately 1%. It can be argued that when the entire model area is taken into consideration, biogenic NO emissions are less than 5% of the anthropogenic emissions, and therefore any modest increase in the biogenic source strength will likely have negligible consequences on tropospheric air quality. However, the majority of the anthropogenic emissions are concentrated in or around areas which contain large power plants or large urban centers. Consequently, in these industrial and urban areas, biogenics are a very small fraction of the total NO inventory. In the more remote/rural areas however, biogenics can be as much as an order of magnitude larger than the anthropogenic NO emissions. Therefore an underestimation of the biogenic NO in these remote regions would result in a significant bias in the emissions inventory for these areas.

Results from the two model scenarios (modified case and base case) revealed that any increased NO from biosolid amended soils produced $\Delta[O_3]$ several orders of magnitude smaller than background concentrations during daytime hours. During the late evening/early morning hours when the mixing volumes are at their smallest, $\Delta[O_3]$ were

found to be reduced at most, by approximately 1%. During one particular episode, both ozone production and ozone depletion were observed during the same time period, possibly indicating that some of the more remote areas of North Carolina are NO_x limited. NO_y species showed slightly larger changes, although most of the increase could be attributed to the increased NO rather than to any of the oxidized products.

Depending on how uniformly the biosolids are distributed throughout the model domain can cause larger impacts in the model results. By applying the biosolids in concentrated areas of the county resulted in ozone depletion of as much as 11% and for the first time, consistent trends of increased ozone production during afternoon hours was evident. While both approaches (concentrating biosolids in one area versus evenly distributing them throughout the county grid cells) are inherently flawed, they do acts as bounds, within which the true situation likely exists. More importantly, this study addresses the importance of biosolid amended soils as a land-use class and that more detailed monitoring is required so that they can be accounted for in future emission inventories.

References

Arya, S.P., Air Pollution Meteorology and Dispersion, Oxford University Press, New York, NY, 1999.

Barnett, K. North Carolina Department of Environment and Natural Resources, Division of Water Quality, Non-Discharge Compliance/Enforcement Unit, Raleigh, personal communication, April 2000.

Gery, M.W., G.Z., Whitten, J.P., Killus and M.C., Dodge, A photochemical kinetics mechanism for urban and regional scale computer modeling. Journal of Geophysical Research, 94, 12,925-12,956, 1989.

Hicks, B.B., M.L. Wesely, J.L. Durham and M.A. Brown, Some direct measurements of atmospheric sulfur fluxes over a pine plantation, Atmospheric Environment, 16, 2899-2903, 1982.

McHenry, J.N., N. Seaman, C. Coats, A. Lario-Gibbs, J. Vukovich, N. Wheeler and E. Hayes, Real-time nested mesoscale forecasts of lower tropospheric ozone using a highly optimized coupled model numerical prediction system, Preprints, AMS Symposium on Interdisciplinary Issues in Atmospheric Chemistry, Dallas, TX, January 10-15, 1999.

MCNC, http://envpro.ncsc.org/NCDAQ/PGM/results; http://airchem.sph.unc.edu/DENR/index.htm, 2001.

Multiscale Air Quality Simulation Platform User's Manual, version 1.0, Environmental Programs, North Carolina Supercomputing Center, Research Triangle Park, NC, 1998.

North Carolina Department of Environment and Natural Resources, Division of Water Quality, Non-Discharge Compliance/Enforcement Unit, Annual Report, 1999.

Peirce, J.J. and V.P. Aneja, Nitric oxide emissions from engineered soil systems, Journal of Environmental Engineering, ASCE, 126(3), 225-232, 2000.

Roberts, J.M. Reactive odd-nitrogen (NO_y) in the atmosphere, in Composition, chemistry, and climate of the atmosphere, edited by H.B. Singh Van Nostrand Reinhold, New York, pp. 176-215, 1995.

Roelle, P.A., V.P. Aneja, J. O'Connor, W. Robarge, D.S. Kim and J.S. Levine, Measurement of nitrogen oxide emissions from an agricultural soil with a dynamic chamber system, Journal of Geophysical Research, 104, 1609-1619, 1999.

Seinfeld, J.H. and S.N. Pandis, Atmospheric chemistry and physics, from Air pollution to climate change, John Wiley and Sons, Inc., New York, pp. 71-74, 1998.

Stull, R.B., An introduction to boundary layer meteorology, Kluwer Academic Publishers, Boston, Ma. 2-26, 1988.

Sullivan, L.J., T.C. Moore, V.P. Aneja and W.P. Robarge, Environmental variables controlling nitric oxide emissions from agricultural soils in the southeast United States, Atmospheric Environment, 30, 3573-3582, 1996.

Thornton, F.C., P.A. Pier and R.J. Valente, NO emissions from soils in the southeastern United States, Journal of Geophysical Research, 102, 21,189-21,195, 1997.

Viessman, W. and M.J. Hammer, Water supply and pollution control, HarperCollins, NY, 1993.

Warneck, P., Chemistry of the natural atmosphere, second edition, Academic Press, Inc., New York, NY, pp. 511-517, 2000.

Walcek, C.J., R.A. Brost, J.S. Chang and M.L. Wesely, SO_2, sulfate, and HNO_3 deposition velocities computed using regional land-use and meteorological data, Atmospheric Environment, 20, 949-964, 1986.

Wesely, M.L., D.R. Cook, R.L. Hart and R.E. Speer, Measurements and parameterization of particulate sulfur dry deposition over grass, Journal of Geophysical Research, 90, 2131-2143, 1985.

Williams, E., A. Guenther and F. Fehsenfeld, An inventory of nitric oxide emissions from soils in the United States, Journal of Geophysical Research, 97, 7511-7519, 1992.

Yienger, J.J. and H. Levy II, Empirical model of global soil-biogenic NO_x emissions. Journal of Geophysical Research, 100, 11,447-11,464, 1995.

File: D:\MO3C5A~1\MECHAN~1\Sources\CB4\rxns\CB4_99.rxn 9/17/99, 9:34:49AM

```
// ************************************************************************
// Updated Carbon Bond Four Principle Mechanism Version 99
//

// I == INORGANIC CHEMISTRY ==========================================
// a) NO2 photolysis -------------------------------------------------

NAMES
 PhotoRateIDs += { NO2_to_O3P };

  R[Ia1]=       NO2     -hv-> NO  + O3P         @ j[NO2_to_O3P];
  R[Ia2]= O3P + O2 + M  ----> O3  + M           @ 6.0E-34*T_300^-2.3;
  R[Ia3]= O3  + NO      ----> NO2 + O2          @ 2.0E-12*EXP(-1400.0/TK);
                                                  // Ia2, Ia3 NASA97, T1
  R[Ia4]= O3P + NO2     ----> NO  + O2          @ 6.5E-12*EXP(120.0/TK);
                                                  // Ia4 NASA97, T1
  R[Ia5]= O3P + NO2     ----> NO3 + O2          @ TROE(9.00E-32*T_300^-2.0,
                                                       2.2E-11,
                                                       b[M], 0.6);
  R[Ia6]= O3P + NO      ----> NO2               @ TROE(9.00E-32*T_300^-1.5,
                                                       3.0E-11,
                                                       b[M], 0.6);
                                                  // Ia5 and Ia6 NASA97, T2
  R[Ia7]= NO  + NO + O2 ----> 2.0*NO2           @ 3.30E-39*EXP(530.0/TK);
                                                  // Ia7 IUPAC97
// b) NO3 CHEMISTRY  -------------------------------------------------

NAMES
 PhotoRateIDs += { NO3_to_NO, NO3_to_NO2 };

  R[Ib1] = O3 +  NO2  ----> NO3 + O2            @ 1.2E-13*EXP(-2450.0/TK);
  R[Ib2] =       NO3  -hv-> NO  + O2            @ j[NO3_to_NO];
  R[Ib2b]=       NO3  -hv-> NO2 + O3P           @ j[NO3_to_NO2];
  R[Ib3] = NO3 + NO   ----> 2.0*NO2             @ 1.50E-11*EXP(170.0/TK);
  R[Ib4] = NO3 + NO2  ----> NO + NO2 + O2       @ 4.50E-14*EXP(-1260.0/TK);

  R[Ib5f]= NO3 + NO2  -M--> N2O5                @ TROE(2.20E-30*T_300^-3.9,
                                                       1.50E-12*T_300^-0.7,
                                                       b[M], 0.6) ;
  R[Ib5r]=       N2O5 ----> NO3 + NO2           @ k[Ib5f]/(2.7E-27*EXP(11000.0/TK)) ;
                                                  // Ib5f NASA97, T2;
                                                  // Ib5r  Ke=2.7E-27*EXP(11000/T)
  R[Ib7]= N2O5 + H2O  ----> 2.0*HNO3            @ 1.5E-21; // homogeneous rate only

// c) OZONE photolysis -----------------------------------------------

NAMES
 PhotoRateIDs += { O3_to_O3P, O3_to_O1D };

 R[Ic1] = O3        -hv-> O3P + O2              @ j[O3_to_O3P] ;
 R[Ic2] = O3        -hv-> O1D + O2              @ j[O3_to_O1D] ;
 R[Ic3] = O1D + M   ----> O3P + M               @ 1.92E-11*EXP( 125.0/TK) ;
                                                  // ave of N2 and O2 rates
 R[Ic4] = O1D + H2O ----> 2.0*OH                @ 2.20E-10;
 R[Ic5] = O3  + OH  ----> HO2 + O2              @ 1.60E-12*EXP(-940.0/TK) ;
 R[Ic6] = O3  + HO2 ----> OH  + 2.0 * O2        @ 1.10E-14*EXP(-500.0/TK) ;

// d) HONO CHEMISTRY  ------------------------------------------------

NAMES
 PhotoRateIDs += { HONO_to_OH };

 R[Id1] = NO   + NO2 + H2O ----> 2.0*HONO       @ 4.4E-40 ;
 R[Id2] = HONO + HONO      ----> NO  + NO2 +H2O @ 1.0E-20 ;
 R[Id3] = OH   + NO        -M--> HONO           @ TROE(7.00E-31*T_300^-2.6,
                                                       3.60E-11*T_300^-0.1,
                                                         b[M], 0.6) ;
 R[Id4] =        HONO      -hv-> OH  + NO       @ j[HONO_to_OH] ;
 R[Id5] = OH   + HONO      ----> NO2 + H2O      @ 1.80E-11*EXP(-390.0/TK);

// e) NO/NO2 with HO2  -----------------------------------------------

 R[Ie1]  = HO2  + NO  ----> OH   + NO2          @ 3.50E-12*EXP(250.0/TK) ;

 R[Ie2f] = HO2  + NO2 -M--> PNA                 @ TROE(1.80E-31*T_300^-3.2,
                                                       4.70E-12*T_300^-1.4,
                                                       b[M], 0.6);
 R[Ie2r] =        PNA -M--> HO2 + NO2           @ k[Ie2f]/(2.1E-27*EXP(10900.0/TK));
                                                  // Ie2f NASA97, T2; Ie2r Ke=2.1E-27*EXP(10900/T)

 R[Ie3]  = OH   + PNA ----> NO2  + H2O + O2     @ 1.30E-12*EXP(380.0/TK) ;
```

Table 4.1. Carbon Bond IV Principle Mechanism.

```
File: D:\MO3C5A~1\MECHAN~1\Sources\CB4\rxns\CB4_99.rxn 9/17/99, 9:34:49AM

// f) HO2 TERMINATION REACTIONS ------------------------------------

NAMES
 PhotoRateIDs += { H2O2_to_OH };

 R[If1] = OH  + NO2       -M--> HNO3          @ TROE(2.6E-30*T_300^-2.9,
                                                     7.5E-11*T_300^-0.6, //IUPAC 6:97
                                                     b[M], 0.41);
 R[If2] = OH  + HNO3      ----> NO3 +H2O      @ 7.2GE-15*EXP(785.0/TK) +
                                                LMHW(1.90E-33*EXP( 725.0/TK),
                                                     4.10E-16*EXP(1440.0/TK),
                                                     b[M]); // NASA97
 R[If3] = HO2 + HO2       ----> H2O2 + O2     @ ( 2.2E-13*EXP( 600.0/TK) +
                                                  1.9E-33*EXP( 980.0/TK) * b[M] ) *
                                                ( 1.0 +
                                                  1.4E-21*EXP(2200.0/TK) * b[H2O] );
                                                  // IUPAC 97
 R[If6] =       H2O2      -hv-> 2.0*OH        @ j[H2O2_to_OH];
 R[If7] = OH  + H2O2      ----> HO2 + H2O     @ 2.90E-12*EXP(-160.0/TK) ;
 R[If8] = OH  + HO2       ----> O2  + H2O     @ 4.80E-11*EXP( 250.0/TK) ;

 // If3--If5 NASA97, T1, note B13

//  g) OH basic PROPAGATION REACTIONS ------------------------------------

 R[Ig1] =  OH + CO  ----> HO2 + CO2           @ 1.50E-13 * (1.0+0.6*Patm) ;
 R[Ig2] =  OH + CH4 ----> XO2 + HCHO + HO2    @ 2.45E-12*EXP(-1775.0/TK);
                                                // NASA 97

// ORGANIC CHEMISTRY ================================================
// C1 == formaldhyde chemistry ------------------------------------

NAMES
 PhotoRateIDs += { HCHO_to_HO2, HCHO_to_H2 };

 R[C1_1] =   HCHO          -hv-> 2.0*HO2 + CO      @ j[HCHO_to_HO2] ;
 R[C1_2] =   HCHO          -hv-> CO  + H2          @ j[HCHO_to_H2] ;
 R[C1_3] =   HCHO    + O3P ----> OH + HO2 + CO     @ 3.4E-11*EXP(-1600.0/TK) ;
 R[C1_4] =   HCHO    + OH  ----> HO2 + CO          @ 8.6E-12*EXP(20.0/TK) ; //IUPAC,97
 R[C1_5] =   HCHO    + NO3 ----> HNO3 + HO2 + CO   @ 2.0E-12*EXP(-2430.0/TK) ;

 // C1_5 is from IUPAC97 and is equal to 5.8E-16 @298K

// C2 == higher aldehyde chemistry ------------------------------------

NAMES
 PhotoRateIDs += { CH3CHO_to_HCO };

 R[C2_1] =  CCHO         -hv-> XO2  + 2.0*HO2 + CO +  HCHO     @ j[CH3CHO_to_HCO] ;
 R[C2_2] =  CCHO   + O3P ----> C2O3 + OH                 @ 1.8E-11*EXP(-1100.0/TK) ;
 R[C2_3] =  CCHO   + OH  ----> C2O3 + H2O                @ 5.6E-12*EXP(  270.0/TK) ;
 R[C2_4] =  CCHO   + NO3 ----> C2O3 + HNO3               @ 1.4E-12*EXP(-1860.0/TK) ;
                                                           // all NASA97, IUPAC97

// PAN == PAN chemistry  ------------------------------------------------------
/*
 *   All PAN Rates from NASA 1997.
 *   The recommended rates for PAN_1 are based on new data in NASA97
 *     that was not used in IUPAC97.  These are consistent with PAN_2
 *   The recommended rates for PAN_2f (see Note Table2, D51) are the
 *     same as IUPAC97, but with F_c=0.6 instead of 0.3; here we use
 *     the original ref's values which are those of IUPAC97.
 *   The equilibrium constant used in PAN_2r is also based on new data in NASA97
 *     that is not cited in IUPAC97.
 */
 R[PAN_1] = C2O3 + NO  ----> NO2 + XO2 +  HCHO + HO2  @ 5.3E-12*EXP(360.0/TK); //NASA97
 R[PAN_2f]= C2O3 + NO2 ----> PAN                      @ TROE(2.7E-28*T_300^-7.1,
                                                             1.2E-11*T_300^-0.9,
                                                             b[M], 0.3);  //IUPAC97==NASA97@0.6
 R[PAN_2r]=        PAN ----> C2O3 + NO2               @ k[PAN_2f]/(9.0E-29*EXP(14000.0/TK)); //NASA9

NAMES
 IgnSpoIDs += { CCO3H,  CCO2H }; // carbonyl peroxide and acetic acid

 R[PAN_3] = C2O3 + HO2  ----> 0.75*(CCO3H + O2) + 0.25*(CCO2H + O3)   @ 4.3E-13*EXP(1040.0/TK);
 R[PAN_4] = C2O3 + C2O3 ----> 2.0*(XO2 +  HCHO    + HO2)              @ 2.8E-12*EXP(530.0/TK);
 // PAN_3 and PAN_4 from IUPAC97  (inoluding produots in PAN_3)


// Organic formulation from Gery, et al., 1989 unless otherwise specified

NAMES
```

Table 4.1. Continued.

```
File: D:\MO3C5A~1\MECHAN~1\Sources\CB4\rxns\CB4_99.rxn 9/17/99, 9:34:49AM

 IgnSpcIDs += { KETENE };

// PARAFFIN CHEMISTRY ------------------------------------------------

SCALARS
 const s_par_1 =  -0.11,  s_par_2 =  -2.1;

 R[PAR_1] = OH  + PAR -----> 0.87*XO2 + 0.13*XO2N + 0.11*HO2 + 0.11*CCHO +
                             0.75*ROR  + s_par_1*PAR  @ 8.14E-13;
 R[PAR_2] =       ROR -----> 1.10*CCHO    + 0.96*XO2  + 0.94*HO2 + s_par_2*PAR +
                             0.04*XO2N    + 0.02*ROR             @ 1.0E+15*EXP(-8000.0/TK);
 R[PAR_3] =       ROR -----> HO2 + KETENE                         @ 1.6E+3;
 R[PAR_4] = ROR + NO2 -----> ALKNO3                               @ 1.5E-11;


// ETHENE CHEMISTRY --------------------------------------------------
// Revised Ethene kinetics (except ETH_1) based on data in
//   Atkinson, J.Phys.Chem.Ref.Data, vol.26,no.2, 1997

 R[ETH_1] = O3P +  ETH  -----> 0.49*HCHO + 0.60*XO2  + 0.95*CO +
                               1.55*HO2  + 0.35*OH         @ 1.04E-11*EXP(-792.0/TK);
 R[ETH_2] =  OH +  ETH  -----> XO2  + 1.56*HCHO + HO2 +
                               0.22*CCHO             @ TROE(7.0E-29*T_300^-3.1,
                                                            9.0E-12, b[M], 0.7);
 R[ETH_3] =  O3 +  ETH  -----> 1.03*HCHO + 0.325*CO + 0.08*HO2 +
                               0.02*H2O2 + 0.08*OH         @ 9.1E-15*EXP(-2580.0/TK);


// OLEFIN CHEMISTRY --------------------------------------------------
//   Olefin Ozonolysis and reaction with O lumping reevaluated based on data in
//    Atkinson, J.Phys.Chem.Ref.Data, vol.26,no.2, 1997

SCALARS
 const s_ole = -1.0 ;

 R[OLE_1] = O3P + OLE -----> 0.49* CCHO    + 0.29*HO2   + 0.19*XO2  + 0.20*CO +
                             0.20* HCHO    + 0.007*XO2N + 0.61*PAR  + 0.10*OH
                                                        @ 4.0E-12 ;
 R[OLE_2] =  OH + OLE -----> HCHO + CCHO  + XO2 + HO2  + s_ole*PAR
                                                        @ TROE(8.0E-27*T_300^-3.5,
                                                               3.0E-11, b[M], 0.5) ;
                                                          // IUPAC, 97
 R[OLE_3] =  O3 + OLE -----> 0.52*CCHO     + 0.86* HCHO    + 0.3947*CO  +
                             0.42*HO2      + 0.45*XO2      + 0.31*OH    +
                             s_ole*PAR     + 0.08*H2O2     + 0.1948*CO2 +
                             0.0595*CH4
                                                        @ 5.5E-15*EXP(-1880.0/TK) ;
 R[OLE_4] = NO3 + OLE -----> 0.91*(XO2 + NO2) + HCHO + CCHO +
                             0.09*XO2N  + s_ole*PAR     @ 4.6E-13*EXP(-1155.0/TK) ;

// ISOPRENE CHEMISTRY--CONDENSED -------------------------------------
// SAI version of the one-product condensed chemistry from Carter (1996).

 R[ISO_1] = O3P  + ISOP -----> 0.25*HO2  + 0.25*XO2 + 0.75*ISPD +
                               0.50*HCHO + 0.25*PAR + 0.25*C2O3
                                                        @ 3.60E-11 ;
 R[ISO_2] = OH   + ISOP -----> 0.991*XO2  + 0.629*HCHO  + 0.912*HO2 +
                               0.088*XO2N + 0.912*ISPD
                                                        @ 2.54E-11*EXP(  407.6/TK) ;
 R[ISO_3] = O3   + ISOP -----> 0.60*HCHO + 0.15*CCHO + 0.35*PAR +
                               0.066*CO  + 0.066*HO2 + 0.266*OH +
                               0.20*C2O3 + 0.20*XO2  + 0.65*ISPD
                                                        @ 7.86E-15*EXP(-1912.0/TK) ;
 R[ISO_4] = NO3  + ISOP -----> XO2 + 0.65*ISPD + 0.80*ISPNO3 + 0.80*HO2 +
                               0.20*NO2  + 0.80*CCHO   + 2.40*PAR
                                                        @ 3.03E-12*EXP( -448.0/TK) ;
 R[ISO_5] = NO2  + ISOP -----> 0.80*CCHO + 2.40*PAR  + 0.80*ISPNO3 +
                                 XO2  + 0.80*HO2  +
                               0.20*ISPD + 0.20*NO       @ 1.50E-19;


 R[ISPD_1] = ISPD + OH  -----> 1.565*PAR  + 0.167*HCHO + 0.713*XO2
                               + 0.503*HO2  + 0.334*CO
                               + 0.168*MGLY + 0.273*CCHO
                               + 0.498*C2O3                    @ 3.36E-11;
 R[ISPD_2] = ISPD + O3  -----> 0.114*C2O3 + 0.150*HCHO + 0.850*MGLY
                               + 0.154*HO2  + 0.268*OH
                               + 0.054*XO2  + 0.020*CCHO
                               + 0.360*PAR  + 0.225*CO     @ 7.11E-18;
 R[ISPD_3] = ISPD + NO3 -----> 0.357*CCHO + 0.282*HCHO + 1.282*PAR
                               + 0.925*HO2  + 0.643*CO
```

Table 4.1. Continued.

File: D:\MO3C5A~1\MECHAN~1\Sources\CB4\rxns\CB4_99.mn 9/17/99, 9:34:49AM

```
                                        + 0.850*ISPND3  + 0.075*C2O3
                                        + 0.075*XO2  + 0.075*HNO3    @ 1.0E-15;
NAMES
 PhotoRateIDs += { ACRO_to_RO2 };

 R[ISPD_4] = ISPD       -hv->  0.333*CO   + 0.067*CCHO + 0.900*HCHO
                                        + 0.832*PAR  + 1.033*HO2
                                        + 0.700*XO2  + 0.967*C2O3    @ j[ACRO_to_RO2];

// TOLUENE CHEMISTRY ------------------------------------------------

 R[TOL_1] = OH  + TOL  ----> 0.08*(XO2 + HO2) + 0.36*(CRES + HO2) + 0.56*TO2
                                                                    @ 1.8E-12*EXP(355.0/TK) ;

 R[TOL_2] = TO2 + NO   ----> 0.90*(NO2 + HO2 + OPEN) + 0.1*ARONO3   @ 8.1E-12 ;
 R[TOL_3] =       TO2  ----> CRES + HO2                             @ 4.2 ;


 R[CR1] =   OH  + CRES ----> 0.40*CRO + 0.60*(XO2 + HO2) + 0.30*OPEN  @ 4.10E-11 ;
 R[CR2] =   NO3 + CRES ----> CRO + HNO3                              @ 2.20E-11 ;
 R[CR3] =   CRO + NO2  ----> ARONO3                                  @ 1.40E-11 ;


SCALARS
 kOPEN_R = 6.0;  // Scaled back from Gery's EPA rpt=9.04xjHCHOr by Bass/Moor=0.78

 R[RF_1] = OPEN      -hv-> C2O3 + HO2 + CO                           @ j[HCHO_to_HO2]*kOPEN_R ;
 R[RF_2] = OPEN + OH ----> XO2 + 2.0*CO + 2.0*HO2 + C2O3 +  HCHO
                                                                     @ 3.0E-11 ;
 R[RF_3] = OPEN + O3 ----> 0.03*CCHO + 0.62*C2O3 + 0.70*HCHO +
                           0.03*XO2  + 0.69*CO   + 0.08*OH   +
                           0.76*HO2  + 0.20*MGLY                     @ 5.48E-17*EXP(-500.0/TK) ;

// XYLENE CHEMISTRY  ------------------------------------------------

 R[XYL_1] = OH + XYL  ----> 0.10*(/* XLO2= */ HO2 + XO2 + PAR) +
                            0.20*(CRES+HO2+PAR) +
                            0.30*TO2 +
                            0.40*(/* XINT= */ MGLY + MGLY + PAR + PAR + HO2)
                                                                    @ 1.70E-11*EXP(116.0/TK) ;
SCALARS
 kMGLY_R = 6.0;  // Scaled back from Gery's EPA rpt 9.64xj HCHO   r by Bass/Moor=0.78

 R[XYL_2] =      MGLY -hv-> C2O3 + HO2 + CO                          @ j[HCHO_to_HO2]*kMGLY_R ;
 R[XYL_3] = OH + MGLY ----> XO2 + C2O3                               @ 1.70E-11 ;

// NOTE WELL::: MGLY here is *not* meant to be real MGLY, but a ring
//              ring fragmentation product of XYL which has been tuned based
//              upon original Bass HCHOr rates and assumed yields. Most
//              importantly the sigma-phi(MGLY) of IUPAC can not be used
//              to compute the j(MGLY).

#if ALT_FUEL_
 R[MN_1] =      MeNO2 ----->  HO2 +  HCHO    + NO       @ j[HONO]

 R[RF_1] = OH + MeOH  ----->  HCHO    + HO2 + H2O       @ 6.7E-12*EXP(-600.0/TK);

 R[RF_2] = OH + EtOH  ----->  0.945*CCHO + HO2 +
                              0.055*XO2  + 0.11*HCHO    @ 7.0E-12*EXP(-235.0/TK);
#end

// Operator Chemistry -----------------------------------------------

 R[XO_1] = XO2  + NO   ----> NO2                         @ 3.0E-12*EXP(280.0/TK); //NASA97,T1
 R[XO_2] = XO2N + NO   ----> XRNO3                       @ k[XO_1] ;
 R[XO_3] = XO2  + XO2  ----->                            @ 2.5E-13*EXP(190.0/TK); // 1.70E-14*EXP(1300
 R[XO_4] = XO2  + HO2  ----->                            @ 3.8E-13*EXP(800.0/TK); // 7.68E-14*EXP(1300
 R[XO_5] = XO2N + HO2  ----->                            @ k[XO_4] ;
 R[XO_6] = XO2N + XO2N ----->                            @ k[XO_3] ;
 R[XO_7] = XO2  + XO2N ----->                            @ k[XO_3]*2.0;


// Declare species NR, which is used to provide
//      mass balance with ambient inputs of propane, etc..

 R[NR_1] =  ----> NR                                     @ 0.0;

// end of principle mechanism file.
```

Table 4.1. Continued.

Grid Cell	Area in Cell	NO Emission Factor ($\mu g\ m^{-2}\ h^{-1}$)	Genus
001 001	1600.000		
417.385,	27 ← **Total hectares in the following 27 categories**		
'Acer'	12.84	4.5	Acer (maple)
'Alnu'	0.00	4.5	Alnus (European alder)
'Betu'	1.30	4.5	Betula (birch)
'Carp'	0.61	4.5	Carpinus (hornbean)
'Cary'	26.67	4.5	Carya (hickory)
'Cerc'	0.39	4.5	Cercis (redbud)
'Coru'	11.72	4.5	Cornus (dogwood)
'Dios'	1.22	4.5	Diospyros (persimmon)
'Fagu'	2.33	4.5	Fagus (american beech)
'Frax'	1.29	4.5	Fraxinus (ash)
'Ilex'	1.91	4.5	Llex (holly)
'Jugl'	1.51	4.5	Juglans (black walnut)
'Juni'	2.53	4.5	Juniperus (east. Red cedar)
'Liqu'	8.54	4.5	Liquidambar (sweetgum)
'Liri'	11.30	4.5	Liriodendron (yellow poplar)
'Magn'	0.22	4.5	Magnolia
'Nyss'	4.87	4.5	Nyssa (blackgum)
'Ofor'	83.90		
'Oxyd'	23.29	4.5	Oxydendrum
'Pinu'	95.59	4.5	Pinus (pine)
'Prun'	0.89	4.5	Prunus (cherry)
'Quer'	120.28	4.5	Quercus (oak)
'Robi'	0.87	4.5	Robinia (black locust)
'Sali'	0.19	4.5	Salix (willow)
'Sass'	0.16	4.5	Sassafras
'Tsug'	2.42	4.5	Tsuga (Eastern hemlock)
'Ulmu'	0.41	4.5	Ulmus (American elm)
0.000,	0		
766.468,	7 ← **Total hectares in the following 7 crop types**		
'Corn'	6.90	577.6	Corn
'Cott'	0.71	256.7	Cotton
'Hay '	202.39	12	Hay
'Mscp'	539.48	12.8	Misc Crops
'Rye '	0.60	12.8	Rye
'Soyb'	5.25	12.8	Soybean
'Whea'	11.11	192.5	Wheat
416.147,	4 ← **Total hectares in the following 4 grass types**		
'Barr'	92.66	0	Barren
'Gras'	1.85	57.8	Grass
'Othe'	321.34	57.8	Other (unknown, asuume grass)
'Scru'	0.28	57.8	Scrub

Table 4.2. Example of land-use statistics that are available for each 4 x 4 km grid cell in the model domain. This data is then used in calculating the biogenic NO budget.

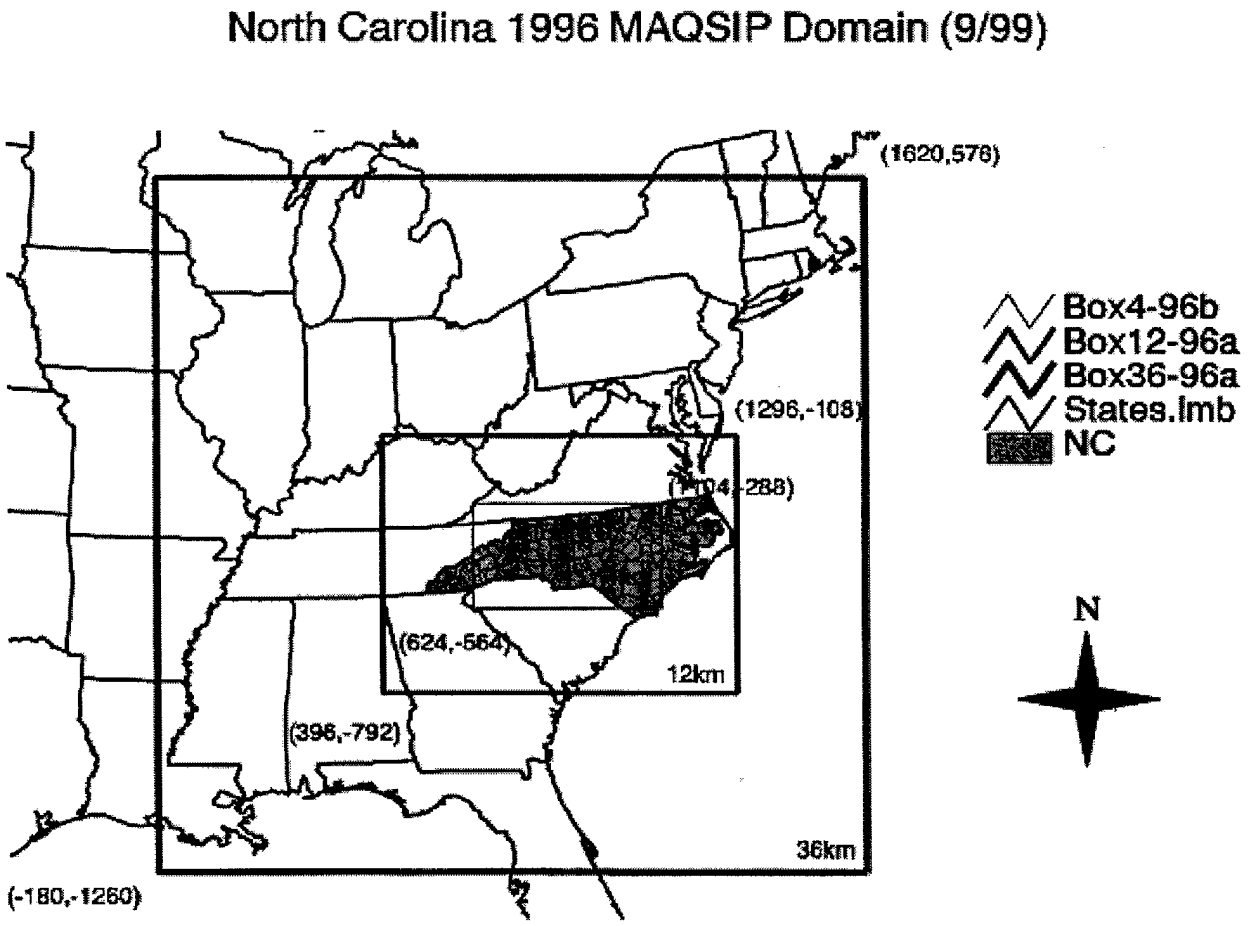

Figure 4.1. Model domain used for this study consists of a 480 km x 276 km area covering most of North Carolina. Grid scale resolution is 4 x 4 km.

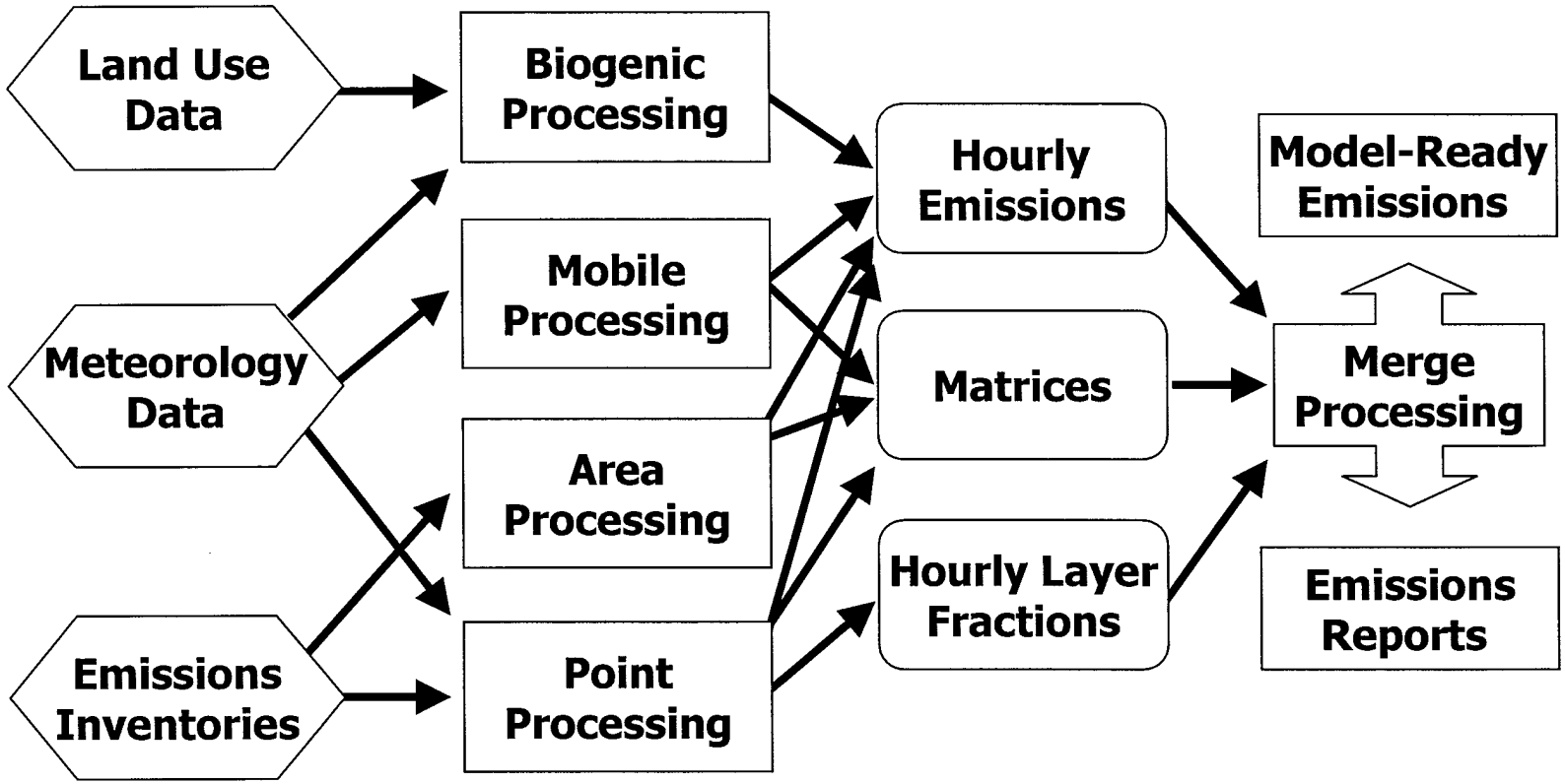

Figure 4.2. Schematic of the Sparse Matrix Operator Kernel Emissions (SMOKE) modeling system. Source: MCNC, North Carolina Supercomputing Center, Environmental Programs.

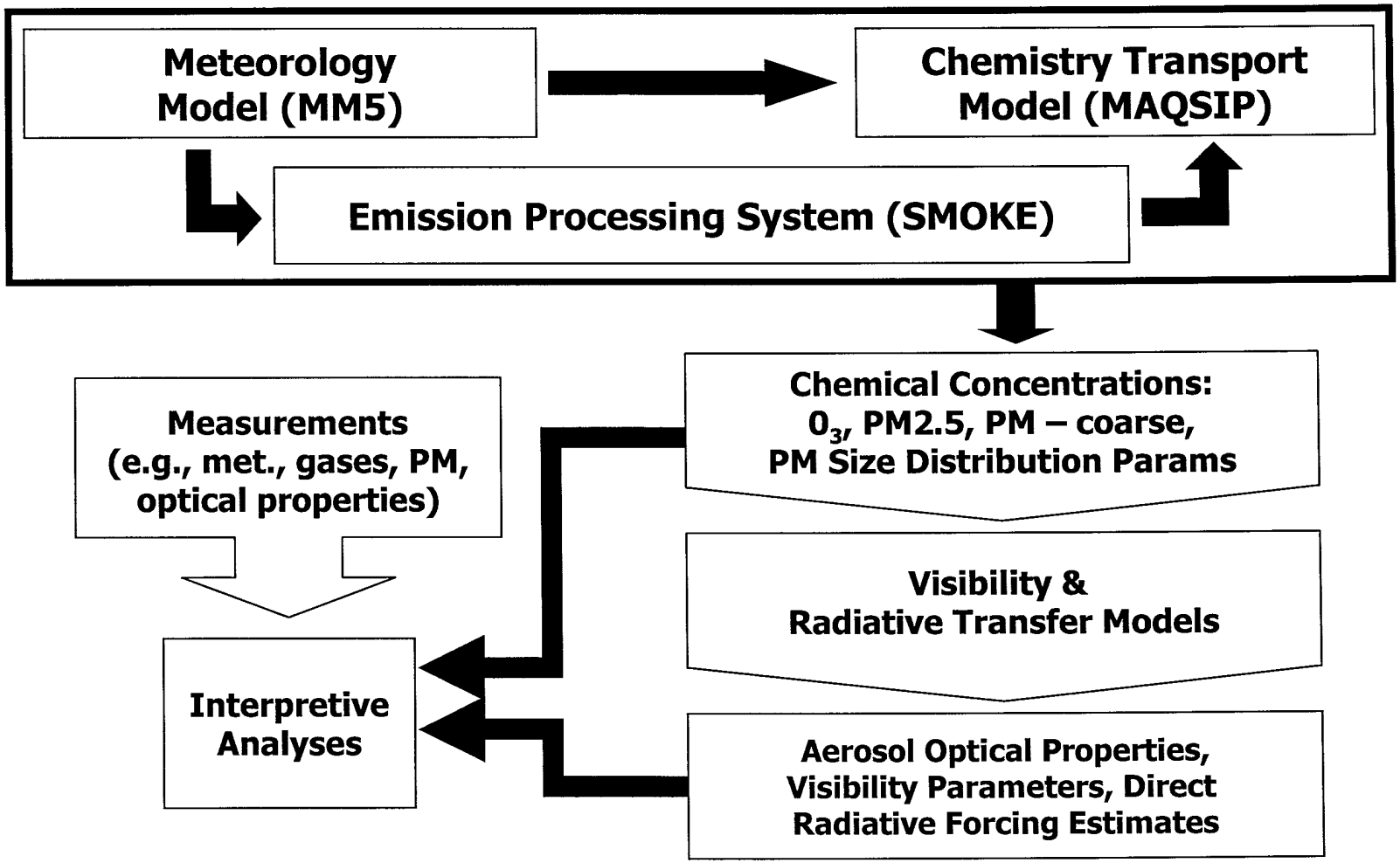

Figure 4.3. Schematic of the Multiscale Air Quality Simulation Platform (MAQSIP). Source: MCNC, North Carolina Supercomputing Center, Environmental Programs.

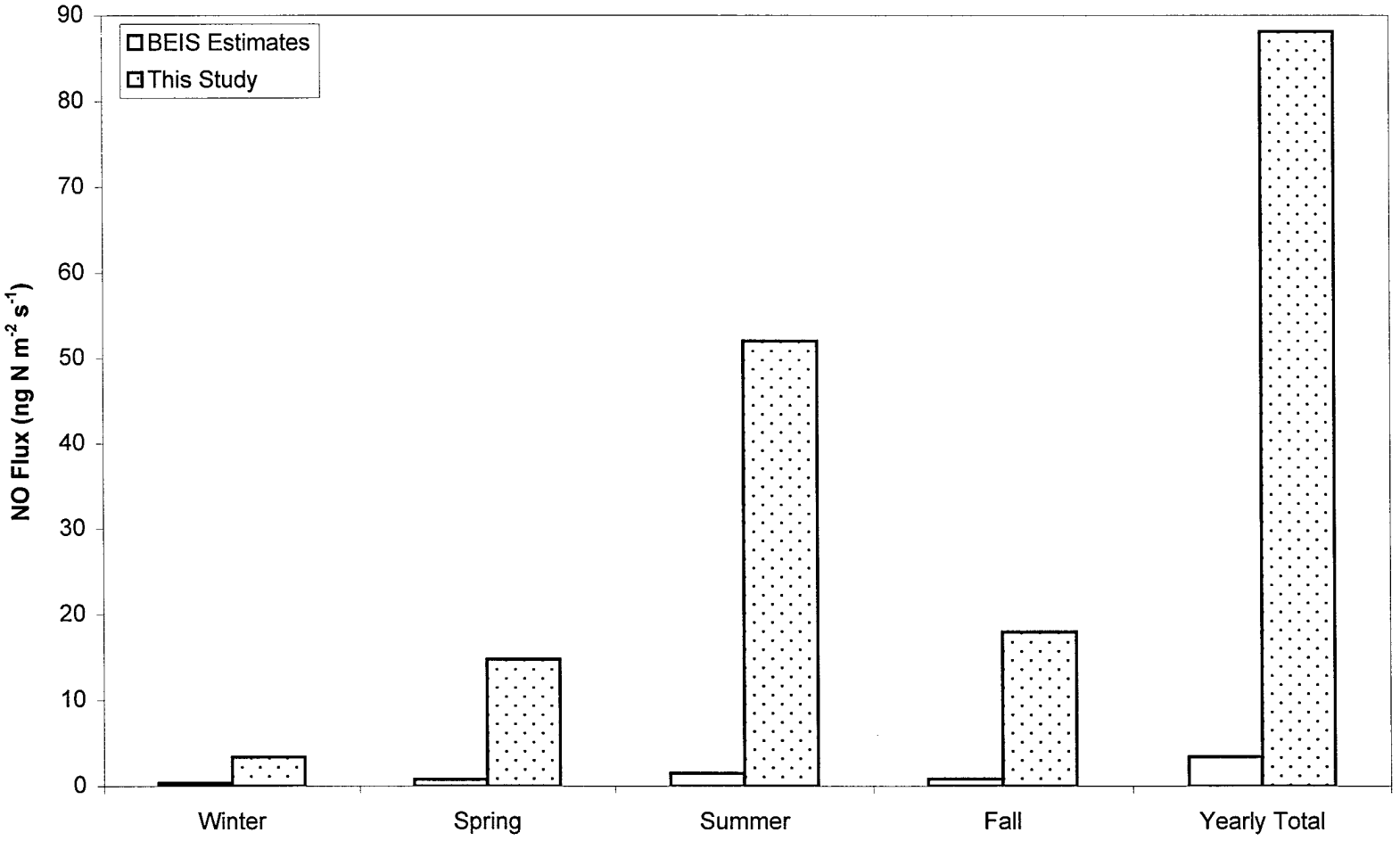

Figure 4.4. Estimated NO flux at field site sampled throughout 1999-2000. Clear bar represents estimates using existing BEIS2 model. Stippled bar represents estimated NO flux using algorithm developed during this study.

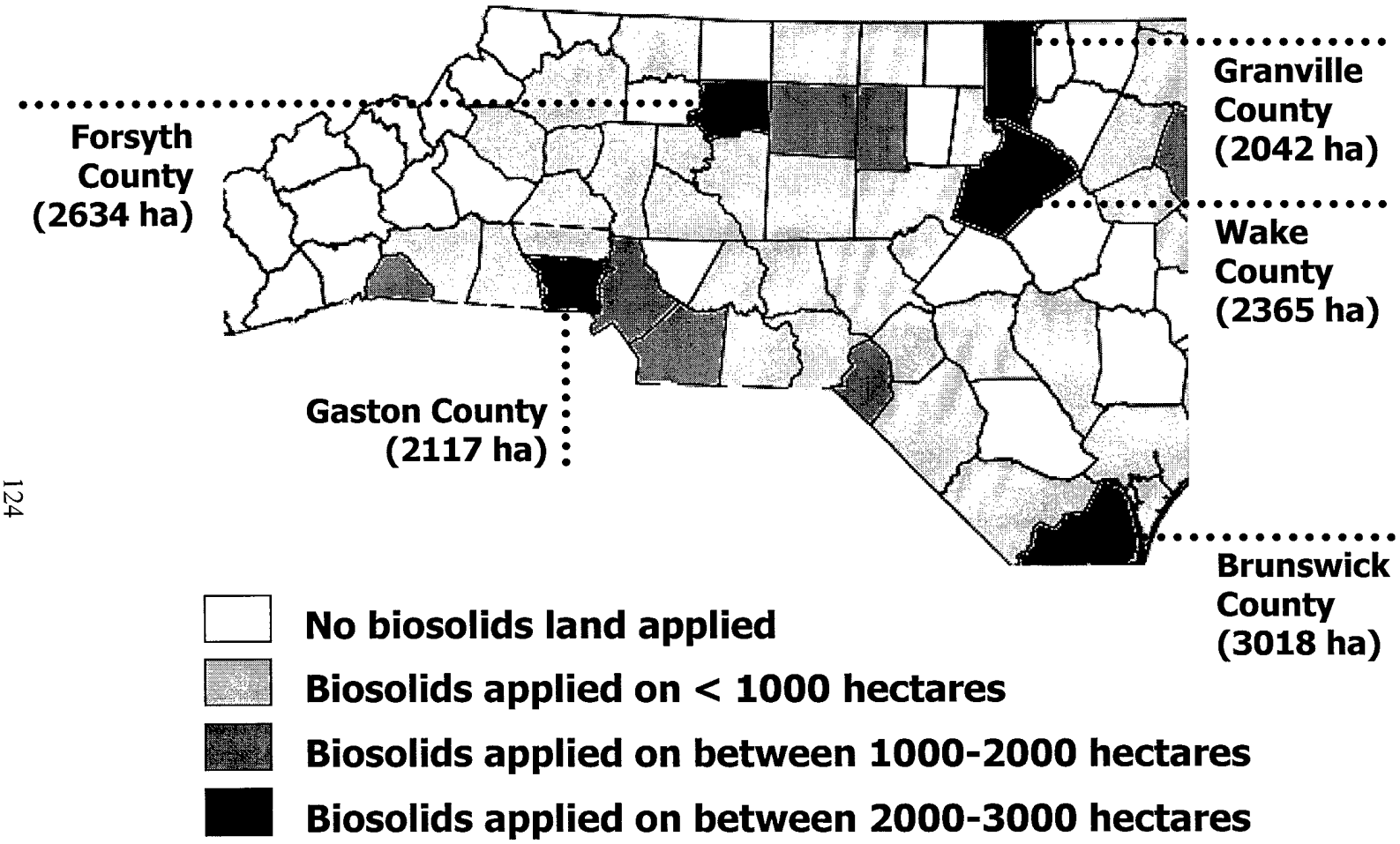

Figure 4.5. Model domain within North Carolina and county-level data of acreages used for application of biosolids.

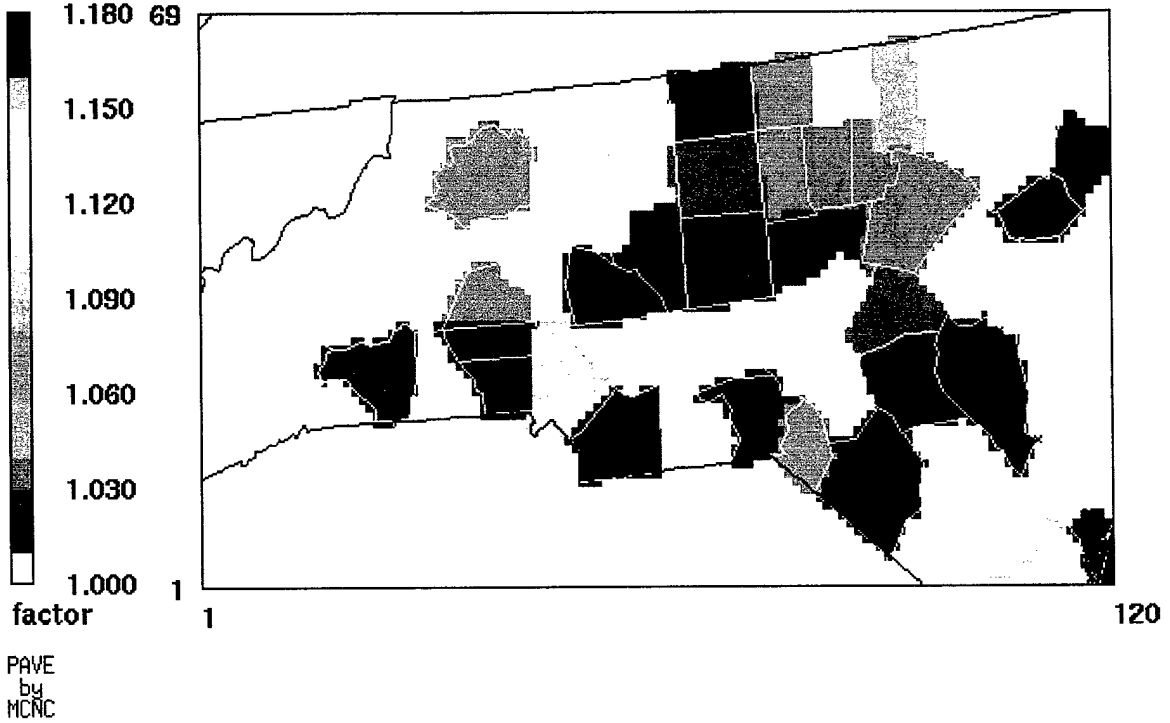

Figure 4.6. NO percent increase factors applied to biogenic NO emissions in all counties of the model domain.

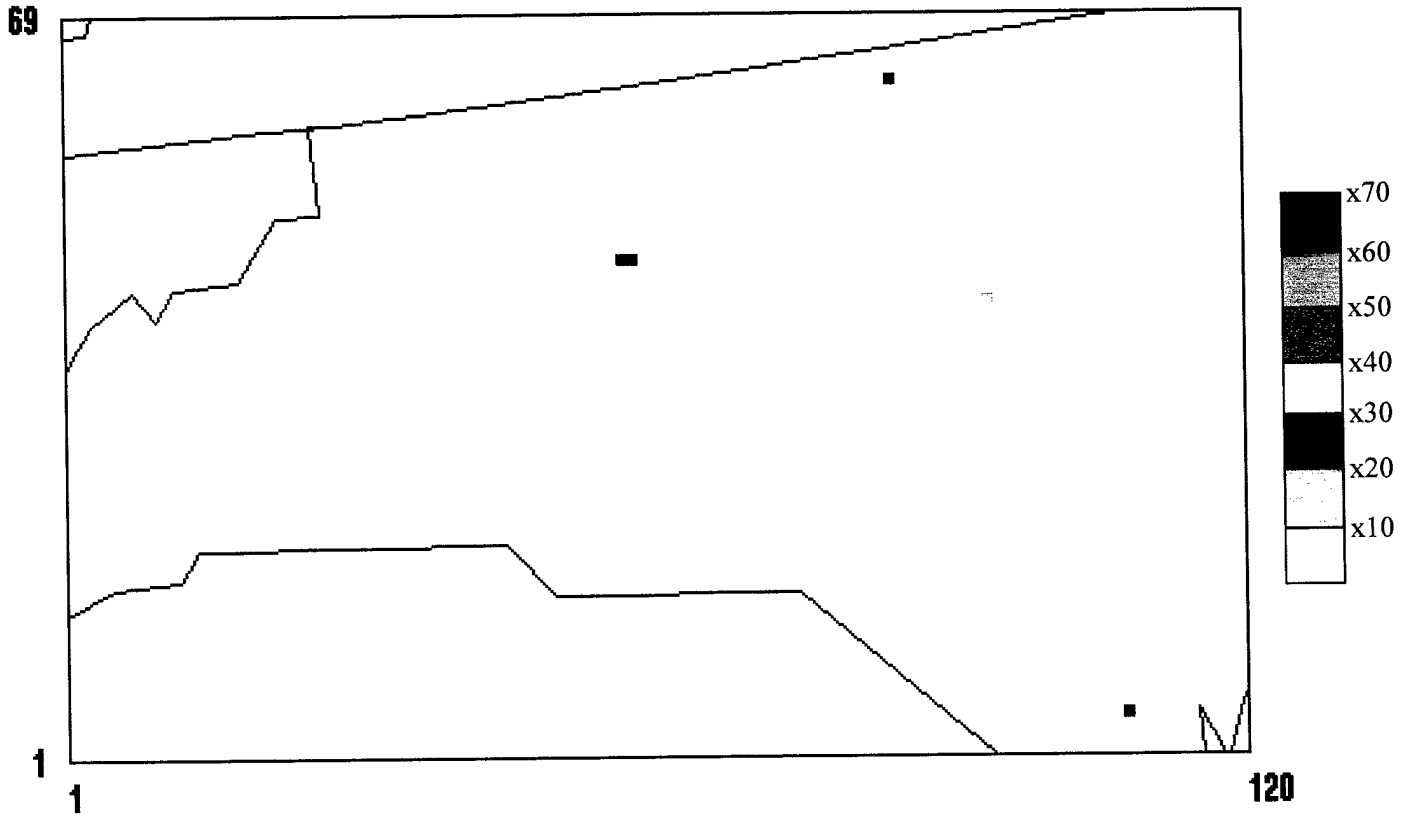

Figure 4.7. Cells in the model domain receiving all of the biosolids which are applied within the respective counties. The scale indicates how much the biogenic NO emissions increase over the base case scenario.

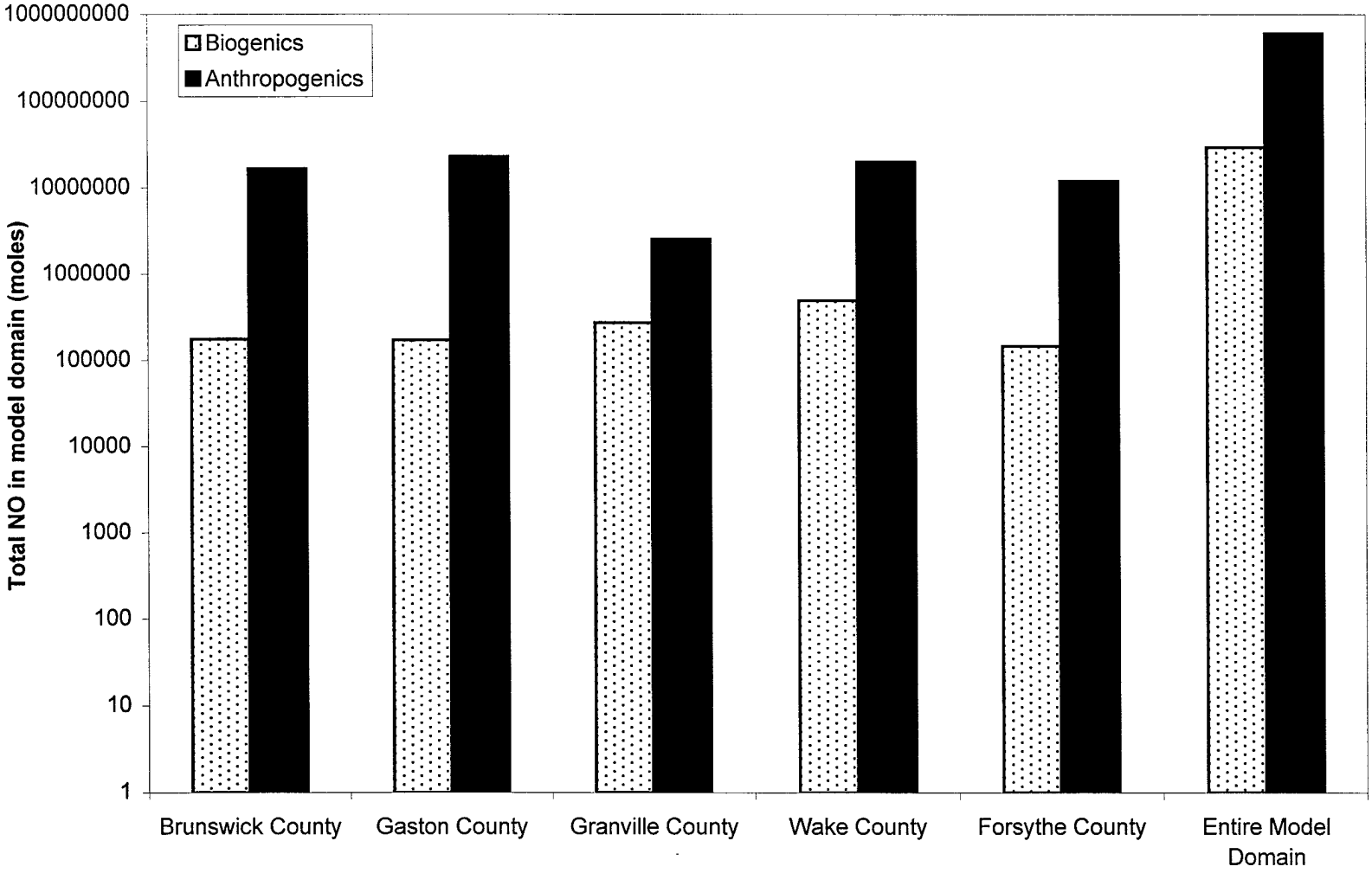

Figure 4.8. Barchart showing relative contribution to the NO inventory from biogenic and anthropogenic sources in the entire model domain and in the 5 counties receiving the largest application of biosolids.

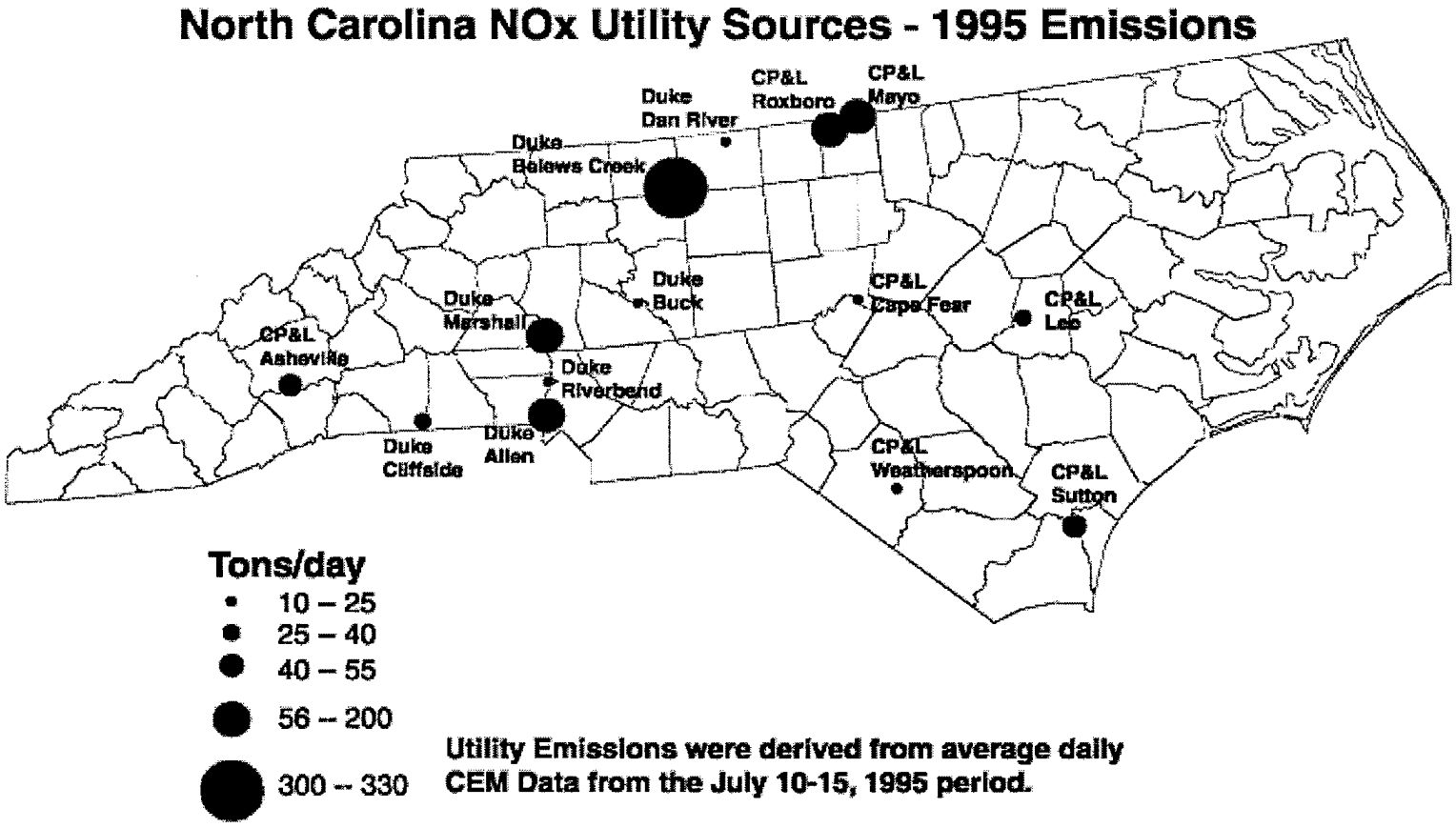

Figure 4.9. North Carolina NO_x utility sources for 1995.

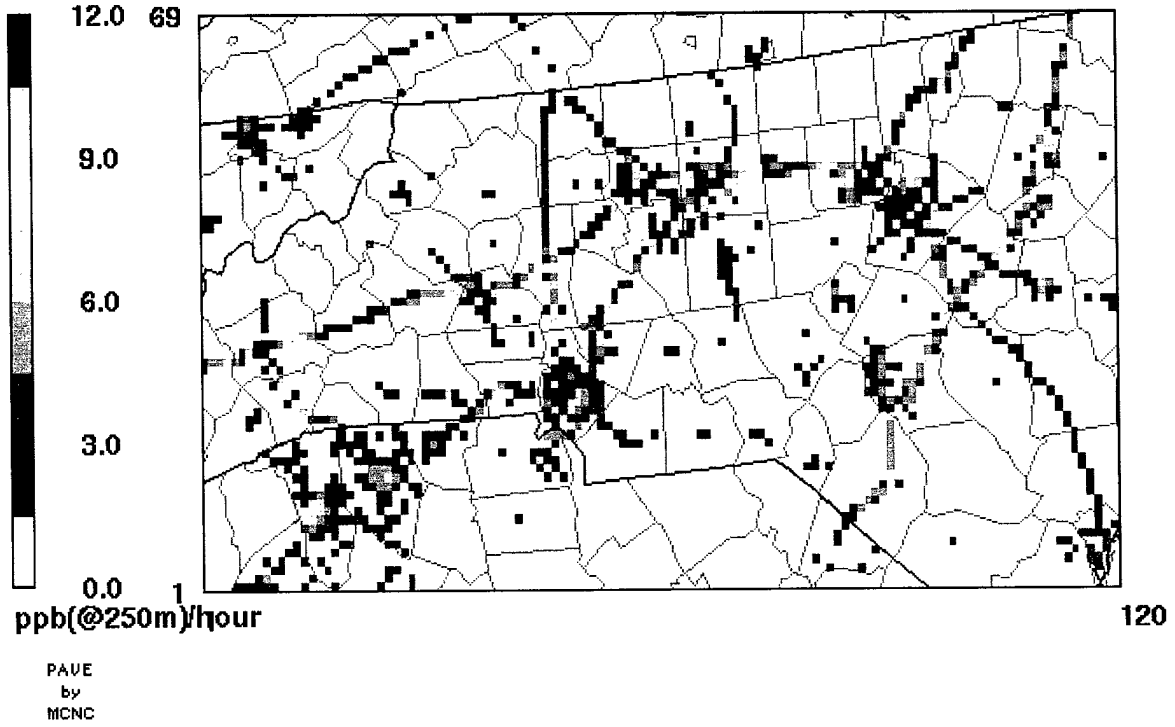

Figure 4.10. Mobile source NO_x emissions.

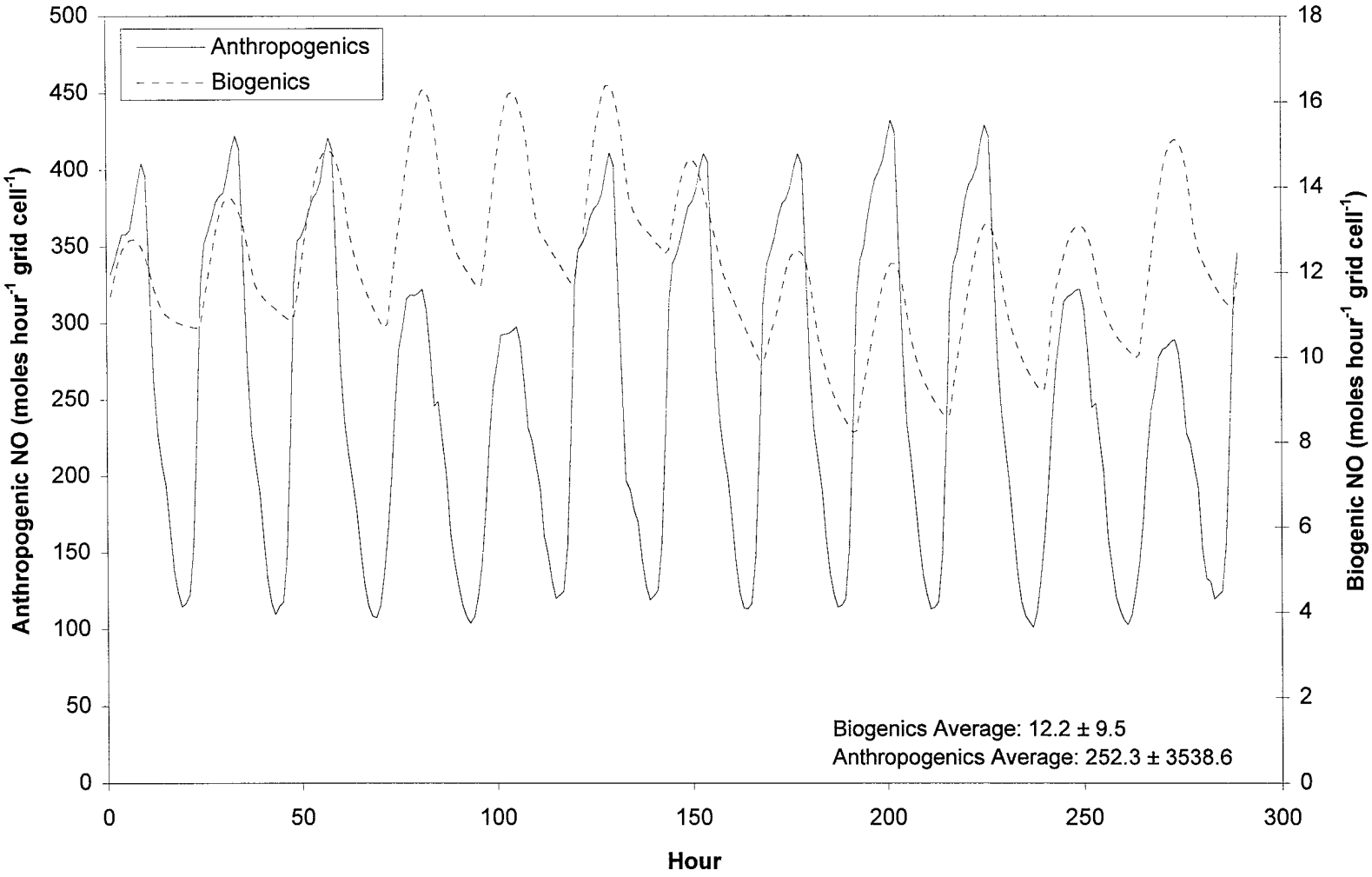

Figure 4.11. Hourly averaged NO emissions (moles/hour) of all the 4 x 4 km grid cells in the model domain. Anthropogenic NO is the solid line (primary axis) and the biogenics are represented by the dashed line (secondary axis).

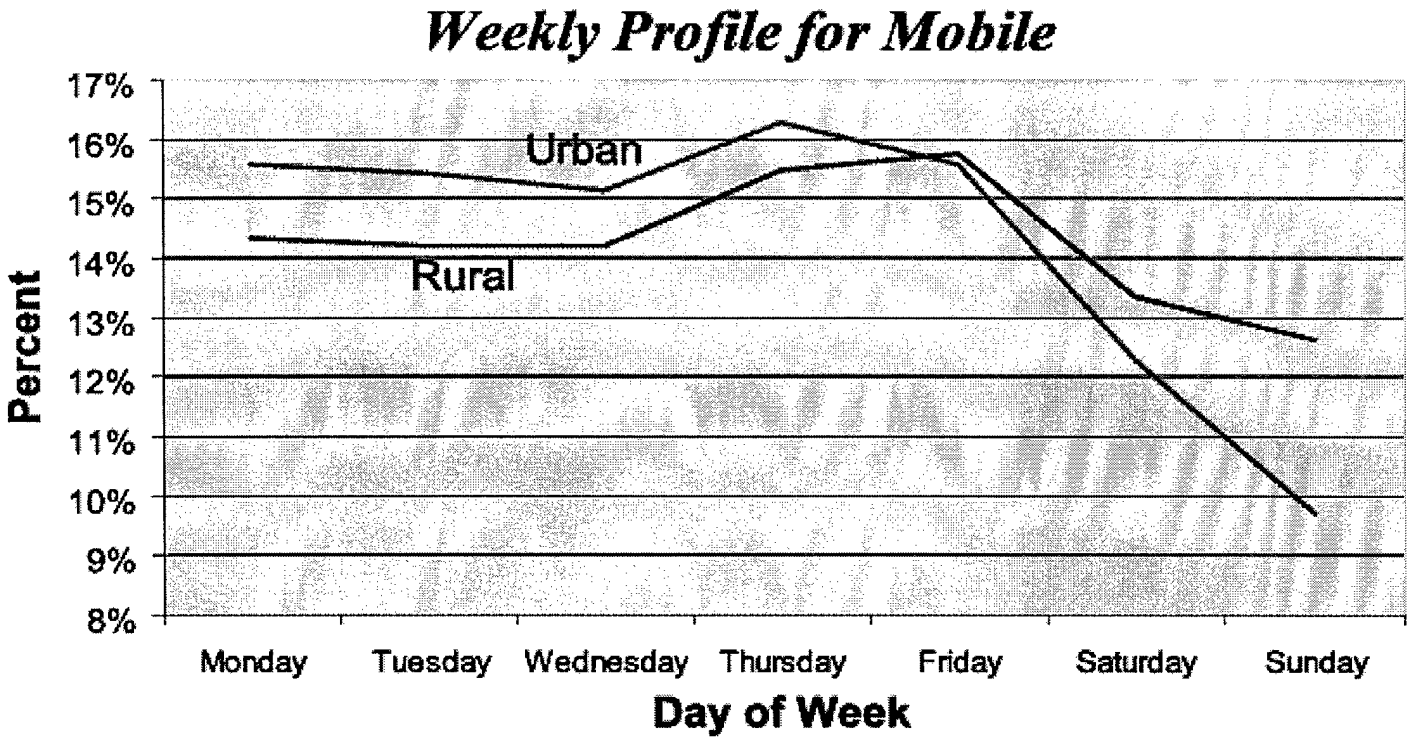

Figure 4.12. Weekly profile of rural and urban mobile sources. Source: MCNC, 2001.

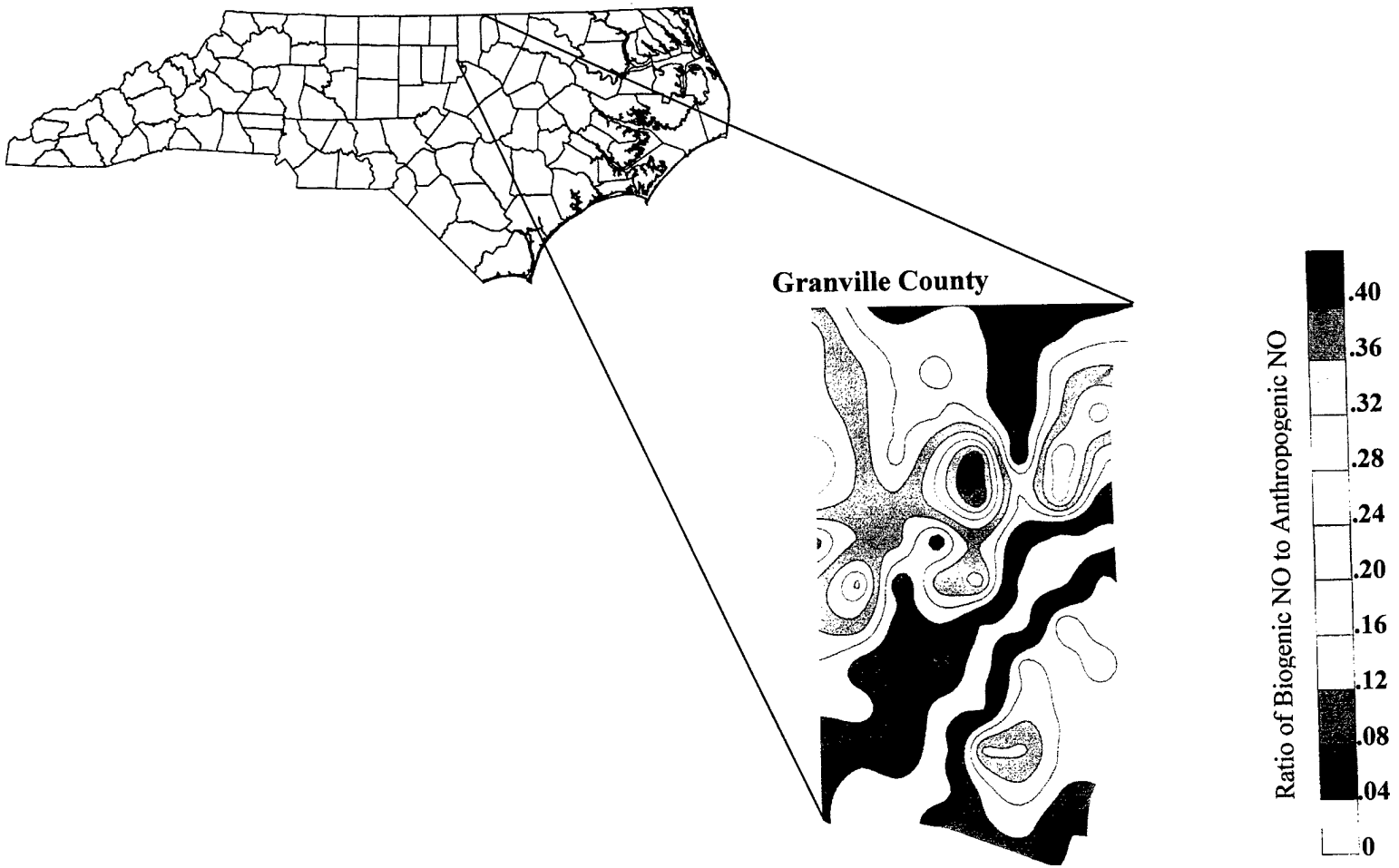

Figure 4.13a. Ratio of biogenic NO to anthropogenic NO in Granville County, NC (mid-week, afternoon).

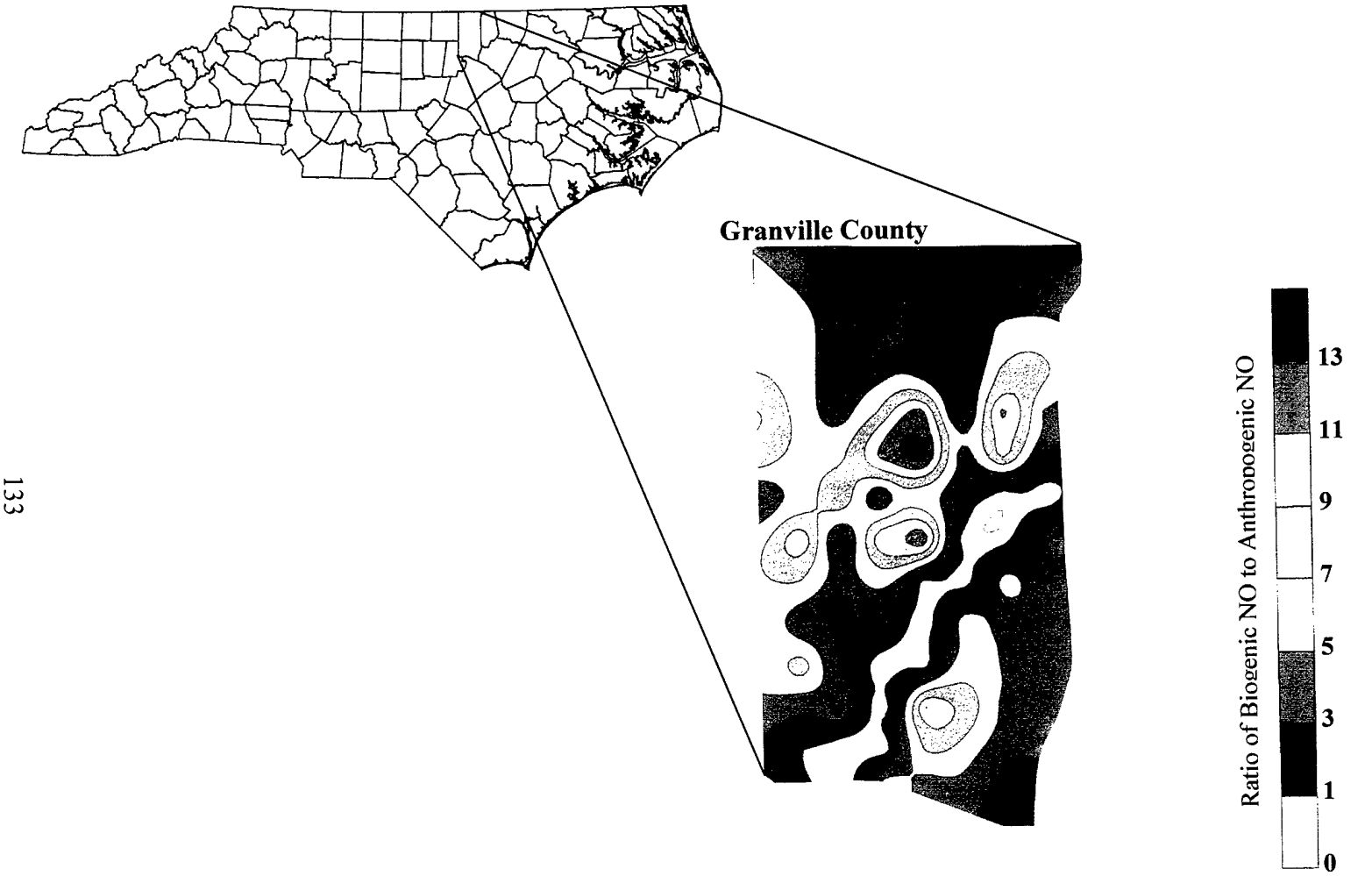

Figure 4.13b. Ratio of biogenic NO to anthropogenic NO in Granville County, NC (weekend, early morning).

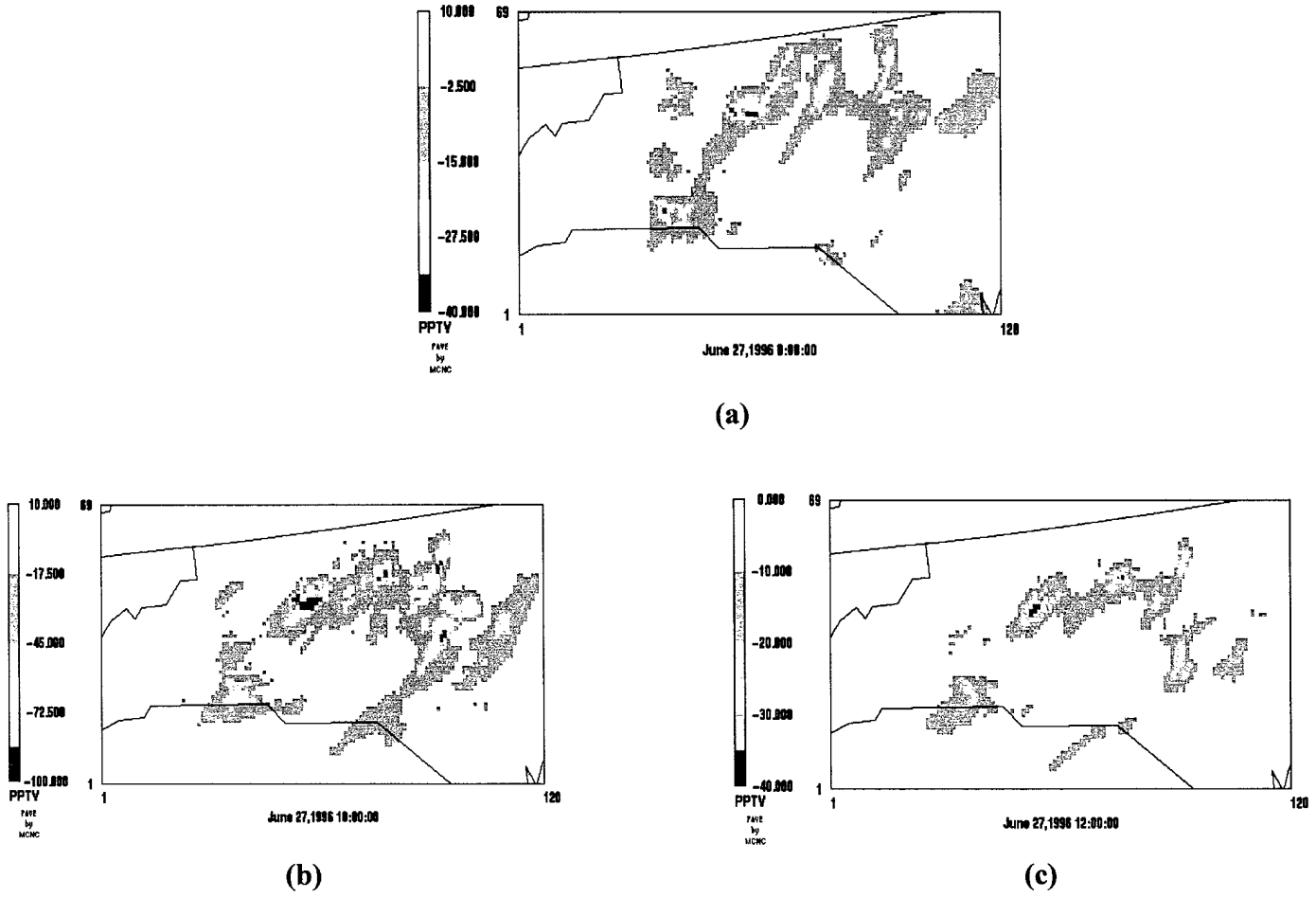

Figure 4.14. Change in O_3 concentrations throughout Wednesday, June 26 and Thursday, June 27, 1996 (Modified case – Base case) plotted at 8:00 pm (a), 6:00 am (b), and 8:00 am (c).

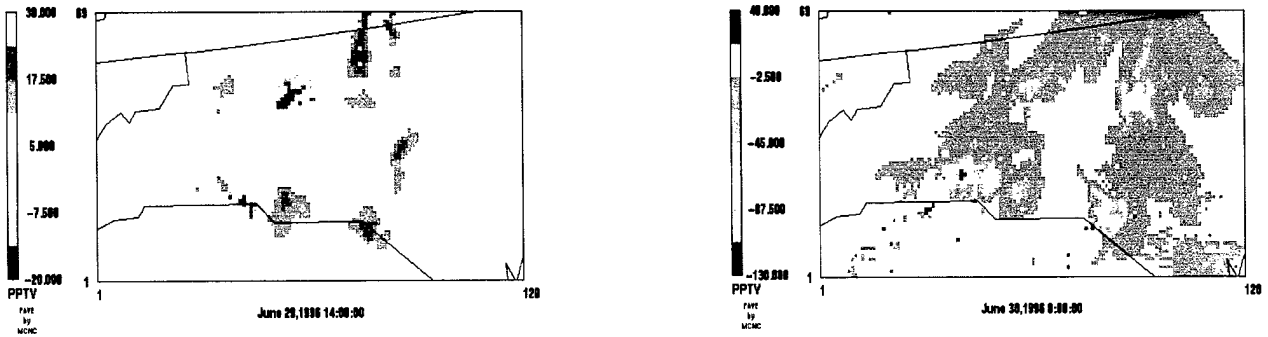

(a) **(b)**

Figure 4.15. Change in O_3 concentrations throughout Saturday, June 29 and Sunday, June 30, 1996 (Modified case – Base case) plotted at 10:00 am (a) and 4:00 am (b).

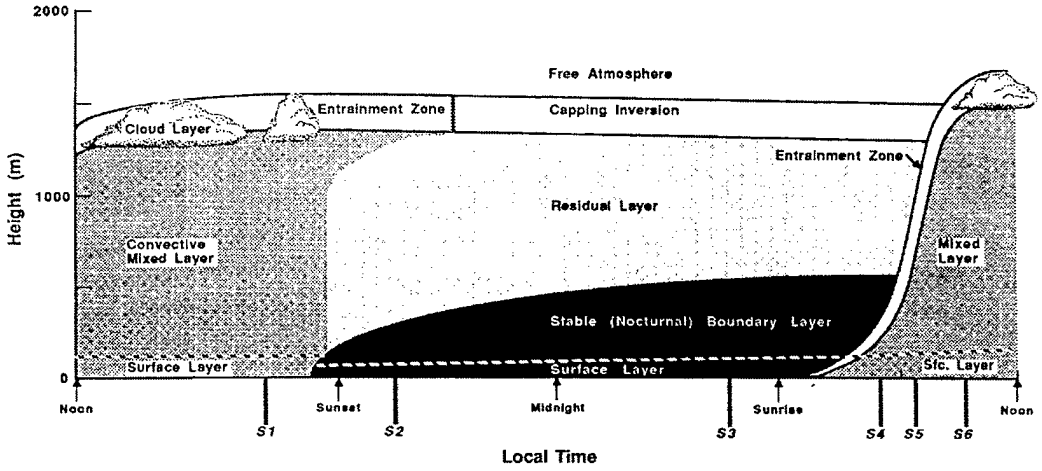

Figure 4.16. Diurnal variation of Planetary Boundary Layer. Source: Stull, 1994.

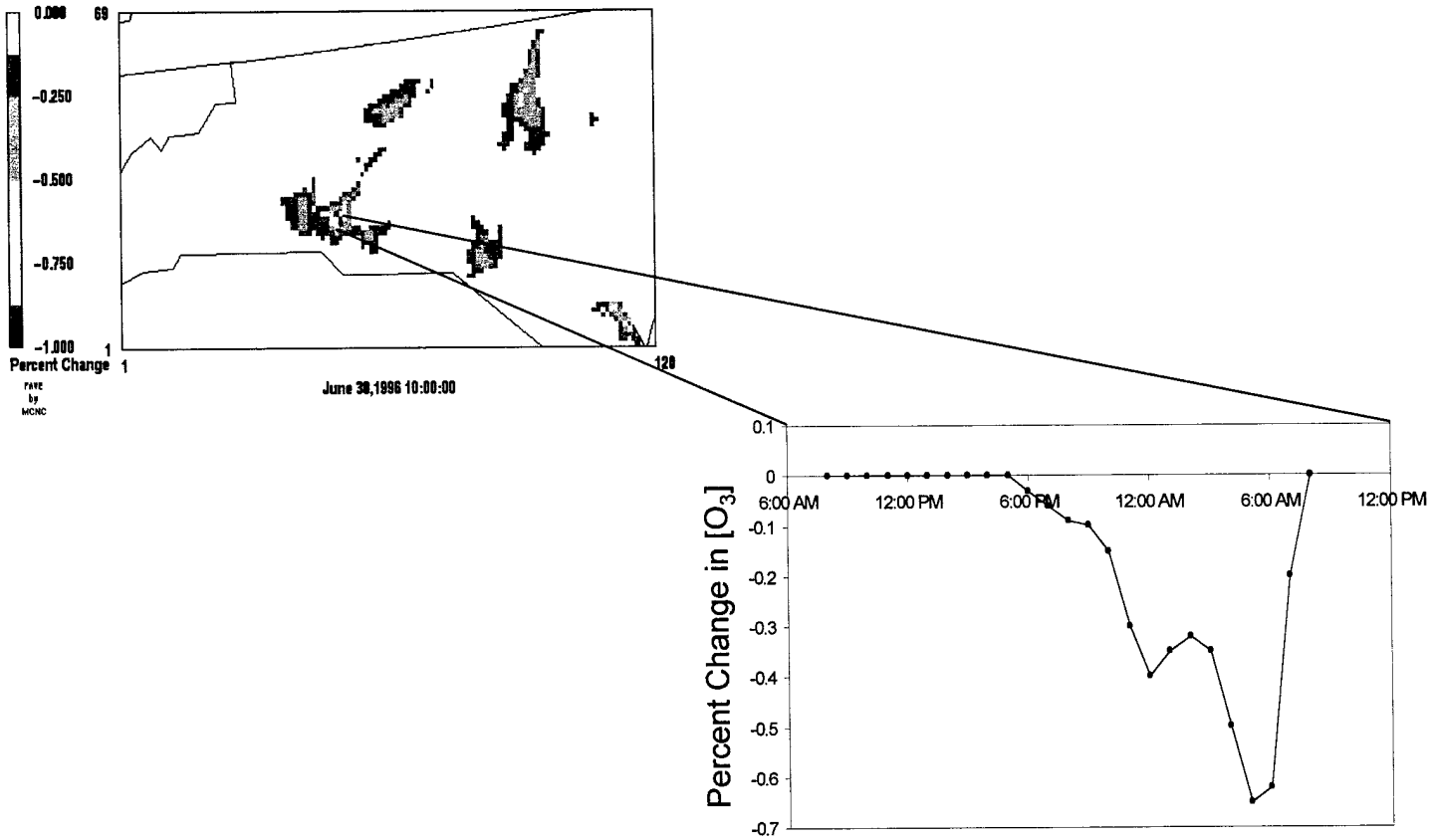

Figure 4.17. Percent change of ozone in the modeling domain. Time series plot represents the average percent change throughout the 24 hour period (8:00 am Saturday – 8:00 am Sunday). Negative values indicate that ozone levels are lower in the modified case than in the base case.

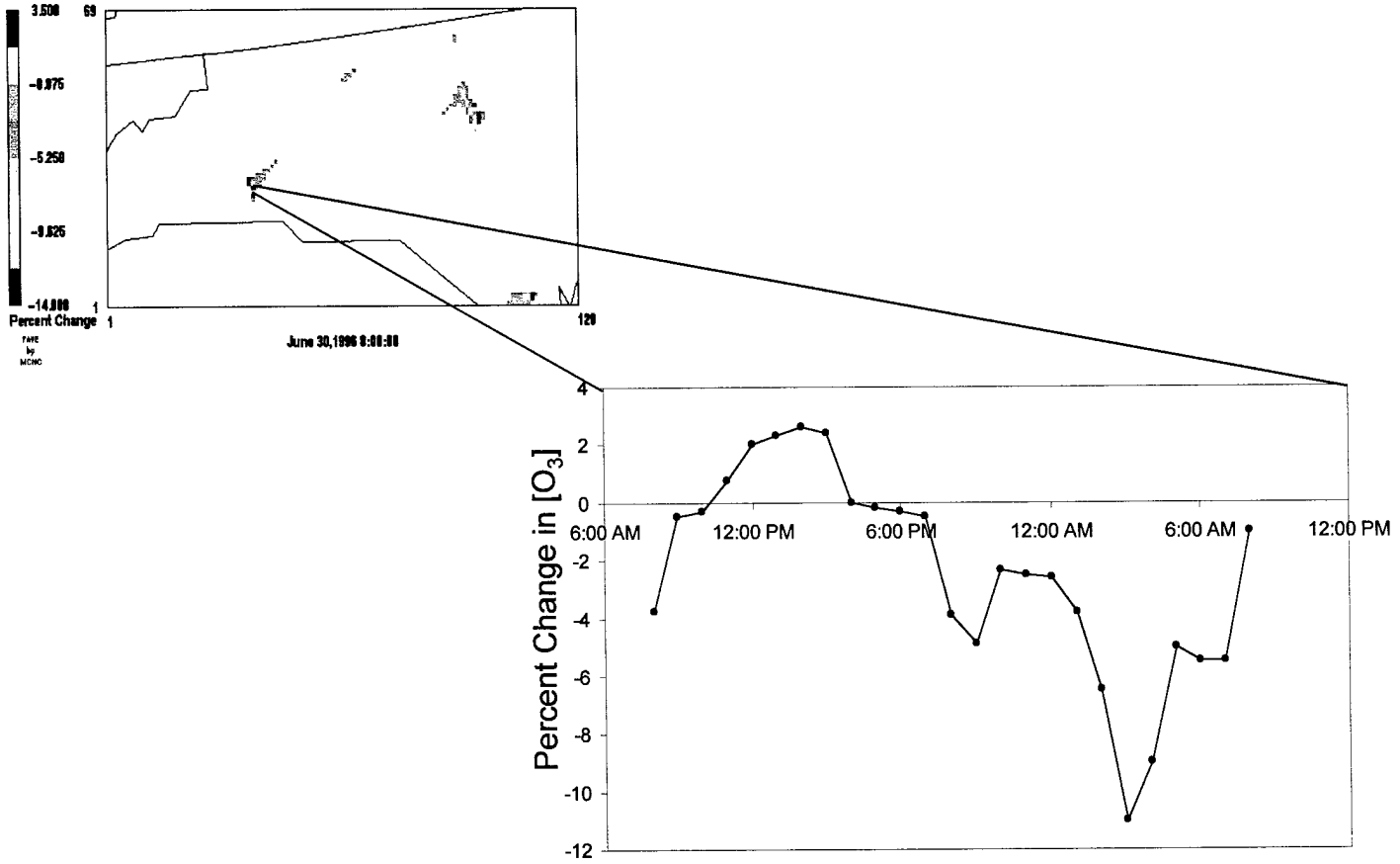

Figure 4.18. Percent change of ozone in the modeling domain with biosolids concentrated within the counties. Time series plot represents the average percent change throughout the 24 hour period (8:00 am Saturday – 8:00 am Sunday). Negative values indicate that ozone levels are lower in the modified case than in the base case.

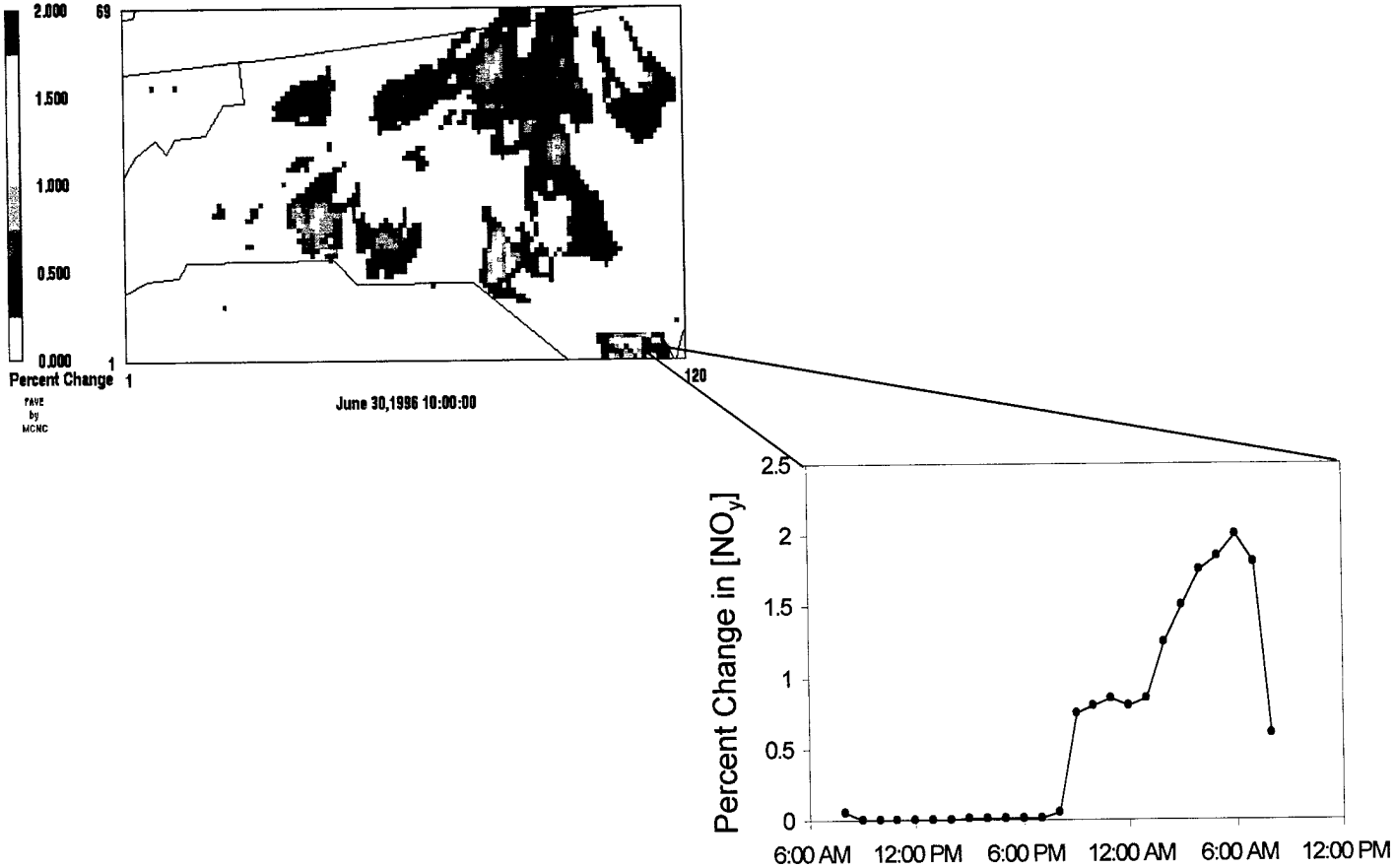

Figure 4.19. Percent change of NO_y concentrations in the modeling domain. Time series plot represents the average percent change throughout the 24 hour period (8:00 am Saturday – 8:00 am Sunday).

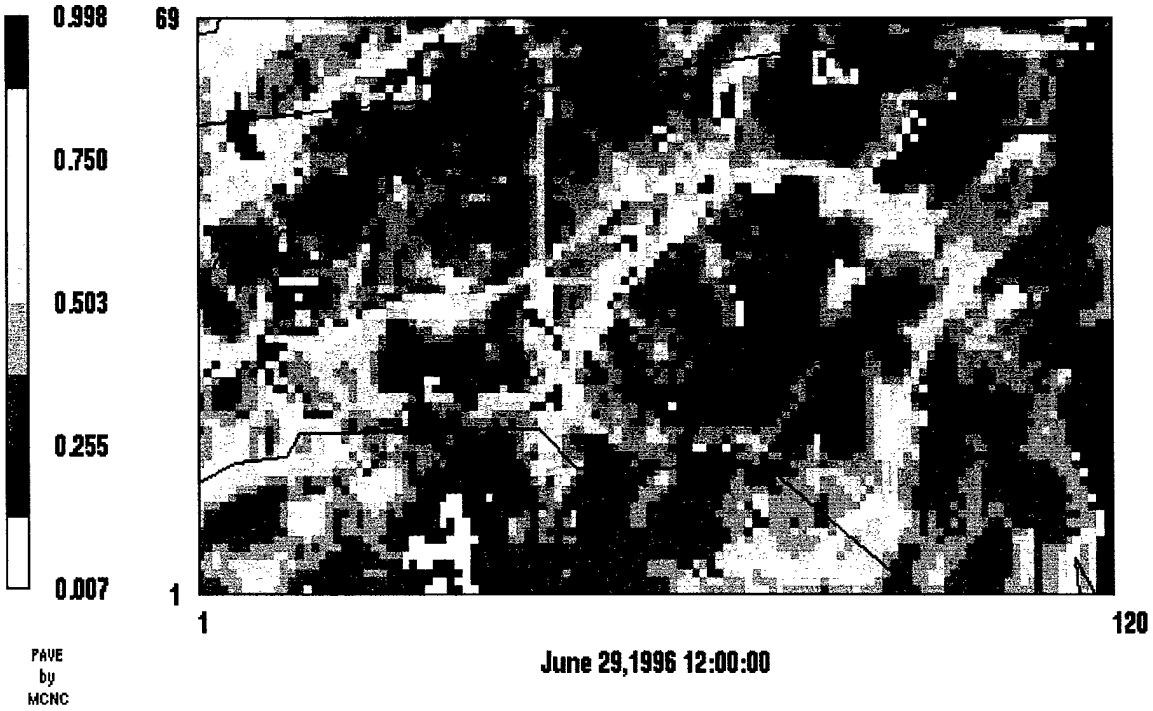

Figure 4.20. Ratio of NO_x to NO_y in MAQSIP modeling domain.

CHAPTER V. CHARACTERIZATION OF AMMONIA EMISSIONS FROM SOILS IN THE UPPER COASTAL PLAIN, NORTH CAROLINA

by

Paul A. Roelle and Viney P. Aneja

Department of Marine, Earth, and Atmospheric Sciences
North Carolina State University
Raleigh, NC 27695-8208

Published in: Atmospheric Environment, in press, 2001.

Abstract

A dynamic flow-through chamber system was used to measure fluxes of ammonia-nitrogen (NH_3-N, where NH_3-N=(14/17)*NH_3) from soil surfaces. The research site was located in eastern North Carolina (35.9°N Latitude; 77.7°W Longitude) and measurements were conducted during spring and winter 2000, in order to assess the NH_3 source strength of intensively managed agricultural soils and the physiochemical properties which control these emissions. Soil temperature (T_{soil}), soil pH, soil moisture, Total Kjeldahl Nitrogen (TKN=organic N+NH_3-N+NH_4^+-N) were monitored throughout both research periods. Soil temperature was found to explain the largest variability in soil NH_3 emissions [$Log_{10}NH_3$-N Flux (ng N m^{-2} s^{-1})= 0.054*T_{soil} (°C) + 0.66; R^2=0.71), suggesting that an approach similar in design to the Biogenic Emissions Inventory System (BEIS2) land use and temperature model for NO emissions, might be effective for modeling biogenic NH_3 emissions. Soil nitrogen was also significant in predicting NH_3 flux [NH_3 Flux =55.5*(NH_3-N)-160, R^2=0.86; NH_3 Flux=0.6*(TKN)-410, R^2=0.27], but only after the two days with the heaviest rainfall were removed from the regression,

emphasizing the role of soil moisture in controlling the transfer of gases across the soil/air interface. Soil pH remained relatively constant throughout both research periods and therefore did not serve as a useful predictor of NH_3 flux. A rain event, followed by a drying period produced a characteristic pulse in ammonia emissions. This pulsing phenomena has been observed for other trace gases by various researchers. This research location was the site of a commercial hog operation, which allowed for the comparison of soil and lagoon emissions (lagoon emissions were based on an algorithm developed by Aneja et al., 2000). An analysis of the source strengths confirmed that lagoon emissions are a larger flux source (average lagoon flux ~ 18,137 ng N m^{-2} s^{-1}; average soil flux ~ 54 ng N m^{-2} s^{-1}), however soil surfaces make up a larger fraction of a commercial hog operation than the lagoon surfaces, and as a result they can not be neglected when developing and apportioning NH_3 emissions. A yearly average of ammonia emissions at this site revealed that soil emissions represent approximately 28% of the lagoon emissions.

Introduction

Ammonia (NH_3) is an important atmospheric trace species, both in terms of its effect on tropospheric chemistry and due to its impact on ecosystems. Ammonia, which is the most abundant alkaline specie in the atmosphere, is critical to neutralizing acids formed through the oxidation of sulfur dioxide (SO_2) and nitrogen oxides (NO_x) (Asman et al., 1998). When NH_3 is deposited onto the soil, it is both taken up by plants and converted by bacteria into nitrate (NO_3^-) (nitrification) (Lekkerkerk et al., 1995). The nitrification process forms hydrogen ions leading to acidification of the soil, leaching of NO_3^- to groundwater, and possible deficiencies of other plant nutrients such as potassium (K^+) and magnesium (Mg^{2+}) (Asman et al., 1998). In addition to acidification, excess nitrogen loading can lead to over enrichment of both land and water ecosystems. Further, excess N deposition can cause the above ground portion of the plant to grow rapidly, leaving the root system relatively smaller and weaker and more susceptible to disease and harsh weather conditions (Lekkerker et al., 1995).

Unlike oxidized nitrogen and sulfur compounds (NO_x and SO_x respectively), which are predominately emitted from industrial processes, NH_3 is primarily emitted by agricultural sources and therefore requires different control strategies (Sutton et al., 1993). A review of the current literature revealed that soil and plant emissions account for anywhere between 11% and 28% of the global NH_3 budget (Table 1.2). In North Carolina, which is currently the second largest pork producing state in the US, the percentage of ammonia emissions from swine is approximately 46% compared to the US average of 10% (Battye et al., 1994) (Figure 1.6 a,b).

Accurate inventories of NH_3 are needed to model both its transport and deposition (Misselbrook et al., 2000). Beyond quantifying this overall source strength and the effects to ecosystems, there needs to be an accurate budget and reliable source apportionment of the various NH_3 emission pathways from these intensively managed animal operations (Figure 5.1). Current inventories that are then used in air quality models are determined using emission factors (ie tons NH_3/animal/year or % NH_3-N emitted/tons of N-fertilized applied), most of which are based on European studies. Therefore, the objectives of this study are to quantify and relate the soil NH_3 flux at an eastern North Carolina site to different environmental variables in the soil, and determine the source strength of these soil emissions. Moreover, the soil ammonia emissions will be compared and contrasted to ammonia emission measurements made over animal (swine) waste treatment and storage lagoons (Aneja et al., 2000).

Methods and Materials

Sampling Site and Sampling Scheme

The NH_3 flux measurements were made at the Upper Coastal Plain Research Station (Figure 5.2), located in Edgecombe County, North Carolina (See Table 5.1 for site/soil characteristics). This facility is operated with typical agronomic and husbandry practices for the respective crops and animals and contains approximately 178 hectares, 101 of which are cropland soils. The facility also maintains a farrow-to-finish hog operation with approximately 1250 hogs on site. The waste from the animals (urine and feces) is flushed from the hog production houses into two uncovered anaerobic waste treatment and storage lagoons (a primary and secondary lagoon, total acreage ~ 1

hectare). The effluent from these lagoons is periodically sprayed to the crops as a nutrient source. A corn crop was planted on April 5th, 2000 and spring measurements began on April 26th and ended on May 14th, 2000. Due to several rain events and equipment malfunctions, only 5 days were suitable for conducting the measurements, all of which are presented in Table 5.1.

Although the field sampled is typically sprayed with lagoon effluent, it was not sprayed during the 2000 measurement campaign and instead received approximately 146 kg N/ha on May 24th, 2000. The corn crop was harvested on August 21st and the stalks were shredded and left on the soil surface. No cover crop was planted and the winter measurements were conducted from Dec 13th-19th, 2000. Rain events prevented measurements on two of the days, although measurements were made on the remaining 5, all of which are presented in Table 5.1.

NH_3 concentration measurements were made on 10 random sampling plots located within a 10 m radius of a mobile laboratory (Modified Ford Aerostar Van, temperature controlled to within the operating range of the instruments). The sampling scheme consisted of measuring concentrations of NH_3 after the sample exited the dynamic flow-through chamber system. The system recorded 60-second, rolling averages of NH_3 concentrations. These values were then binned and averaged every 15 minutes. The 15-minute binned averages were used in all flux calculations. N in Table 5.1 refers to the number of these binned averages (to also include soil temperature as discussed in *Soil Analysis).*

A daily experiment consisted of placing the chamber on the stainless steel collar, which had been inserted into the soil the previous evening. The collars were all located on bare soil with no plants being enclosed within the collar or chamber system. The chamber was placed on the collar at approximately 8:00 AM and flushed with zero grade air for at least one hour before data collection began at 9:00 AM. This sampling scheme ensured that the concentrations within the chamber reached steady state prior to any data acquisition and allowed for the instruments to undergo their daily calibrations. Daily experiments ended at approximately 5:00 PM and the stainless steel collar was relocated to a random location within a 10 m radius of the mobile laboratory, in preparation for the next days experiment. This procedure allowed a minimum of 16 hours for any effect on soil NH_3 flux, due to soil disturbances caused by the insertion of the stainless steel collar, to dissipate.

Instrumentation and Flux Calculation

The chamber design, associated mass balance equation and calibration procedures are described in full in Chapter I.

Soil Analysis

A soil sample was taken from the center of the chamber footprint at the end of each measurement period (1 sample per measurement period), and analyzed for soil pH, soil moisture and Total Kjeldahl Nitrogen (TKN=organic N+NH_3-N+NH_4^+-N) by the North Carolina State University Department of Biological and Agricultural Engineering. Percent water filled pore space (% WFPS) is a measure of soil water content and can be expressed as the percentage of pore spaces in the soil that are filled with water. The

%WFPS is a convenient expression to describe soil moisture because it accounts for the differing bulk and particle densities of soils and therefore allows for the comparison of soil moisture from different soil types. Soil temperature was measured with a Campbell Scientific temperature probe (accuracy ± 3%) inserted into the soil to a depth of approximately 5 cm. Air temperatures (Campbell Scientific; accuracy ± 3%) were measured inside of a radiation shield at a height of 1.5 meters. Soil data was stored in 15 minute binned averages utilizing a Campbell Scientific 21X Micrologger.

Results and Discussion

Environmental Controls on NH_3 Flux

The ammonia-water and ammonia-soil system have been studied in the past because of their industrial importance and as a means for studying the absorption/desorption mechanism (Whitman and Davis, 1924; Godfrey, 1973; Levenspiel and Godfrey, 1974; Ibusuki and Aneja, 1984; Leuning et al., 1984; Warneck, 2000). These previous studies indicate that the three most important parameters in the biological and chemical processes which determine the NH_3 equilibrium and production rate are temperature, pH and nitrogen content of the soil. In the soil environment these variables translate to soil temperature, soil pH, and the soil moisture content.

Soil Temperature

The temperature dependence is linked to the NH_3 production/emission through chemical and biological processes occurring simultaneously in the soil environment. In the absence of recent N fertilization, ammonia appears in the soil through a process called mineralization or ammonification whereby microorganisms satisfy their energy needs in

the soil by converting amino acids in the dead organic matter to NH_3 as in the following reaction (Delwiche, 1970; Kinzig and Socolow, 1994):

$$CH_2NH_2COOH + 11/2O_2 \rightarrow 2CO_2 + H_2O + NH_3 \quad (1)$$

Given that biochemical reactions have been shown to rise exponentially with temperature in the range between 288 – 308 K, one would expect there to be a corresponding increase in the soil NH_3 concentration as soil temperature increases (assuming that the system is not limited by soil organic matter content) (Warneck, 2000). In fact, this exponential dependence of both reduced and oxidized nitrogen trace species on soil temperature has been repeatedly demonstrated in both field and laboratory studies (Sherlock and Goh, 1985; Van der Molen et al., 1990; Roelle et al., 1999).

The NH_3 and NH_4^+ in the soil solution are in aqueous equilibrium,

$$NH_4^+{}_{(aq)} \leftrightarrow NH_{3(aq)} \quad (2)$$

and if the NH_3 vapor pressure in solution is greater than the vapor pressure of NH_3 in the surrounding air than the NH_3 will be volatilized (Sherlock and Goh, 1985). This relationship can be expressed in the form of Henry's Law, where the dimensionless Henry coefficient (H) can be written as:

$$H = (NH_{3(aq)})/ (NH_{3(g)}) \text{ and} \quad (3)$$

$$\text{Log } H = -1.69 + 1477.7/T \quad (4)$$

(Hales and Drewes, 1979; Sherlock and Goh, 1985).

From equations 3 and 4 above, it can be shown that an increase in soil temperature will produce a corresponding increase of the $NH_{3(g)}$ concentrations in the soil. This same Henry's law equilibrium applies in water bodies (such as hog waste

lagoons) and Aneja et al. (2001a) have developed a fundamental mechanistic ammonia model to predict lagoon NH_3 emissions based on this equilibrium. The Aneja et al. (2000) study confirmed that lagoon temperature was the dominant parameter affecting NH_3 emissions from lagoons and the temperature dependence model that they developed was then compared to a temperature dependence model developed in this study for NH_3 emissions from soil surfaces. Other physiochemical parameters that influence NH_3 emissions are pH, nitrogen content, and moisture content of the soil.

The calculated NH_3 fluxes (including rainfall totals which are discussed later) during the spring and winter 2000 measurement period can be seen in Figure 5.3. The values calculated during this study fall within the range of NH_3 soil fluxes reported by other researchers (Table 5.2). The daily averaged NH_3 flux values plotted versus the daily averaged soil temperature (Figure 5.4) reveal a statistically significant relationship ($p<0.01$) with NH_3 flux increasing exponentially as soil temperature increases. The next best fit to this data was a linear model which resulted in an $R^2=0.62$ [NH_3-N Flux (ng N m^{-2} s^{-1}) = 6.9* T_{soil} (^oC)-35.6]. The soil temperature model in this study [$Log_{10}NH_3$-N Flux (ng N m^{-2} s^{-1}) = $0.054*T_{soil} + 0.66$; $R^2=0.71$] and the lagoon temperature model in the Aneja et al. (2000) study [$Log_{10}NH_3$-N Flux (μg N m^{-2} min^{-1}) = $0.048*T_{lagoon} + 2.1$; $R^2=0.78$] indicate approximately the same amount of variability in the NH_3 flux from the soil and lagoon surfaces. This strong exponential dependence of NH_3 emissions on temperature has been cited for other nitrogen (N) trace gases (NO, NO_2 and N_2O) with approximately the same results (Kim et al., 1994; Sullivan et al., 1996; Roelle et al., 1999). In fact, the US Environmental Protection Agency (EPA), currently utilizes this

exponential temperature dependence in the Biogenic Emissions Inventory System (BEIS) model to estimate the biogenic nitric oxide emissions (NO) which are then used as input data for ozone and air quality models (Birth and Geron, 1995; Thornton et al., 1997). The strong temperature dependence reported in this study suggests that a similar approach may also be effective in estimating the biogenic NH_3 emissions.

Soil pH, Soil Moisture and Soil Nitrogen Content

As previously discussed, other parameters such as soil pH and soil moisture have been identified as controlling NH_3 production. The $[OH^-]$ produced as a result of the following dissociation in the soil solution

$$NH_{3(aq)} \leftrightarrow NH_4^+{}_{(aq)} + OH^- \quad (5)$$

can be represented by:

$$[OH^-] = K_w/[H^+], (K_w\text{=water dissociation constant}) \quad (6)$$

As the soil pH increases ($[OH^-]$ increases), the equilibrium is shifted towards more NH_3 being released (Warneck, 2000; Li, 2000), and studies have demonstrated pH to effect NH_3 emissions (Singh and Nye, 1988; Aneja et al., 2001a). However, in intensively managed agricultural soils, the pH value of a soil column (~20 cm) tends to remain fairly uniform (see Table 5.1), and therefore no significant relationships between soil pH and NH_3 flux can be discerned. The studies which identified soil pH as a significant variable typically looked at pH in the top 1-3 cm of the soil and were during fertilization events, both of which found much larger changes in pH values (1-3 pH units). Therefore it is recommended that future field studies should also include an analysis of soil pH over a few different sampling depths.

The soil moisture conditions at this field site are best described by Figure 5.3, which shows the rain events in relation to the sampling days and measured flux values. The percent water filled pore space (%WFPS) (Table 5.1) also describes moisture conditions, however the effects of our soil sampling technique (20 cm depth), has the potential to dilute the actual moisture content in the top few centimeters of the soil column, where the largest concentration of ammoniacal nitrogen has been shown to reside (Singh and Nye, 1986). As more water is introduced, pores in the soil matrix begin to fill and hinder the diffusion of NH_3 gas from the soil to the air (Kirk and Nye, 1991). Additionally, from an equilibrium standpoint, as the water content in the soil increases, the NH_3 decreases as the equilibrium moves towards the right hand side of equation (5).

Increases in emissions have been observed when soils with high moisture content are subjected to drying via high winds or temperature. This increase or "pulse" is believed to be caused by the combination of an increase in the ammoniacal nitrogen concentration of the soil and greater diffusion through the relatively drier soil (Burch and Fox, 1989; Battye et al., 1994). A similar "pulse" in emissions (day 3 in Figure 5.3) may be causing the large increase in emissions which occurred after the sharp decrease in soil moisture (decreased from 40.5 %WFPS to 24.9 %WFPS). While this observation is based on only one data point, prior to which there was a lapse of several days of data, it is supported by similar observations from other researchers (Burch and Fox, 1989; Battye et al., 1994).

The relationship of NH_3 volatilization and N content of the soil can be seen in Figure 5.5(a,b). Several investigators have attempted to develop models describing the physical and chemical processes affecting the release of NH_3 from soil surfaces (Sherlock and Goh, 1985; Singh and Nye, 1986). Based on their mechanistic models, a linear dependence of NH_3 flux on soil nitrogen content was expected and found to explain more variability in the data than other attempted relationships. In both plots (a and b), there was a relatively weak dependence of NH_3 flux on NH_3-N and TKN content of the soil (R^2=0.12 and 0.02 for NH_3-N and TKN respectively) when all data points are considered in the regression. Given the strong influence that soil moisture has on NH_3, both in terms of its equilibrium and in its control of diffusion through the soil, both a and b were reanalyzed taking the moisture conditions into account. When 2 sampling days (rain events > 0.3 cm and standing water evident in some parts of the field) were removed, there was an appreciable increase in the significance of N content on NH_3 release. The rain events which occurred on December 13th and 16th were both light mists with the majority of the total rainfall occuring after the sampling period. Interestingly, the largest rainfall event (December 17th) did not suppress NH_3 emissions on December 18th, relative to the other wintertime measurements. However strong winds associated with the frontal passage following the rainfall event did act to dry out the surface layer even though the soil core had the highest % WFPS. The greater dependence of NH_3 volatilization rates on NH_3 content (R^2=0.86) as compared to TKN (R^2=0.27) is expected as TKN is the sum of both ammoniacal N and organic N.

Budget for Site

Aneja et al. (2000) described a temperature based model similar to the model described in this study, although their model related NH_3 emissions from hog waste lagoons to lagoon temperature. While the processes regulating NH_3 emissions from lagoon surfaces differ from those regulating soil NH_3 emissions, the temperature relationship is found to be applicable to both. The physical and chemical processes regulating the emissions from the lagoon and soil surfaces and their dependence on soil temperature are described in detail in Aneja et al. (2001a) and Warneck (2000), respectively. Utilizing the temperature model developed in this study to estimate NH_3 emissions from soils and the temperature based algorithm developed by Aneja et al. (2000) to estimate NH_3 emissions from lagoons (See Table 5.2 for measured lagoon NH_3 emission averages), it is possible to estimate the relative seasonal source strengths of the soil and the lagoon.

Although this yearly estimate is based on a model developed from two seasons of data, the temperature dependence is assumed to remain consistent, during periods when the soil has not been recently fertilized, throughout diurnal cycles and throughout the year (Van der Molen et al., 1990; Aneja et al., 2000; Warneck, 2000). Using the daily averaged temperatures (Information obtained from North Carolina State Climate Office), the seasonally averaged emissions from the 101 hectares of soil surface at this site during spring, summer, fall and winter were determined to be 324 kg NH_3-N, 933 kg NH_3-N, 383 kg NH_3-N and 83 kg NH_3-N respectively (Figure 5.6). Similarly, the seasonally averaged lagoon emissions from the 1 hectare of lagoon surface during spring, summer,

fall and winter were determined to be 1,140 kg NH_3-N 2,953 kg NH_3-N, 1,315 kg NH_3-N and 340 kg NH_3-N respectively. Therefore, the NH_3 emissions from soil surfaces represent approximately 28%, 32%, 29% and 24% of the spring, summer, fall and winter lagoon emissions. The typical practice in most hog operations is to spray the fields with the hog waste effluent instead of fertilizing them with commercially derived fertilizers. This field, however, was not sprayed and therefore this budget may be biased low, as emission factors for land spreading of slurry are often cited as being larger (~15-76%) than the factors for the commercially derived fertilizers (Misselbrook et al., 2000).

Conclusions and Recommendations

Utilizing a dynamic flow-through chamber technique, NH_3 flux values were calculated for the spring and winter (2000) at an upper coastal plain site in North Carolina. Soil pH remained relatively constant throughout the measurement period and therefore was not useful as a NH_3 flux predictor. The NH_3 flux values were most strongly correlated with soil temperature [$Log_{10}NH_3$-N Flux (ng N m^{-2} s^{-1}) = 0.054*T_{soil} + 0.66; R^2=0.71], which may help to steer the way towards developing a temperature and land use type model (similar in design to the EPA's Biogenic Emissions Inventory System (BEIS) model for estimating biogenic NO emissions) to estimate biogenic NH_3 emissions. However, when the major rain events were eliminated, the role of soil nitrogen (both NH_3-N and TKN) in explaining the variability in NH_3 flux improved significantly.

The average NH_3 flux values from this study corresponded well with other reported values and confirmed that soils have smaller fluxes of NH_3 than lagoons (Table

5.2). However, as in most commercial animal operations the land area used for crops is significantly larger than the surface area for lagoons. A preliminary analysis revealed that given the relative sizes of the agricultural soils in comparison to the lagoons, the soils (soils represent ~28% of the lagoon NH_3 emissions) cannot be neglected when developing and apportioning NH_3 budgets. Further, the soil algorithm developed in this study was based on a crop which had not been fertilized for several months prior to the experimental period. Given that land spreading of slurry is estimated to release approximately 15-76% of the applied nitrogen may indicate that estimates presented in this study should be considered as a lower limit. It should be noted that the data used to produce this inventory was only from this one field site during the time periods discussed. The exponential temperature relationship reported here, however has been consistently reported throughout the literature and therefore provides some basis for this study to be extended throughout the year and at different soil and crop types. It should not be assumed, however that this temperature dependence can be extended to all temperatures, as temperatures outside the range of 15-35 °C are often found to alter the often-cited exponential relationship.

While temperature has often been shown to be a controlling variable in nitrogen trace gas emissions, other variables (pH, N-content, % WFPS) have displayed more mixed results (Williams et al., 1992; Matson et al., 1997). Therefore, future work should consist of field and laboratory studies to further investigate these relationships and data following slurry application should also be obtained to help refine the NH_3 budget for intensively managed agricultural soils. While this research does help to quantify the soil

source strength, it does not shed much light on transport through canopies or on the effect ambient NH_3 concentrations have on deposition versus emissions. Even though the values reported in this study are within the range of other reported values, a side-by-side comparison of the differing NH_3 flux methodologies would be extremely beneficial in furthering our knowledge of this species. A simple model based on first principles will be proposed and analyzed in the following chapter.

References

Aneja, V.P., J.P. Chauhan and J.T. Walker, Characterization of atmospheric ammonia emissions from swine waste storage and treatment lagoons, Journal of Geophysical Research, 105, 11,535-11,545, 2000.

Aneja, V.P., B.P. Malik, Q. Tong and D. Kang, Measurement and modeling of ammonia emissions at waste treatment lagoon-atmospheric interface, Water, Air and Soil pollution, in press, 2001a.

Aneja, V.P., P.A. Roelle, G.C. Murray, J. Southerland, J.W. Erisman, D. Fowler, W. Asman and N. Patni, Atmospheric nitrogen compounds II: emissions, transport, transformation, deposition and assessment, Atmospheric Environment, 35, 1903-1911, 2001b.

Asman, W.A.H., P. Cellier, S. Genermont, N.J. Hutchings and S.G. Sommer, Ammonia emission research: from emission factors to process descriptions, Eurotrac newsletter, 20, 2-10, 1998.

Battye, R. W. Battye, C. Overcash and S. Fudge, Development andselection of ammonia emission factors. EPA Contract Number 68-D3-0034, Work Assign. 0-3, USEPA, Research Triangle Park, North Carolina, 1994.

Birth, T.L. and C.D. Geron, User's guide to the personal computer version of the biogenic emissions inventory system (PC-BEIS2), EPA-600/R-95-091, July 1995.

Burch, J.A. and R.H. Fox, The effect of temperature and initial soil moisture content on the volatilization of ammonia from surface applied urea, Soil Science, 147, 311-318, 1989.

Delwiche, C.C., The nitrogen cycle, Scientific American, 223, 137-146, 1970.

Godfrey, J.M., A new apparatus for studying mass transfer and reaction between two fluid phases, PhD thesis, p. 154, Oregon State University, Corvallis, 1973.

Hales, J.M. and D.R. Drewes, Solubility of ammonia at low concentrations, Atmospheric Environment, 13, 1133-1147, 1979.

Ibusuki, T. and V.P. Aneja, Mass transfer of NH_3 into water at environmental concentrations, Chemical Engineering Science, 39, 1143-1155, 1984.

Kim, D.S., V.P. Aneja and W.P. Robarge, Characterization of nitrogen oxide fluxes from soil of a fallow field in the central piedmont of North Carolina, Atmospheric Environment, 28, 1129-1137, 1994.

Kinzig, A.P. and R.H. Socolow, Human impacts on the nitrogen cycle, Physics Today, 24-31, Nov. 1994.

Kirk, G.J.D. and P.H. Nye, A model of ammonia volatilization from applied urea. V. The effects of steady-state drainage and evaporation, Journal of soil science, 42, 103-113, 1991.

Lekkerkerk, L.J.A., G.J. Heij and M.J.M. Hootsmans, Dutch priority programme on acidification, Ammonia: the facts, Secretariat Additional Programme on Acidification Research, Report no. 300-06, April 1995.

Levenspiel, O. and J.M. Godfrey, A gradientless contactor for experimental study of interface mass transfer with/without reaction, Chemical Engineering Science, 29, 1723-1730, 1974.

Li, C.S., Modeling trace gas emissions from agricultural ecosystems, Nutrient cycling in agroecosystems, 58, 259-276, 2000.

Matson, P., M. Firestone, D. Herman, T. Billow, N. Kiang, T. Benning and J. Burns, Agricultural systems in the San Juaquin Valley: Development of Emission Estimates for Nitrogen Oxides, Technical Report, U. of Ca, Berkeley, Contract Numb: 94-732, 1997.

Misselbrook, T.H., T.J. Van Der Weerden, B.F. Pain, S.C. Jarvis, B.J. Chambers, K.A. Smith, V.R. Phillips and T.G.M. Demmers, Ammonia emission factors for UK agriculture, Atmospheric Environment, 34, 871-880, 2000.

Roelle, P.A., V.P. Aneja, J. O'Connor, W.P. Robarge, D.S. Kim and J.S. Levine, Measurement of nitrogen oxide emissions from an agricultural soil with a dynamic chamber system, Journal of Geophysical Research, 104, 1609-1619, 1999.

Sherlock, R.R. and K.M. Goh, Dynamics of ammonia volatilization from simulated urine patches and aqueous urea applied to pasture. II. Theoretical derivation of a simplified model, Fertilizer Research, 6, 3-22, 1985.

Singh, R. and P.H. Nye, A model of ammonia volatilization from applied urea. I. Development of the model, Journal of Soil Science, 37, 9-20, 1986.

Sullivan, L.J., T.C. Moore, V.P. Aneja and W.P. Robarge, Environmental variables controlling nitric oxide emissions from agricultural soils in the southeast United States, Atmospheric Environment, 30, 3573-3582, 1996.

Sutton, M.A., C.E.R. Pitcairn and D. Fowler, The exchange of ammonia between the atmosphere and plant communities, in Advances in Ecological Research, Vol. 24, edited by M. Begon and A.H. Fitter, pp. 301-390, 1993.

Thornton, F.C., P.A. Pier and R.J. Valente, NO emissions from soils in the southeastern United States, Journal of Geophysical Research, 102, 21,189-21,195, 1997.

Van der Molen, J., A.C.M. Beljaars, W.J. Chardon, W.A. Jury and H.G. Van Faassen, Ammonia volatilization from arable land after application of cattle slurry. 2. Derivation of a transfer model. Netherlands journal of agricultural science, 38, 239-254, 1990.

Warneck, P., Chemistry of the natural atmosphere, second edition, Academic Press, Inc., New York, NY, pp. 511-530, 2000.

Weber, A., Gutser, R. and U. Schmidhalter, Results from field experiments on ammonia losses after urea application with regard to measurement methodologies, in Proceedings of UN/ECE Ammonia Expert Group, edited by H. Menzi, Swiss College of Agriculture, Berne, 18-20 September, 2000.

Whitman, W.G. and D.S. Davis, Comparative absorption rates for various gases, Industrial Engineering Chemistry, 16, 1233-1237, 1924.

Williams E., A. Guenther and F. Fehsenfeld, An inventory of nitric oxide emissions from the soil in the United States, Journal of Geophysical Research, 97, 7511-7519, 1992.

Site: Upper Coastal Plain Research Station
35.9° N Latitude
77.7° W Longitude
Elevation: 35.5 Meters
Soil Type: Norfolk Loamy Sand

Sampling Period (N=)	Crop / Fertilization	pH	WFPS %	N – Content µg/g			Soil Temp (°C)	NH_3 Flux (ng N m^{-2} s^{-1})
				NH_3-N	NO_3-N	TKN		
5 April 00	**Corn Planted**							
26 April 00 (33)		5.2	38.6	6.1	16.9	909	16.2 ± 2.3	145.4 ± 33.5
27 April 00 (28)		5.2	40.5	7.7	17.7	1070	15.1 ± 1.7	38.4 ± 11.7
12 May 00 (21)		5.1	24.9	7.0	19.2	963	28.4 ± 3.0	271.1 ± 135.1
13 May 00 (20)		5.2	22.9	4.5	8.1	889	30.4 ± 3.0	128.8 ± 45.5
14 May 00 (20)		5.5	24.3	5.1	5.4	806	28.6 ± 2.2	90.3 ± 13.6
24 May 00	**146 kg N/ha**							
21 Aug 00	**Corn Harvested**							
13 Dec 00 (29)		4.9	33.1	3.5	12.0	933	6.8 ± 1.0	26.1 ± 10.9
14 Dec 00 (27)		5.2	39.9	8.5	11.1	1004	8.3 ± 0.6	7.3 ± 3.4
16 Dec 00 (34)		5.2	28.6	3.0	5.3	941	8.8 ± 1.5	9.6 ± 5.7
18 Dec 00 (29)		5.1	53.9	3.9	9.1	776	7.4 ± 1.8	13.7 ± 6.0
19 Dec 00 (27)		5.3	35.8	2.4	8.6	737	6.9 ± 1.9	3.4 ± 3.1

TKN = Total Kjeldahl Nitrogen = organic N+NH_3-N+NH_4^+-N

Table 5.1. Site and soil characteristics for Spring 2000 and Winter 2000 measurement campaigns at the Upper Coastal Plain Research Station, Edgecombe County, NC.

Researcher	Site Description	Reported NH_3 Flux Values
Harrison et al., 1989	Grass and Crop Surfaces	-20 to 100 ng N m^{-2} s^{-1}
Meixner et al., 1991	Wheat	-12 to 25 ng N m^{-2} s^{-1}
Weber et al., 2001	Post-Fertilization (80 kg N ha^{-1}) Winter Wheat	
	1999	64 ng N m^{-2} s^{-1}
	2000	178 ng N m^{-2} s^{-1}
This Study		
▪ Spring	Corn Crop, pre-fertilization	38 to 271 ng N m^{-2} s^{-1}
▪ Winter	No Crop Planted	3 to 26 ng N m^{-2} s^{-1}
Aneja et al., 2000	Anaerobic Lagoon Surface	
▪ Spring		1706 ± 552 μg N m^{-2} min^{-1}
▪ Summer		4017 ± 987 μg N m^{-2} min^{-1}
▪ Fall		844 ± 401 μg N m^{-2} min^{-1}
▪ Winter		305 ± 154 μg N m^{-2} min^{-1}

Table 5.2. List of researchers and reported NH_3 flux values measured under various crop and fertilization scenarios.

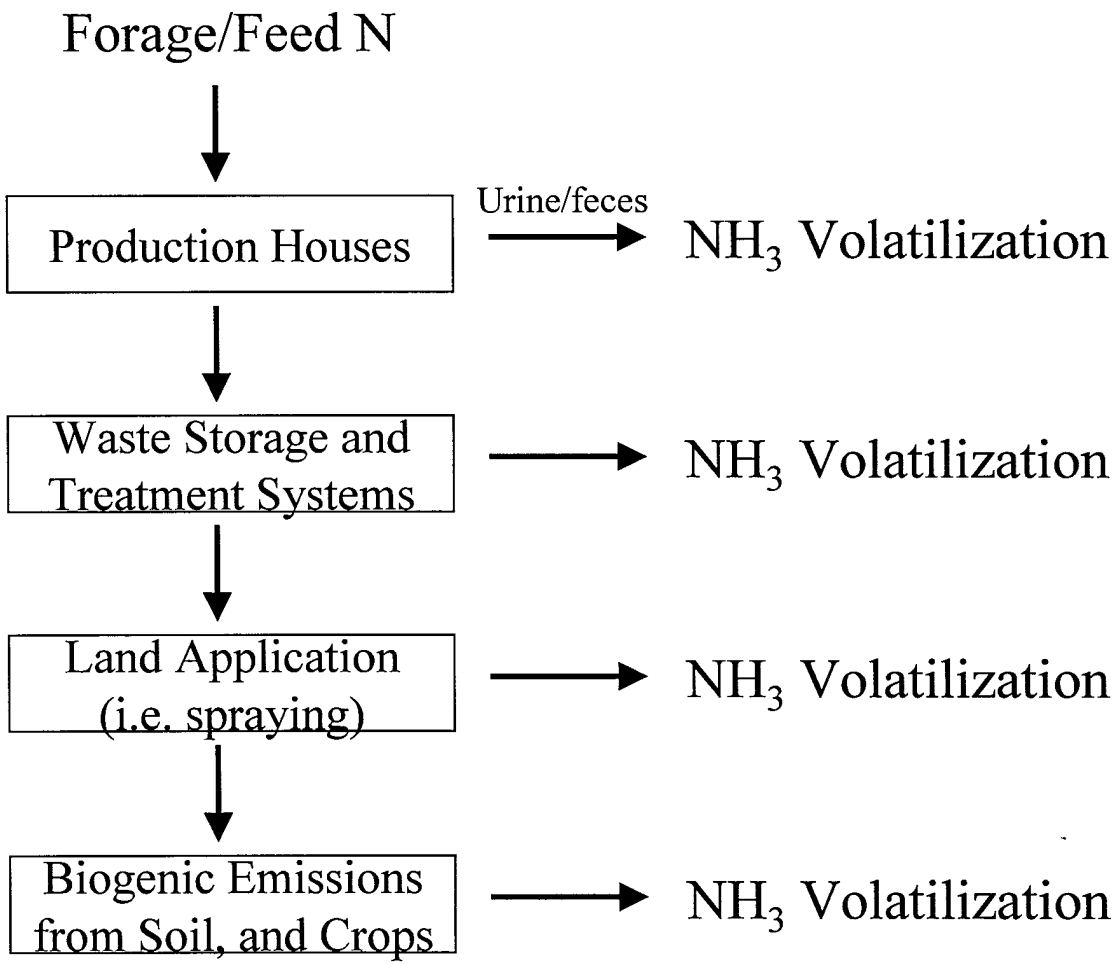

Figure 5.1. Major routes for NH_3 emissions from intensively managed animal operations in North Carolina, USA. Source: Aneja et al., 2001b.

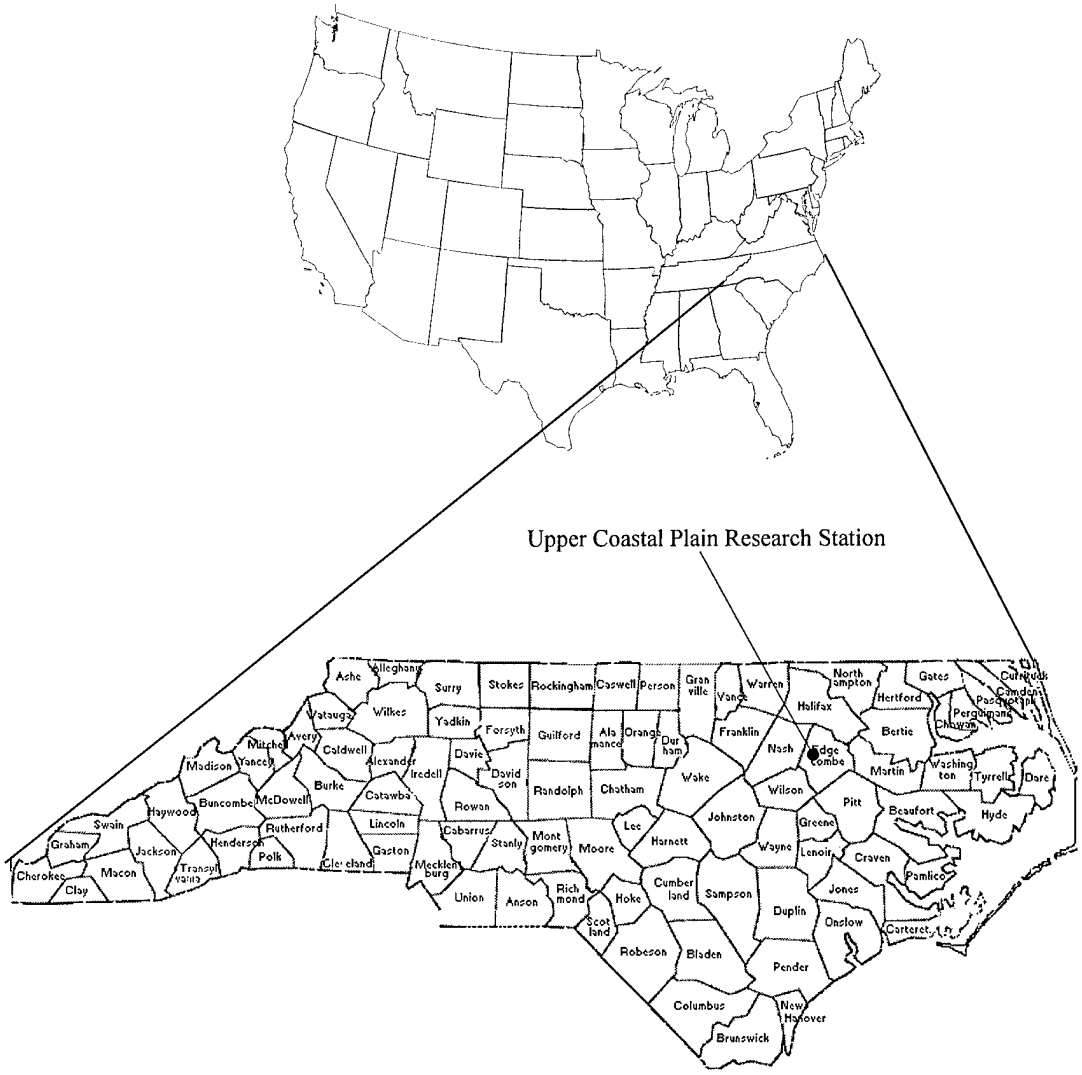

Figure 5.2. Site of Upper Coastal Plain Research Station.

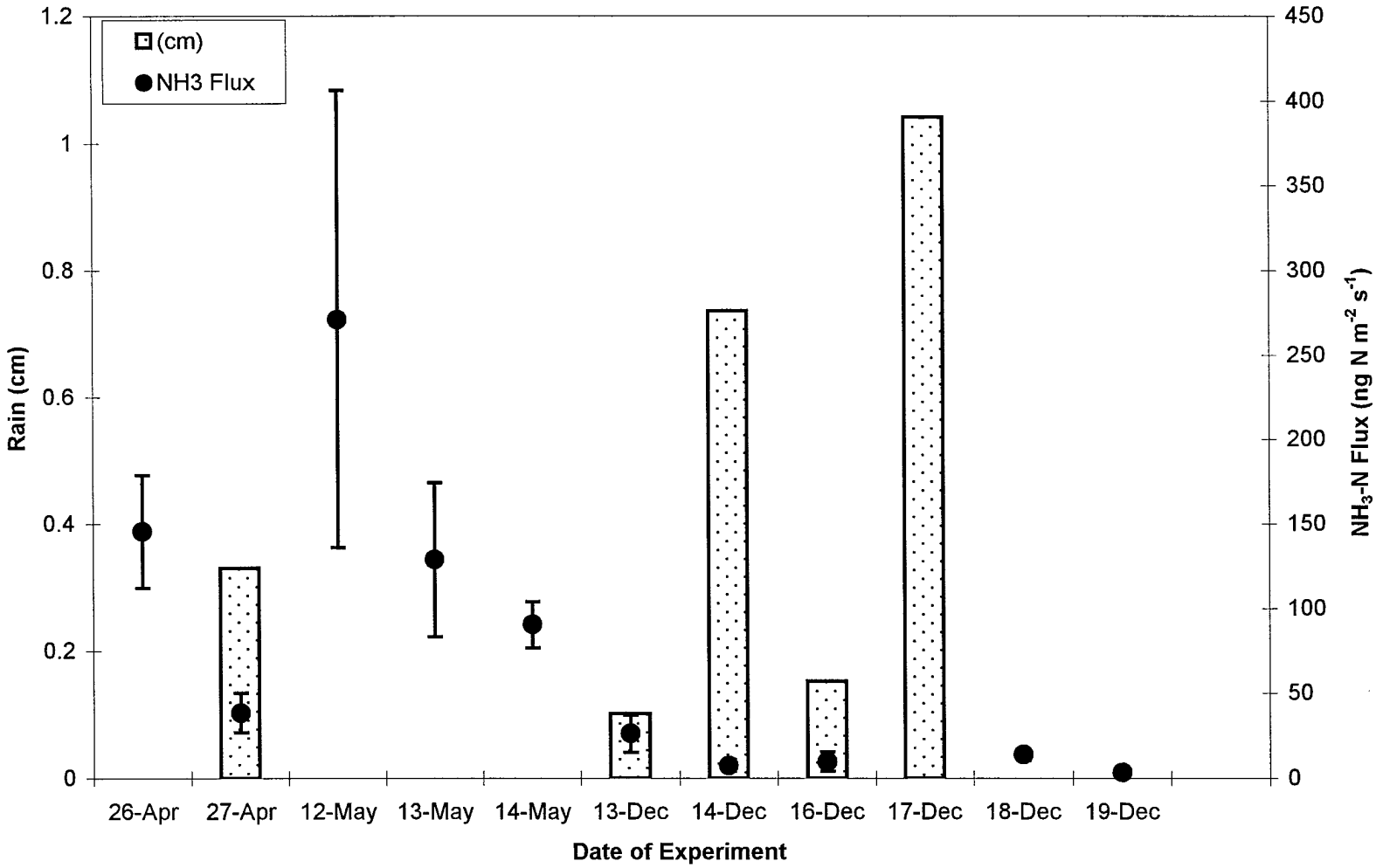

Figure 5.3. Total rainfall (primary axis) and NH_3-N flux (secondary axis) versus day of experiment. Vertical bars represent one standard deviation of the ammonia flux.

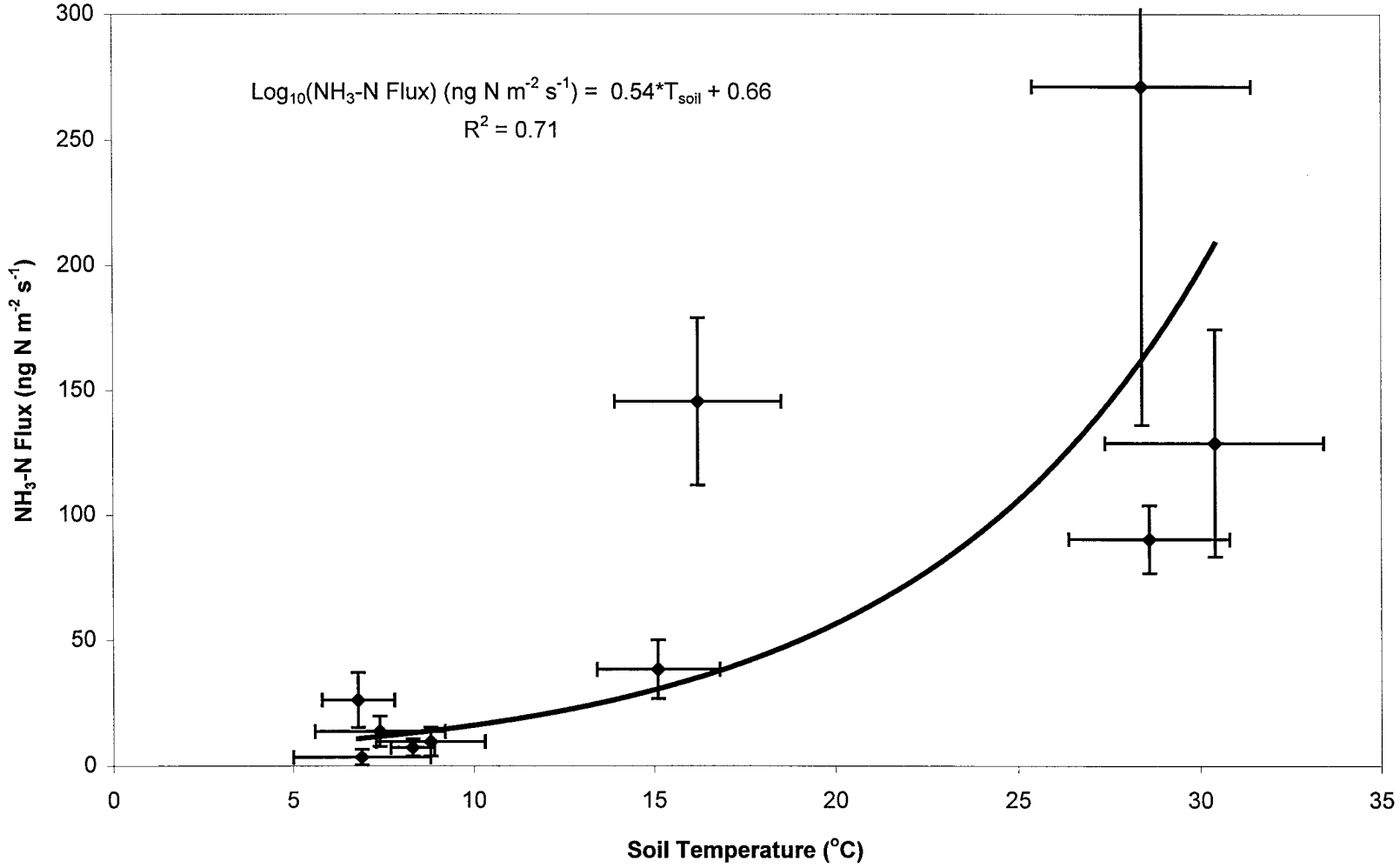

Figure 5.4. Plot of NH_3-N Flux versus soil temperature. Vertical lines represent one standard deviation of the average NH_3 Flux, and horizontal bars represent one standard deviation of the temperature during that flux measurement period.

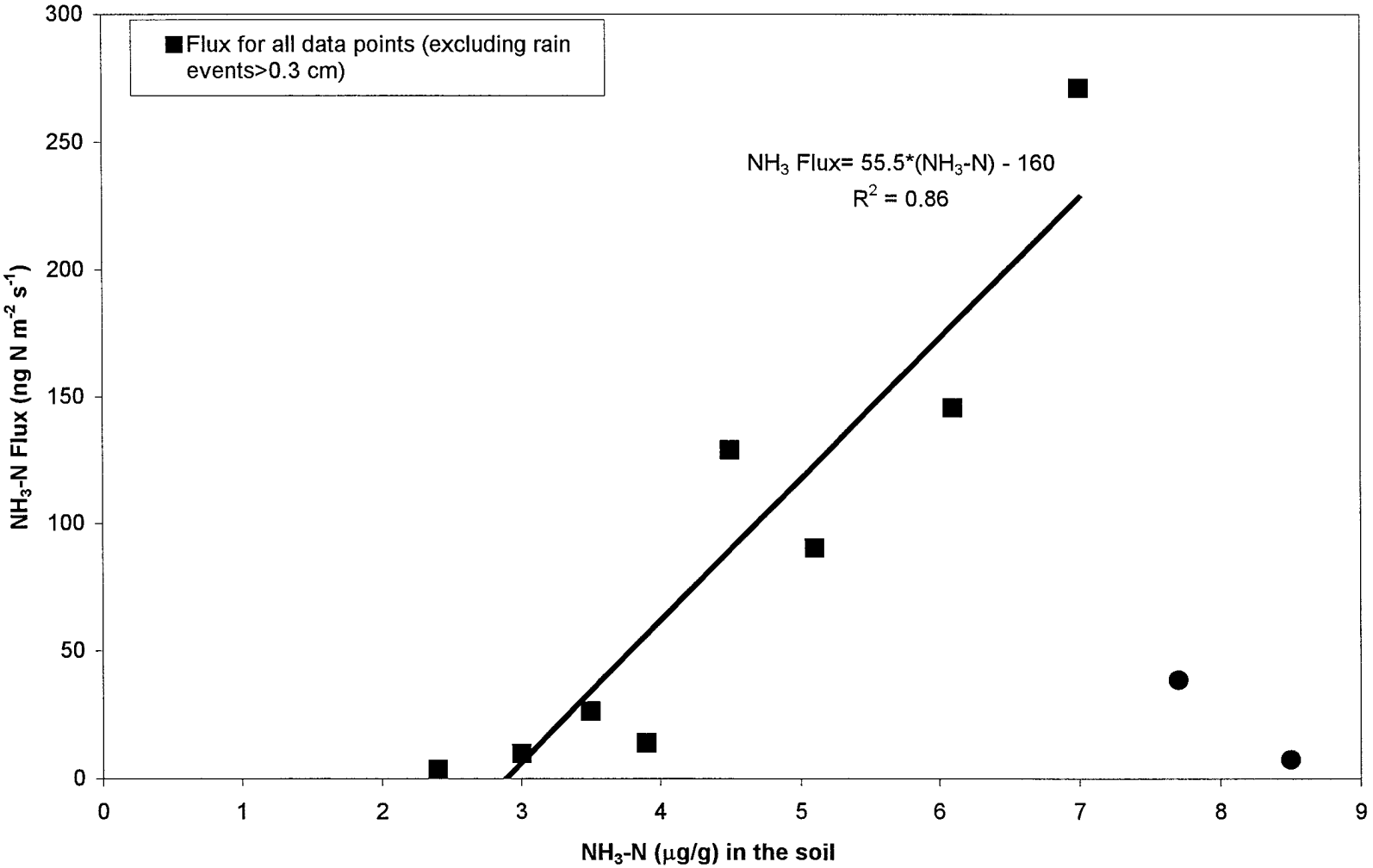

Figure 5.5a. Plot of NH_3-N Flux versus NH_3-N content of the soil. Note that (■) represents the data points without rain events >0.3 cm and (●) represents those data points that were measured on days having rain >0.3 cm.

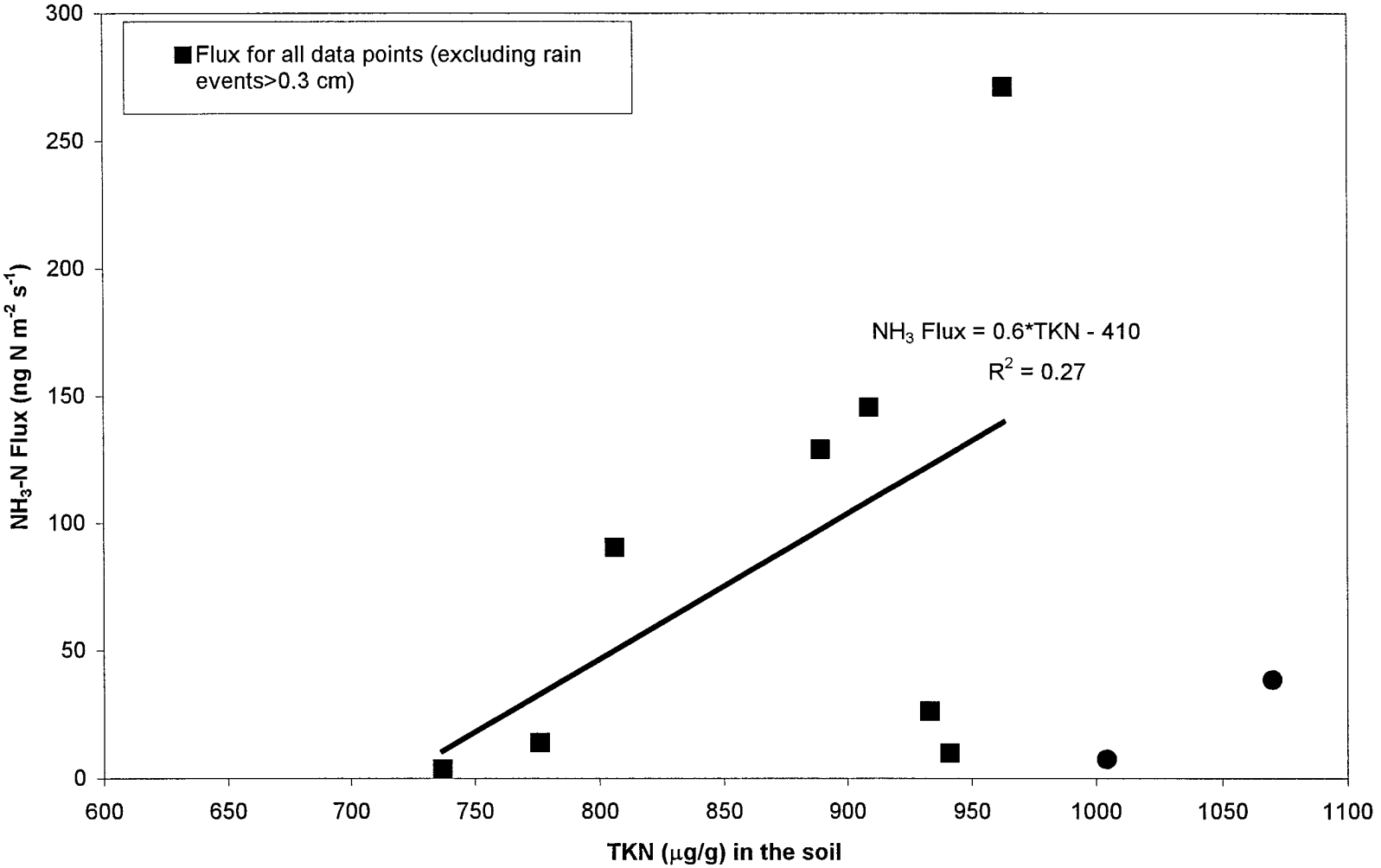

Figure 5.5b. Plot of NH_3-N Flux versus Total Kjeldahl Nitrogen content of the soil. Note that (■) represents the data points without rain events >0.3 cm and (●) represents those data points that were measured on days having rain >0.3 cm.

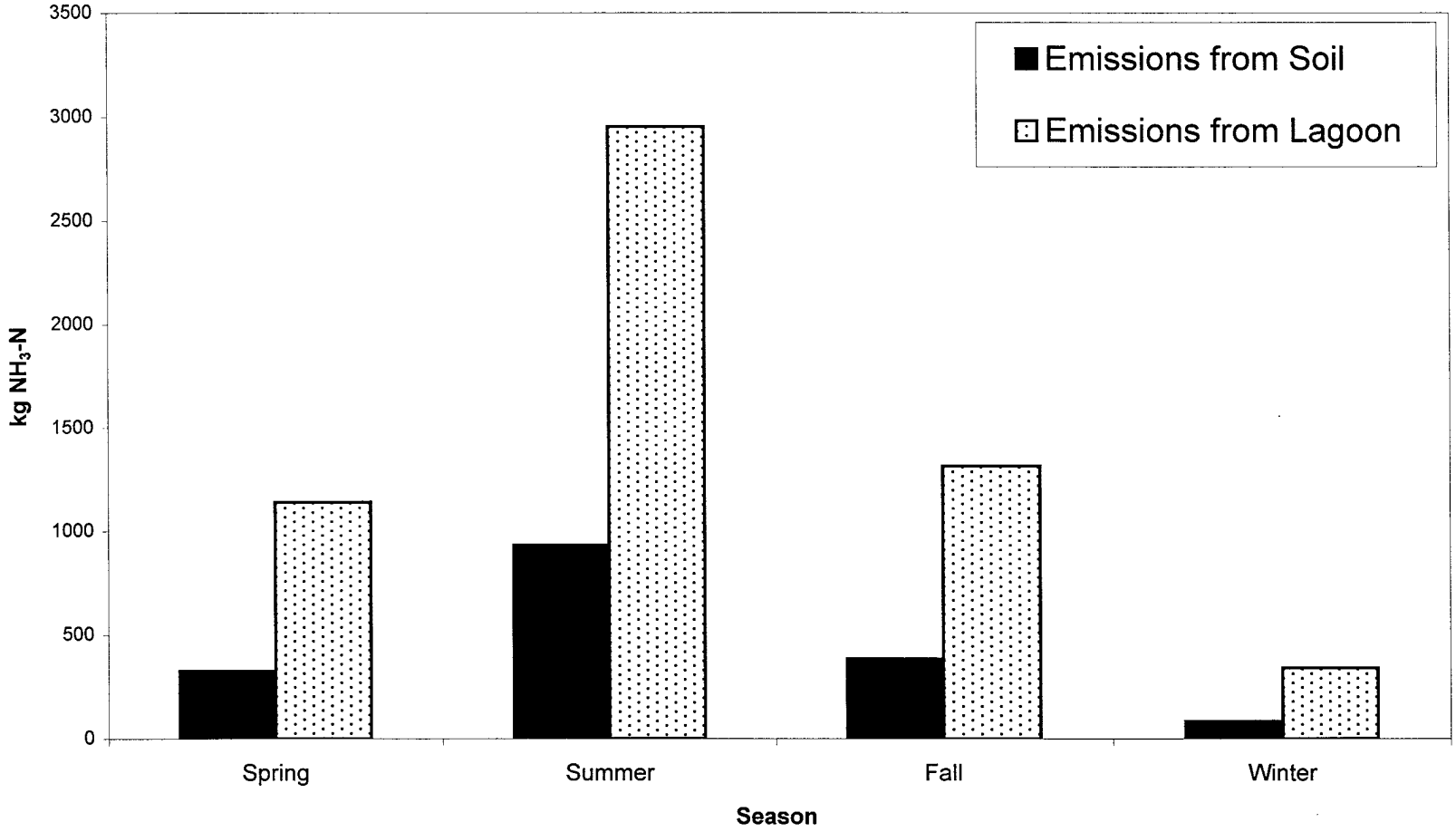

Figure 5.6. Budget of NH_3-N estimates from soil and lagoon surfaces at the Upper Coastal Plain Research Site. Soil estimates were determined by applying the flux algorithm developed in this study to the total land area (~101 ha). Lagoon estimates were determined by applying the flux algorithm developed by Aneja et al. (2000) to the total lagoon surface area (~ 1 ha).

CHAPTER VI. MODELING OF AMMONIA EMISSIONS FROM SOILS

Abstract

Using a dynamic flow-through chamber system in conjunction with a Thermo Environmental 17C Chemiluminescence ammonia (NH_3) analyzer, emissions from slurry-amended (~ 33 kg N ha^{-1}) and non-amended soils were calculated at a swine farm in eastern North Carolina. The average NH_3-N flux values during the period when the soils were not amended with any slurry were ~ 54 ng N m^{-2} s^{-1} while the average NH_3-N flux values measured immediately following the application of slurry to the soil were 1723.9 ng N m^{-2} s^{-1}. An empirical model relating soil temperature to NH_3 flux for non-amended soils explained over 70% of the variability in NH_3 emissions, however a similar empirical model relating soil temperature to NH_3 flux for slurry amended soils was able to explain only 39% of the variability in NH_3 emissions. A mass transport model, based on physical and chemical processes to estimate NH_3 emissions from recently amended soils is also presented and compared and contrasted to the empirical model. The variables used in the mechanistic model are pH, soil temperature and total ammoniacal nitrogen content. When using the mass transport model, the percentage difference between predicted and measured values for the non-amended and slurry-amended soils were 164% and 16 % respectively, indicating that the mechanistic model is only applicable for periods when nitrification/denitrification, plant uptake and immobilization are small enough in comparison to the chemical and physical processes following slurry application that they can be ignored. The percentage of the nitrogen (N) applied which was emitted as NH_3 increased at its greatest rate immediately following slurry application

(1-2 days) and then began to level out at a value of approximately 20% by day 4. Previous laboratory studies found these volatilization events to be short lived (few days-2 weeks) and this study corroborates those findings.

Introduction

Emissions of ammonia (NH_3) from soils has been found to be a significant source of NH_3 into the atmosphere (Table 1.2). The vast majority (approx. 90%) of the NH_3 in the atmosphere is converted into NH_4^+ aerosols by the irreversible reactions of ammonia with sulfuric acid (H_2SO_4), nitric acid (HNO_3), hydrochloric acid (HCl), water and to a lesser extent (approximately 10%) the hydroxyl radical (OH) in the atmosphere (Warneck, 2000). These NH_4^+ aerosol producing reactions can be summarized as follows:

$$NH_3(g) + H_2SO_4(l) \rightarrow NH_4HSO_4(l) \quad (1)$$

$$NH_3(g) + HNO_3(g) \leftrightarrow NH_4NO_3(s) \quad (2)$$

$$NH_3(g) + HCl(g) \leftrightarrow NH_4Cl(s) \quad (3)$$

$$NH_3(g) + H_2O(l) \rightarrow NH_4^+ + OH^- \quad (4)$$

$$NH_3 + OH \rightarrow NH_2 + H_2O(l) \quad (5)$$

(Finlayson Pitts and Pitts, 1986).

The conversion of NH_3 to NH_4^+ dictates the spatial scale of the contribution of NH_3 to the total atmospheric nitrogen input (Aneja et al., 2001a). Due to ammonia's relatively shorter lifetime in the atmosphere (less than 5 days), low source height and high deposition velocities, its distribution is usually limited to its nearby surroundings (Warneck, 2000; Aneja et al., 2001a). The NH_4^+ aerosols, however have lifetimes on the order of 15 days and therefore can travel and deposit at larger distances from the ammonia source.

Control strategies to minimize NH_3 emissions require a more thorough understanding of the relative source strengths of the various emission pathways. Furthermore, computers used to model the fate of this increased ammonia can only be as accurate as the input data, and failing to capture any of the spatial or temporal variability in the NH_3 emissions will result in poor model output. This study describes a mass transport model, relating NH_3 release from the soil to the soil nitrogen content, pH and soil temperature. The model will then be assessed with field measurements with the aim of gaining a better understanding of the physical and chemical processes controlling the NH_3 emissions from soils and the applicability of this proposed mass transfer model.

Methods and Materials

Sampling Site and Sampling Scheme

The NH_3 flux measurements were made at the Upper Coastal Plain Research Station, located in Edgecombe County, North Carolina (See Figure 5.2 for measurement location; See Table 6.1 for site/soil characteristics). This facility (contains approximately 178 hectares, 101 of which are cropland soils) is operated with typical agronomic and husbandry practices for the respective crops and animals. The facility also maintains a farrow-to-finish swine operation with approximately 1250 swine on site. The waste from the animals (urine and feces) is flushed from the swine production houses into two uncovered anaerobic waste treatment and storage lagoons (a primary and secondary lagoon, total acreage ~ 1 hectare). The effluent from these lagoons is periodically sprayed to the crops as a nutrient source. A corn crop was harvested on August 21st and

the stalks were shredded and left on the soil surface. No cover crop was planted nor was the field fertilized throughout the winter and Spring of 2001.

NH_3 concentration measurements were made on 13 randomly selected plots located within a 10 m radius of a mobile laboratory (Modified Ford Aerostar Van, temperature controlled to within the operating range of the instruments). Portions of the research facility were being sprayed with the slurry during this measurement period. For the purposes of this study and to avoid contamination of the research equipment, the plots used in this study were amended individually. Twelve of the plots were surface applied with 750 ml of slurry collected from the hog waste lagoon and the last plot, which was used as the control, was unamended. Based on chemical analysis conducted on April 25th, 2001 by the North Carolina Agronomy Division, this equated to approximately 33 kg N ha^{-1}, an amount representative of typical agronomic practices (Troeh and Thompson, 1993). The daily sampling scheme was identical to the procedures described in Chapter V.

Instrumentation and Flux Calculation

The chamber design, associated mass balance equation and calibration procedures are described in full in Chapter I.

Soil Analysis

A soil sample (top 2 cm) was taken from the center of the chamber footprint at the end of each measurement period (approximately 1 sample per day), and analyzed for soil pH, soil moisture, NH_x (NH_x=NH_4^++NH_3), NO_3-N and Total Kjeldahl Nitrogen (TKN=organic N+NH_3-N+NH_4^+-N) by the North Carolina State University Department

of Biological and Agricultural Engineering. Based on previous studies, the unamended plots are found to remain fairly consistent in terms of pH and N-content and therefore the unamended plot was only sampled once. Soil temperature was measured with a Campbell Scientific temperature probe (accuracy ± 3%) inserted into the soil to a depth of approximately 5 cm. Air temperatures (Campbell Scientific; accuracy ± 3%) were measured inside of a radiation shield at a height of 1.5 meters. Data was stored in 15 minute binned averages utilizing a Campbell Scientific 21X Micrologger, in conjunction with a Toshiba laptop computer.

Model

The exchange of NH_3 gas from the soil into the atmosphere is assumed to be related to the resistances in both the liquid and gas phases and the gas concentration gradient between the soil-air interface. The mechanistic model describing this exchange can be written as:

$$\text{Flux}(NH_3)_{gas} = K\left([NH_3]_{(gas,soil)} - [NH_3]_{(gas,air)}\right) \quad (6)$$

where K is the transfer coefficient from the NH_3 gas in the soil to the NH_3 gas in the air (Singh and Nye, 1986a). Total ammonia (NH_x=$NH_3 + NH_4^+$) in the soil is dependent on the plant uptake rate, immobilization rate, nitrification/denitrification rates and volatilization of the gas from the soil (Sherlock and Goh, 1985). Previous researchers have shown that during the time period immediately following fertilization (4 days-2 weeks), the volatilization process is sufficiently strong so that other processes (plant uptake, immobilization, nitrification/denitrification) can be neglected (Sherlock and Goh,

1985). Furthermore, following slurry application the $[NH_3]_{(gas,soil)}$ will generally be significantly larger than the $[NH_3]_{(gas,air)}$ and the NH_3 flux equation can be rewritten as:

$$Flux(NH_3)_{gas} = K[NH_3]_{(gas,soil} \tag{7}$$

Therefore the determination of the NH_3 flux from the soil is dependent on knowing the NH_3 gas concentration in the soil/slurry environment and the exchange coefficient K.

The NH_3 gas concentration in the soil solution can be calculated by examining the chemical equilibrium between NH_3 and NH_4^+. As slurry is initially applied to the soil it is rapidly hydrolyzed to produce ammonium ions in the soil:

$$(Urea) \longrightarrow NH_4^+{}_{(aq)} \tag{8}$$

The subsequent dissociation of NH_4^+ in the solution can be described by:

$$NH_4^+ + H_2O \overset{K_{NH_4^+}}{\leftrightarrow} NH_{3(aq)} + H_3O^+{}_{(aq)} \tag{9}$$

where $K_{NH_4^+}$ is the equilibrium constant and is given by:

$$K_{NH_4^+} = \frac{[NH_{3(aq)}][H_3O^+{}_{(aq)}]}{[NH_4^+{}_{(aq)}]} \tag{10}$$

The ammonium equilibrium constant is found to be dependent on temperature through the following equations described by Bates and Pinching, 1950; Hales and Drewes, 1979; Aneja et al., 2001b.

$$K_{NH_4^+} = 5.67 * 10^{-10} * \exp\left[-6286 * \left(\frac{1}{273.15 + T_{soil}} - \frac{1}{298.15}\right)\right] \tag{11}$$

or similarly

$$\mathrm{Log}\left(K_{NH_4^+}\right) = -0.09018 - \frac{2729.92}{T} \tag{12}$$

where T is the soil temperature in Kelvin.

This first order equilibrium between $NH_4^+{}_{(aq)}$ and $NH_{3(aq)}$ is extremely fast and in terms of the volatilization it will not be rate limiting (Sherlock and Goh, 1985).

The total ammoniacal nitrogen content of the soil ($NH_{x(aq)}$) can be rewritten as:

$$NH_4^+{}_{(aq)} = NH_{x(aq)} - NH_{3(aq)} \tag{13}$$

and substituting equation (13) into equation (10) yields:

$$\frac{\left[NH_{3(aq)}\right]\left[H_3O^+{}_{(aq)}\right]}{K_{NH_4^+}} = \left[NH_{x(aq)}\right] - \left[NH_{3(aq)}\right] \tag{14}$$

Solving for $NH_{3(aq)}$, equation (14) can be rewritten as:

$$\left[NH_{3(aq)}\right] = \frac{\left[NH_{x(aq)}\right]}{\left(1 + \frac{H_3O^+}{K_{NH_4^+}}\right)} \tag{15}$$

Recognizing that H_3O^+ will also hydrolyze to produce H^+ ions and that $H^+ = 10^{-pH}$, equation (15) can be rewritten in the form:

$$\left[NH_{3(aq)}\right] = \frac{\left[NH_{x(aq)}\right]}{1 + \frac{10^{-pH}}{K_{NH_4^+}}} \tag{16}$$

Substituting for the equilibrium constant $K_{NH_4^+}$ from equation (12), we are left with:

$$NH_{3(aq)} = \frac{\left[NH_{x(aq)}\right]}{1 + 10^{\left(0.09018 + \frac{2729.92}{T} - pH\right)}} \tag{17}$$

At the interface of the air and liquid film in the soil solution, the aqueous NH_3 concentration is assumed to be related to the gaseous NH_3 concentration through Henry's Law equilibrium where:

$$NH_{3(gas)} = HNH_{3(aq)} \tag{18}$$

and the Henry's Law equilibrium constant H can be expressed as:

$\text{Log}(H^{-1}) = -1.69 + \frac{1477.7}{T}$ (Hales and Drewes, 1979).

Substituting the Henry's Law relationship (equation 18) into the flux equation (7) yields the following expression for NH_3 Flux:

$$\text{Flux}(NH_{3(gas)}) = K[NH_{3(aq)}]H \tag{19}$$

Substituting the $NH_{3(aq)}$ from equation (17) into equation (18) yields the following NH_3 flux equation:

$$\text{Flux}(NH_{3(gas)}) = \frac{K[NH_{x(aq)}]H}{(1+10^{(0.09018+\frac{2729.92}{T}-pH)})} \tag{20}$$

The mass transport model given in equation (20) is the same model used by Aneja et al. (2001b) for estimating NH_3 flux from lagoon surfaces. While all parameters in equation 20 can be measured or calculated in both the lagoon and soil environments, the flux is critically dependent upon accurate representation of the mass transfer coefficient (K), and the value of the Henry's law coefficient (H). Aneja et al. (2001b) used two-film theory which accounts for the role of air velocity and temperature in the gas (k_g) and

liquid phase (k_L) resistance to NH_3 transfer across an interface and is given by the following equation:

$$K = \left(\frac{H}{k_l} + \frac{1}{k_g} \right)^{-1} \tag{21}$$

In a review of over 30 publications, it was discovered that the reported values of this overall mass transfer coefficient ranges from 1.3×10^{-6} m s^{-1} to 1.2×10^{-2} m s^{-1}. Several researchers have attempted to relate this overall mass transfer coefficient to various properties such as roughness length, friction wind velocity and height of the internal boundary layer (van der Molen et al., 1990; Olesen and Sommer, 1993). Using a micrometeorological technique, Svensson and Ferm (1993) calculated mass transfer coefficients from soils amended with manure and reported values ranging from 4.3×10^{-3} m s^{-1} to 1.2×10^{-2} m s^{-1}. Researchers in a laboratory using swine manure, however reported the overall mass transfer coefficient to range between 1.3×10^{-6} m s^{-1} and 5.2×10^{-6} m s^{-1} (Zhang, 1992). Great variability does exist in the range of reported values. However conditions during which these measurements were made do differ. In general, a review of these published reports indicated that for the slurry mixture alone, values of the overall mass transfer coefficient were on the order of 10^{-6} m s^{-1} – 10^{-5} m s^{-1} while field and laboratory experiments on slurry/soil mixtures were on the order of 10^{-4} m s^{-1} – 10^{-3} m s^{-1}.

Singh and Nye (1986b) described a controlled laboratory experiment in which the exchange coefficient was measured under a variety of flow and pH conditions. These researchers reported that the value of K increased linearly as the flow rate over the soil

surface increased from 0 to 1 l min^{-1}. However, they reported that as flow rates increased beyond 1 l min^{-1}, the rate of increase becomes smaller and begins to level out at a value of 3.7×10^{-3} m s^{-1}. Sherlock and Goh (1985) theororized that in soils, water movement and the diffusion of ions is probably more restricted than in flooded soils or water bodies. Therefore they concluded that volatilization of NH_3 from non-flooded soils is more likely to be controlled by the rate of diffusion through the soil than on wind speed.

Numerous studies conducted by Denmead et al. (1974) and Beauchamp et al. (1978, 1982) reported no positive relationships between wind speed and NH_3 emissions from non flooded soils. Given the good reproducibility of the measurements in the experiments conducted by Singh and Nye (1986b) (±6%), their experimentally measured value of 3.7×10^{-3} m s^{-1} will be used in this study. For comparison purposes, the NH_3 flux using the empirically determined K value based on temperature and wind speed (equation 21) and as described by Aneja et al. (2001b) will also be presented.

Results and Discussion

Temperature

Positive relationships between the release of nitrogen trace gases from soils and soil temperature are well established in the literature. For example, the solid line (plotted on a logarithmic scale) in Figure 6.1 shows this temperature dependence in an empirical model [$Log_{10}(NH_3\text{-N Flux}) = 0.054*T_{soil} + 0.66$; $R^2=0.71$] developed by Roelle and Aneja (2001). This empirical model was developed from measurements made at the same measurement location as this slurry-amended study and was conducted during 2 different seasons (winter and spring, 2000) when no fertilizer (slurry or chemically

derived) was applied to the soil (within 3 months of data collection). The R^2 of 0.71 in this study is consistent with many nitrogen trace gas experiments from various soil and crop types which have reported R^2 values ranging between 0.42 and 0.87 (Sullivan et al., 1996; Thornton et al., 1997; Roelle et al., 1999; Roelle and Aneja, 2001).

The four data points (solid squares) surrounding the solid line in Figure 6.1 represent the control plots (no slurry applied to the plot) from this (Spring 2001) measurement campaign. These data points fit the general form of the model, and in fact including these four new data points into the model changes the R^2 only slightly from 0.71 to 0.70. The 12 data points (solid triangles) in this graph represent the data from the spring 2001 slurry amended plots. Although these 12 data points did fall within the range of soil temperatures used to develop the empirical model, attempting to estimate the fluxes from the slurry amended plots using the empirical model in Figure 6.1 would result in an underestimation of at least an order of magnitude. An empirical model developed from only the slurry amended soil data results in an R^2= 0.26 and a new empirical relationship taking all data points (amended and non-amended) into account results in a decreased R^2 value from 0.71 to 0.39.

These results highlight that temperature will explain over 70% of the variability in NH_3 emissions when it is developed from, and applied to, soils that have not been recently amended (fertilized). However, similar empirical models relating temperature to NH_3 flux developed from recently amended soils or a combination of both amended and non-amended soils reduces the explanatory capability of the model to 26% and 39% respectively. This suggests that when nitrification/denitrification, plant uptake and

immobilization are sufficiently small to be neglected in comparison to the chemical and physical processes during time periods immediately following slurry application, than temperature alone can not adequately estimate the NH_3 flux. During non-fertilized episodes, this relationship can be attributed to the fact that the biochemical reaction rates of microorganisms responsible for the production/consumption of NH_3 respond to changes in temperature (Sullivan et al., 1996; Roelle et al., 1999; Roelle et al., 2000; Warneck, 2000). However, during recently fertilized events, as shown through the development of the mass transfer model, parameters other than temperature such as ammoniacal nitrogen content and pH must be considered.

Similarly to the empirical model, the mass transport model relates the NH_3 flux to soil temperature (exponential dependence). Maintaining all other parameters constant (typically observed agronomic values before$_{(1)}$ and after$_{(2)}$ slurry application: $NH_{x(1)}$=6 μg/g; $pH_{(1)}$=5.5; $K_{(1)}$=3.69x10^{-3} m s^{-1}; $NH_{x(2)}$=90 μg/g; $pH_{(2)}$=6.5; $K_{(2)}$=3.69x10^{-3} m s^{-1}) and varying the temperature between 16.3 and 20.6 °C (typical range during a measurement period) in both the mechanistic and empirical model produces similar profiles, yet at different magnitudes (Figure 6.2). The average NH_3 flux measured before and after slurry application was 54 and 1724 ng N m^{-2} s^{-1}, respectively. Although soil temperatures from the different seasons did overlap, it is apparent that a temperature based empirical relationship will fail to capture the magnitude of the emissions. While Figure 6.2 reemphasizes the exponential dependence of NH_3 flux on soil temperature, it also highlights the role that other parameters, namely pH and ammoniacal nitrogen must play in the mass transfer equation.

Applying the mechanistic model to the non-amended field site data collected during the spring and winter 2000 measurement campaign (Figure 6.3-first 10 data points) results in much weaker model performance than when the mechanistic model is used for time periods immediately following slurry application (Figure 3-last 4 data points). The average percent difference between modeled and measured values for the slurry amended plots was 16% while the average percent difference for non-amended plots was 164%. This weaker relationship for the non-amended plots is explained by the fact that the assumptions in deriving the mechanistic model were that nitrification/denitrification, plant uptake and immobilization processes were much slower than the volatilization processes, and that ambient [NH_3] were negligible, all of which are invalid assumptions during the unamended measurement period. Therefore, during the slurry amended measurement periods, it is important to consider the other controlling parameters from the mass transfer equation.

Based on measured wind speeds and temperature during this measurement period, the mass transfer coefficient ranged from 1.5×10^{-3} m s^{-1} to 2.4×10^{-3} m s^{-1} as opposed to the experimentally measured value of 3.69×10^{-3} m s^{-1}. Results using the same soil conditions and the calculated mass transfer coefficient from equation 21 are also plotted in Figure 6.3. From the results of this study, the experimentally measured mass transfer coefficient is more accurate in estimates of the NH_3 flux. This may confirm that in soil environments, NH_3 emissions are limited more by rate of diffusion of the NH_3 to the soil/air interface than by windspeed or temperature, as suggested by Sherlock and Goh (1985).

Ammoniacal Nitrogen Content and pH

Figure 6.4 shows both the daily trend of the NH_3-N content of the soil (primary axis) and the averaged NH_3 flux from the 3 sample plots on each of the successive measurement days (secondary axis). The solid squares in Figure 6.4 represent the average flux from the control (unamended) plots. The decreasing trends in both NH_3-N flux and NH_x content of the soil are expected based on the fact that as volatilization of NH_3 from the soil continues, in the absence of other NH_3 production mechanisms, there will be progressively smaller concentrations of NH_3 in the soil. To examine how changes in $[NH_x]$ effect the NH_3 flux predicted by the mechanistic model, all parameters in the mechanistic model are kept constant (T=20 °C; pH=6.5; $K=3.69x10^{-3}$ m s^{-1}) and only the $[NH_x]$ is varied (Figure 6.5). This modeled linear relationship is supported by an earlier study conducted by Roelle and Aneja, (2001) during a non-fertilized period which showed the NH_3 flux from the soil being highly correlated to the NH_3-N content of the soil [NH_3 Flux=55.5*(NH_x)-160; R^2=0.86]. Using this empirical relationship, which is based on soil conditions with much smaller [NH_x-N] (<9 μg/g compared to ~ 105 μg/g) results in significantly higher NH_3 flux estimates (solid line) than the mechanistic model for values of $[NH_x]$ greater than approximately 5 μg/g.

Producing a new empirical model [NH_3 Flux=22.7*(NH_x)- 91.4; R^2 = 0.75] taking both the slurry-amended and non-slurry amended soils into account shows that the soils ammoniacal nitrogen content is significant ($p<0.01$) in estimating NH_3 emissions both prior to and after slurry application. The shaded and dashed lines in Figure 6.5 differ by approximately 40% at lower values of NH_x (~10 μg/g) and less than 7% at the higher

values of NH_x (~120 μg/g). Although it appears that the mechanistic and empirical models yield approximately equivalent flux estimates, it should be noted that in this example the pH was kept constant in the mechanistic model. While many field studies have found pH to remain fairly uniform throughout non-fertilized periods, this assumption is invalid during periods immediately following fertilization (Sullivan et al., 1996; Roelle et al., 1999; Li et al., 1999).

As slurry is initially applied to the soil it is rapidly hydrolyzed to produce ammonium and carbonate ions which causes an increase in the soil pH. As the ammonia volatilizes, H^+ ions accumulate in the soil and throughout the volatilization event there is a gradual decrease of the soil pH. Therefore, during recently fertilized episodes, pH and $[NH_x]$ can not be considered in isolation because a change in $[NH_x]$ causes a change in the pH. This effect can be seen clearly in Table 6.1, which shows the pH beginning at approximately 6.6 for the amended plots and gradually decreasing to 6.2, while the control plot is assumed, based on previous studies, to remain fairly constant at 5.4.

While the overall change during these 4 days is less than ½ of a pH unit, the effects on the estimated ammonia flux can be large. Based on the mass transport model, changing only the soil pH by 1 unit and maintaining all other variables constant at ($T=20^oC$, $NH_x=90$ μg/g, $K=3.69 \times 10^{-3}$ m s^{-1}) results in changes of NH_3 flux of approximately an order of magnitude (Figure 6.6-solid line). However, in a more realistic situation, varying both the pH and $[NH_x]$ (as shown on the secondary axis) results in the NH_3 flux as seen in Figure 6.6 (solid squares).

Figure 6.7 shows the measured NH_3-N volatilized as a % of the N applied. At a rate of N-application of 33 Kg N ha^{-1}, nearly 20% of the applied N is lost as NH_3 within the first 4 days after application. The predicted NH_3-N volatilized as a % of the N applied is shown by the solid line in Figure 6.7, which is based on the daily averaged soil parameters measured and the mass transfer equation with the constant mass transfer coefficient (3.69×10^{-3} m s^{-1}). The solid line appears to accurately predict the percent of N lost as NH_3 during the first three days following slurry application. However, while the measured rate of loss begins to level out at approximately 20%, the solid line (predicted value) tends to be increasing although at a slower rate. Other modeling and experimental studies have found that the percent of N applied, which is lost as NH_3, typically levels out at approximately 30% and that this usually occurs within the first 1-2 weeks after fertilizer application (Singh and Nye, 1986b and 1988). While the NH_3 volatilized (as a percent of the N applied) in this study appears to level out slightly faster than other reported studies, this may be a factor of the amount of nitrogen initially applied to the soil. Whereas, the Singh and Nye (1986a) study applied nearly 210 kg N ha^{-1}, this study applied 33 kg N ha^{-1}. Furthermore, the $[NH_x]$ was still elevated (in comparison to background levels) at the conclusion of the measurement period indicating that this volatilization event may have persisted for a few more days. Regardless, the consistent trend among the model, measurements and previous lab and field studies indicates that these volatilization events are short-lived (few days-2 weeks), and generally result in emissions of 20-30% of the applied nitrogen.

Conclusions and Recommendations

Using a mechanistic/mass transport model and measured soil parameters, ammonia emissions were estimated and compared to calculated flux values at an eastern North Carolina swine farm. A mechanistic model developed for volatilization events performed well (average of 16% difference between modeled and measured flux values) immediately following a slurry application, however performed poorly on the non-amended soils (average of 164% difference between modeled and measured flux values). This relationship is not surprising given that the assumptions in the mass transport model, namely negligible plant uptake and ammonification processes relative to the ammonia in the soil/slurry mixture, both of which (plant uptake and ammonification processes) are not valid assumptions during periods prior to or long after slurry/fertilizer application. Further, during time periods prior to slurry application the assumption of ammonia concentration in the air being negligible in comparison to the ammonia concentration in the soil cannot be assumed to be valid and therefore ammonia concentrations in the air must be included in the mass transfer model.

In this study, the value of the mass transfer coefficient was kept constant at 3.7 x 10^{-3} m s^{-1} based on laboratory results reported by Singh and Nye (1986b) and research conducted by other investigators. Using an equation to describe the exchange coefficient in terms of wind speed and temperature resulted in calculated exchange coefficients ranging from 1.5 x 10^{-3}m s^{-1} to 2.4 x 10^{-3} m s^{-1}. The literature currently describes mass transfer coefficients ranging from 1.3 x 10^{-6} m s^{-1} to 1.2 x 10^{-2} m s^{-1} and therefore a more thorough understanding of this parameter must be obtained. The fact that the

experimentally measured exchange coefficient performed better than the calculated exchange coefficient may indicate that for soil systems the NH_3 flux is rate limited by diffusion to the soil/air interface as opposed to wind speed or temperature. Soil ammoniacal nitrogen content was found to be linearly related to NH_3 while pH and temperature were both found to have an exponential dependence. The measurements revealed that the applied N is lost at the greatest rate in the first 2 days following application and begin to level out by day 4, although additional field data is required to confirm this relationship.

While the currently used emission factor approach may adequately capture the total NH_3 emitted to the atmosphere on a yearly basis, these results show that they would perform poorly in resolving any temporal or spatial trends. In an effort to further refine global Nitric Oxide (NO) emission estimates, Yienger and Levy (1995) proposed a "pulsing" mechanism to account for the large bursts of NO following the wetting of dry soils. Similarly, it would appear that a mechanism should be incorporated into the emission estimate process to further refine the budget of ammonia emissions from soils, especially intensively managed soils which are consistently amended with both commercially derived fertilizers and animal waste. As a first approach during non-amended periods, the temperature-based model appears to capture the majority of the variation in NH_3 emissions. A possible approach for the amended periods would be to adopt the same procedures commonly used in the estimates of biogenic NO emissions, which is to apply a temperature algorithm and a factor to adjust for the amount of fertilizer the crop receives. Unfortunately, this approach requires a large set of data

conducted over many different soil and crop types to empirically determine these factors, which to date is still unavailable.

References

Aneja, V.P., P.A. Roelle, G.C. Murray, J. Southerland, J.W. Erisman, D. Fowler, W. Asman and N. Patni, Atmospheric nitrogen compounds II: emissions, transport, transformation, deposition and assessment, Atmospheric Environment, 35, 1903-1911, 2001a.

Aneja, V.P., B.P. Malik, Q. Tong and D. Kang, Measurement and modeling of ammonia emissions at waste treatment lagoon-atmospheric interface, Water, Air and Soil pollution, in press, 2001b.

Bates, R.G. and G.D. Pinching, Dissociation Constant of aqueous ammonia at 0 to 50-degrees from EMF studies of the ammonium salt of a weak acid, Journal of the American Chemical Society, 72, 1393-1396, 1950.

Beauchamp, E.G., G.E. Kidd and G. Thurtell, Ammonia volatilization from sewage sludge applied in the field, Journal of Environmental Quality, 7, 141-146, 1978.

Beauchamp, E.G., G.E. Kidd and G. Thurtell, Ammonia volatilization from liquid dairy cattle manure in the field, Canadian Journal of Soil Science, 62, 11-19, 1982.

Denmead O.T., J.R. Simpson, and J.R. Freney, Ammonia flux intothe atmosphere froma grazed pasture, Science, 185, 609-610, 1974.

Erisman, J.W., T. Brydges, K. Bull, E. Cowling, P. Grennfelt, L. Nordberg, K. Satake, T. Schneider, S. Smeulders, K. W. Van der Hoek, J.R. Wisniewski and J. Wisniewski, Summary statement, Proceedings of the First International Nitrogen Conference, Noordwijkerhout, The Netherlands, 23-27 March, 1998.

Finlayson-Pitts, B.J., and Pitts, J.N. Jr., Atmospheric Chemistry: Fundamentals and Experimental Techniques. John Wiley & Sons, New York, New York, 1986.

Hales, J.M. and D.R. Drewes, Solubility of ammonia at low concentrations, Atmospheric Environment, 13, 1133-1147, 1979.

Li,Y., V.P.Aneja, S.P. Arya, J.Rickman, J.Brittig, P.A. Roelle and D.S. Kim, Nitric oxide emission from intensively managed agricultural soil in North Carolina, Journal of Geophysical Research 104, 26,115 – 26,123, 1999.

Ni, J., Mechanistic models of ammonia release from liquid manure: a review, Journal of Agricultural Engineering Research, 72, 1-17, 1999.

Olesen, J.E. and S.G. Sommer, Modelling effects of wind speed and surface cover on ammonia volatilization from stored pig slurry, Atmospheric Environment, Part A, General Topics, 27(16), 2567-2574, 1993.

Paerl, H.W., Coastal eutrophication and harmful algal blooms: Importance of atmospheric deposition and groundwater as "new" nitrogen and other nutrient sources, Limnology and Oceanography, 42, 1154-1165, 1997.

Roelle, P.A., V.P. Aneja, J. O'Connor, W.P. Robarge, D.S. Kim and J.S. Levine, Measurement of nitrogen oxide emissions from an agricultural soil with a dynamic chamber system, Journal of Geophysical Research, 104, 1609-1619, 1999.

Roelle, P.A., V.P. Aneja, B. Gay, C. Geron and T. Pierce, Biogenic nitric oxide emissions from cropland soils, Atmospheric Environment, 35, 115-124, 2001.

Roelle, P.A. and V.P. Aneja, Characterization of ammonia emissions from soils in the upper coastal plain, North Carolina, Atmospheric Environment, in press, 2001.

Sherlock, R.R. and K.M. Goh, Dynamics of ammonia volatilization from simulated urine patches and aqueous urea applied to pasture. II. Theoretical derivation of a simplified model, Fertilizer Research, 6, 3-22, 1985.

Singh, R. and P.H. Nye, A model of ammonia volatilization from applied urea. I. Development of the model, Journal of Soil Science, 37, 9-20, 1986a.

Singh, R. and P.H. Nye, A model of ammonia volatilization from applied urea. II. Experimental testing, Journal of Soil Science, 37, 21-29, 1986b.

Singh, R. and P.H. Nye, A model of ammonia volatilization from applied urea. IV. Effect of method of Urea application, Journal of Soil Science, 39, 9-14, 1988.

Sullivan, L.J., T.C. Moore, V.P. Aneja and W.P. Robarge, Environmental variables controlling nitric oxide emissions from agricultural soils in the southeast United States, Atmospheric Environment, 30, 3573-3582, 1996.

Svensson, L. and M. Ferm, Mass transfer coefficient and equilibrium concentration as key factors in a new approach to estimate ammonia emission from livestock manure. Journal of Agricultural Engineering Research, 56, 1-11, 1993.

Thornton, F.C., P.A. Pier and R.J. Valente, NO emissions from soils in the southeastern United States, Journal of Geophysical Research, 102, 21,189-21,195, 1997.

Troeh F.R. and Thompson L.M., Soils and Soil Fertility, Oxford University Press, pp. 184-185, New York, 1993.

Van der Molen, J. A.C.M. Beljaars, W.J. Chardon, W.A. Jury and H.G. Vanfaassen, Ammonia volatilization from arable land after application of cattle slurry. 2. Derivation of a transfer model, Netherlands Journal of Agricultural Science, 38(3), 239-254, 1990.

Warneck, P., Chemistry of the natural atmosphere, second edition, Academic Press, Inc., New York, NY, pp. 511-530, 2000.

Yienger, J.J., Levy II H., Empirical model of global soil-biogenic NO_X emissions. Journal of Geophysical Research, 100, 11,447-11,464, 1995.

Zhang, R., Degradation of swine manure and a computer model for predicting the desorption rate of ammonia from an under-floor pit, PhD Thesis, University of Illinois at Urbana-Champaign, pp. 131, 1992.

Site: Upper Coastal Plain Research Station
35.9° N Latitude
77.7° W Longitude
Elevation: 35.5 Meters
Soil Type: Norfolk Loamy Sand

Sampling Period	n	pH	% Moisture Content	N – Content μg/g			Soil Temp (°C)	NH_3 Flux (ng N m^{-2} s^{-1})
				$[NH_x]$	NO_3-N	TKN		
30 April - Plot 1	4	6.48	13.39	105	7.81	882	23.8 ± 0.3	3390.8 ± 98.5
30 April - Plot 2	4	6.46	11.83	86	8.88	882	24.1 ± 0.02	2813.2 ± 100.0
30 April - Plot 3	4	6.77	12.19	95	8.88	906	24.6 ± 0.1	2200.4 ± 177.5
30 April - unamended	4						23.1 ± 0.2	87.3 ± 20.8
1 May - Plot 4	4	6.41	6.96	79.7	22.76	980	17.9± 0.7	2114.4 ± 136.4
1 May - Plot 5	4	6.54	5.32	84	15.07	828	18.2 ± 0.6	1708.7 ± 40.1
1 May - Plot 6	4	6.55	4.93	78.3	26.42	1028	18.5 ± 0.2	2323.8 ± 18.9
1 May - unamended	4						17.4 ± 0.1	71.3 ± 23.4
2 May - Plot 7	4	6.36	6.79	94.3	18.3	996	19.1 ± 0.7	1199.1 ± 12.0
2 May - Plot 8	4	6.2	7.33	73	17.07	943	19.4 ± 0.2	1071.0 ± 47.1
2 May - Plot 9	4	6.17	7.98	69.7	18.55	861	19.7 ± 0.1	1273.0 ± 124.6
2 May - unamended	4						18.6 ± 0.2	80.3 ± 19.2
3 May - Plot 10	4	6.1	4.6	59	33.2	924	17.9 ± 0.8	791.2 ± 32.3
3 May - Plot 11	4	5.95	4.08	82	29.15	976	18.1 ± 0.7	556.1 ± 9.5
3 May - Plot 12	4	6.29	4.26	76	42.27	1200	18.3 ± 0.6	1245.1 ± 4.1
3 May - unamended	4	5.4	1.19	6.03	12.93	1072	17.3 ± 0.2	67.4 ± 15.4

TKN = Total Kjeldahl Nitrogen = organic N+NH_3-N+NH_4^+-N

Table 6.1. Site and soil characteristics for the Spring 2001 measurement campaign at the Upper Coastal Plain Research Station, Edgecombe County, NC.

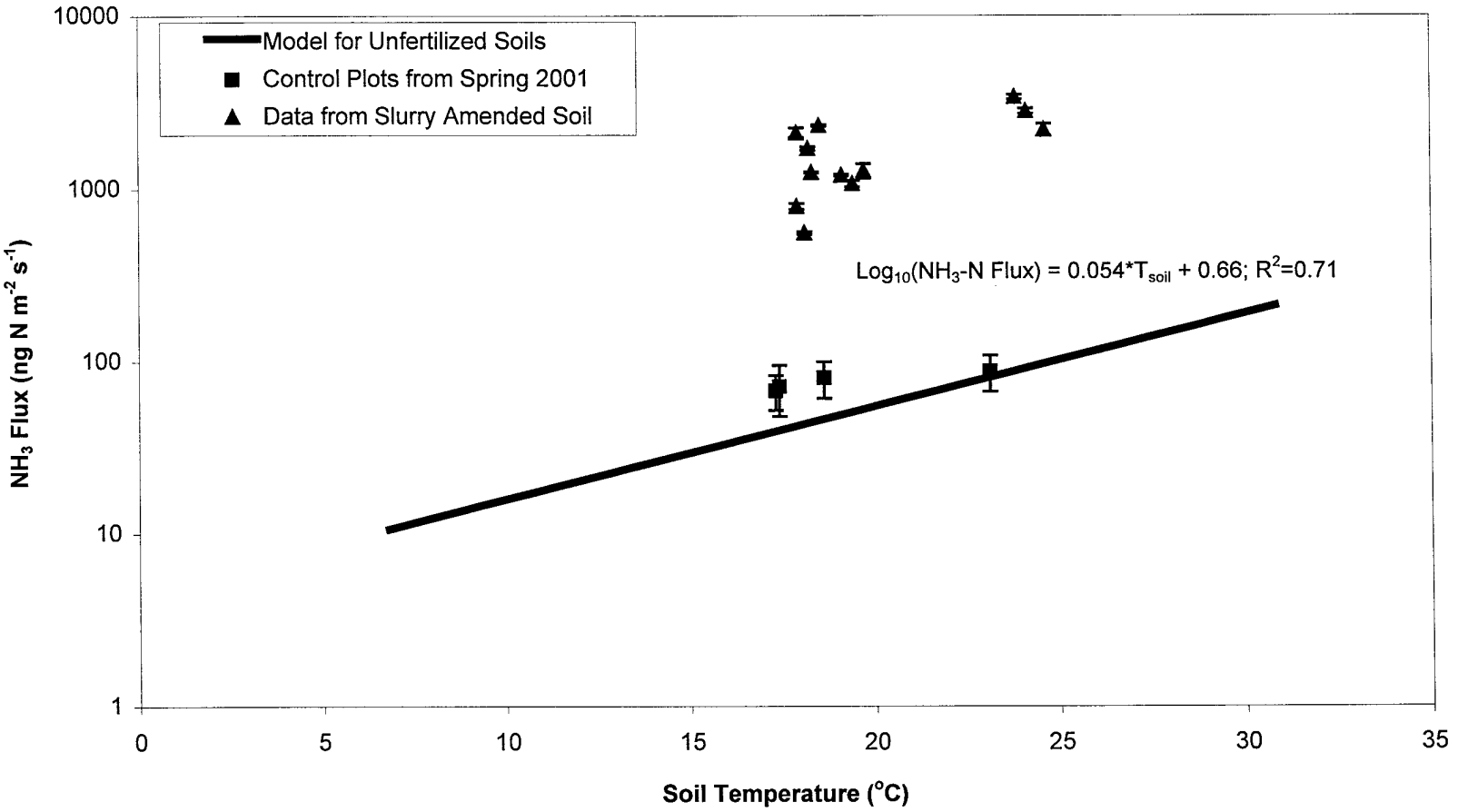

Figure 6.1. Measured NH_3-N flux versus soil temperature. The solid line represents a temperature based algorithm developed as part of an earlier study (Roelle and Aneja, 2001). The solid squares represent the control plots from spring 2001 measurements while the solid triangles represent the NH_3-N flux from the slurry applied soils. Vertical bars represent one standard deviation of the NH_3 flux.

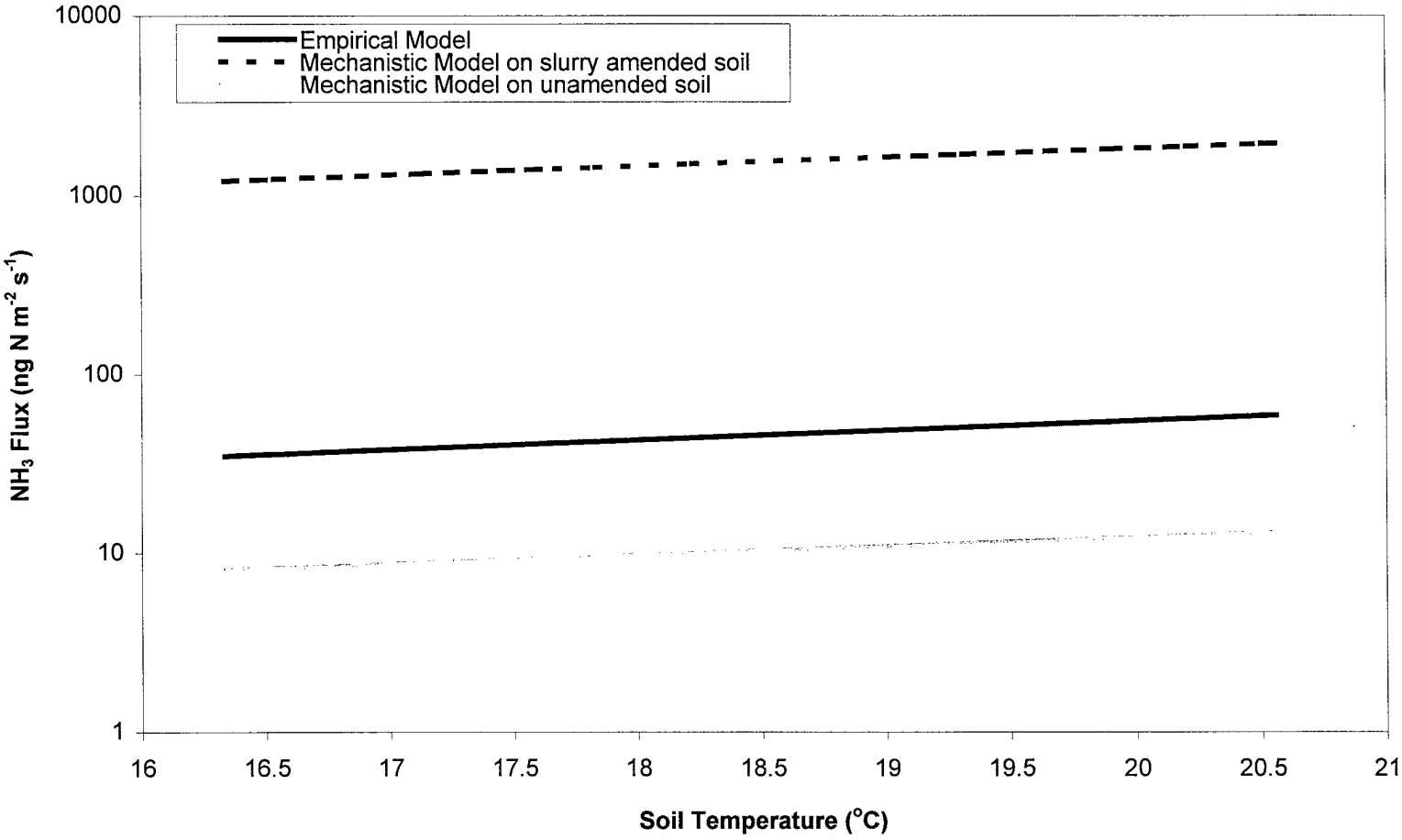

Figure 6.2. Modeled NH_3-N flux versus soil temperature. The solid line represents the empirical model and the shaded$_{(1)}$ and dashed$_{(2)}$ lines represent a mechanistic model with all parameters constant at: $NH_{x(1)}$=6 μg/g; $pH_{(1)}$=5.5; $K_{(1)}$=3.69 x 10^{-3} m s^{-1}; $NH_{x(2)}$=90 μg/g; $pH_{(2)}$=6.5; $K_{(2)}$=3.69 x 10^{-3} m s^{-1}. Soil temperature was varied between 16.3 and 20.6 °C.

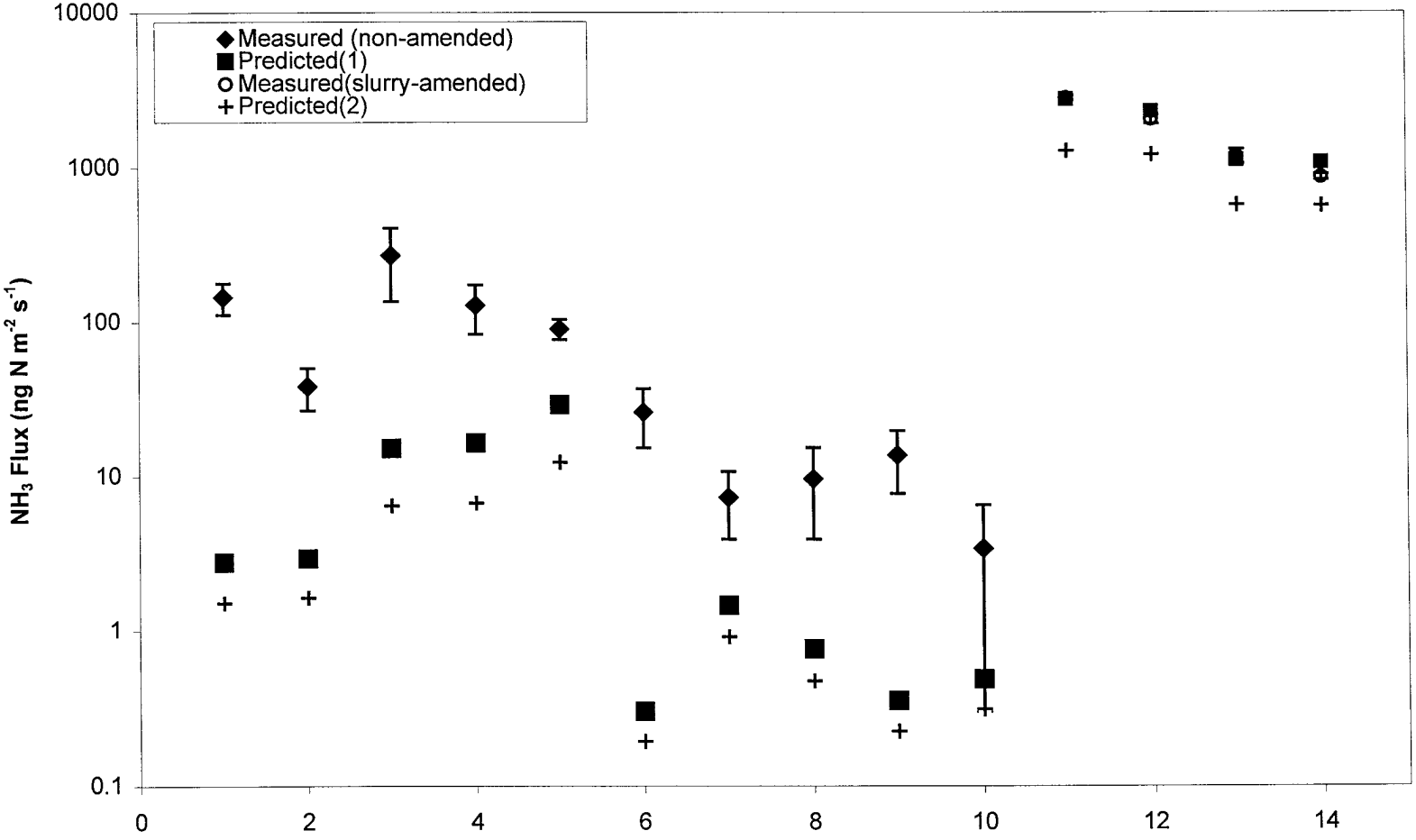

Figure 6.3. Plots of measured and predicted (mechanistic model) NH_3-N flux on different measurement days. The first 10 data points represent the non-amended plots, while the last 4 data points represent the slurry amended plots. Predicted(1) are estimated using $K=3.69 \times 10^{-3}$ m s^{-1} while Predicted(2) calculates K from equation (21).

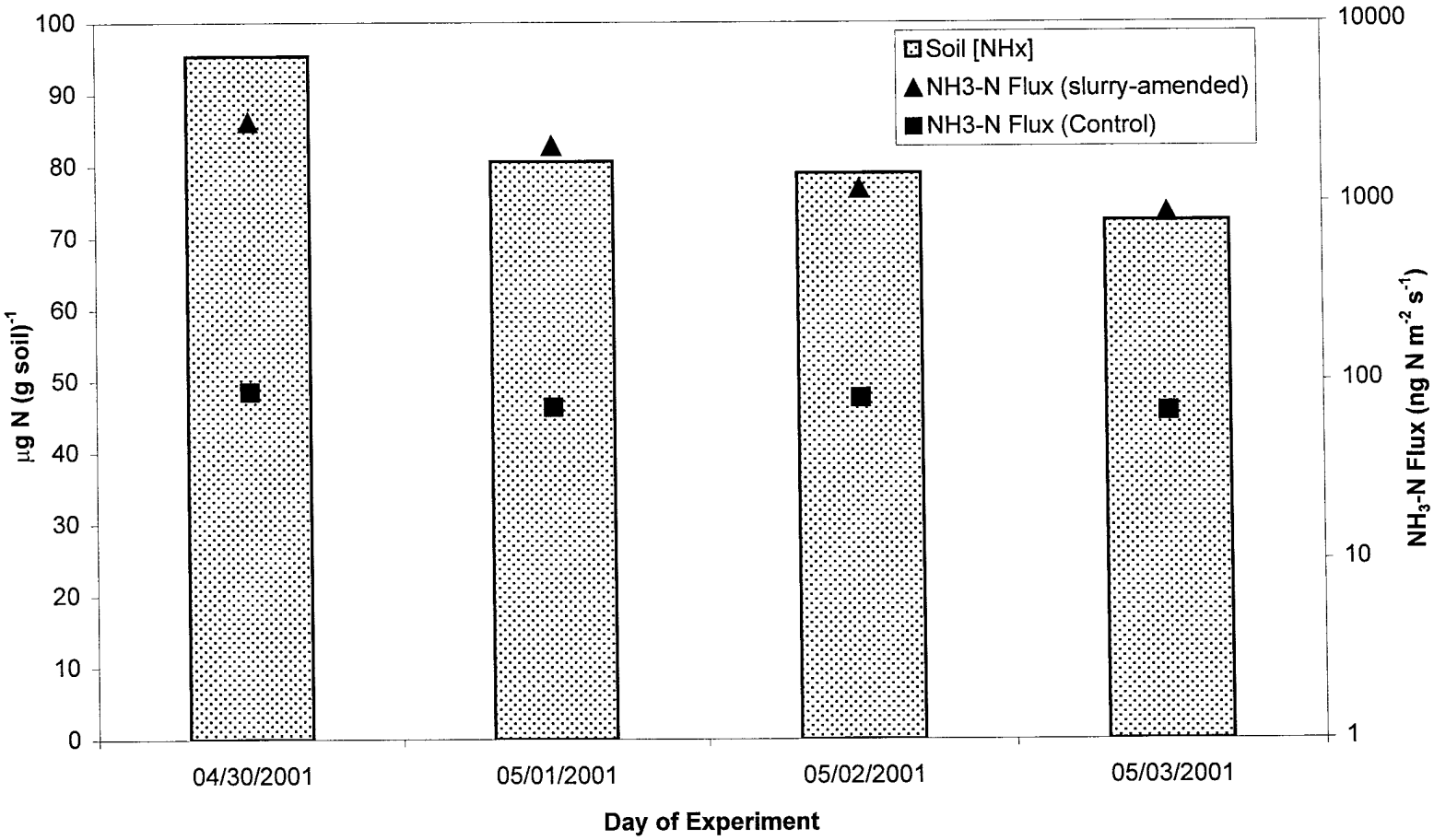

Figure 6.4. NH_x-N content (primary axis) and NH_3-N Flux (secondary axis) versus the day of the experiment. Solid triangles represent the daily averaged NH_3-N flux from the slurry amended plots, while the solid squares represent the daily averaged NH_3 flux from the control (unfertilized) plots.

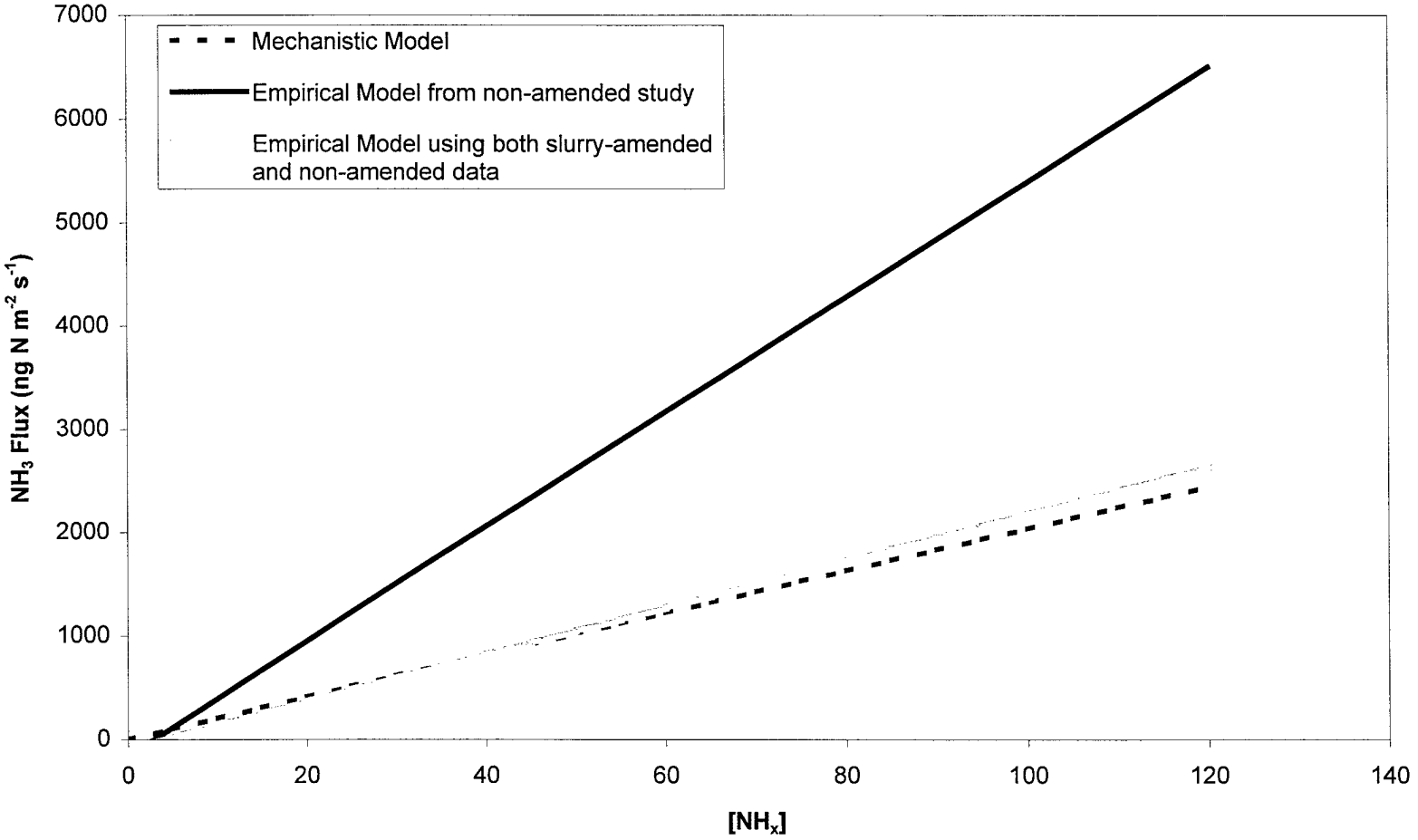

Figure 6.5. NH_3 flux versus ammoniacal nitrogen content of the soil. The solid line represents the mechanistic model and the dashed and shaded lines represents empirical models from the non-amended and combined data sets repectively. All values kept constant at T=20°C; pH=6.5; K=3.69 x 10^{-3} m s^{-1}.

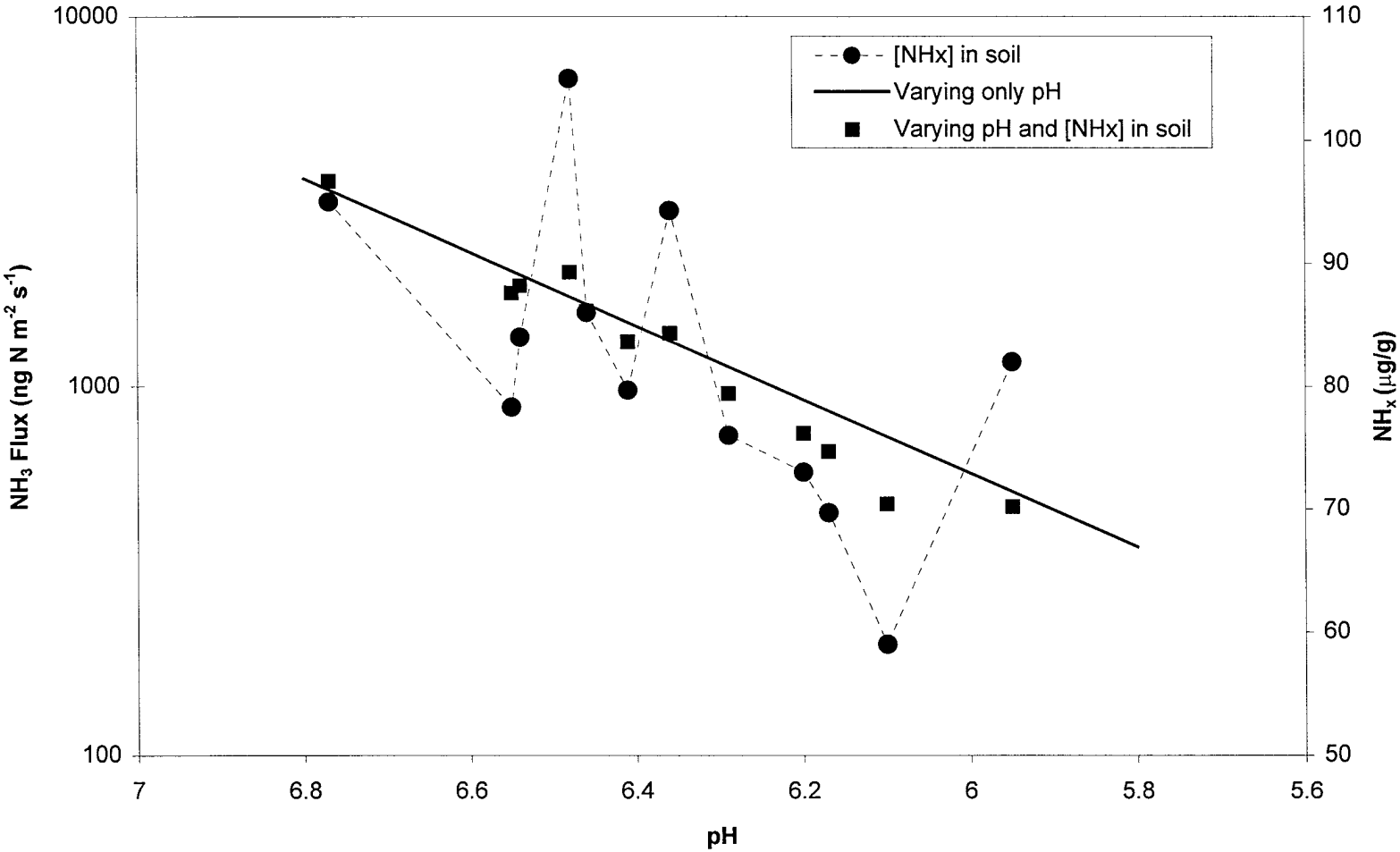

Figure 6.6. NH_3 flux versus soil pH. Solid line represents the mechanistic model, and only varying the pH. All values in the model are kept constant at T=20°C; NH_x=90 µg/g; K=3.69x10^{-3} m s^{-1}. The solid squares (■) represent the mechanistic model, varing both the pH and the [NH_x] in the soil (●), as indicated on the secondary axis.

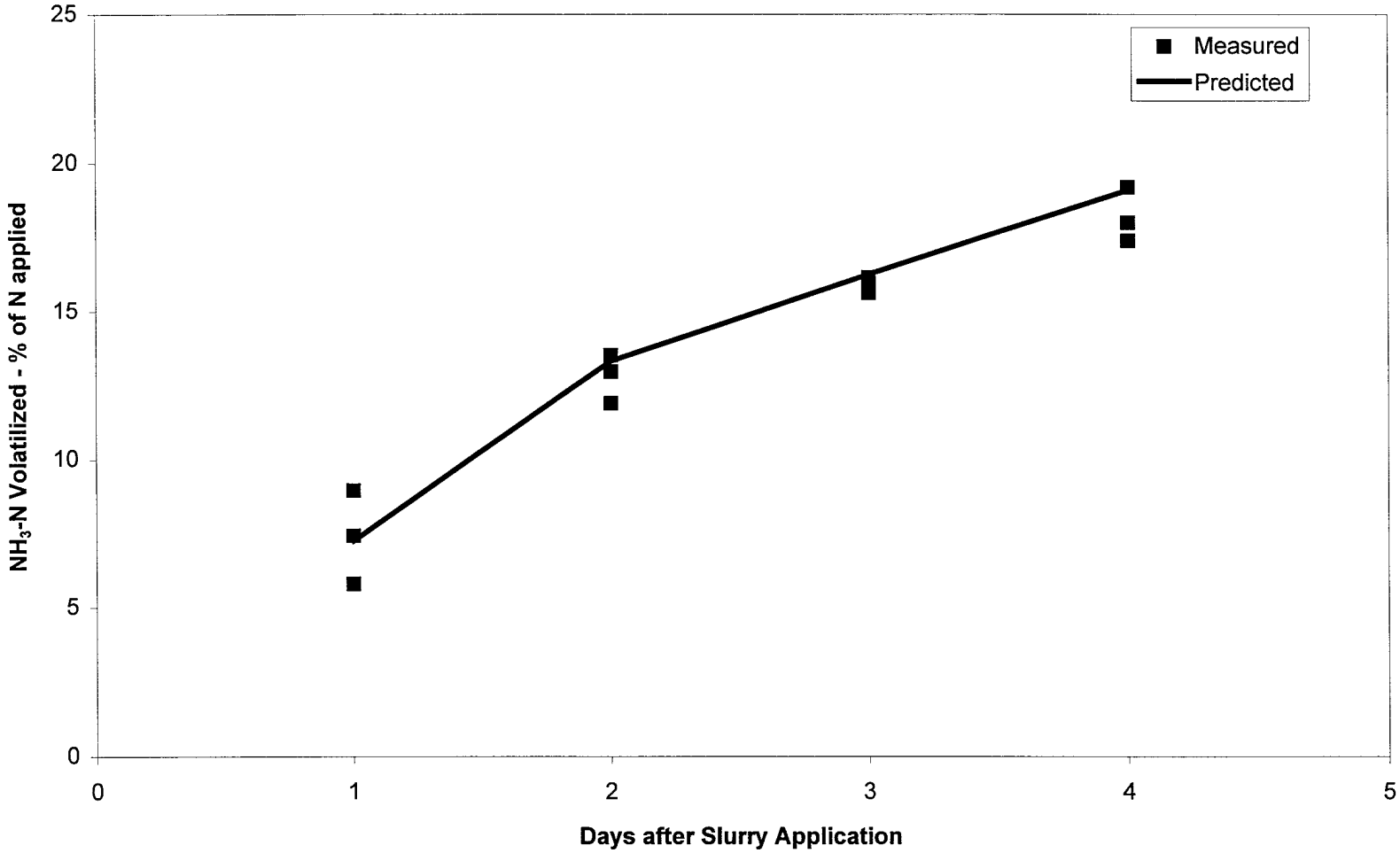

Figure 6.7. NH_3-N volatilized as a percent of the N applied. Solid squares represent the measured values from each plot on the 4 measurement days. The solid line represents the modeled NH_3-N volatilized using the soil parameters measured.

CHAPTER VII. SUMMARY AND SUGGESTIONS FOR FUTURE RESEARCH

A dynamic flow-through chamber technique was used to measure oxidized and reduced biogenic nitrogen compound emissions into the rural troposphere. This research initially focused on soils amended with chemically derived fertilizers and investigated the chemical and physical parameters which are often cited as being significant in controlling the emissions from soils. NO emissions and soil properties were studied at several croplands throughout North Carolina and were generally found to follow a diurnal profile with maximum emissions coinciding with maximum soil temperatures. The exponential dependence of NO flux on soil temperature existed at all sites, but to different levels of significance. It was also observed that NO flux did respond to varying amounts of both total extractable nitrogen (TEN) in the soil and soil moisture content.

Throughout the 1990's two processes were identified as potentially contributing significant nitrogen to the ecosystem throughout North Carolina. Considering the experience that our research group had in measuring nitrogen trace gas emissions it was decided that these two relatively new nitrogen sources should be characterized to determine their source strength and modeled to determine possible impacts. The first of these processes was the land application of biosolids, which are the byproduct of the wastewater treatment process. These biosolids are land applied for their nutrient content and as a cost effective way for the wastewater treatment plant to dispose of this byproduct. Measurements were made at a field site amended with biosolids throughout 1999-2000 and NO emissions were found to be dependent primarily on soil temperature.

The exponential dependence of NO emissions on soil temperature is the relationship most often cited in the literature and has been found to be consistent across soil and crop types. Using this temperature relationship and also taking into consideration the nitrogen fertilizer being applied to the crop results in an NO emissions model which is described by Williams et al. (1992) (Chapter III). The Williams model combines soil temperatures and a land use database to produce NO emission inventories which can then be used in air quality models. Currently, land use databases have multiple categories for different crop and vegetation types but there is no category for soils which are amended with biosolids. Considering that this study found biosolid amended soils to have high emissions of NO, relative to soils amended with chemically derived fertilizers, indicates that biogenic emission inventory's can be underestimated and can therefore cause biases in air quality models.

In this study we have determined how many acres of biosolid amended soils exist in the various counties of North Carolina and have applied our observationally based temperature algorithm (Chapter III) to determine a modified NO emissions inventory. It was not possible to determine where within the counties these biosolids were being applied, so therefore we had to use our discretion in apportioning this land-use throughout the grid cells of the various counties. We used two approaches, the first of which was to evenly distribute the biosolids throughout all the grid cells of the county and the other was to concentrate them within the county. The Multiscale Air Quality Simulation Platform (MAQSIP) was then run in two scenarios, the first of which we call the base case and the second being the modified case. In the base case, the current

biogenic NO emissions inventory is used and in the modified case MAQSIP is run with a modified NO emissions inventory which takes the biosolid amended acreages into consideration. It was found that, in general, the greatest change in the model output occurred in the evening and consisted of ozone being depleted. Concentrating the biosolids within a few grid cells of the respective counties resulted in changes where ozone was depleted by as much as 11% in the evening and increased by approximately 2% in the afternoon. While neither scenario is likely to be representative of actual conditions, this approach does serve as boundaries with which the significance of this land use class can be assessed. These results indicate that the biosolids can have significant impacts on model results and therefore data needs to be made available describing where these biosolids are being applied and then they need to be included in future land use databases.

Future research concerning the emissions of nitric oxide from biosolid amended soils should focus on emissions from various crop and soil types amended with bioslids to verify the relationships reported in this study. A comparison of these field results and a similarly designed laboratory study found the differences between the measured emissions to be statistically significant. While this initial comparison looked at soil temperature and soil moisture, it did not consider nitrogen content and microbial population. Therefore a more detailed comparison should be conducted to assess how these factors (nitrogen content and microbial population) in the field and laboratory environments may act to control the emissions of NO.

The second process which is contributing increased nitrogen to the environment of North Carolina is the land application of slurry from swine facilities. During the 1990's the swine population in North Carolina increased from approximately 3 million animals to approximately 10 million today, making North Carolina the second largest swine producing state in the U.S. Therefore, in an attempt to quantify the strength of the ammonia being emitted via the swine operations, ammonia emissions were calculated during various seasons and for time periods prior to and after the slurry was applied to the soil. An observationally based model to estimate ammonia emissions prior to slurry application was developed and then compared to a similar model for estimating emissions from lagoon surfaces. A comparison of these two models revealed that on a yearly basis, ammonia emissions from the soil contribute approximately 28% of the lagoon emissions. Before the results of this one study are extrapolated to farms throughout North Carolina, similar studies should be conducted at other swine facilities. However, given that the temperature dependence of nitrogen trace gases has consistently been shown to follow this exponential relationship across soil and crop types and during different times of the year, it is expected that these results will be similar at other locations.

Ammonia emissions were also measured for time periods immediately following slurry application and, as expected, the emissions were larger by approximately an order of magnitude. For time periods prior to slurry application, soil temperature alone was found to be the best predictor of ammonia flux, explaining over 70% of the variability in the ammonia emissions. However for time periods after slurry application, soil temperature explained approximately 40% of the ammonia emissions. These results

indicate that microbial processes are responsible for the majority of the ammonia in the soil prior to slurry application. In an attempt to estimate ammonia emissions for time periods after slurry application, a fundamental mechanistic mass transfer model was investigated and assessed with the field data from this site. This mass transfer model was found to predict the ammonia emissions, within approximately 15%, but only for time periods immediately following slurry application.

Future research concerning the emissions of ammonia from soils amended with lagoon effluent should consist of additional measurements at various swine farms to verify the relationships reported here. Further, an extended study for time periods after slurry application should be conducted to determine the length of time that emissions remain elevated following application of the slurry. Once this relationship is determined, a better ammonia inventory can be developed for this region which takes into consideration not only microbial production of ammonia in the soil but also the volatilization events associated with lagoon effluent application.

Appendix 1. Variations of Nitric Oxide Fluxes from Diverse Physiographic Agricultural Soils in North Carolina

Paul A. Roelle and Viney P. Aneja

Department of Marine, Earth and Atmospheric Sciences
North Carolina State University
Raleigh, NC 27695-8208

Emissions of nitric oxide (NO) were determined during late spring and summer 1995 and the spring of 1996 from four crop types, located at four different physiographic regions in North Carolina. Emission rates were calculated using a dynamic flow-through chamber system coupled to a state-of-the-art mobile laboratory for in-situ analysis. Average NO fluxes during late spring 1995 were: 50.9 ± 47.7 ng N m^{-2} s^{-1} for corn in the lower coastal plain. Average NO fluxes during summer 1995 were: 6.4 ± 4.6 and 20.2 ± 19.0 ng N m^{-2} s^{-1} respectively for corn and soybean in the coastal region; 4.2 ± 1.7 ng N m^{-2} s^{-1} for tobacco in the piedmont region; and 8.5 ± 4.9 ng N m^{-2} s^{-1} for corn in the upper piedmont region. Average NO fluxes for spring 1996 were: 66.7 ± 60.7 ng N m^{-2} s^{-1} for wheat in the lower coastal plain; 9.5 ± 2.9 ng N m^{-2} s^{-1} for wheat in the coastal plain; 2.7 ± 3.4 ng N m^{-2} s^{-1} for wheat in the piedmont region; and 56.1 ± 53.7 ng N $m^{-}s^{-1}$ for corn in the upper piedmont region. An exponential dependence of NO flux on soil temperature was present at all of the locations. Further, all locations displayed a diurnal trend of NO emissions which revealed a peak in NO emissions that coincided with the maximum soil temperature for the day. The composite data of all the research sites revealed a general positive trend of increasing NO flux with soil water content and extractable nitrogen.

Presented at:
Workshop on Atmospheric Nitrogen Compounds II: Emissions, Transport, Transformation, Deposition and Assessment
Chapel Hill, North Carolina
June 7 – 9, 1999

Appendix 2. Biogenic Nitric Oxide Source Strengths

Paul A. Roelle and Viney P. Aneja

Department of Marine, Earth and Atmospheric Sciences
North Carolina State University
Raleigh, NC 27695-8208

Emissions of nitric oxide (NO) were determined during late spring and summer 1995 and the spring of 1996 from four crop types, located at four different physiographic regions in North Carolina. Emission rates were calculated using a dynamic flow-through chamber system coupled to a state-of-the-art mobile laboratory for in-situ analysis. Average NO fluxes during late spring 1995 were: 50.9 ± 47.7 ng N m^{-2} s^{-1} for corn in the lower coastal plain. Average NO fluxes during summer 1995 were: 6.4 ± 4.6 and 20.2 ± 19.0 ng N m^{-2} s^{-1} respectively for corn and soybean in the coastal region; 4.2 ± 1.7 ng N m^{-2} s^{-1} for tobacco in the piedmont region; and 8.5 ± 4.9 ng N m^{-2} s^{-1} for corn in the upper piedmont region. Average NO fluxes for spring 1996 were: 66.7 ± 60.7 ng N m^{-2} s^{-1} for wheat in the lower coastal plain; 9.5 ± 2.9 ng N m^{-2} s^{-1} for wheat in the coastal plain; 2.7 ± 3.4 ng N m^{-2} s^{-1} for wheat in the piedmont region; and 56.1 ± 53.7 ng N $m^{-}s^{-1}$ for corn in the upper piedmont region. An exponential dependence of NO flux on soil temperature was present at all of the locations. Further, all locations displayed a diurnal trend of NO emissions, which revealed a peak in NO emissions that coincided with the maximum soil temperature for the day. The composite data of all the research sites revealed a general positive trend of increasing NO flux with soil water content and extractable nitrogen

Presented at:
Air & Waste Management Association's 92nd Annual Meeting and Exhibition
St. Louis, Missouri
June 20 – 24, 1999

Appendix 3. Biogenic Air Pollution

Viney P. Aneja and Paul A. Roelle

Department of Marine, Earth and Atmospheric Sciences
North Carolina State University
Raleigh, NC 27695-8208

and Jeffrey Peirce

Department of Civil and Environmental Engineering
Duke University
Durham, NC 27708-0287

Microorganisms in soil and in aquatic environments play an extremely important role in the cycling of atmospheric pollutants, but one which is difficult to assess quantitatively and not been examined under laboratory controlled environments. Chemical transformations performed by certain bacteria in a media may be important to indoor air pollution and conservation efforts. These organisms break down the complex organic molecules. In general, moisture and temperature promote large populations of decomposers and high rates of metabolism.

Laboratory experiments are conducted to measure pollutant flux from natural and engineered multimedia systems under controlled conditions. New test chambers designed and fabricated in triplicate mimic larger scale test chambers utilized in the field. In the most recent design, construction, and use of this experimental apparatus; pollutant flux is monitored in the laboratory at the multimedia (i.e. soil-air) interface in a controlled dynamic system. The laboratory test chambers are constructed with glass walls (10 cm diameter X 20 cm height), Teflon top and bottom plates, viton o-rings, and Teflon tubing and valves throughout the test system to minimize wall interactions with the materials and the gases under consideration. Pollutant concentrations in the head space above the media samples are monitored continually at one second intervals using a Thermo Environmental Instrument Model 42S Chemiluminescence NO-NO_2-NO_x analyzer with computer data recording. Comprehensive physical, chemical, and microbiological testing of the samples is performed in the laboratory to fully characterize the materials in the test chamber. Selected conditions during controlled experiments include temperature, pH, water filled pore space and nitrogen loadings.

Soil temperatures were examined at 5° C intervals between 3° C and 48° C, for various levels of soil moisture. The soil moisture is represented as % water filled pore space and ranged in values from 1.82 and 96.76. In general NO flux was found to increase linearly with temperature, and also responded to varying amounts of soil moisture. For a fixed temperature, NO flux reached maximum values for % water filled pore space (WFPS) between the range of 20-45%, indicating that moisture stress (low levels of %WFPS) or saturation (high levels of %WFPS) may inhibit NO emissions. NO flux was also examined for various levels of pH between the ranges of 4.3 and 8.3. No

significant trends were observed for pH levels between 5 and 7, however NO was found to increase linearly with increasing pH above 7.3, and maximum NO emissions were observed for acidic soil (pH=4.3). Further implications of these controlled studies to indoor pollution and conservation will be discussed.

Presented at:
An International Conference on Microbiology and Conservation (ICMC '99)
Florence, Italy
June 16 – 19, 1999

Appendix 4. Seasonal Variations of Nitric Oxide Fluxes from Diverse Physiographic Agricultural Soils in North Carolina

Paul A. Roelle, Viney P. Aneja and Wayne Robarge*

Department of Marine, Earth and Atmospheric Sciences
*Department of Soil Science, Box 7619
North Carolina State University, Box 8208
Raleigh, NC 27695

and Bruce Gay, Thomas Pierce and Chris Geron

US EPA
MD-80
Research Triangle Park, NC

Emissions of nitric oxide (NO) were determined during late spring and summer 1995 and the spring of 1996 from four crop types, located at four different physiographic regions in North Carolina. Emission rates were calculated using a dynamic flow-through chamber system coupled to a state-of-the-art mobile laboratory for in-situ analysis. Average NO fluxes during late spring 1995 were: 50.9 ± 47.7 ng N m^{-2} s^{-1} for corn in the lower coastal plain. Average NO fluxes during summer 1995 were: 6.4 ± 4.6 and 20.2 ± 19.0 ng N m^{-2} s^{-1} respectively for corn and soybean in the coastal region; 4.2 ± 1.7 ng N m^{-2} s^{-1} for tobacco in the piedmont region; and 8.5 ± 4.9 ng N m^{-2} s^{-1} for corn in the upper piedmont region. Average NO fluxes for spring 1996 were: 66.7 ± 60.7 ng N m^{-2} s^{-1} for wheat in the lower coastal plain; 9.5 ± 2.9 ng N m^{-2} s^{-1} for wheat in the coastal plain; 2.7 ± 3.4 ng N m^{-2} s^{-1} for wheat in the piedmont region; and 56.1 ± 53.7 ng N $m^{-}s^{-1}$ for corn in the upper piedmont region. An exponential dependence of NO flux on soil temperature was present at all of the locations. Further, all locations displayed a diurnal trend of NO emissions, which revealed a peak in NO emissions that coincided with the maximum soil temperature for the day. The composite data of all the research sites revealed a general positive trend of increasing NO flux with soil water content and extractable nitrogen.

Presented at:
International Global Atmospheric Chemistry Conference
Bologna, Italy
September 12 – 17, 1999

Appendix 5. Measurements and Analysis of Criteria Pollutants in New Delhi, India

Viney P. Aneja, Paul A. Roelle, Sharon B. Phillips, Quansong Tong, Nealson Watkins and Richard Yablonsky

Department of Marine, Earth and Atmospheric Sciences
North Carolina State University
Raleigh, NC 27695-8208

and A. Agarwal
Centre for Science and Environment
New Delhi 110062, India

Ambient concentrations of Carbon Monoxide (CO), Nitrogen Oxides (NO_x), Sulfur Dioxide (SO_2) and Total Suspended Particulates (TSP) were measured from January 1997 to November 1998 in the center of downtown (the Income Tax Office (ITO) located on B.S.G. Marg) New Delhi, India. The data consists of 24-hour averages of SO_2, NO_x, TSP; and 8 and 24-hour averages of CO. The measurements were made in an effort to characterize air pollution in the urban environment of New Delhi and assist in the development of an Air Quality Index. The yearly average CO, NO_x, SO_2 and TSP concentrations for 1997 and 1998 were found to be 4810 ± 2287 μg m^{-3} and 5772 ± 2116 μg m^{-3}; 83 ± 35 μg m^{-3} and 64 ± 22 μg m^{-3}; 20 ± 8 μg m^{-3} and 23 ± 7 μg m^{-3}; 409 ± 110 and 365 ± 100 μg m^{-3} respectively. In general, the maximum CO, SO_2, NO_x and TSP values occurred during the winter with minimum values occurring during the summer, which can be attributed to a combination of meteorological conditions and photochemical activity in the region. The ratio of CO to NO_x (~50) indicates that mobile sources are the predominant contributors for these two compounds in the urban air pollution problem in New Delhi. The ratio of SO_2 to NO_x (~0.6) indicates that point sources are contributing to SO_2 pollution in the city. The averaged background CO concentrations in New Delhi were also calculated (~1939 μg m^{-3}) which exceed those for Eastern USA (~500 μg m^{-3}). Further, all measured concentrations exceeded the US National Ambient Air Quality Standards (NAAQS) except for SO_2. TSP was identified as exceeding the standard on the most frequent basis.

Presented at:
Workshop on Air Quality and Pollution Inventory for the City of Delhi
New Delhi, India
June 6 – 8, 2000

Appendix 6. Characterization of Nitric Oxide Emissions from Sludge Amended Soils

Paul A. Roelle and Viney P. Aneja

Department of Marine, Earth and Atmospheric Sciences
North Carolina State University
Raleigh, NC 27695-8208

and Jeffrey Peirce

Department of Civil and Environmental Engineering
Duke University
Durham, NC 27708-0287

Land spreading nitrogen-rich municipal sludge to human food and non-food chain land is a practice followed throughout the US. This practice may lead to the recovery and utilization of the nitrogen by vegetation, but it may also lead to emissions of biogenic nitric oxide (NO), which may enhance ozone pollution in the lower levels of the troposphere. Recent global estimates of biogenic NO emissions from soils are cited in the literature, which are based on field measurements of NO emission from various agricultural and non-agricultural fields. However, biogenic emissions of NO from sludge-amended soils are lacking. Using a state-of-the-art mobile laboratory and a dynamic flow-through chamber system, in-situ concentrations of nitric oxide (NO) were measured during the summer of 1999 from a sludge amended agricultural soil. The field site was sampled both prior to and immediately following an application of the municipal waste sludge. The average NO flux for the entire time period prior to the sludge application (June 9 – September 3) was ~ 50 ng N m^{-2} s^{-1}. The results of the research segregated into time periods prior to and immediately following the sludge application will be presented. NO emissions responded to changes in soil temperature where daily maximums in NO emissions coincided with daily maximums in soil temperatures. Relationships between NO flux and pH and percent water filled pore space (%WFPS) will also be presented.

Presented at:
Air & Waste Management Association's 93rd Annual Meeting and Exhibition
Salt Lake City, Utah
June 18 – 22, 2000

Appendix 7. Nitric Oxide Emissions from Soils Amended with Municipal-waste Biosolids

Paul A. Roelle and Viney P. Aneja

Department of Marine, Earth and Atmospheric Sciences
North Carolina State University
Raleigh, NC 27695-8208

and Jeffrey Peirce

Department of Civil and Environmental Engineering
Duke University
Durham, NC 27708-0287

Land spreading nitrogen-rich municipal waste biosolids ($N\text{-}NO_3^-$ ~ 443 mg/Kg Dry biosolid, $N\text{-}NO_2^-$ ~ 443 mg/Kg dry biosolid, Phosphorus ~ 11,970 mg/Kg Dry biosolid, Total N ~ 42,586 mg/Kg Dry biosolid) to human food and non-food chain land is a practice followed throughout the US. This practice may lead to the recovery and utilization of the nitrogen by vegetation, but it may also lead to emissions of biogenic nitric oxide (NO), which may enhance ozone pollution in the lower levels of the troposphere. Recent global estimates of biogenic NO emissions from soils are cited in the literature, which are based on field measurements of NO emission from various agricultural and non-agricultural fields. However, biogenic emissions of NO from soils amended with biosolids are lacking. Using a state-of-the-art mobile laboratory and a dynamic flow-through chamber system, in-situ concentrations of nitric oxide (NO) were measured during the Summer/Fall of 1999 and Winter/Spring of 2000 from an agricultural soil which is routinely amended with municipal waste biosolids. The average NO flux for the entire time period prior to a biosolids application (June 9 – September 3) was 57.8 ± 34.6 ng N-NO m^{-2} s^{-1}. Field experiments were conducted which indicated that the application of biosolids increase the emissions of NO. The results of the research segregated into time periods prior to and immediately following the biosolids application will be presented. NO emissions responded to changes in soil temperature where daily maximums in NO emissions coincided with daily maximums in soil temperatures. Relationships between NO flux and pH and percent water filled pore space (%WFPS) will also be presented.

Presented at:
The Sixth International Conference on Air-Surface Exchange of Gases and Particles
Edinburgh, United Kingdom
July 3 – 7, 2000

Appendix 8. Measurement and Modeling of Biogeochemical Cycling of Nitrogen Compounds

Paul A. Roelle and Viney P. Aneja

Department of Marine, Earth and Atmospheric Sciences
North Carolina State University
Raleigh, NC 27695-8208

Land spreading nitrogen-rich municipal sludge to human food and non-food chain land is a practice followed throughout the US. This practice may lead to the recovery and utilization of the nitrogen by vegetation, but it may also lead to emissions of biogenic nitric oxide (NO), which may enhance ozone pollution in the lower levels of the troposphere. Recent global estimates of biogenic NO emissions from soils are cited in the literature, which are based on field measurements of NO emission from various agricultural and non-agricultural fields. However, biogenic emissions of NO from sludge-amended soils are lacking. Using a state-of-the-art mobile laboratory and a dynamic flow-through chamber system, in-situ concentrations of nitric oxide (NO) were measured during the summer of 1999 from a sludge amended agricultural soil. The field site was sampled both prior to and immediately following an application of the municipal waste sludge. The average NO flux for the entire time period prior to the sludge application (June 9 – September 3) was ~ 50 ng N m^{-2} s^{-1}. The results of the research segregated into time periods prior to and immediately following the sludge application will be presented. NO emissions responded to changes in soil temperature where daily maximums in NO emissions coincided with daily maximums in soil temperatures. Relationships between NO flux and pH and percent water filled pore space (%WFPS) will also be presented.

Presented at:
Meteorology at the Millennium, 150th Anniversary Conference
Cambridge, United Kingdom
July 10 – 14, 2000

Appendix 9. Measurement and Modeling of Nitric Oxide Emissions from Biosolid Amended Soils

Paul A. Roelle and Viney P. Aneja

Department of Marine, Earth and Atmospheric Sciences
North Carolina State University
Raleigh, NC 27695-8208

and Sonia Aneja
Summer Intern
Broughton High School
Raleigh, NC

Land spreading nitrogen-rich municipal biosolids to human food and non-food chain land is a practice followed throughout the US. This practice may lead to the recovery and utilization of the nitrogen by vegetation, but it may also lead to emissions of biogenic nitric oxide (NO), which may enhance ozone pollution in the lower levels of the troposphere. Recent global estimates of biogenic NO emissions from soils are cited in the literature, which are based on field measurements of NO emission from various agricultural and non-agricultural fields. However, biogenic emissions of NO from biosolid-amended soils are lacking. Using a state-of-the-art mobile laboratory and a dynamic flow-through chamber system, in-situ concentrations of nitric oxide (NO) were measured during the summer, winter and spring of 1999/2000 from agricultural soils amended with biosolids. The field site was sampled prior to and immediately following applications of the biosolids. The average NO flux for summer, winter and spring were 57.8 ± 34.6 ng NO-N m^{-2} s^{-1}, 3.62 ± 3.93 ng NO-N m^{-2} s^{-1} and 59.05 ± 54.21 ng NO-N m^{-2} s^{-1} respectively. NO emissions responded to changes in soil temperature where daily maximums in NO emissions coincided with daily maximums in soil temperatures.

Presented at:
International Symposium on the Measurement of Toxic and Related Air Pollutants
Research Triangle Park, North Carolina
September 12 – 14, 2000

Appendix 10. Effect of Environmental Variables on NO Emissions from Agricultural Soils

Viney P. Aneja, Paul A. Roelle and Yongxian Li

Department of Marine, Earth and Atmospheric Sciences
North Carolina State University
Raleigh, NC 27695-8208

Nitric oxide (NO) is an important air pollutant which leads to the production of ozone and acidic precipitation. Biogenic emissions of NO are gaining in importance for ozone formation in semi-urban and rural regions of the Southeast United States. Using a dynamic chamber system interfaced to a mobile laboratory for continuous NO analysis, soil emissions of NO were measured over typical row crops in North Carolina during 1994 - 1996. This paper investigates the effect of soil temperature, soil water content and soil extractable nitrogen on soil NO emissions from corn and soybean canopies. Three of five sets of measurements from corn and two of four sets of measurements from soybean displayed an exponential relationship between soil NO emissions and soil temperature. No significant correlation between soil NO emissions and water filled pore space (WFPS) was observed. The best correlation observed between soil NO emissions and total extractable nitrogen (TEN) was found to be linear for soybean (NO emission = 0.67 + 1.43*TEN, R^2 = 0.34), and logarithmic for corn (NO emission = 21.20*Ln (TEN) – 27.27, R^2 = 0.17). Multiple regression models (Ln (NO emission) = 1.5017 + 0.0786*TEN – 0.0006*TEN^2; R^2 = 0.58 for corn; Ln (NO emission) = 77.917 – 6.19*T + 0.1243*T^2 + 0.0068*TEN^2; R^2 = 0.65 for soybean) appear to be the best overall model for predicting soil NO emissions.

Presented at:
Internet Conference: Nitrogen Emissions from Soil
"Programme based on an Austrian research co-operation between the Magistrat der Stadt Wien, MA 49 (City of Vienna) and the Bundesministerium für Bildung, Wissenschaft und Kultur (Austrian Federal Ministry of Education, Science and Culture)
<www.nitro-soil.at>
September 18 – December 31, 2000

Appendix 11. Characterization of Sources of Biogenic Atmospheric Ammonia

Paul A. Roelle and Viney P. Aneja

Department of Marine, Earth and Atmospheric Sciences
North Carolina State University
Raleigh, NC 27695-8208

Atmospheric ammonia (NH_3) has recently reached a heightened awareness as a result of its environmental impact on particulate matter formation, soil acidification, aquatic eutrophication and odor issues. Animal waste (22 Tg NH_3 yr^{-1}) contributes the largest emissions to the total global NH_3 budget (45 Tg NH_3 $year^{-1}$) (Dentener and Crutzen, 1994), hence areas of intensive livestock operations are potential sources of significant ammonia emissions. North Carolina is currently the second largest hog producing state in the USA and the current technology to manage the waste is known as the lagoon and spray system, which consists of an exposed waste lagoon and mechanisms through which the waste is periodically sprayed onto the soil as a nutrient source. It has been reported that a substantial fraction of the total NH_3 emissions in NC are from these intensive livestock operations (9.21 kg NH_3 $animal^{-1}$ $year^{-1}$) (Aneja et al., 1998; Battye et al., 1994). The objective of this study is to characterize the sources of biogenic atmospheric ammonia. Fluxes of NH_3 were determined in-situ using a dynamic flow-through chamber system, in conjunction with a high sensitivity chemiluminescence ammonia analyzer. Soil and water samples from the center of the chamber footprint were collected and analyzed for pH, Total Kjeldahl Nitrogen (TKN) content, and percent water filled pore space. Results indicate that NH_3 fluxes from the agricultural field sites ranged from 45 – 100 ng N m^{-2} s^{-1} for soils and 305-4017 μg N m^{-2} min^{-1} for lagoons. NH_3 emissions responded to changes in temperature where daily maximums in NH_3 emissions coincided with daily maximums in temperatures. Relationships between NH_3 flux, temperature, pH and TKN will also be presented.

Presented at:
Atmospheric Sciences and Applications to Air Quality (ASAAQ) and Exhibition
Taipei, Taiwan
October 31 – November 2, 2000

Appendix 12. Nitric Oxide Emissions from Biosolid Amended Soils

Paul A. Roelle and Viney P. Aneja

Department of Marine, Earth and Atmospheric Sciences
North Carolina State University
Raleigh, NC 27695-8208

Land spreading nitrogen-rich municipal biosolids to human food and non-food chain land is a practice followed throughout the US. This practice may lead to the recovery and utilization of the nitrogen by vegetation, but it may also lead to emissions of biogenic nitric oxide (NO), which may enhance ozone pollution in the lower levels of the troposphere. Recent global estimates of biogenic NO emissions from soils are cited in the literature, which are based on field measurements of NO emission from various agricultural and non-agricultural fields. However, biogenic emissions of NO from biosolid-amended soils are lacking. Using a state-of-the-art mobile laboratory and a dynamic flow-through chamber system, in-situ concentrations of nitric oxide (NO) were measured during the summer, winter and spring of 1999/2000 from agricultural soils amended with biosolids. The field site was sampled both prior to and immediately following an application of the biosolids. The average NO flux for the entire time period prior to the sludge application (June 9 – September 3) was ~ 50 ng N m^{-2} s^{-1}. The results of the research segregated into time periods prior to and immediately following the sludge application will be presented. NO emissions responded to changes in soil temperature where daily maximums in NO emissions coincided with daily maximums in soil temperatures. Relationships between NO flux and pH and percent water filled pore space (%WFPS) will also be presented.

Presented at:
2000 Annual Meeting and International Conference of the American Institute of Hydrology: Atmospheric, Surface and Subsurface Hydrology and Interactions
Research Triangle Park, North Carolina
November 5 – 8, 2000